NATIONAL AERONAUTICS AND SPACE ADMINISTRATION

Technical Report 32-1505

Satellite Auxiliary-Propulsion Selection Techniques

Lee B. Holcomb

JET PROPULSION LABORATORY
CALIFORNIA INSTITUTE OF TECHNOLOGY
PASADENA, CALIFORNIA

November 1, 1970

NATIONAL AERONAUTICS AND SPACE ADMINISTRATION

Technical Report 32-1505

Satellite Auxiliary-Propulsion Selection Techniques

Lee B. Holcomb

JET PROPULSION LABORATORY
CALIFORNIA INSTITUTE OF TECHNOLOGY
PASADENA, CALIFORNIA

November 1, 1970

Prepared Under Contract No. NAS 7-100
National Aeronautics and Space Administration

Preface

The work described in this report was sponsored by the NASA/OSSA Applications Technology Satellites Program Office and was performed by the Propulsion Division of the Jet Propulsion Laboratory.

Acknowledgment

The author would like to acknowledge the cooperation of the many corporations, NASA agencies, and other government agencies for permission to reproduce photographs and data, and for freely discussing various technical areas. The author would further like to acknowledge the continuous assistance and contributions of C. N. Jennings, J. H. Kelley, D. J. Kerrisk, P. I. Moynihan, N. R. Thach, and G. J. Nunz.

Contents

Tables

Contents (contd)

Tables (contd)

Contents (contd)

Tables (contd)

Figures

Contents (contd)

Figures (contd)

Contents (contd)

Figures (contd)

Contents (contd)

Figures (contd)

Contents (contd)

Figures (contd)

Abstract

In order to establish criteria for the selection of attitude- and station-keeping propulsion systems for future satellites and other unmanned spacecraft, current auxiliary propulsion systems were surveyed and parameterized. Thruster systems considered were inert gas, monopropellant hydrazine, vaporizing liquid, electrolysis, Tridyne, resistojet, radioisojet, and subliming solid. Electrostatic and electromagnetic thrusters were also surveyed, but were not included in the detailed study. A generalized auxiliary propulsion system selection technique, based on cost-effectiveness criteria, is presented. Three specific missions are included as examples of the use of the selection criteria: a synchronous satellite, a subsynchronous satellite, and a Grand Tour planetary spacecraft.

Satellite Auxiliary-Propulsion Selection Techniques

I. Introduction

With the advent of long life earth-orbiting and interplanetary three-axis stabilized spacecraft, the technology of low-thrust (10^{-5} to 5 lbf) propulsion systems has received increased emphasis. The selection of the optimum[1] auxiliary-propulsion system for a given mission is extremely important and can severely impact the spacecraft payload and the probability of success. An auxiliary-propulsion system can be characterized by parameters such as mass, power, performance, cost, volume, leakage, reliability, and others. The selection of an optimum system involves the tradeoff of these variables for the specific mission under consideration.

In order to meaningfully relate or normalize such diverse parameters as cost, reliability, mass, power, etc., a cost-effectiveness technique can be used, which produces a measure of excellence for each system option for a given mission.

The utilization of cost effectiveness in technology decisions has received varied attention in the past. A cost-effectiveness comparison of auxiliary-propulsion systems was undertaken by General Electric on the Orbiting Astronomical Observatory (OAO) and Nimbus programs (Ref. 1). A report on the design criteria for spacecraft propulsion system selection (Ref. 2) has been used as a basis for the cost-effectiveness techniques presented herein. Section II presents a more in-depth discussion of what the terminology cost-effectiveness means to a subsystem designer, what some of the misconceptions of the term are, what benefit can be gained from a cost-effectiveness analysis, and finally how to go about a cost-effectiveness analysis of candidate auxiliary propulsion systems. This report is a continuation of earlier thruster tradeoff studies at the Jet Propulsion Laboratory.

Before a meaningful tradeoff of thruster systems can begin, an up-to-date survey of existing technology is necessary. An extensive survey of available thruster systems is presented in Appendix A. System types included in the survey are as follows:

(1) Inert gas: H_2, He, Ne, N_2, A, K, Xe, CF_4, and CH_4. The inert gas system is characterized by a high-pressure gas, which is reduced in pressure by a regulator and expelled through a nozzle.

(2) Tridyne (gaseous O_2, H_2, and N_2). The tridyne system is identical to the inert gas system except that the gas is catalytically reacted to increase the gas temperature prior to expulsion through a nozzle.

[1] "Optimum" in this report means the most applicable subsystem for a given mission, based on maximized cost effectiveness, rather than the optimized subsystem without regard for existing technology and cost.

(3) Hydrazine direct catalyst. The hydrazine direct catalyst system is composed of a liquid expulsion feed system and a catalytic thrust chamber that decomposes the hydrazine prior to expulsion.

(4) Hydrazine resistojet. The hydrazine resistojet system is similar to the hydrazine direct catalyst system; however, the hydrazine is decomposed by an electrically heated resistance element in the thrust chamber.

(5) Hydrazine plenum. The hydrazine plenum system has a liquid hydrazine feed system that is fed into a catalytic gas generator; the gases generated are stored in a plenum for later gas expulsion.

(6) Vaporizing liquid: ammonia, Freon 12, butane, and propane. The vaporizing liquid system is characterized by a liquid propellant pressurized by its own equilibrium vapor pressure and the expulsion of this vapor through a nozzle.

(7) Resistojets: ammonia, nitrogen, hydrogen, and ammonia carbamate. The resistojet is not really a system, but a subsystem. Cold fluid (gaseous or liquid) is increased in temperature by passing through an electrically heated heat exchanger.

(8) Radioisojet: ammonia and hydrogen. The radioisojet is similar to a resistojet; however, a radioisotope heat source is employed rather than an electrical resistance heater.

(9) Electrolysis: water (hot or cold gas thrusting mode) and hydrazine. Electrolysis auxiliary propulsion systems produce a low-molecular weight, gaseous propellant by the electrolysis of a suitable liquid. The gaseous propellant is then expelled as an inert gas or ignited as in the case of water electrolysis.

(10) Subliming solid: ammonium hydrosulfide, ammonium carbamate, and monomethyl ammonium carbamate. The subliming solid system is characterized by a solid propellant, which when heated is pressurized by its own vapor pressure and this vapor is expelled through a nozzle.

Additional systems (ion, colloid, pulsed plasma, "cap pistol," and "honeycomb") have been included in the preliminary survey.

In Table 1 some favorable and unfavorable characteristics of auxiliary propulsion systems are presented. This table is not meant to serve as a selection criterion for candidate systems; however, it may serve to narrow the selection to a few candidate thrusters.

The performance and mass of the ten system types listed above are included in Appendix B. Thruster system performance is tabulated for various propellants, duty cycles, and power. Feed system mass is parameterized as a function of propellant mass. Tabulations of component masses are available for redundancy calculations. Subsystem reliability calculations are presented in Appendix C; a survey of mechanical component failure rates and reliability theory is included. System redundancy equations are developed along with detailed system reliability calculations. Estimated system costs are presented in Appendix D; both hardware and development costs are listed.

Seven system configurations are referenced throughout the report. These configurations are presented in Fig. 1. The first three configurations (a, b, and c) are single systems with six thrusters ($\pm$yaw, $\pm$roll, and $\pm$pitch). These configurations provide three-axis attitude control. Thrusters will operate about a moment and can cause small translations of the spacecraft. The fourth configuration (d) has twelve thrust chambers (T/C) which provide couples in all three axes. In a degraded mode one of the two thrusters in any of the couples could fail closed and the other would provide moments about that axis. The last three configurations (e, f, g) are double systems, two complete systems, each able to provide three-axis attitude control in case of a failure in the other system.

Auxiliary propulsion systems/spacecraft interactions must be studied before a specific system can be selected. One of the most subtle propulsion system/spacecraft interactions is plume impingement on spacecraft surfaces, other subsystems, and scientific instruments. This subject will be addressed in an addendum to this report.

The advent of momentum wheels has greatly changed the major role of an attitude propulsion system in that limit cycle operation is not a primary design criterion. Impulses for unloading momentum wheels are separated by large time intervals (on the order of hours to weeks) with respect to limit cycle operation, thus reducing the number of thruster cycles. In addition, total impulse requirements are reduced because of the removal of cyclical disturbances by the momentum wheels. The pointing accuracy with momentum wheels is limited by parameters such as sensor accuracy and wheel inertia, assuming thruster transients are small. This implies that thruster selection will not affect pointing accuracy, provided a reasonable thrust level can be obtained. In a detailed dynamic six-degree-of-freedom simulation of an ATS-type satellite, various system thrust profiles were investigated and compared with square wave pulse shapes. If autopilot

Table 1. General characteristics of thruster systems

Thruster system	Favorable characteristics	Unfavorable characteristics
Inert gas	Inexpensive. Repeatable impulse bit. Flight experience.	Low specific impulse. Long-term leakage, for long missions. High-pressure tankage required. Excessive mass for high total impulse missions.
Tridyne (gaseous monopropellant)	Same feed system as inert gas. Increased performance over inert gas. Repeatable impulse bit.	Medium-to-low specific impulse. Long-term leakage, for long missions. High pressure tankage required. Low-power heater required.
Vaporizing liquid	Relatively inexpensive. Low-pressure storage. Repeatable impulse bit. Flight experience.	Relatively low reliability of present feed system designs. Medium-to-low specific impulse. Leakage for long missions.
Hydrazine catalyst	Relatively high reliability of feed system. Medium specific impulse. Flight experience. Low leakage of propellant for long-term storage.	Moderately expensive. Poor repeatability at very low impulse bit with cold catalyst bed. "Limited" catalyst bed life.
Hydrazine resistojet (liquid)	Relatively high reliability of feed system. Medium specific impulse. Low leakage of propellant for long-term storage.	Relatively expensive development. Poor pulse response at low thrust.
Hydrazine resistojet (gaseous)	Relatively high reliability of feed system. Medium specific impulse. Low leakage of propellant. Repeatable impulse bit.	Relatively expensive development. Thermal control of vaporizer required.
Hydrazine plenum	Relatively inexpensive. Repeatable impulse bit. Flight qualified system.	Relatively low reliability of nonpassive feed system. Medium-to-low specific impulse.
Water electrolysis	Medium-to-high specific impulse. Cell has undergone flight qualification. Repeatable impulse bit.	Low reliability. Relatively high development cost.
Hydrazine electrolysis	Repeatable impulse bit. Could also self-pressurize in "dual-mode."	Low reliability. Relatively high development cost.
Subliming solid	High reliability. Low thrust.	Thermal control problems. Long on–off times. Moderately low specific impulse.
"Cap pistol" and "honeycomb"	No leakage. Medium specific impulse.	Complex mechanisms and logic circuitry. Large fixed mass.

Table 1 (contd)

Thruster system	Favorable characteristics	Unfavorable characteristics
Ion	High specific impulse. Flight experience.	High voltages and large power requirement. Complex system. Exhaust neutralizer required. Expensive.
Colloid	High specific impulse. Low power-to-thrust ratio. Low propellant vapor pressure.	Some power required. High voltages. Complex system. Exhaust neutralizer required. Expensive.
Pulsed plasma	High specific impulse. Simple system. Flight experience. Relatively inexpensive.	Large power requirement. Limited thruster life. RF noise. Potential feed system problems.
Resistojet, NH_3	Low pressure storage. Repeatable impulse bit. Flight experience. Medium specific impulse.	Relatively low reliability of present feed system designs. Thruster heater power required. Leakage for long missions.
Resistojet, N_2	Relatively inexpensive. Repeatable impulse bit.	Medium-to-low specific impulse. Long-term leakage. Leakage for long missions.
Radioisojet, NH_3	Medium-to-high specific impulse. Repeatable impulse bit.	High cost. Isotope handling problems. Influence of isotopes on spacecraft and thruster design. Leakage for long missions. Relatively low reliability of present feed system designs.

stability problems are not created by the initial delay and rise time, the effect of the thrust transient characteristics will result in a somewhat larger transient position error, rate error, and propellant consumption. However, for most realistic thruster systems these additional errors arising from transient rather than square pulse shape are very small and are considered acceptable in a conservative system design. The subliming solid system is the only system considered in this report that could lead to large errors in propellant estimation if a square wave approximation is used. If the subliming solid system is restricted to a long-pulse, or steady-state thrusting, then a square wave approximation to the thrust profile can be assumed.

Other major roles of a secondary propulsion system are tipoff rate reduction, reference acquisition, orbit trim, and station keeping. North-South station keeping requirements (typically 150 ft/s/yr or so) can impose a relatively large total impulse requirement on an auxiliary-propulsion system.

Three mission profiles are presented as examples in this report: a synchronous satellite, a subsynchronous satellite, and a planetary space vehicle. These three missions, coupled with the ten basic systems and combinations of these systems, present a wide variety of tradeoffs of system designs.

The tradeoff examples of Sections III, IV, and V show that the preferred auxiliary-propulsion system for the synchronous satellite considered (*Intelsat IV*) is a 10-mlbf ammonia resistojet. The optimum auxiliary-propulsion system for the subsynchronous satellite considered, Earth Resources Technology Satellite (ERTS), is a combination

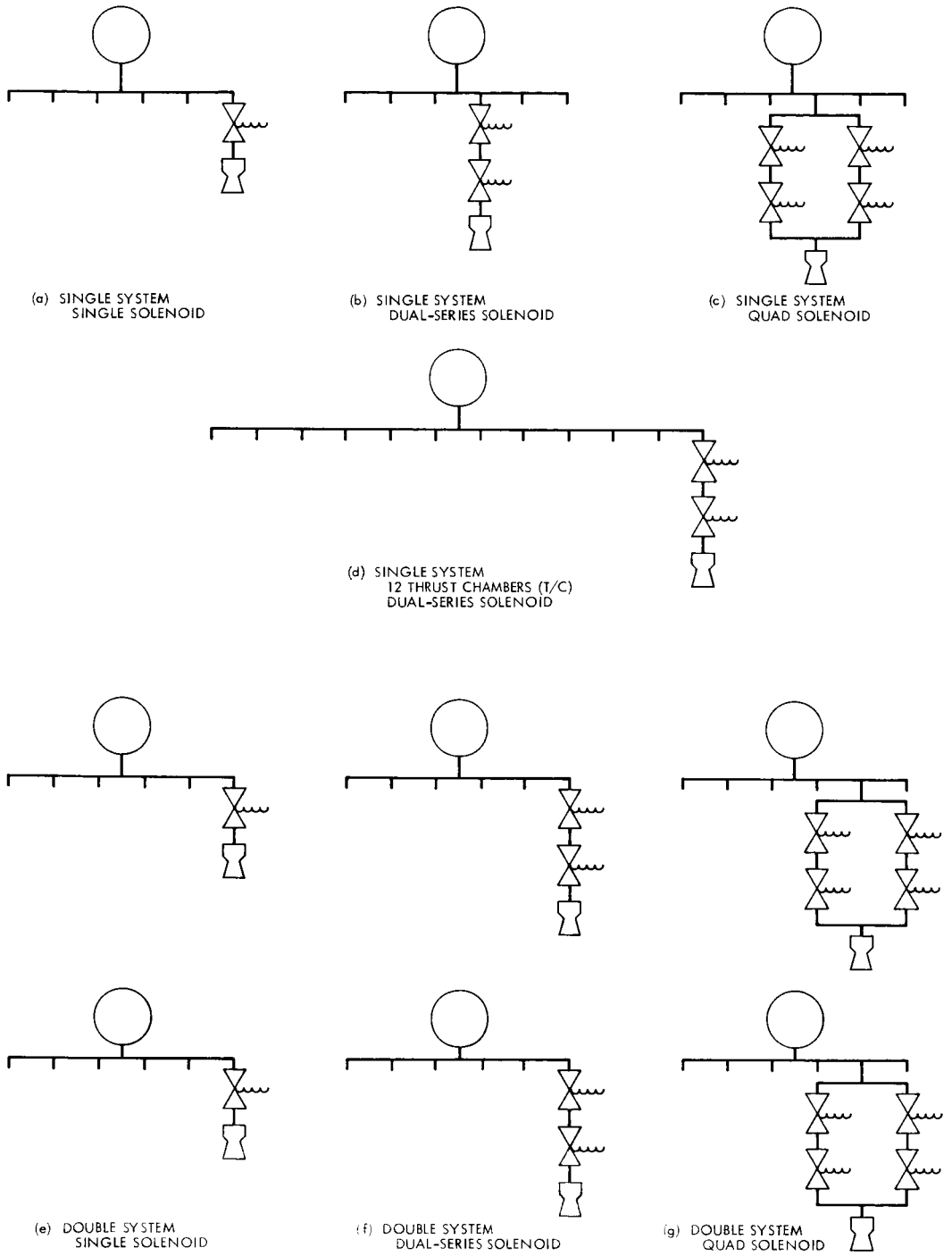

Fig. 1. System configurations

of hydrazine plenum low-level thruster and hydrazine catalyst high-level thruster. The hydrazine catalyst system is the optimum for the planetary spacecraft under consideration, Thermoelectric Outer Planet Spacecraft (TOPS).

The techniques presented in Section II are valid for comparing auxiliary propulsion systems. The parametric data presented in the appendixes is based on a new mission with little or no previous development effort. In the case of missions that are merely continuations of previous programs the cost and other data associated with previously used subsystems will differ from the generalized data in the appendixes. It is emphasized that the results in this report are completely dependent on the mission and subsystem assumptions, and that they not only change from mission to mission but also may change with time for the same mission as technology evolves and as the relations of the values of cost, mass, reliability, etc., vary.

II. Cost-Effectiveness Techniques

Before a discussion of cost-effectiveness techniques can begin, the terminology of this Section must be introduced. Several terms that require accurate definitions will appear in the discussion. The term "worth" may be defined as a composite measure of multiple program objectives and the degree to which those objectives are met within the assumed structure of the particular program being analyzed (Ref. 3). Worth may be a decaying function with time as in the case of a satellite which is constantly returning data. "Probability of success" is defined as the probability that all the required subsystems are functioning properly (or in redundant backup modes) at a given time. The failure of a required subsystem (e.g., communication, power, attitude control) will result in the loss of satellite usefulness. "Utility" means usefulness; the satisfying of a need (Ref. 4). As applied in this resort, utility is the product of two factors, worth and probability of success. "Effectiveness" is considered equivalent to utility. "Cost" requires little definition; it may be categorized as consumption of physical resources, employment of human resources, and dissipation of time (Ref. 5). Costs may be indexed by a dollar-value scale. The value of an outcome or the measure of utility is the result of a subjective evaluation by the decision-maker. An obvious scale for value is dollars, but many times this is an inappropriate unit of measure; for example, military decision makers assess the value of lives lost, or targets damaged.

The application of cost-effectiveness methods as a criterion for subsystem design tradeoffs and design selections has received considerable attention recently. Development of the cost-effectiveness discipline, and its widespread use by planners, has been extremely rapid—so much so that cost-effectiveness analysis is still relatively ill-defined within the technical community.

Cost effectiveness is often criticized, as in this statement by Rep. L. Mendel Rivers, Chairman of House Armed Services Committee (Ref. 6):

> "All of this is being rationalized on the basis of cost/effectiveness studies. Do you know that the M14 rifle costs more than a bow and arrow? From a cost/effectiveness standpoint we obviously would be better off if we went back to bows and arrows. A beer bottle filled with gasoline and stuffed with a rag wick is a fairly effective weapon at close quarters, and it is cheaper to produce than a land mine or a hand grenade. From a cost/effectiveness viewpoint, we should be collecting beer bottles and old rags."

Why such violent opposition to cost-effectiveness? It is something a man always practices when he buys a house or plans a vacation. It is seldom the mathematics or computation that is questioned or at fault; almost always it is how we decide what assumptions to make, what contingencies to consider, what objectives to choose, what the costs are and what the gains are; and, above all, it is the things we did not consider at all (Ref. 7).

The essence of decision making is a tradeoff of cost and utility. Cost is usually easy to predict, within a given error band, whereas utility is quite difficult to predict. Disagreement on assigned utilities is common, and care must be taken to select realistic utilities. The broad application of the cost-effectiveness discipline to aerospace systems like missiles, communication satellites, launch vehicles, program planning, and earth station profit analysis was the subject of an AIAA Lecture Series in 1966. A further refinement of cost-effectiveness techniques as applied to spacecraft propulsion systems is presented in Ref. 2; the techniques and principles of this work have been utilized herein.

What benefit can be gained from a cost-effectiveness analysis of auxiliary propulsion systems? Ultimately, when faced with a list of candidate systems and their associated mass, cost, reliability, and power, a selection of a single system for a given mission must be performed. These characteristics (weight, reliability, etc.) have different relative effects on the system capability depending on the particular mission in question. With cost-effectiveness techniques these diverse characteristics can be normalized

into one figure-of-merit, thereby establishing the quantitative relative importance of each characteristic. In the past, selections have too often been made on unclear and undefined criteria and have therefore been subject to conflicting personal opinions. Use of the proposed cost-effectiveness selection criteria, if nothing else, forces the decision maker to document his input data and assumptions; traceability is vastly increased. The method presented herein is not difficult to use and sophisticated mathematics is not required. The following theory may at first appear abstract, but the example which follows should clarify the use of the techniques.

A. Theory

Is the objective of a cost-effectiveness study to find a program or system that offers the maximum ratio of utility to cost? In general, when considering the unbounded problem of comparing broad programs and systems, decisions based on maximizing the ratio of effectiveness over cost can be misleading. Maximum gain is infinitely large, and minimum cost is zero. Seek the policy which has that outcome, and you shall not find it. Comparisons of alternative large systems or programs should be approached either with total cost fixed by attempting to maximize utility, or with utility fixed and attempting to minimize cost. The spacecraft subsystem designer, however, is faced with a different problem. He must select from competitive systems, which offer several values of total spacecraft utility at several values of cost. The subsystem utilities and costs are therefore bounded, but not fixed. Is the ratio of utility to cost a valid selection criterion for spacecraft subsystems? For this purpose the ratio appears to be valid. Each subsystem within the spacecraft is usually assigned a baseline budget, which will probably not be equal to any of the projected costs of the candidate subsystems. Competition between subsystem designers for incremental increases to their allotted budgets should be based on attendant gains in total spacecraft utility per added dollar. This criterion will force some subsystems below their initial budgets and hence to less expensive designs. The initially stated problem thus degenerates to a feedback cycle where changes in the proposed spacecraft program goals and objectives are incorporated to suit the restricted funds (Ref. 2).

Cost effectiveness may be described in several ways. It is expressed here as:

$$CE = \frac{\sum_i U_i}{\sum_i C_i} = \frac{\sum_i P_i W_i}{\sum_i C_i} \tag{1}$$

where U_i are incremental utility values and C_i are concurrent cost increments. Utility is expressed as the product of worth and probability of success. The increments are expressed as time points. For purposes of this report, an averaging and summation of functions over time increments will replace a formal integration.

Worth is a function of spacecraft payload mass. Probability of success is a function of individual subsystem reliability and, in this study, is directly a function of auxiliary propulsion reliability. Since spacecraft probability of success is a function of subsystem redundancy, it is therefore a function of redundancy mass. Mission cost is directly a function of subsystem cost. Equation (1) is therefore a function of mass, cost, and reliability:

$$CE = f(\text{mass}, \text{cost}, \text{reliability}) \tag{2}$$

The initial step in a tradeoff study is the characterization of competitive systems in terms of their design parameters. The comparison of systems becomes a comparison of groups of parameters. System descriptions can usually be mapped into three parameters: mass, reliability, and cost. The relative influence of these parameters can be expressed in terms of system cost effectiveness.

Partial differentiation of Eq. (2) results in the following expression:

$$dCE = \frac{\partial CE}{\partial \text{mass}} d\,\text{mass} + \frac{\partial CE}{\partial \text{cost}} d\,\text{cost} + \frac{\partial CE}{\partial \text{reliability}} d\,\text{reliability} \tag{3}$$

For purposes of this report this expression should be simplified to match the accuracy of supplied mission data:

$$\Delta CE = \left|\frac{\Delta CE}{\Delta \text{mass}}\right| \Delta\text{mass} + \left|\frac{\Delta CE}{\Delta \text{cost}}\right| \Delta\text{cost} + \left|\frac{\Delta CE}{\Delta \text{reliability}}\right| \Delta\text{reliability} \tag{4}$$

A baseline value of cost effectiveness may be assigned as:

$$CE_{\text{baseline}} = CE\,(\text{mass}_{\text{baseline}}, \text{cost}_{\text{baseline}}, \text{reliability}_{\text{baseline}}) \tag{2a}$$

Any modifications to this reference value can be measured in terms of the individual changes in mass, reliability, and cost:

$$CE = CE_{\text{baseline}} + \Delta CE$$

$$= CE_{\text{baseline}} + \left|\frac{\Delta CE}{\Delta \text{mass}}\right| \Delta\text{mass} + \left|\frac{\Delta CE}{\Delta \text{cost}}\right| \Delta\text{cost}$$

$$+ \left|\frac{\Delta CE}{\Delta \text{reliability}}\right| \Delta\text{reliability} \qquad (5)$$

Where Δmass, Δcost, and Δreliability are the differences in the baseline and comparative system mass, cost, and reliability (deltas). The terms $\Delta CE/\Delta$mass; $\Delta CE/\Delta$cost; and $\Delta CE/\Delta$reliability are called "influence coefficients" and must be determined for each mission. The influence of one parameter on mission utility and cost must be evaluated while the other parameters are fixed. A more general form of Eq. (5) could contain many more terms, each consisting of a differential parameter and its corresponding influence coefficient (e.g., power, volume). The mapping of these additional parameters into mass, cost, and reliability should be implemented when available data make this effort practical. Without quantification, the influence of these considerations must be qualitatively superimposed on the quantitative analytical results.

Influence coefficients in general are determined by noting the effect of subsystems other than the auxiliary propulsion system on the mission cost effectiveness. The influence of these changes can then be used to compare the small changes in auxiliary propulsion characteristics that exist between candidate thrusting systems.

Since most space vehicles are constrained by mass, relative worth must be assigned to subsystem mass (i.e., there exists a mass influence coefficient). Mission utility may be affected by two types of mass allocation:

(1) The allocation of additional mass to scientific payload (direct effect on mission value or worth).

(2) The allocation of additional mass to subsystem redundancy (direct effect on mission probability of success).

If spacecraft mass is constrained, then the reduction in mass, achieved by changing from a heavy alternative subsystem to a lighter subsystem, may be assigned to either additional scientific payload or subsystem redundancy.

Cost influence coefficients are relatively easy to obtain; however, care must be taken when cost data are compiled. The following two types of costs must be identified:

(1) Nonrecurring developmental costs.

(2) Recurring hardware costs.

Nonrecurring costs must be spread over the total number of missions.

Since the auxiliary propulsion subsystem is continually in use, a change in subsystem reliability will impact the entire mission success. If the probability of mission success is given by a function (P_i), then incorporated into this function is the baseline thruster reliability. If a new subsystem is compared, then the corresponding probability of mission success is given by:

$$P_{MS_i} = \frac{R_{NS}}{R_{BL}} P_i \qquad (6)$$

where P_{MS} is the new probability of mission success; R_{NS} and R_{BL} are the reliabilities of the new comparative subsystem and the baseline subsystem, respectively.

Competitive subsystems (e.g., inert gas vs hydrazine catalyst) can now be compared with a common figure of merit. A system is selected as the baseline for comparisons. This selection of a baseline system can be arbitrary for the first iteration. The baseline value of cost effectiveness is calculated with Eq. (1) and is assigned to the selected baseline system. Equation (5) is then used with the proper influence coefficients inserted. The differences in values of mass, cost, and reliability between the baseline system and the comparative system (deltas) are inserted into Eq. (5) and a combined figure of merit is obtained. The calculated optimum system is the one with the maximum value of cost-effectiveness and can be graphically displayed when the various options are plotted. To illustrate this method, a hypothetical example will now be explored.[2]

B. Example

Auxiliary propulsion system mission requirements are necessary to begin a comparison of competitive systems. From these requirements, the desired thrust level, duty cycle, and total impulse are calculated. Competitive subsystems may then be fully defined utilizing the performance and design information in Appendixes B, C, and D. Assume that a comparison of an inert gas and a hydrazine

[2]Examples showing actual design cases are presented in Sections III, IV, and V.

Table 2. System data

System	Configuration	Mass, lbm	Reliability	Cost,[a] $ million	Cost effectiveness
Inert gas	Single system, 6 thrust chambers	150	0.900	0.120	0.0775
Inert gas	Single system, 12 thrust chambers	160	0.910	0.140	0.0764
Inert gas	Double system, 6 thrust chambers	250	0.980	0.200	0.06483
Hydrazine catalyst	Single system, 6 thrust chambers	140	0.850	0.250	0.0762
Hydrazine catalyst	Single system, 12 thrust chambers	150	0.880	0.300	0.07564
Hydrazine catalyst	Double system, 6 thrust chambers	190	0.900	0.400	0.06949

[a]For the detailed treatment of cost see Appendix C.

direct catalyst system is conducted, resulting in the matrix of design characteristics given in Table 2. The auxiliary propulsion designer, now faced with this matrix of characteristics, must decide which system should be selected for the application being considered; relative importance of cost, mass, and reliability must be assessed for the specific mission/program in order to make a meaningful design decision. The cost-effectiveness criteria described earlier provides us with a technique to relate the propulsion characteristics into one figure of merit.

Note that the designer is faced with all of the same data (e.g., mass, reliability, and cost), he would otherwise use to form a basis for a design selection; however, now a quantitative technique is available to aid in judging the importance of the different characteristics of the candidate systems.

Mission data and reference total program cost are as follows: Assume that the program is a $100,000,000 weather satellite; mission worth and probability of success are presented in Figs. 2 and 3; relative worth of increased scientific payload mass (150 lbm is the baseline mass allocated to the scientific payload) is expressed in Fig. 4. Figure 5 is based on a system redundancy study.

With these data, computation can begin. The calculations will follow these steps:

(1) Calculate baseline cost effectiveness.

(2) Calculate mass influence coefficients.
   (a) Influence coefficient determined by addition or subtraction of spacecraft redundancy mass.
   (b) Influence coefficient determined by addition or subtraction of spacecraft payload mass.

(3) Calculate reliability influence coefficient.

(4) Calculate cost influence coefficient.

(5) Determine the incremental (delta) values of mass, cost, and reliability between the individual subsystems and the baseline subsystem.

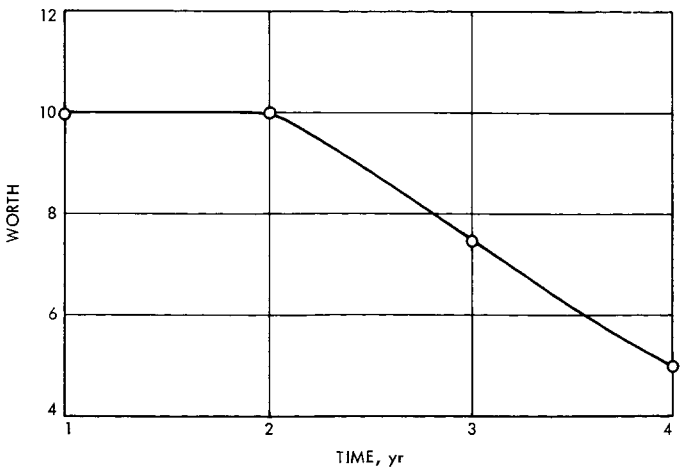

Fig. 2. Worth of data returned from satellite

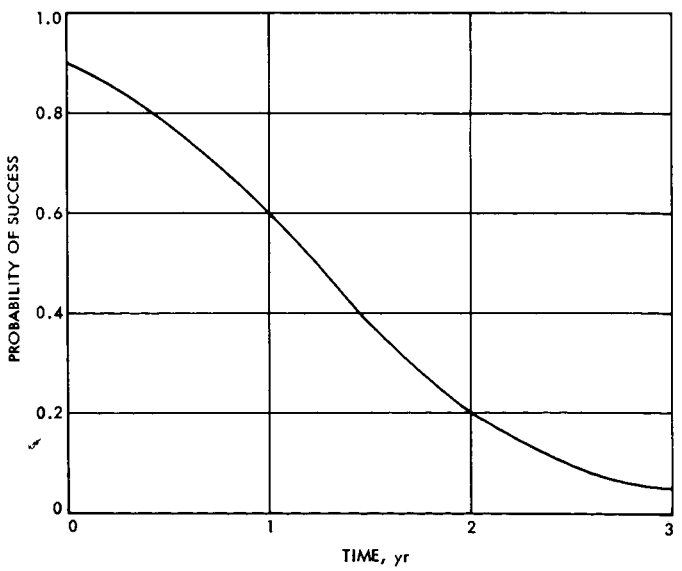

Fig. 3. Mission probability of success

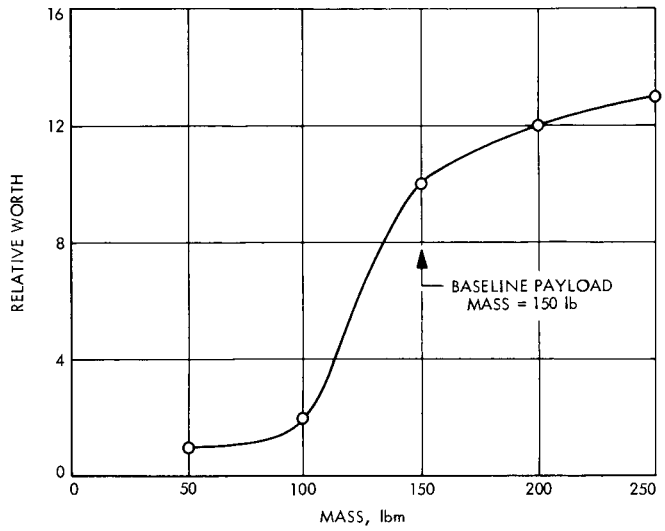

Fig. 4. Relative worth of scientific payload vs mass

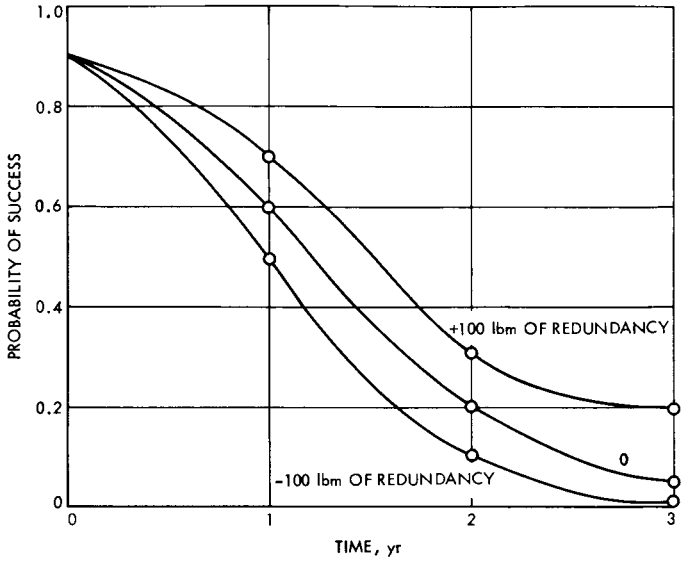

Fig. 5. Effect of redundancy on mission probability of success

(6) Select the proper mass influence coefficient for spacecraft mass addition and for spacecraft mass subtraction.

(7) Insert influence coefficients into Eq. (5) and compare subsystems.

(8) Plot the results.

(9) Perform sensitivity analysis (optional).

An influence coefficient calculation summary is presented in Table 2. From Eq. (1) the baseline cost effectiveness can be computed:

$$CE_{\text{baseline}} = \frac{\sum_i P_i W_i}{\sum_i C_i}$$

$$= \frac{10.0\,(0.60) + 7.5\,(0.20) + 5.0\,(0.05)}{100} \frac{\text{units}}{\$\,\text{million}}$$

$$= 0.0775 \frac{\text{units}}{\$\,\text{million}} \qquad (1)$$

where

W_i = baseline worth from Fig. 2,

P_i = baseline mission probability of success with zero lbm of redundance from Fig. 3,

and

$\sum_i C_i$ = total mission cost of \$100 million

If the inert gas 6-thrust-chamber system is assumed as the baseline thruster system, then baseline attitude propulsion mass, reliability, and cost are 150 lbm, 0.900, and \$120,000, respectively. The baseline thruster reliability is included in the baseline mission probability of success. The \$120,000 is included in the baseline of \$100,000,000 system cost.

The effect of 100 lbm of additional spacecraft redundancy is presented in Fig. 5. With the aid of Eq. (1) utilizing the modified probability of success we get:

$$CE = \frac{\sum_i P_i W_i}{\sum_i C_i}$$

$$= \frac{10.0\,(0.70) + 7.5\,(0.30) + 5.0\,(0.20)}{100} \frac{\text{units}}{\$\,\text{million}}$$

$$= 0.0925 \frac{\text{units}}{\$\,\text{million}} \qquad (1)$$

where

W_i = baseline worth from Fig. 2,

P_i = mission probability of success with 100 lbm of redundancy from Fig. 5,

and

$\sum_i C_i$ = total mission cost of \$100 million

When the baseline and modified cost effectiveness are introduced into Eq. (5), the following influence coefficient for redundancy mass allocation can be determined:

$$CE = CE_{\text{baseline}} + \left.\frac{\Delta CE}{\Delta \text{mass}}\right| \Delta\text{mass} + \left.\frac{\Delta CE}{\Delta \text{cost}}\right| \Delta\text{cost} + \left.\frac{\Delta CE}{\Delta \text{reliability}}\right| \Delta\text{reliability}$$

$$0.0925 \frac{\text{units}}{\$\,\text{million}} = 0.0775 \frac{\text{units}}{\$\,\text{million}} + \left.\frac{\Delta CE}{\Delta \text{mass}}\right| (100\,\text{lbm}) + \left.\frac{\Delta CE}{\Delta \text{cost}}\right| (0) + \left.\frac{\Delta CE}{\Delta \text{reliability}}\right| (0)$$

$$\left.\frac{\Delta CE}{\Delta \text{mass}}\right| = \frac{(0.0925 - 0.0775)\left(\frac{\text{units}}{\$\,\text{million}}\right)}{100\,\text{lbm}} = 1.5 \times 10^{-4} \frac{\left(\frac{\text{units}}{\$\,\text{million}}\right)}{\text{lbm}} \tag{5}$$

A similar calculation for reduction of redundancy mass is included in the calculation summary table. The effect of additional mass allocated to spacecraft payload on mission cost effectiveness can also be determined. The mission worth curve (Fig. 2) is modified for each addition or subtraction of spacecraft payload mass. The reference relative worth is 10 units at 150 lbm of payload. To compute the effect that changes in payload mass have on mission worth, the ratio of the new relative worth to the baseline quantity is used as a multiplier of the mission worth curve. As an example, the new mission worth that results if 50 lbm is added to the payload would be computed by the following equation:

$$W_i\,(\text{baseline mass} + 50\,\text{lbm}) = \frac{RWSP\,(\text{baseline mass} + 50\,\text{lbm})}{RWSP\,(\text{baseline mass})} W_i$$

where

W_i = baseline worth from Fig. 2,

$RWSP\,(X)$ = relative worth from Fig. 4 of a payload mass at X lbm,

and baseline mass refers to the baseline scientific payload mass, which is 150 lbm in Fig. 4.

The cost effectiveness of a spacecraft with 50 lbm added to payload would be:

$$CE = \frac{\sum_i P_i W_i\,(\text{baseline mass} + 50\,\text{lbm})}{\sum_i C_i}$$

$$= \frac{\left(\frac{12}{10}\right)(10.0)\,(0.60) + \left(\frac{12}{10}\right)(7.5)\,(0.20) + \left(\frac{12}{10}\right)(5.0)\,(0.05)}{100} \frac{\text{units}}{\$\,\text{million}}$$

$$= \frac{12}{10}\left[\frac{(10.0)\,(0.60) + (7.5)\,(0.20) + (5.0)\,(0.07)}{100}\right] \frac{\text{units}}{\$\,\text{million}}$$

$$= \frac{12}{10} CE_{\text{baseline}} = 0.093 \frac{\text{units}}{\$\,\text{million}} \tag{1}$$

Use of Eq. (5) again gives

$$\left.\frac{\Delta CE}{\Delta \text{mass}}\right| = \frac{(0.0930 - 0.0775) \frac{\text{units}}{\$\,\text{million}}}{50\,\text{lbm}} = 5.1 \times 10^{-4} \frac{\left(\frac{\text{units}}{\$\,\text{million}}\right)}{\text{lbm}}$$

Reduction in payload mass is treated similarly. Calculations are included in Table 3.

The effect of an increase or decrease in subsystem reliability is easy to compute. In this example, the baseline reliability is 0.900. With the aid of Eq. (6), the effect of a 0.01 increase in subsystem reliability would be

$$P_{MS_i} = \frac{R_{NS}}{R_{BL}} P_i$$

$$= \frac{0.910}{0.900} P_i = 1.01 P_i \tag{6}$$

From Eq. (1):

$$CE = \frac{\sum_i P_i W_i}{\sum_i C_i} \tag{1}$$

when evaluating effect of increased subsystem reliability, P_i is replaced by P_{MS_i}

$$CE = \frac{\sum_i P_{MS_i} W_i}{\sum_i C_i}$$

$$CE = \frac{(10.0)(0.60)\frac{0.910}{(0.900)} + (7.5)(0.20)\frac{0.910}{(0.900)} + (5.0)(0.05)\frac{0.910}{(0.900)}}{100} \frac{\text{units}}{\$\,\text{million}}$$

$$CE = 0.0784 \frac{\text{units}}{\$\,\text{million}} \tag{7}$$

Table 3. Influence coefficient calculations

$$CE_{\text{baseline}} = \frac{\sum_i P_i W_i}{\sum_i C_i}$$

where

P_i = probability of success (Fig. 3)
W_i = mission worth (Fig. 2)
$\sum_i C_i$ = total mission cost of \$100 million

$$CE_{\text{baseline}} = \frac{10\,(0.60) + 7.5\,(0.2) + 5.0\,(0.05)}{\$100} = 0.0775 \frac{\text{units}}{\$\text{ million}}$$

Addition and subtraction of mass to system redundancy:

+100 lbm:

$$CE = \frac{10\,(0.70) + 7.5\,(0.3) + 5.0\,(0.20)}{\$100} = 0.0925 \frac{\text{units}}{\$\text{ million}}$$

Table 3 (contd)

0 to +100 added:

$$\frac{\Delta CE}{\Delta \text{mass}} = \frac{0.0925 - 0.0775}{100} = \frac{0.015}{100} = 1.5 \times 10^{-4} \frac{\left(\frac{\text{units}}{\$\text{ million}}\right)}{\text{lbm}}$$

−100 lbm:

$$CE = \frac{10\,(0.50) + 7.5\,(0.1) + 5.0\,(0.01)}{100} = 0.0580\ \frac{\text{units}}{\$\text{ million}}$$

0 to −100 lbm:

$$\frac{\Delta CE}{\Delta \text{mass}} = \frac{0.0580 - 0.0775}{-100} = \frac{0.0195}{100} = 1.95 \times 10^{-4} \frac{\left(\frac{\text{units}}{\$\text{ million}}\right)}{\text{lbm}}$$

Addition and subtraction of mass to scientific payload:

0 to +50 lbm:

Relative worth 12 instead of 10

$$CE = \frac{12}{10}\, CE_{\text{baseline}} = 0.0930\ \frac{\text{units}}{\$\text{ million}}$$

0 to +50 lbm:

$$\frac{\Delta CE}{\Delta \text{mass}} = \frac{0.0930 - 0.0775}{50} = 5.1 \times 10^{-4} \frac{\left(\frac{\text{units}}{\$\text{ million}}\right)}{\text{lbm}}$$

0 to −50 lbm:

$$CE = \frac{2}{10}\,(CE_{\text{baseline}}) = 0.0155\ \frac{\text{units}}{\$\text{ million}}$$

0 to −50 lbm:

$$\frac{\Delta CE}{\Delta \text{mass}} = \frac{0.0155 - 0.0775}{-50} = 1.24 \times 10^{-3} \frac{\left(\frac{\text{units}}{\$\text{ million}}\right)}{\text{lbm}}$$

Change in reliability of 0.01:

$$CE = \frac{\left(\frac{0.910}{0.900}\right)(10.0)\,(0.60) + \left(\frac{0.910}{0.900}\right)(7.5)\,(0.20) + \left(\frac{0.910}{0.900}\right)(5.0)\,(0.05)}{\$100}\ \frac{\text{units}}{\$\text{ million}} = 0.0784\ \frac{\text{units}}{\$\text{ million}}$$

$$\frac{\Delta CE}{\Delta \text{reliability}} = \frac{0.0784 - 0.0775}{0.01}\ \frac{\left(\frac{\text{units}}{\$\text{ million}}\right)}{\text{increase in reliability}} = 8.61 \times 10^{-2}\ \frac{\left(\frac{\text{units}}{\$\text{ million}}\right)}{\text{increase in reliability}}$$

Addition of $1,000,000 to cost:

$$CE = \frac{10\,(0.60) + 7.5\,(0.2) + 5.0\,(0.05)}{\$100 + \$1} = 0.0767\ \frac{\text{units}}{\$\text{ million}}$$

$$\frac{\Delta CE}{\Delta \text{cost}} = 0.0767 - 0.0775 = -7.67 \times 10^{-4} \frac{\left(\frac{\text{units}}{\$\text{ million}}\right)}{\$\text{ million}}$$

where

$P_{MS_i} = \left(\frac{R_{NS}}{R_{BL}}\right) P_i$, and P_i is taken from Fig. 3,

W_i = baseline worth from Fig. 2,

$\sum_i C_i$ = total mission cost of \$100 million,

R_{BL} = reliability of the baseline system (0.90),

and

R_{NS} = increased reliability (0.900 + 0.01 = 0.91)

Use of Eq. (5) again gives

$$\left|\frac{\Delta CE}{\Delta \text{reliability}}\right| = \frac{0.0784 - 0.0775}{0.01} \frac{\left(\frac{\text{units}}{\$\text{ million}}\right)}{\text{increase in reliability}}$$

$$= 8.61 \times 10^{-2} \frac{\left(\frac{\text{units}}{\$\text{ million}}\right)}{\text{increase in reliability}}$$

The influence of subsystem cost on mission cost effectiveness can be demonstrated by increasing program cost by \$1 million:

$$CE = \frac{\sum_i W_i P_i}{\sum_i C_i + 1.0}$$

$$CE = \frac{(10.0)(0.60) + (7.5)(0.20) + (5.0)(0.05)}{100 + 1} \frac{\text{units}}{\$\text{ million}}$$

$$CE = 0.0767 \frac{\text{units}}{\$\text{ million}}$$

Use of Eq. (5) again gives

$$\left|\frac{\Delta CE}{\Delta \text{cost}}\right| = \frac{0.0767 - 0.0775}{1} \frac{\left(\frac{\text{units}}{\$\text{ million}}\right)}{\$\text{ million}}$$

$$= -7.67 \times 10^{-4} \frac{\left(\frac{\text{units}}{\$\text{ million}}\right)}{\$\text{ million}}$$

The inert gas 6-thrust-chamber system, as was mentioned before, is the baseline attitude propulsion system. To compute the relative cost-effectiveness of each of the other competitive systems, Eq. (5) is used with the proper influence coefficients inserted (e.g., $\Delta CE/\Delta$mass; $\Delta CE/\Delta$cost).

The differences in mass, cost, and reliability of each of the comparative systems from that of the baseline system can now be computed. For example, the single inert gas system with the 12-thrust-chamber arrangement would compare with the baseline system in the following manner:

$$\Delta\text{mass} = \text{mass}_{\text{baseline}} - \text{mass}_{\text{comparative system (12 T/C)}}$$

$$= 150 \text{ lbm} - 160 \text{ lbm} = -10.0 \text{ lbm}$$

$$\Delta\text{cost} = \text{cost}_{\text{comparative system (12 T/C)}} - \text{cost}_{\text{baseline}}$$

$$= 0.140 \$ \text{ million} - 0.120 \$ \text{ million}$$

$$= +0.02 \$ \text{ million}$$

$$\Delta\text{reliability} = \text{reliability}_{\text{comparative (12 T/C)}} - \text{reliability}_{\text{baseline}}$$

$$= 0.910 - 0.900 = +0.010$$

where increases in subsystem mass and cost will decrease cost effectiveness, and increases in reliability will increase cost effectiveness. Influence coefficients should not be used when deltas greatly exceed those that were used for influence coefficient computation.

The proper influence coefficients must be specified. Since there are only one cost and one reliability influence coefficient in this example, these two selections are obvious. However, selection of the proper mass influence coefficient requires a little more investigation. When the incremental mass value (Δmass) is negative (i.e., the comparative subsystem has more mass than the baseline subsystem), then the influence coefficient which results in the minimum decrease of mission cost effectiveness should be selected. The mass influence coefficient for subtraction of mass from the payload would result in a decrease in cost effectiveness of

$$\Delta CE = \left|\frac{\Delta CE}{\Delta \text{mass}}\right| \Delta\text{mass}$$

$$= \left[1.24 \times 10^{-3} \left(\frac{\text{units}}{\$\text{ million}}\right)\right] [-10 \text{ lbm}]$$

$$= -0.0124 \frac{\text{units}}{\$\text{ million}}$$

The mass influence coefficient for redundancy mass reduction would result in a decrease in cost-effectiveness of

$$\Delta CE = \frac{\Delta CE}{\Delta \text{mass}} \Delta \text{mass}$$

$$= \left[1.95 \times 10^{-4} \frac{\left(\frac{\text{units}}{\$\,\text{million}}\right)}{\text{lbm}} \right] [-10\,\text{lbm}]$$

$$= -0.00195 \frac{\text{units}}{\$\,\text{million}}$$

The two decreases in cost effectiveness should be nearly equal if the hypothetical system were designed from a cost effectiveness basis; however, this is not always accomplished in practice. The result is that for this particular system, the least loss in utility with an increase in auxiliary propulsion subsystem mass will result from a reduction in system redundancy mass. Therefore, for this example mission all comparative subsystems with a mass that is increased over that of the baseline subsystem (i.e., increases in auxiliary propulsion mass above baseline) should be compared using the mass influence coefficient calculated for redundancy mass reduction. A similar analysis will show that all auxiliary propulsion subsystems with a lower mass than the baseline subsystem should be compared using the mass influence coefficient calculated for scientific payload mass increase, because this will result in the greatest increase in cost effectiveness. Equation (5) can now be used to compare the baseline 6-thrust-chamber inert gas subsystem with the 12-thrust-chamber inert gas subsystem:

$$CE\,(12\,\text{T/C}) = CE_{\text{baseline}} + \left.\frac{\Delta CE}{\Delta \text{mass}}\right| \Delta \text{mass} + \left.\frac{\Delta CE}{\Delta \text{cost}}\right| \Delta \text{cost} + \left.\frac{\Delta CE}{\Delta \text{reliability}}\right| \Delta \text{reliability}$$

$$CE\,(12\,\text{T/C}) = 0.0775 \frac{\text{units}}{\$\,\text{million}}$$

$$+ \left[1.95 \times 10^{-4} \frac{\left(\frac{\text{units}}{\$\,\text{million}}\right)}{16\,\text{lbm}} \right] [-10\,\text{lbm}]$$

$$+ \left[-7.67 \times 10^{-4} \frac{\left(\frac{\text{units}}{\$\,\text{million}}\right)}{\$\,\text{million}} \right] [+0.02\,\$\,\text{million}]$$

$$+ \left[8.61 \times 10^{-2} \frac{\left(\frac{\text{units}}{\$\,\text{million}}\right)}{\text{increase in reliability}} \right] [0.01]$$

$$= 0.0764 \frac{\text{units}}{\$\,\text{million}} \qquad (5)$$

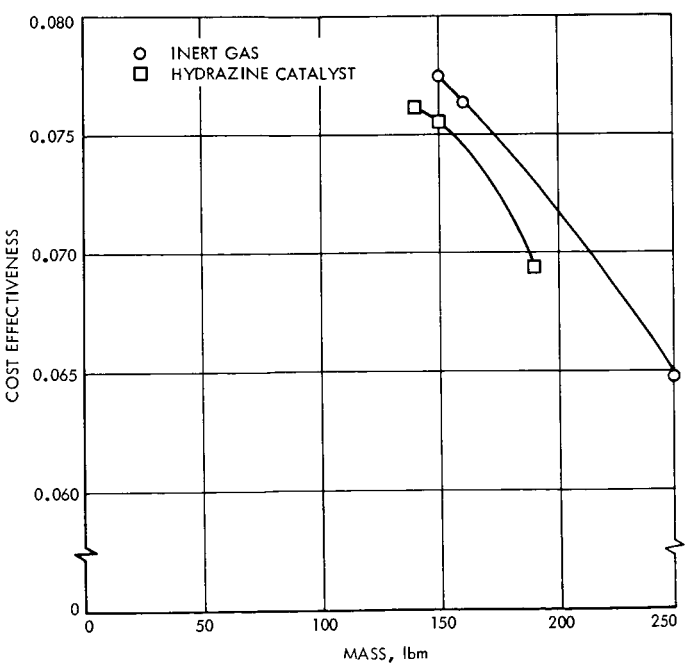

Fig. 6. Cost effectiveness vs mass

The remaining system cost effectiveness values were calculated, and are presented in the last column of Table 2 and in Fig. 6. The recommended system, based on factors presented herein, has the maximum value of cost-effectiveness. This is the 6-thrust-chamber single inert gas system.

C. Sensitivity Analysis

In order to establish confidence in the results of a cost-effectiveness study, the sensitivity of these results to the original input data and assumptions must be calculated. In many instances the outcome of a cost-effectiveness analysis is indeed quite sensitive to the assumptions made. In this analysis, the assumptions that were made initially are modified, different values of the variables are assumed, and then the impact of the variations on the final evaluation is determined. If the results of the analysis are very sensitive to certain assumptions, either justification for the

use of the assumed values must be presented or the sensitivity of conclusions to the assumed values should be indicated.

III. Subsynchronous Satellite Mission

Typical subsynchronous satellites are the Nimbus and the Orbiting Geophysical Observatory (OGO). Extensions of these programs have been proposed. Earth Resources Technology Satellite A (ERTS A), an earth resources satellite design based on existing satellite designs, is presently being studied under separate contracts at General Electric and TRW Systems. This 30 million dollar satellite is intended to survey the earth's surface for resources. The baseline system will be designed for a one-year life, permitting repetitive coverage and seasonal observations. The spacecraft mass will be about 1300 lbm and will be placed in a circular, sun-synchronous (subsynchronous) orbit of about 500 nautical miles altitude. It will view the entire earth in 100-mile-wide increments in less than 3 weeks.

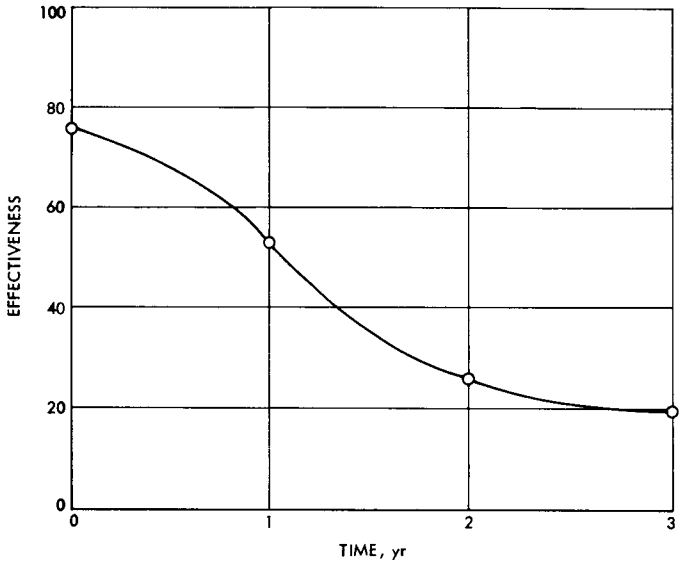

Fig. 7. Average mission effectiveness on OGO I, II, and III

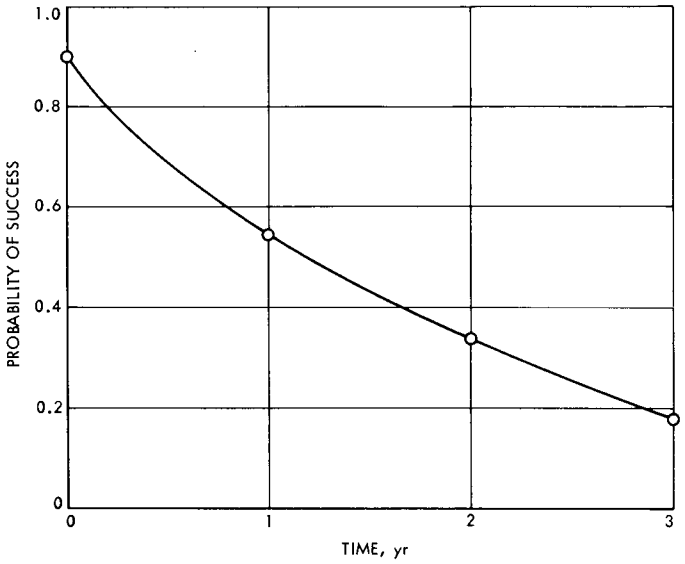

Fig. 9. Predicted mission probability of success for ERTS A

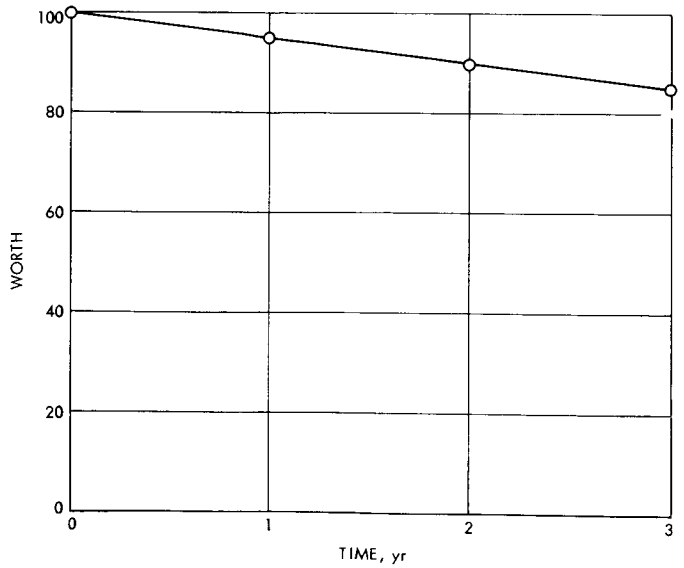

Fig. 8. Predicted mission worth for ERTS A

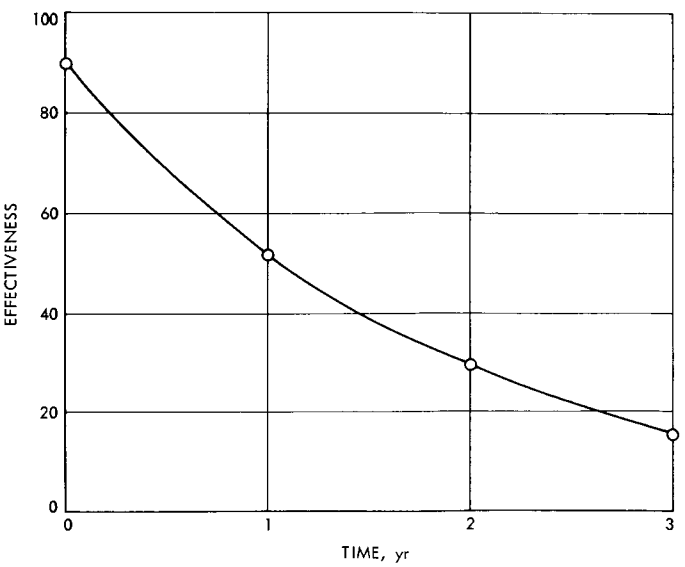

Fig. 10. Predicted effectiveness for ERTS A

The ERTS spacecraft configuration will be similar to either Nimbus or OGO, therefore for the purpose of these calculations these missions are assumed equivalent.

Assignment of mission worth and probability of success is based upon previous estimates of OGO and Nimbus effectiveness (Refs. 1 and 8). Effectiveness in this sense is defined as the product of the mission "worth" and probability of success. In an early study of the OGO, predicted values of spacecraft effectiveness were compared with the actual spacecraft effectiveness of OGO I, II, and III, resulting in a rather poor correlation. The poor correlation is mainly due to the omission of some system characteristics in the analysis model. If an average of the actual OGO spacecraft effectiveness is used, then Fig. 7 results. For this specific mission the degradation of scientific instruments with time causes a slight decrease in mission worth; however, worth is nearly constant with time (see Fig. 8). The mission probability of success was modified from an early estimate of a mean time between failure of three years to a mean time between failure of two years. Figures 8–10 present predicted worth, probability of success, and effectiveness. The actual and predicted effectiveness are nearly identical, as can be demonstrated by a comparison of Figs. 7 and 10.

The effect of additional mass allocated to the auxiliary-propulsion system will not have a large impact on launch accuracy, since spacecraft mass is below the capability of the launch vehicle. The effect of subsystem mass on overall spacecraft cost effectiveness was studied in Ref. 1. Figure 11 is extracted from this report. From this curve and existing launch vehicle information, a representative mass influence coefficient can be derived. With the aid of Figs. 8, 9, and 11 along with the cost-effectiveness techniques outlined in Section II, mass, reliability, and cost influence coefficients can be calculated (see Table 4).

Table 4. Influence coefficient calculations for ERTS A

$$CE_{baseline} = \frac{\sum_i P_i W_i}{\sum_i C_i}$$

where

P_i = probability of success (Fig. 9)

W_i = mission worth (Fig. 8)

$\sum_i C_i$ = total mission cost of \$30 million

$$CE_{baseline} = \frac{95\,(0.546) + 90\,(0.331) + 85\,(0.18)}{\$30} = 6.33\ \frac{\text{units}}{\$\ \text{million}}$$

Addition or subtraction of mass:

$$\frac{\Delta CE}{\Delta \text{mass}} = 5.73 \times 10^{-4}\ \frac{\left(\frac{\text{units}}{\$\ \text{million}}\right)}{\text{lbm}}$$

(See Fig. 11, extracted from Ref. 1)

Change in reliability of 0.01:

$$CE = \frac{\left(\frac{0.9975}{0.9875}\right)(95)(0.546) + \left(\frac{0.9975}{0.9875}\right)(90)(0.331) + \left(\frac{0.9975}{0.9875}\right)(85)(0.18)}{\$30}\ \frac{\text{units}}{\$\ \text{million}} = 6.39\ \frac{\text{units}}{\$\ \text{million}}$$

$$\frac{\Delta CE}{\Delta \text{reliability}} = \frac{6.39 - 6.33}{0.01}\ \frac{\left(\frac{\text{units}}{\$\ \text{million}}\right)}{\text{increase in reliability}} = 6.41\ \frac{\left(\frac{\text{units}}{\$\ \text{million}}\right)}{\text{increase in reliability}}$$

Addition of \$1,000,000 to cost:

$$CE = \frac{95\,(0.546) + 90\,(0.331) + 85\,(0.18)}{\$30 + \$1} = 6.13\ \frac{\text{units}}{\$\ \text{million}}$$

$$\frac{\Delta CE}{\Delta \text{cost}} = 6.13 - 6.33 = -2.04 \times 10^{-1}\ \frac{\left(\frac{\text{units}}{\$\ \text{million}}\right)}{\$\ \text{million}}$$

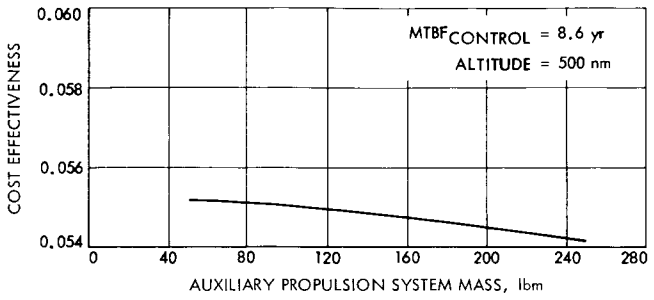

Fig. 11. Effect of auxiliary propulsion mass on Nimbus-type mission cost effectiveness

The next step in the tradeoff of candidate thruster systems is the definition of mission requirements. The auxiliary-propulsion subsystem must serve two functions: (1) low-level attitude control (momentum wheel unloading, tipoff rate reduction, and reference acquisition) and (2) high level orbital corrections (ΔV). The ERTS spacecraft is three-axis-stabilized and requires 6 low-level thrusters (10 to 200 mlbf thrust).[3] These thrusters will perform initial tipoff rate reduction, reference acquisition, and the necessary momentum wheel unloading. A total impulse of 455 lbf-s is required for these 6 thrusters. The high-level ΔV thrusters (0.1 to 5 lbf) must correct the initial injection orbit to a sun-synchronous orbit (orbit with precessing period of 1 yr). Initial requirements for ΔV were nearly 150 ft/s including satellite orbital velocity and inclination. With improvements in the *Thor-Delta* launch vehicle injection accuracy, this requirement is now estimated at 50 ft/s, with no anticipated inclination error. This results in the requirement for two ΔV thrusters with a combined 2100 lbf-s total impulse. The only low-level thruster system not considered for comparison is the subliming solid system for which the impulse bit requirements are too stringent.

The following combination of systems were considered:

(1) Inert gas low level thrusters (LLT) (6T)[4] with
Inert gas high level thrusters (HLT) (2T)[5]
Resistojet, NH_3 HLT (2T)
Subliming solids HLT (2T)
Inert gas resistojet HLT (2T)[5]
Hydrazine catalyst HLT (2T)

(2) Tridyne LLT (6T) with
Tridyne HLT (2T)[5]
Hydrazine catalyst HLT (2T)
Resistojet, NH_3 HLT (2T)
Subliming solid HLT (2T)

(3) Inert Tridyne LLT (6T) with
Tridyne HLT (2T)[5]

(4) Hydrazine catalyst LLT (6T) with
Hydrazine catalyst HLT (2T)[5]

(5) Hydrazine resistojet LLT (6T) with
Hydrazine resistojet HLT (2T)[5]

(6) Hydrazine plenum LLT (6T) with
Hydrazine plenum HLT (2T)[5]
Hydrazine catalyst HLT (2T)[5]

(7) Vaporizing liquid, NH_3 LLT (6T) with
Vaporizing liquid, cold HLT (2T)[5]
Resistojet, NH_3 HLT (2T)[5]
Subliming solid HLT (2T)
Hydrazine catalyst HLT (2T)

(8) Resistojet, NH_3 LLT (6T) with
Resistojet, NH_3 HLT (2T)[5]

(9) Radioisojet, NH_3 LLT (6T) with
Radioisojet, NH_3 HLT (2T)[5]

(10) Electrolysis LLT (cold mode) (6T) with
Electrolysis HLT (hot mode)[5] (2T)

Based on mission requirements, and with the aid Appendixes B, C, and D, mass, reliability, and cost wer calculated. Development cost was spread over four mi sions. Tabulation of these values is presented in Table 5 The inert gas low level/inert gas high level system in th quad valve, single system, configuration is assigned as th baseline for which cost effectiveness of 6.33 units/$ mil lion is calculated. System cost effectiveness is plotted as a function of auxiliary-propulsion system mass in Fig. 12 with the peak portions of the system curves presented in Fig. 13.

The combination with the highest value of cost effectiveness is the hydrazine plenum/hydrazine catalyst system. The value of this system could be even higher if the passive (plenum-pressure) feed system were utilized. The next most favorable group of systems consists of combinations of thrusters with common feed systems, and systems with eight similar thrusters. Included in this group are:

(1) Inert Tridyne (6T) + Tridyne (2T).

[3]In this report the following abbreviations are used: mlbf, millipounds of force; mlbm, millipounds of mass.

[4]Refers to number of required thrusters.

[5]High-level thrusters using same propellant feed system as the low-level thrusters.

Table 5. Auxiliary-propulsion system data for ERTS A[a]

Parameters		Single systems				Double systems		
		Single	Dual series	Quad	16 T/C dual series	Single	Dual series	Quad
Inert gas, N_2 (8T)[b]	Mass	144	146	149[c]	152	428	432	438
	Reliability	0.9392	0.9621	0.9875[c]	0.9883	0.996	0.999	0.9998
	Cost	0.250	0.275	0.325[c]	0.335	0.475	0.525	0.625
	CE	6.038	6.179	6.330[c]	6.331	6.192	6.198	6.179
Hydrazine direct catalyst (8T)	Mass	23	25	28	32	61	64	70
	Reliability	0.9268	0.9494	0.9745	0.9948	0.995	0.997	0.9993
	Cost	0.480	0.505	0.555	0.675	0.910	0.960	1.060
	CE	5.979	6.118	6.263	6.372	6.309	6.309	6.300
Hydrazine direct thermal (8T)	Mass	23	25	27	31	59	62	69
	Reliability	0.9268	0.9494	0.9745	0.9948	0.995	0.997	0.9993
	Cost	0.680	0.705	0.755	0.875	1.310	1.360	1.460
	CE	5.941	6.079	6.229	6.332	6.228	6.228	6.218
Hydrazine plenum (8T)	Mass	33	34.5	38	40	90	94	100
	Reliability	0.9343	0.9571	0.9823	0.9831	0.996	0.998	0.9997
	Cost	0.350	0.375	0.425	0.435	0.675	0.725	0.825
	CE	6.047	6.189	6.350	6.342	6.347	6.347	6.333
Vaporizing liquid (8T)	Mass	35	36	40	42	96	100	106
	Reliability	0.9369	0.9598	0.9851	0.9859	0.996	0.998	0.9998
	Cost	0.350	0.375	0.425	0.435	0.675	0.725	0.825
	CE	6.079	6.205	6.357	6.359	6.343	6.343	6.331
Resistojet, NH_3 (8T)	Mass	40	42	45	73.5	92	96	102
	Reliability	0.9309	0.9537	0.9788	0.9860	0.995	0.998	0.9996
	Cost	0.480	0.505	0.555	0.675	0.910	0.960	1.060
	CE	5.996	6.137	6.287	6.292	6.291	6.297	6.283
Radioisojet, NH_3 (8T)	Mass	39	40.6	43.8	68	89	92	98
	Reliability	0.9353	0.9581	0.9834	0.9859	0.996	0.998	0.9997
	Cost	1.55	1.57	1.61	1.70	2.45	2.49	2.57
	CE	5.818	5.955	6.103	6.086	5.982	5.984	5.974
Tridyne (8T)	Mass	79	81	84	87	135	138	142
	Reliability	0.9332	0.9560	0.9812	0.9884	0.996	0.998	0.9996
	Cost	0.480	0.505	0.555	0.675	0.910	0.960	1.060
	CE	5.990	6.130	6.280	6.300	6.272	6.273	6.260
Electrolysis (8T)	Mass	68	69	74	78			
	Reliability	0.8886	0.9181	0.9483	0.9168			
	Cost	1.2	1.23	1.28	1.48			
	CE	5.577	5.756	5.933	5.696			
Inert Tridyne (6T) Tridyne (2T)	Mass	41	45	49	50			
	Reliability	0.9376	0.9605	0.9859	0.9894			
	Cost	0.250	0.280	0.330	0.365			
	CE	6.05	6.19	6.34	6.36			

[a]Mass, lbm; cost, $ million; *CE*, units/$ million.
[b]Number in parentheses indicates number of required thrusters.
[c]Baseline system configuration.

Table 5 (contd)

Parameters		Single systems				Double systems		
		Single	Dual series	Quad	16 T/C dual series	Single	Dual series	Quad
Inert gas, N_2 (6T) resistojet, N_2 (2T)	Mass	108	109	113	125			
	Reliability	0.9376	0.9605	0.9859	0.9894			
	Cost	0.250	0.280	0.330	0.365			
	CE	6.047	6.188	6.341	6.348			
Inert gas, N_2 (6T) resistojet, NH_3 (2T)	Mass	52	54	57	60			
	Reliability	0.9249	0.9474	0.9724	0.9748			
	Cost	0.575	0.600	0.650	0.690			
	CE	5.933	6.011	6.220	6.225			
Inert gas, N_2 (6T) hydrazine catalyst (2T)	Mass	44	46	49	53			
	Reliability	0.9236	0.9529	0.9780	0.9838			
	Cost	0.575	0.600	0.650	0.690			
	CE	5.929	6.111	6.297	6.287			
Inert gas, N_2 (6T) subliming solid (2T)	Mass	67	68	70	72			
	Reliability	0.9435	0.9608	0.9797	0.9803			
	Cost	0.550	0.570	0.610	0.620			
	CE	6.049	6.155	6.267	6.268			
Hydrazine plenum (6T) hydrazine catalyst (2T)	Mass	24.5	26.1	29.3	32.8			
	Reliability	0.9408	0.9638	0.9892	0.9950			
	Cost	0.355	0.380	0.430	0.465			
	CE	6.093	6.236	6.388	6.416			
Vaporizing liquid, NH_3 (6T) and hydrazine catalyst (2T)	Mass	27.2	29	32	36			
	Reliability	0.9279	0.9506	0.9756	0.9814			
	Cost	0.700	0.730	0.790	0.830			
	CE	5.942	6.080	6.226	6.253			
Vaporizing liquid, NH_3 (6T) and subliming solid (2T)	Mass	50	51	53	55			
	Reliability	0.9412	0.9585	0.9773	0.9779			
	Cost	0.700	0.725	0.755	0.785			
	CE	6.014	6.118	6.225	6.220			
Vaporizing liquid, NH_3 (6T) resistojet, NH_3 (2T)	Mass	31	33	36	39			
	Reliability	0.9354	0.9583	0.9835	0.9859			
	Cost	0.355	0.380	0.430	0.465			
	CE	6.054	6.196	6.348	6.354			
Tridyne (6T) and hydrazine catalyst (2T)	Mass	33	35	37	42			
	Reliability	0.9258	0.9484	0.9734	0.9839			
	Cost	0.830	0.860	0.920	1.070			
	CE	5.900	6.037	6.183	6.217			
Tridyne (6T) and resistojet, NH_3 (2T)	Mass	41	42	45	49			
	Reliability	0.9205	0.9429	0.9678	0.9749			
	Cost	0.830	0.860	0.920	1.070			
	CE	5.862	5.998	6.144	6.156			
Tridyne (6T) and subliming solid (2T)	Mass	55	56	59	61			
	Reliability	0.9390	0.9562	0.9750	0.9804			
	Cost	0.830	0.855	0.905	1.025			
	CE	5.972	6.076	6.184	6.193			

(2) Vaporizing, NH_3 (6T) + resistojet, NH_3 (2T).

(3) Inert gas (6T) + resistojet, inert gas (2T).

(4) Hydrazine catalyst (8T).

(5) Vaporizing, NH_3 (8T).

(6) Hydrazine plenum (8T).

(7) Hydrazine resistojet (8T).

The hydrazine resistojet low-level thrusters offer advantages over the hydrazine direct catalytic low-level thrusters. The increased cold thruster first pulse specific impulse of the resistojet thruster can lead to considerable mass savings when large quantities of propellant are required for momentum wheel unloading or other short pulse low duty cycle operation. The present resistojet hydrazine system must be penalized for its high development cost, since this system is still in early development. However, when it becomes fully developed, it can be expected to approach the hydrazine plenum/direct catalyst system combination in cost effectiveness (e.g., ERTS type of mission). The combination systems are ranked high in the comparison. Their high values of cost effectiveness is a direct result of the use of a common feed system, which reduces system cost and mass while increasing system reliability. The inert Tridyne low-level/reacting Tridyne high-level system combination was ranked high in the combination systems. The inert gas/inert gas resistojet system combination has no duty cycle restrictions, while the vaporizing ammonia/ammonia resistojet system combination is limited by heat transfer to pulse lengths less than 300 to 400 s. Both the vaporizing ammonia and hydrazine plenum 8-thruster systems suffer from pulse length limitations.

The inert gas 8-thruster system ranked next, followed by the Tridyne 8-thruster system. Since the mass influence

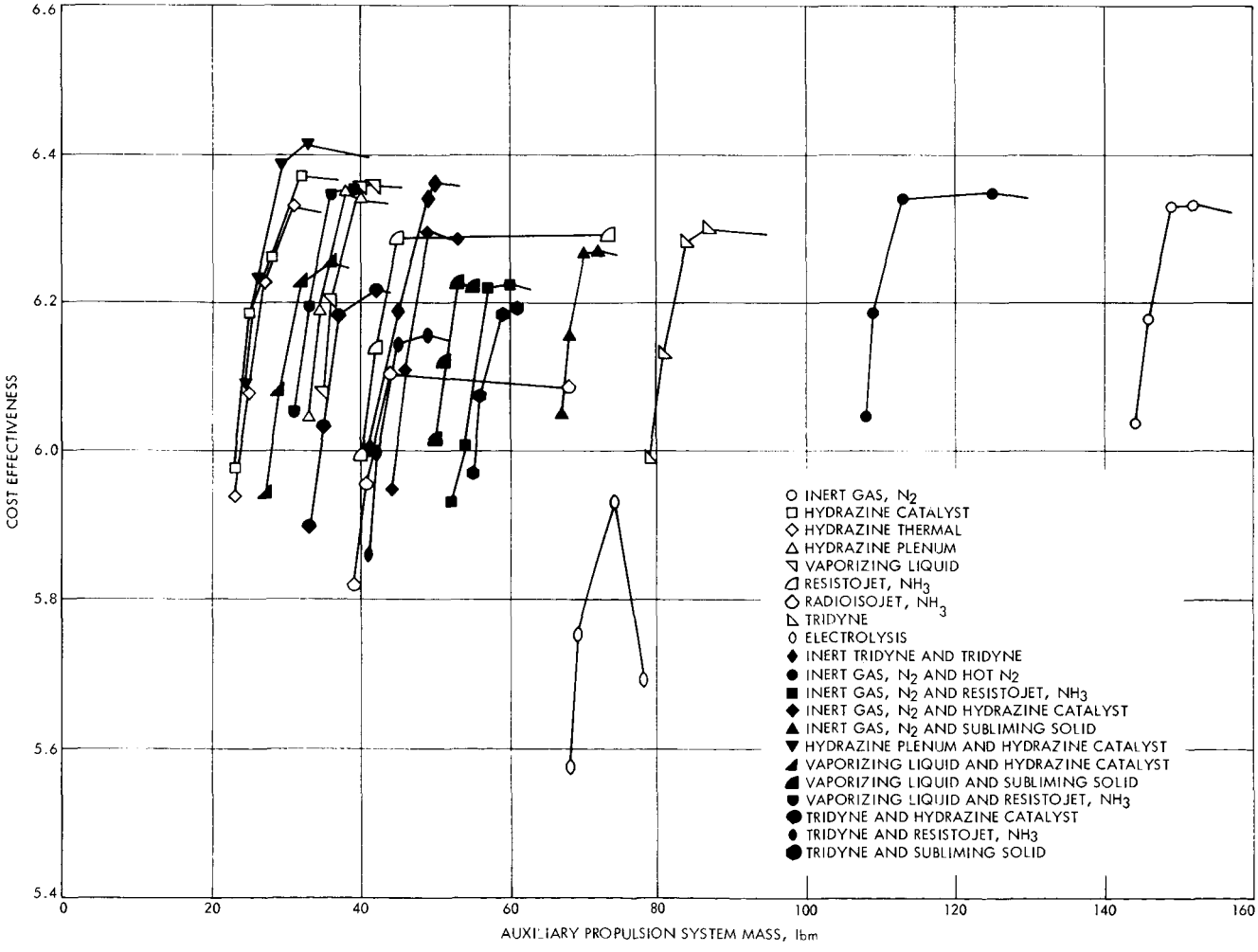

Fig. 12. Auxiliary propulsion system cost effectiveness for the ERTS mission

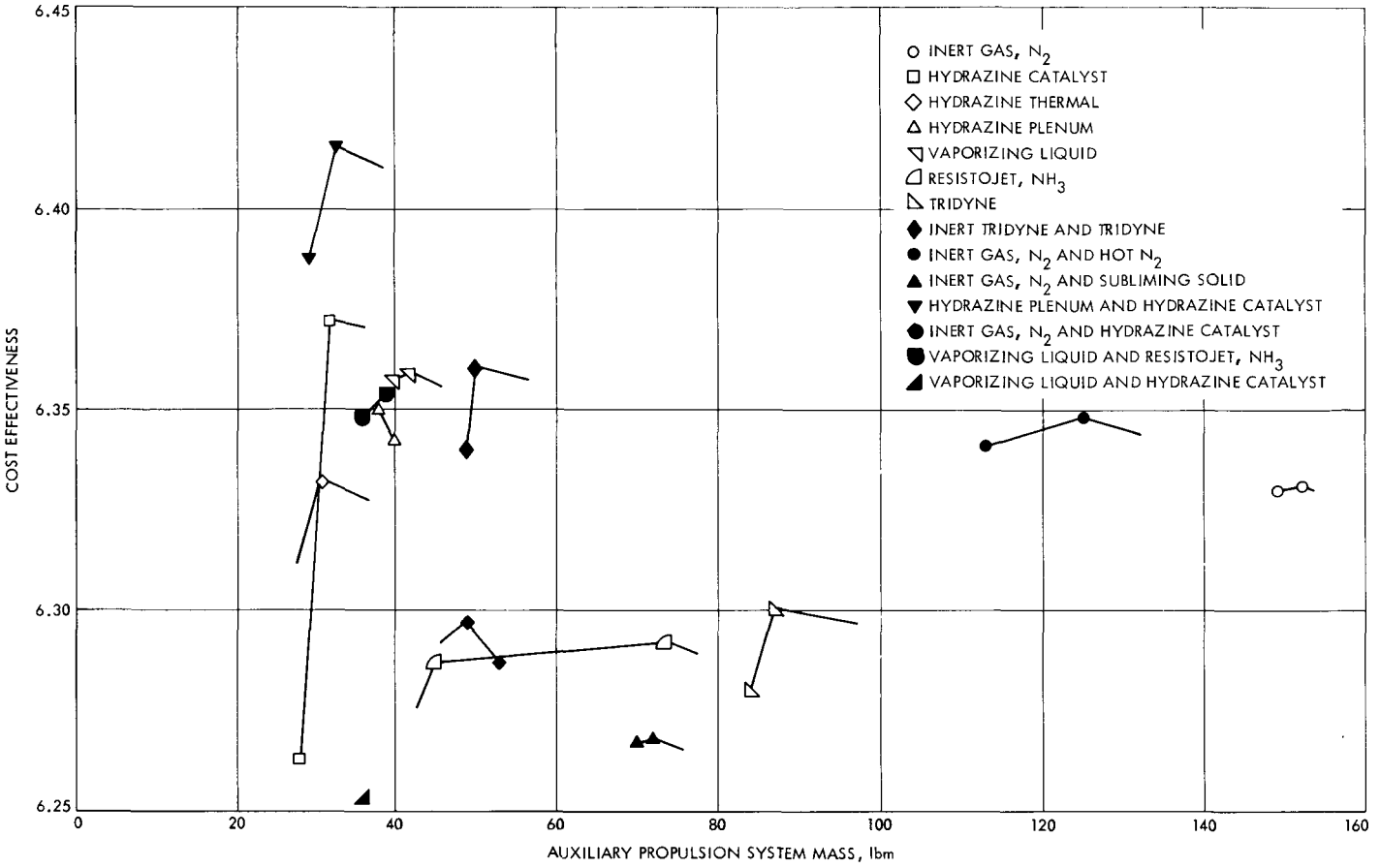

Fig. 13. Maximum auxiliary propulsion system cost effectiveness for the ERTS mission

coefficient is small for this mission, the effect or cost effectiveness of mass savings is small. Although the 8-thruster Tridyne system is lighter than the inert-gas system and the inert gas/inert gas resistojet, its increased cost and slightly decreased reliability penalize the system. With the development of the Tridyne system, its cost will approach that of the inert gas systems. As a result, the Tridyne system will become more favorable, exceeding inert gas and rivaling the inert gas/inert gas resistojet system. The ammonia resistojet 8-thruster system is next most effective.

The next highest ranking thruster systems are combinations of two independent systems. They are ranked in order of cost effectiveness as follows:

(1) Inert gas (6T) and hydrazine catalyst (2T) combination.

(2) Inert gas (6T) and subliming solid (2T) combination.

(3) Vaporizing ammonia (6T) and hydrazine catalyst (2T) combination.

(4) Vaporizing ammonia (6T) and subliming solid (2T) combination.

(5) Inert gas (6T) and resistojet, NH_3 (2T) combination.

(6) Tridyne (6T) and hydrazine catalyst (2T) combination.

(7) Tridyne (6T) and subliming solid (2T) combination.

(8) Tridyne (6T) and resistojet, NH_3 (2T) combination.

The use of two types of systems in combination is costly. The inert gas (6T) and hydrazine catalyst (2T) combination gives rise to the most cost effective system combination. If mission cost is increased, then the increased cost of combining two systems with independent feed systems has a diminishing influence on cost effectiveness.

The radioisojet and electrolysis systems are too costly for this mission, and have high initial masses. The total impulse of the auxiliary propulsion system was not great enough to result in substantial mass savings with either system.

The preferred configurations of all systems were either the quad-valve single system or the 16 T/C dual-series valve single system. This was due to the small increase in cost and mass with redundancy, balanced by greatly increased system reliability. Cost data was an important factor in the ERTS mission system tradeoffs. If more appropriate cost data becomes available, the application of this data to the system descriptions (Table 5) is suggested. With new cost data, additional system comparisons can be made.

IV. Synchronous Satellite Mission

Typical synchronous satellite missions are those of the *Intelsat* family. The *Intelsat IV*, which is presently under joint development by Hughes and Comsat, is the largest and most complex of the *Intelsat* family. The planned *Intelsat IV* satellite injection mass is 1300 lbm, with a cost between 150 and 200 million dollars. Useful satellite design lifetime has been planned for 7 yr. The spacecraft is spin-stabilized, and the position and orientation propulsion system must perform the spinup immediately after vehicle separation. Injection into a near circular orbit is performed by a solid propellant apogee motor.

Assignment of mission worth is based on the number of operating communication channels. The cost of satellite usage by customers is based on the amount of channel width used and length of time in use. Two economic factors affect the worth of satellite service. These are the demand for usage and the rate of inflation. The rates of expected demand and depreciation over a seven year period tend to balance each other resulting in a near constant worth assignment. Degradation in quality and loss of channels with time can be expected. The design goal is for 10 of 12 channels to be working after seven years (Ref. 9). A combination of the above data results in Fig. 14. One aspect of a communications satellite is that the allowed bandwidth is fixed and cannot be expanded. Thus, baseline worth of 12 channels cannot be increased by the mere addition of more communication channels.

Reliability has been a subject of great concern in the *Intelsat* program. Total utility is most strongly affected by increased mission life. In the *Intelsat IV* program, extensive studies have been conducted on the addition of redundancy to subsystems (Ref. 10). Several methods of redundancy additions were explored. The optimum method of redundancy addition is presented in Fig. 15. The probability of successful launch and orbit insertion was obtained from a combination of a reliability logic diagram, a fault tree, and judicious appointment of failure categories.

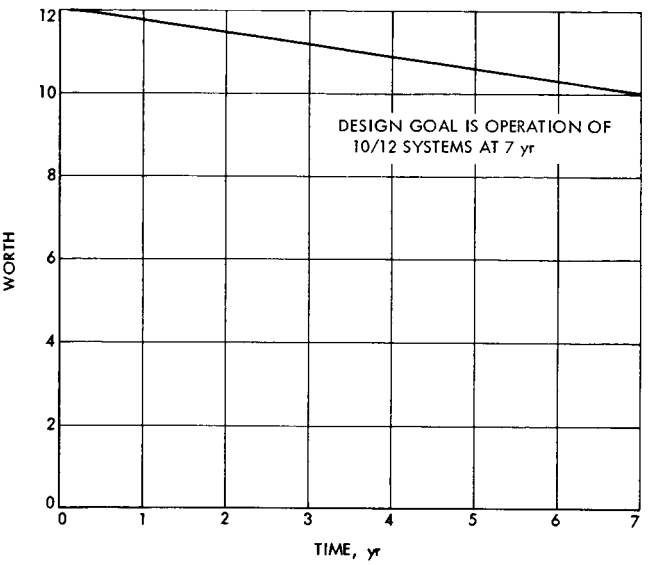

Fig. 14. Predicted worth for *Intelsat IV*

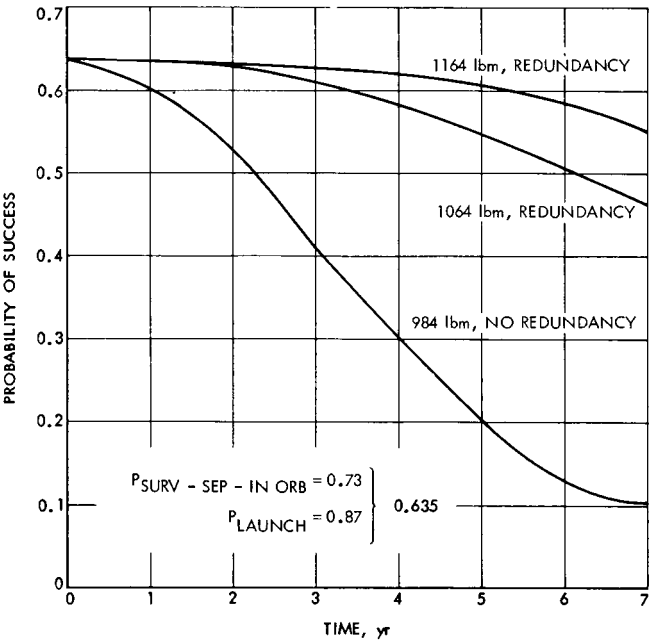

Fig. 15. Predicted probability of success with added redundancy

From these curves and the techniques outlined in Section II, mass, reliability, and cost influence coefficients can be calculated. These calculations are summarized in Table 6.

Table 6. Influence coefficient calculations for *Intelsat IV*

$$CE_{baseline} = \frac{\sum_i P_i W_i}{\sum_i C_i}$$

where

P_i = probability of success (Fig. 15)

W_i = mission worth (Fig. 14)

ΣC_i = total mission cost of $175 million

$$CB_{baseline} = \frac{(11.71)(0.635) + (11.43)(0.626) + (11.14)(0.610) + (10.86)(0.584) + (10.57)(0.546) + (10.29)(0.508) + (10.00)(0.457)}{\$175} = 0.247 \frac{\text{units}}{\$\text{ million}}$$

Addition and subtraction of mass to system redundancy:

+100 lbm:

$$CE = \frac{(11.71)(0.635) + (11.43)(0.632) + (11.14)(0.626) + (10.86)(0.619) + (10.57)(0.606) + (10.29)(0.584) + (10.00)(0.550)}{\$175} = 0.264 \frac{\text{units}}{\$\text{ million}}$$

0 to +100 lbm added

$$\frac{\Delta CE}{\Delta \text{mass}} = \frac{0.264 - 0.247}{100} = 1.7 \times 10^{-4} \frac{\left(\frac{\text{units}}{\$\text{ million}}\right)}{\text{lbm}}$$

−80 lbm:

$$CE = \frac{(11.71)(0.603) + (11.43)(0.527) + (11.14)(0.406) + (10.86)(0.305) + (10.57)(0.546) + (10.29)(0.508) + (10.00)(0.457)}{\$175} = 0.145 \frac{\text{units}}{\$\text{ million}}$$

0 to −80 lbm

$$\frac{\Delta CE}{\Delta \text{mass}} = \frac{0.145 - 0.247}{-80.0} = 1.28 \times 10^{-3} \frac{\left(\frac{\text{units}}{\$\text{ million}}\right)}{\text{lbm}}$$

Change in reliability of 0.005

$$CE = \frac{\left(\frac{0.996}{0.991}\right)(11.71)(0.635) + \left(\frac{0.996}{0.991}\right)(11.43)(0.626) + \left(\frac{0.996}{0.991}\right)(11.14)(0.610) + \left(\frac{0.996}{0.991}\right)(10.86)(0.584) + \left(\frac{0.996}{0.991}\right)(10.57)(0.546) + \left(\frac{0.996}{0.991}\right)(10.29)(0.508) + \left(\frac{0.996}{0.991}\right)(10.00)(0.457)}{\$175} = 0.24825 \frac{\text{units}}{\$\text{ million}}$$

$$\frac{\Delta CE}{\Delta \text{reliability}} = \frac{0.24825 - 0.247}{0.005} = 0.25 \frac{\left(\frac{\text{units}}{\$\text{ million}}\right)}{\text{increase in reliability}}$$

Addition of $1,000,000 to cost:

$$CE = \frac{(11.71)(0.635) + (11.43)(0.626) + (11.14)(0.610) + (10.86)(0.584) + (10.57)(0.546) + (10.29)(0.508) + (10.00)(0.457)}{\$175 + \$1} = 0.246$$

$$\frac{\Delta CE}{\Delta \text{cost}} = 0.246 - 0.247 = -1.41 \times 10^{-3} \frac{\left(\frac{\text{units}}{\$\text{ million}}\right)}{\$\text{ million}}$$

The next step in the tradeoff is the selection of the candidate systems. A look at the requirements of the position and orientation thrusters is necessary to further screen systems. The system has several functions. They are initial spinup, orientation, trim of circular orbit, and station keeping. Six thrusters are required; their orientations are presented in Fig. 16. Continuous thrusting spinup thrusters will increase the spin rate of the satellite. Continuous thrusting of the axial engines will impart a ΔV to the spacecraft in the axial direction. Pulsing of one of the axial thrusters will act to reorient spin axis. The radial engines on a properly timed pulse will impart a ΔV in the radial direction. The spinup maneuver is accomplished by two burns of the spinup thrusters, requiring a total of 660 lbf-s impulse. Circularization of the orbit requires a ΔV of about 175 ft/s. Station-keeping requirements are 7 and 180 ft/s/yr in the east-west and north-south directions, respectively. A total impulse of 54,000 lbf-s is required for seven years of operation with an estimated 10,000 actuations/thruster. All maneuvers are either long duration steady-state thrusting or long chain pulse mode operation (500 pulses).

Twin tanks located 180 deg apart may be used to eliminate changes in the center of gravity. The initial supply of propellant during the spinup maneuver may be acquired by the use of retention screens or a small auxiliary tank. Retention screens would be the simplest, lightest, and possibly most reliable. Once the spin is begun, propellant-pressurant separation is achieved.

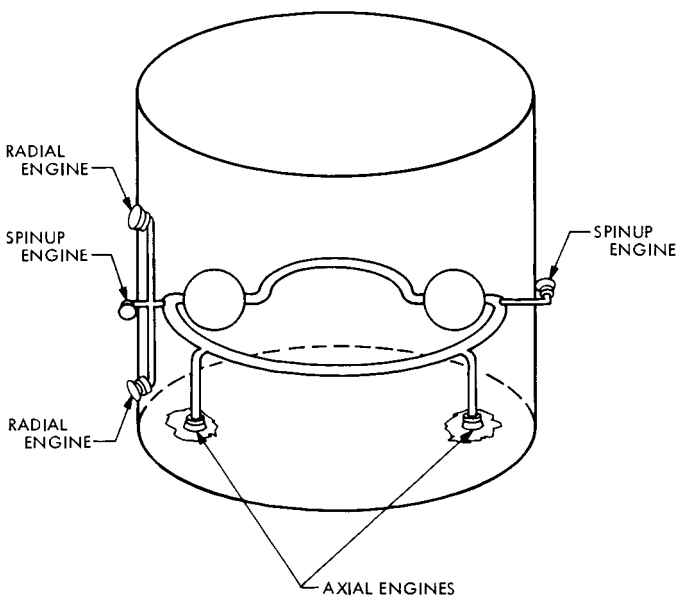

Fig. 16. *Intelsat IV* position and orientation system

The gains in steady-state specific impulse of a hydrazine resistojet thruster, operating at zero power and a thrust level above 0.1 lbf over a hydrazine direct catalytic thruster are so small that only the direct catalytic thruster has been considered. The pulse mode operation eliminates the subliming solid unit from consideration (most of the station keeping requirements are met by pulse mode operation). Radioisojet systems have not been considered for the following reasons:

(1) The steady-state or long pulse mode operation cannot be performed if the temperature and resulting performance are to remain high.

(2) Long mission life leads to decay in radioactive thermal power; plutonium may be used but is quite expensive.

(3) Preference for high-thrust (2 to 5 lbf) thrusters leads to large isotope heaters and thus major shielding requirements.

(4) Nuclear radiation effects on communications subsystem are possible.

The hydrazine plenum, vaporizing ammonia, and ammonia resistojet systems can be designed for pulse lengths of 200–300 s duration. The duty cycle must be modified to limit pulse widths and pulse chain lengths to less than 200–300 s. The following systems are worthy of serious considerations:

(1) Inert gas, N_2.

(2) Liquid hydrazine, direct catalyst.

(3) Liquid hydrazine, plenum.

(4) Liquid ammonia, cold.

(5) Liquid ammonia, resistojet.

(6) Tridyne.

(7) Electrolysis, water.

Based on the mission requirements and Appendixes B, C, and D, mass, reliability, and cost were calculated. Development cost was spread over five missions. A tabulation of these values is presented in Table 7.

The large spread of thruster system mass is noted. Before any cost-effectiveness tradeoffs can begin, the inert nitrogen and Tridyne systems must be eliminated from consideration. The mass of the inert gas system is greater than the spacecraft, apogee motor and propellant and spacecraft adapter. The mass of the Tridyne system is equal to the injected spacecraft mass. Two ammonia

Table 7. Auxiliary-propulsion system data for *Intelsat IV*[a]

Parameters		Single Systems			
		Single	Dual series	Quad	12 T/C Dual series
Inert gas 1 lbf	Mass	3104.0	3105.0	3107.0	3110.0
	Cost	0.235	0.255	0.295	0.305
	Reliability	0.8822	0.9295	0.980	0.980
Direct catalyst hydrazine 4 to 2 lbf	Mass	322.0	324.0	326.0	331.0[b]
	Cost	0.455	0.475	0.515	0.605[b]
	Reliability	0.853	0.899	0.947	0.991[b]
	CE	0.237	0.247	0.257	0.262[b]
Hydrazine plenum 10 mlbf	Mass	534.0	535.0	537.0	540.0
	Cost	0.355	0.375	0.415	0.425
	Reliability	0.8619	0.908	0.957	0.958
	CE	0.063	0.066	0.068	0.067
Resistojet, NH_3 10 mlbf	Mass	263.0	265.0	267.0	289.0
	Cost	0.455	0.475	0.515	0.605
	Reliability	0.866	0.912	0.962	0.965
	CE	0.248	0.261	0.275	0.273
Resistojet, NH_3 50 mlbf	Mass	335.0	337.0	339.0	451.0
	Cost	0.455	0.475	0.515	0.605
	Reliability	0.866	0.912	0.962	0.965
	CE	0.227	0.234	0.244	0.090
Vaporizing liquid NH_3 10 mlbf	Mass	576.0	577.0	579.0	582.0
	Cost	0.355	0.375	0.415	0.425
	Reliability	0.8689	0.9155	0.9648	0.965
	CE	0.053	0.056	0.058	0.057
Tridyne 10 mlbf	Mass	1064.0	1066.0	1068.0	1071.0
	Cost	0.455	0.475	0.515	0.605
	Reliability	0.879	0.927	0.977	0.980
Electrolysis, 1 lbf (I_{sp} = 236 lbf-s/lbm)	Mass	315.0	318.0	322.0	352.0
	Cost	1.12	1.15	1.20	1.40
	Reliability	0.804	0.862	0.925	0.968
	CE	0.222	0.238	0.254	0.227
Electrolysis, 1 lbf (I_{sp} = 250 lbf-s/lbm)	Mass	300.0	303.0	307.0	337.0
	Cost	1.12	1.15	1.20	1.40
	Reliability	0.804	0.862	0.925	0.968
	CE	0.222	0.238	0.254	0.227

[a]Mass, lbm; cost, $ million; *CE*, units/$ million.
[b]Baseline system configuration.

resistojet systems have been considered (10 and 50 mlbf). Two electrolysis systems were considered (I_{sp} of 250 and 236 lbf-s/lbm).

The hydrazine dual-series valve, single system is assigned as the baseline for which a cost effectiveness of 0.247 units/$ million is calculated. The hydrazine system was selected as the baseline system since all Comsat and Hughes reliability and redundancy studies were conducted about a design mass based on a hydrazine position and orientation subsystem. Incremental values of mass, cost, and reliability are calculated and the baseline value of cost effectiveness is modified. The resulting values of cost-effectiveness are presented in Table 7. Their values are plotted in Fig. 17. The values of cost effectiveness for the systems cluster in two groups. Hydrazine catalyst, water electrolysis, and ammonia resistojets combine to form the first group, which is significantly higher than

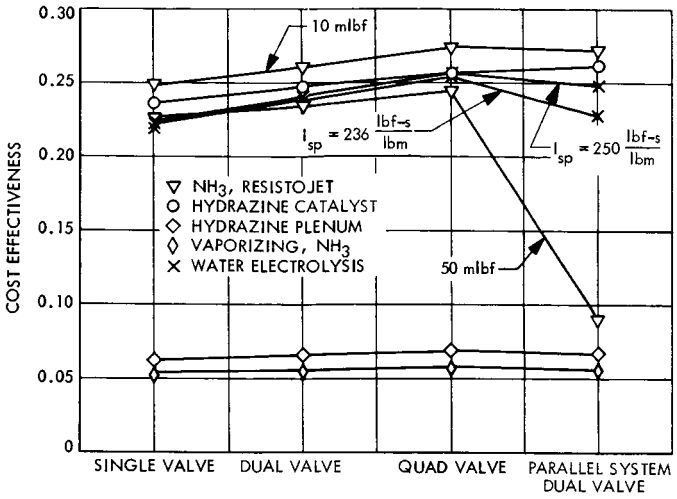

Fig. 17. Auxiliary propulsion cost effectiveness for *Intelsat IV*

the second group, consisting of vaporizing ammonia and hydrazine plenum systems.

The large mass variations between the design reference mass and those required for either of the two systems in the second group presented problems in that the Δ mass values exceeded the amount of redundancy mass on the spacecraft. After the removal of 120 lbm of redundancy, the spacecraft was reduced down to single system configurations. Additional mass removal was implemented by reduction in the communications payload, which has the effect of linearly decreasing the worth of the payload. As a result of the low subsystem reliability and decreased payload, the hydrazine plenum and vaporizing ammonia systems are unfavorable.

Both the hydrazine direct catalyst and ammonia resistojet systems are favorable. The tradeoff between these two systems reduces to a function of what reposition times (thrust level) and power usage can be accepted. If a thrust level of 10 mlbf can be accepted and the power is available then the ammonia resistojet becomes the favorable system. In all calculations, power has been penalized by the addition of the appropriate mass penalty. This penalty can only be imposed if the power is available. If the requirement for reposition and station keeping is strict then the hydrazine direct catalyst system is definitely the preferred auxiliary-propulsion system. Although the electrolysis system is favorable, its ranking must be qualified. The water electrolysis system is based on several theoretical calculations. The specific impulse delivered from an O_2/H_2 thruster operating at a mixture ratio of 8 to 1 is based on the use of large quantities of hydrogen for film cooling. However this thruster has not been operated at an 8-to-1 mixture ratio. Spark plug and thrust chamber reliability calculations were based on a 2000°F chamber temperature. Temperatures in excess of this will lead to lower component reliability.

V. Planetary Mission

The Thermoelectric Outer Planets Spacecraft (TOPS) has been selected as a representative planetary vehicle. TOPS is representative of a spacecraft which would be launched during the 1977–1979 period to use the outer planet gravitational fields with corrective ΔV maneuvers to fly a Grand Tour trajectory. The four-planet plan has been selected as a design mission (see Fig. 18). The flyby of Jupiter, Saturn, Uranus, and Neptune will take roughly 10 yr. Radioisotope thermoelectric generators (RTG) are provided for spacecraft electrical power and thermal control. As a consequence, the penalty for power usage is great (approximately 0.59 lbm/W).

An assignment of mission "worth" to each of the four planetary encounters is difficult. Several factors make scientific information returned from Jupiter important:

(1) Jupiter is presently assumed in a primordial state similar to when life originated on earth.

(2) The presence of low frequency radio waves emanating from the approximate location of one of its moons (Io).

(3) High measured equilibrium surface temperature of approximately 129°K compared to a theoretical equilibrium temperature of 105°K.

(4) Increase in emissivity of one of its moons as it travels around the night side of the planet.

(5) The composition of its atmosphere, especially the relatively large quantity of He suspected in the atmosphere.

There are other reasons for the exploration of Jupiter. The importance of data returned from Saturn is less important; however; there are a great number of unanswered questions concerning this planet. The assignment of representative mission "worth" is presented in Fig. 19.

The assignment of mission probability of success, which involves determining the effects of redundancy on spacecraft life, is a complete study in itself. An early attempt to assign mission probability of success and redundancy

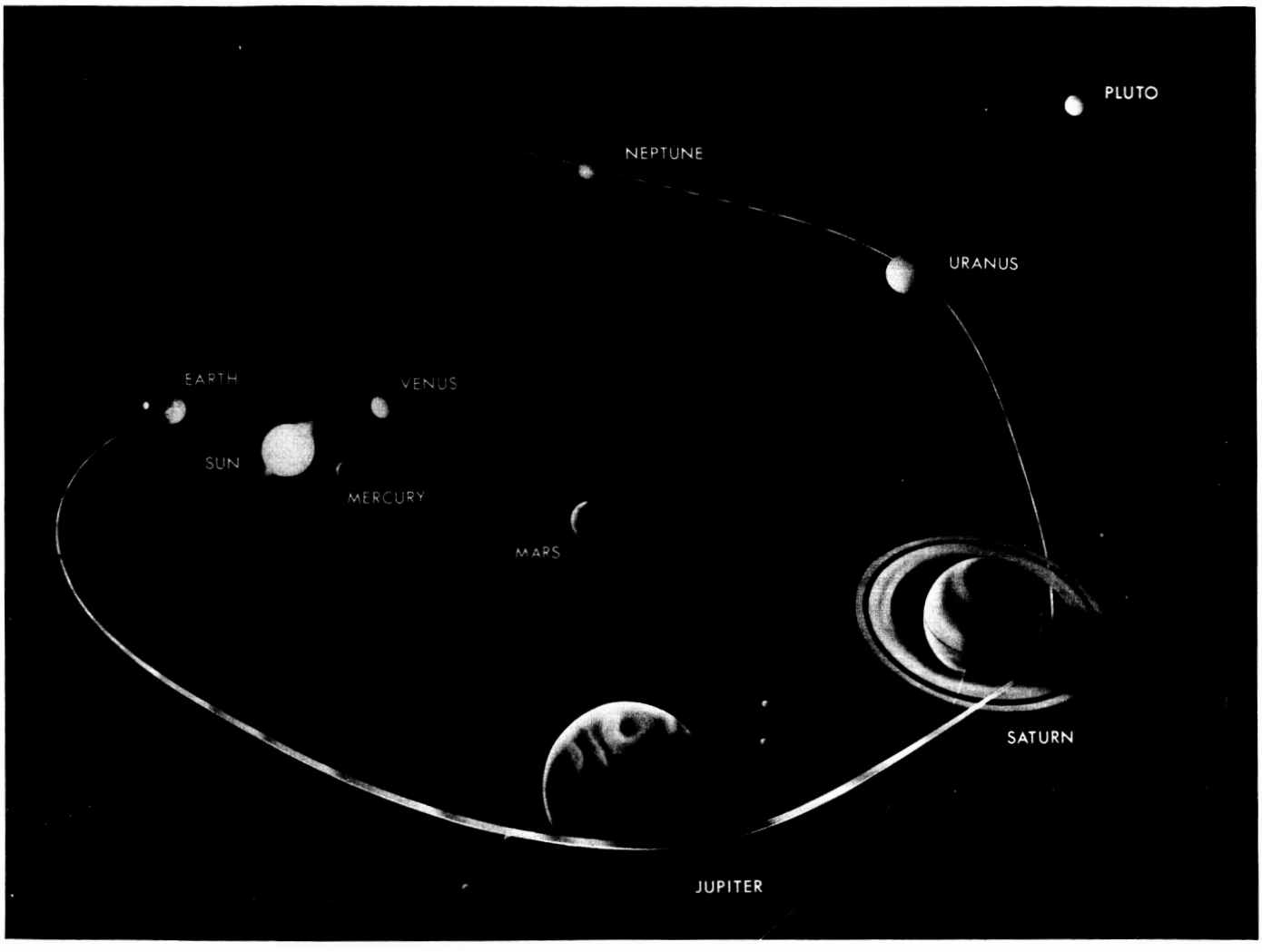

Fig. 18. The Grand Tour trajectory

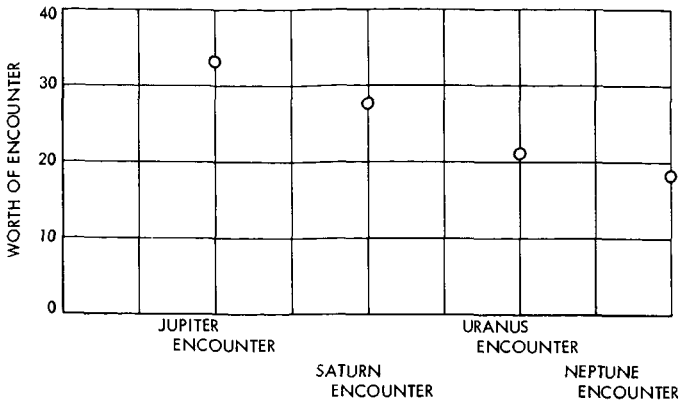

Fig. 19. Predicted worth of planetary encounter

effects was carried out at JPL in 1968. A principal curve extracted from this study is presented in Fig. 20. In order to assess the impact of additional scientific payload mass, a further study was undertaken; the curve in Fig. 21 is the result of this study. The addition of 1.0 lbm of scientific payload requires 0.8 lbm support equipment.

From these curves and the techniques outlined in Appendix B, mass and cost influence coefficients can be calculated. These calculations are summarized in Table 8.

The second step in a thruster tradeoff is the selection of the candidate systems. With the aid of the above determined influence coefficients and power penalty assumptions, a screening of candidate systems is appropriate. Resistojets (both ammonia and inert gas feed) require around 100 W of electrical power to operate in the 10-mlb thrust range (2000°F). The anticipated conversion factor of 1.7 W/lbm puts the mass for these systems in excess of any of the other considered systems (range 7 to 30 lbm).

A look at the requirements of attitude propulsion thrusters is necessary to further screen systems. The system will perform three primary functions. They are initial tipoff rate reduction, reference acquisition, and periodic unloading of the momentum wheels (TOPS is 3-axis stabilized). The tipoff requirement is for the steady-state operation of the required jets to suppress initial roll rates (up to 300 s of operation). This will require a maximum total impulse of 25 lbf-s. Acquisition will require an additional 25 lbf-s total impulse. The tentative momentum wheel unloading requirement is for 1000 unloadings of each wheel; an estimate of 150 lbf-s is required for this operation. Both operations can be performed with thrusters in the 10–100 mlbf thrust range. These calculations were based on moment arms of 2 ft.

The long (300 s) steady-state thrust places restrictions on the design of both the cold ammonia system and the hydrazine plenum systems. Both systems suffer from thermal limitations in opposite respects. Sufficient heat-transfer area must be included in the ammonia system design to allow for the complete vaporization of liquid ammonia.

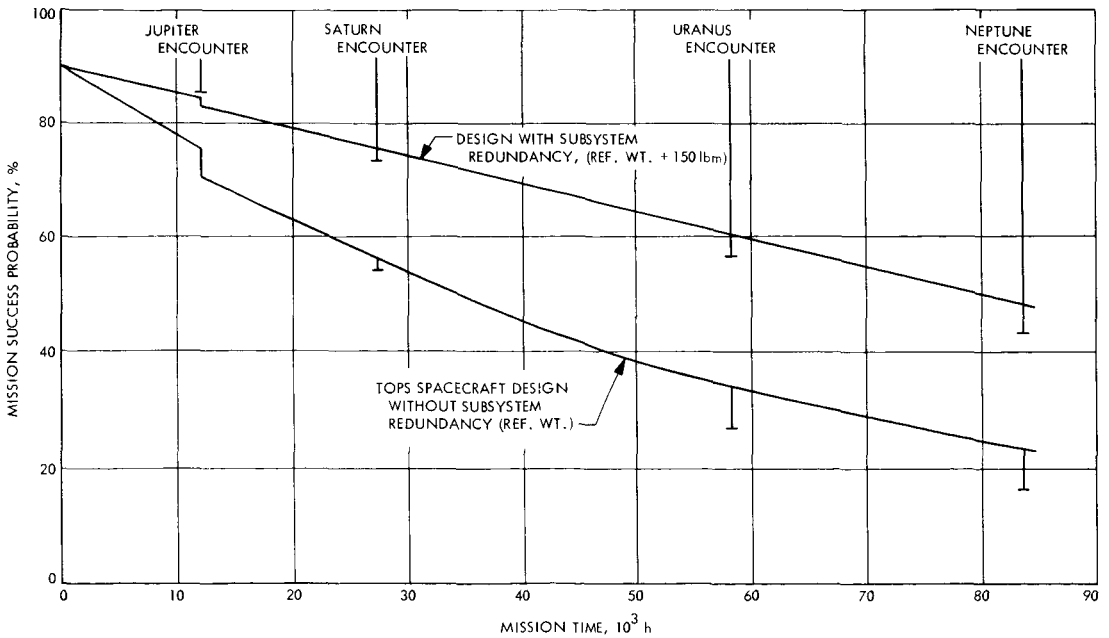

Fig. 20. Effects of subsystem redundancy on TOPS mission success-probability

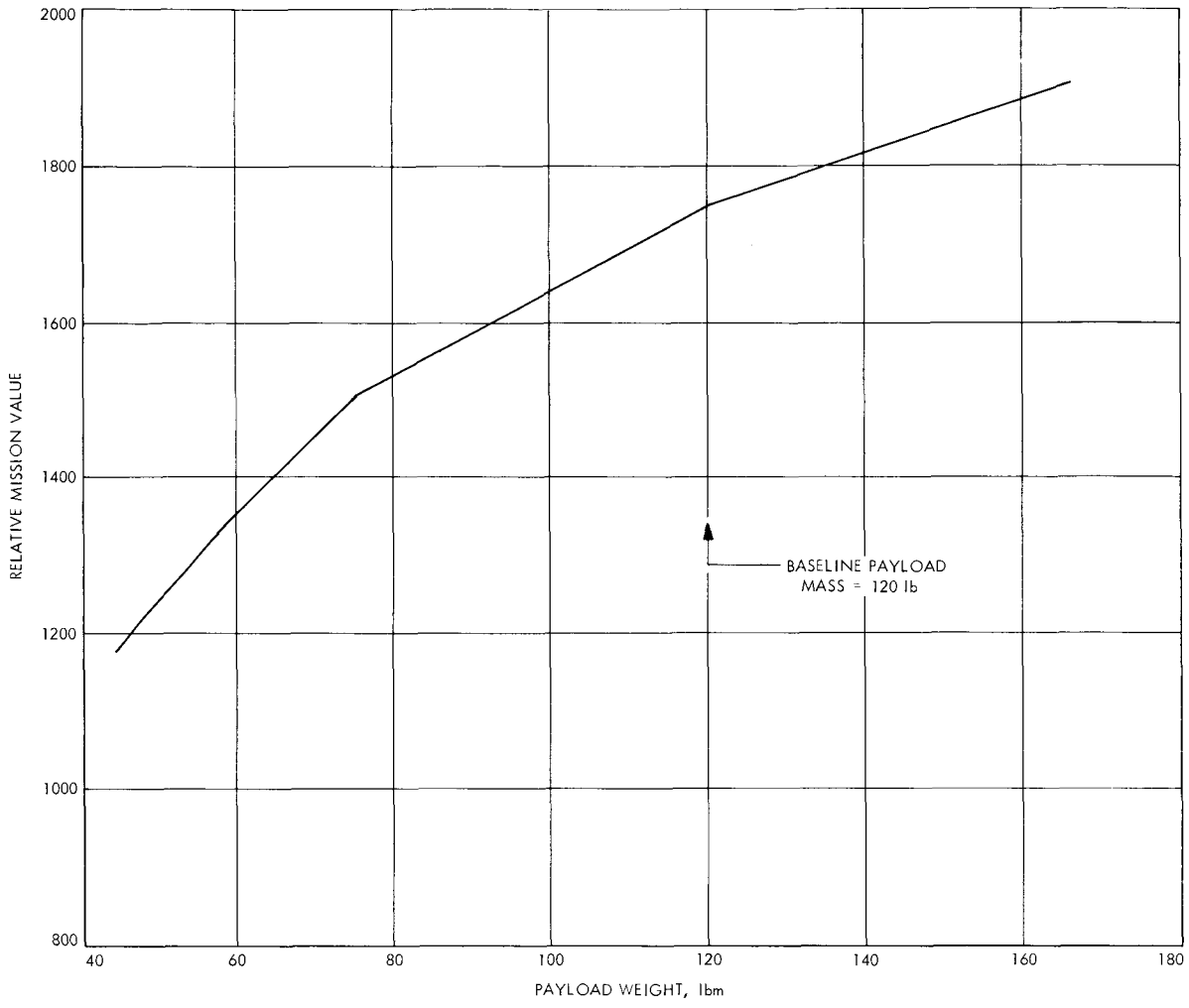

Fig. 21. TOPS mission value vs payload weight

The hydrazine plenum system must be designed to dissipate the excessive heat generated during the tipoff maneuver. Both of these systems can be designed to meet the overall system requirements. The advantage of water electrolysis systems is the relatively high specific impulse achieved with combustion (hot mode) of the generated bipropellants. However, the initial mass (electrolysis cell and stored tipoff propellant) is excessive. This tends to eliminate electrolysis units from consideration. The requirement for small impulse-bit operation eliminates "valveless" subliming solid systems from consideration because of their long on–off transients. The following systems are suitable for serious consideration:

(1) Inert gas.

(2) Liquid hydrazine, direct catalyst.

(3) Liquid hydrazine, resistojet.

(4) Liquid hydrazine, plenum.

(5) Liquid ammonia, cold.

(6) Liquid ammonia, radioisojet.

(7) Tridyne.

All systems consist of a baseline of 6 thrusters (±roll, ±yaw, ±pitch). The thrust level is set at a nominal 50 mlbf, which may be altered slightly from system to system.

Based on the above-mentioned mission requirements and the aid of Appendixes B, C, and D, mass, reliability, and cost were calculated. Development costs were spread over two missions. A tabulation of these values is presented in Table 9. The inert gas, single solenoid, double system is assigned as the baseline for which a cost-effectiveness of 0.3421 units/$ million is calculated. Incremental values in mass, reliability, and cost are calculated and the baseline value of cost-effectiveness is modified.

Table 8. Influence coefficient calculations for TOPS

$$CE_{baseline} = \frac{\sum_i P_i W_i}{\sum_i C_i}$$

where

P_i = probability of success (Fig. 20)

W_i = mission worth (Fig. 19)

$\sum_i C_i$ = total mission cost of \$200 million

$$CE_{baseline} = \frac{(33.5)(0.83) + (27.5)(0.76) + (21.0)(0.57) + (18.0)(0.43)}{\$200} = 0.342 \frac{\text{units}}{\$\text{ million}}$$

Addition or subtraction of mass to system redundancy:

−150 lbm:

$$CE = \frac{(33.5)(0.78) + (27.5)(0.54) + (21.0)(0.35) + (18.0)(0.24)}{\$200} = 0.255 \left(\frac{\text{units}}{\$\text{ million}}\right)$$

150 to −150 lbm added or subtracted:

$$\frac{\Delta CE}{\Delta \text{mass}} = \frac{0.255 - 0.342}{-150} = 5.81 \times 10^{-4} \frac{\left(\frac{\text{units}}{\$\text{ million}}\right)}{\text{lbm}}$$

Addition or subtraction of mass to scientific payload:

+45 lbm + (45) (0.8) support mass:

$$CE = \frac{1900}{1750} CE_{baseline} = 0.371 \frac{\text{units}}{\$\text{ million}}$$

0 to 72 lbm:

$$\frac{\Delta CE}{\Delta \text{mass}} = \frac{0.371 - 0.342}{72} = 4.06 \times 10^{-4} \frac{\left(\frac{\text{units}}{\$\text{ million}}\right)}{\text{lbm}}$$

−45 lbm − (45) (0.8) support mass:

$$CE = \frac{1500}{1750}(0.342) = 0.293 \frac{\text{units}}{\$\text{ million}}$$

0 to −72 lbm:

$$\frac{\Delta CE}{\Delta \text{mass}} = \frac{0.293 - 0.342}{-72} = 0.697 \times 10^{-3} \frac{\left(\frac{\text{units}}{\$\text{ million}}\right)}{\text{lbm}}$$

Change in reliability of 0.002:

$$CE = \frac{\left(\frac{1.00}{0.998}\right)(33.5)(0.83) + \left(\frac{1.00}{0.998}\right)(27.5)(0.76) + \left(\frac{1.00}{0.998}\right)(21.0)(0.57) + \left(\frac{1.00}{0.998}\right)(18.0)(0.43)}{\$200} = 0.343$$

$$\frac{\Delta CE}{\Delta \text{reliability}} = \frac{0.343 - 0.342}{0.002} = 0.345 \frac{\left(\frac{\text{units}}{\$\text{ million}}\right)}{\text{increase in reliability}}$$

Addition of \$1,000,000 in cost:

$$CE = \frac{(33.5)(0.83) + (27.5)(0.76) + (21.0)(0.57) + (18.0)(0.43)}{\$200 + \$1} = 0.340 \frac{\text{units}}{\$\text{ million}}$$

$$\frac{\Delta CE}{\Delta \text{cost}} = 0.340 - 0.342 = -1.7 \times 10^{-3} \frac{\left(\frac{\text{units}}{\$\text{ million}}\right)}{\$\text{ million}}$$

Table 9. Auxiliary-propulsion system data for TOPS[a]

Parameters		Single systems				Double systems		
		Single	Dual series	Quad	12 T/C Dual series	Single	Dual series	Quad
Inert gas, N_2 50 mlbf	Mass	12.48	13.68	16.08	17.88	32.28[b]	34.68	39.48
	Reliability	0.9513	0.9691	0.9878	0.9884	0.998[b]	0.999	0.9998
	Cost	0.250	0.270	0.310	0.320	0.450[b]	0.490	0.510
	CE	0.336	0.342	0.347	0.346	0.342[b]	0.341	0.337
Vaporizing, NH_3 10 mlbf	Mass	8.55	9.75	12.25	13.95	19.6	22.0	26.8
	Reliability	0.949	0.9668	0.985	0.986	0.997	0.999	0.9998
	Cost	0.400	0.420	0.460	0.470	0.700	0.740	0.820
	CE	0.337	0.343	0.348	0.347	0.348	0.347	0.345
Hydrazine direct catalyst 50 mlbf	Mass	7.15	8.35	10.75	13.25	16.5	18.9	23.7
	Reliability	0.944	0.961	0.980	0.995	0.997	0.998	0.9996
	Cost	0.500	0.520	0.560	0.650	0.900	0.940	1.02
	CE	0.336	0.341	0.347	0.351	0.349	0.348	0.346
Hydrazine resistojet 50 mlbf	Mass	7.1	8.2	10.6	13.0	15.2	17.6	22.4
	Reliability	0.944	0.961	0.980	0.995	0.997	0.998	0.9996
	Cost	0.900	0.920	0.960	1.05	1.30	1.34	1.42
	CE	0.340	0.341	0.346	0.350	0.349	0.341	0.346
Hydrazine plenum, active 50 mlbf	Mass	8.15	9.35	11.75	13.55	18.3	20.7	23.7
	Reliability	0.946	0.964	0.983	0.983	0.997	0.999	0.9997
	Cost	0.400	0.420	0.460	0.470	0.700	0.740	0.820
	CE	0.336	0.342	0.347	0.347	0.349	0.348	0.347
Tridyne 10 mlbf	Mass	9.90	11.10	13.50	16.18	23.76	26.16	31.0
	Reliability	0.947	0.964	0.983	0.988	0.997	0.999	0.9997
	Cost	0.500	0.520	0.560	0.650	0.900	0.940	1.02
	CE	0.337	0.342	0.347	0.347	0.346	0.345	0.342
Radioisojet, NH_3 10 mlbf	Mass	17.2	18.4	20.8	33.0	34.8	37.2	42.0
	Reliability	0.948	0.966	0.984	0.986	0.997	0.999	0.9997
	Cost	2.20	2.22	2.26	2.35	3.10	3.14	3.22
	CE	0.330	0.336	0.341	0.334	0.336	0.335	0.332
Hydrazine plenum, passive 50 mlbf	Mass	7.50	8.70	11.10	12.90	17.0	19.4	22.4
	Reliability	0.946	0.964	0.983	0.983	0.997	0.999	0.9997
	Cost	0.400	0.420	0.460	0.470	0.700	0.740	0.820
	CE	0.339	0.345	0.350	0.349	0.350	0.349	0.348

[a]Mass, lbm; cost, $ million; CE, units/$ million.
[b]Baseline system configuration.

The development cost is spread over two missions. The resulting values of cost-effectiveness are presented in Table 9.

The general trend of subsystem cost effectiveness as a function of its level of redundancy is a curve with a maximum cost effectiveness located somewhere between the redundancy extremes (see Fig. 22). The maximum portion of Fig. 22 is enlarged in Fig. 23. Hydrazine direct catalyst in the 12 T/C dual-series valve, single system configuration, is the optimum system for a TOPS-type mission. Hydrazine plenum and hydrazine resistojet systems are next in preference. The cold ammonia system is next in line after the hydrazine systems. Inert gas (nitrogen) was next with the Tridyne system immediately following. The least favorable system of the cost effectiveness tradeoff was the ammonia radioisojet, since the two 3-thruster clusters have an initial mass of over 10 lbm. Included in this curve is a hydrazine plenum system utilizing a passive pressure control device. The assignment of a reliability

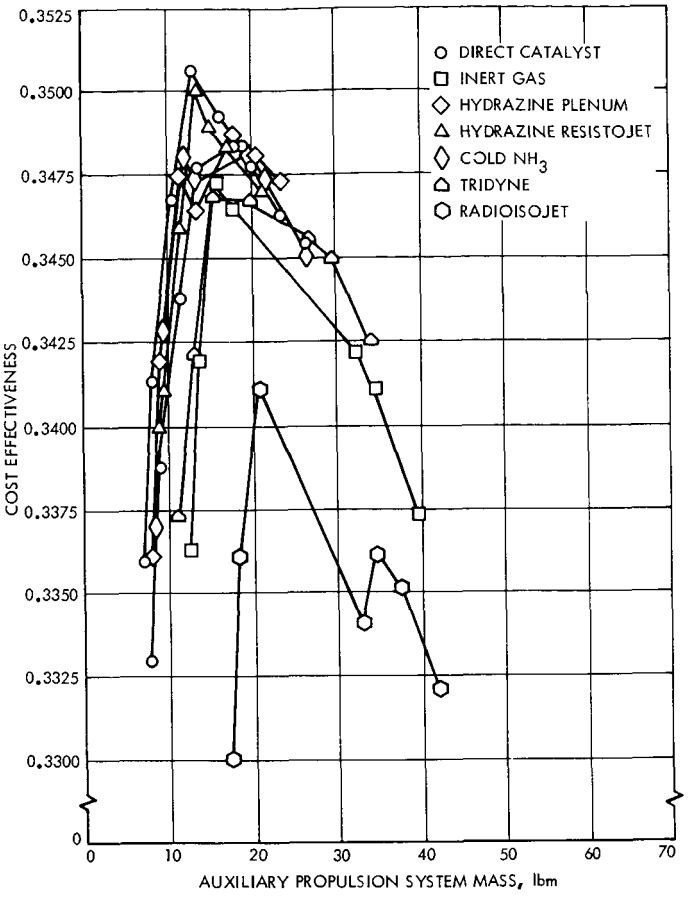

Fig. 22. Auxiliary propulsion system cost effectiveness for TOPS mission

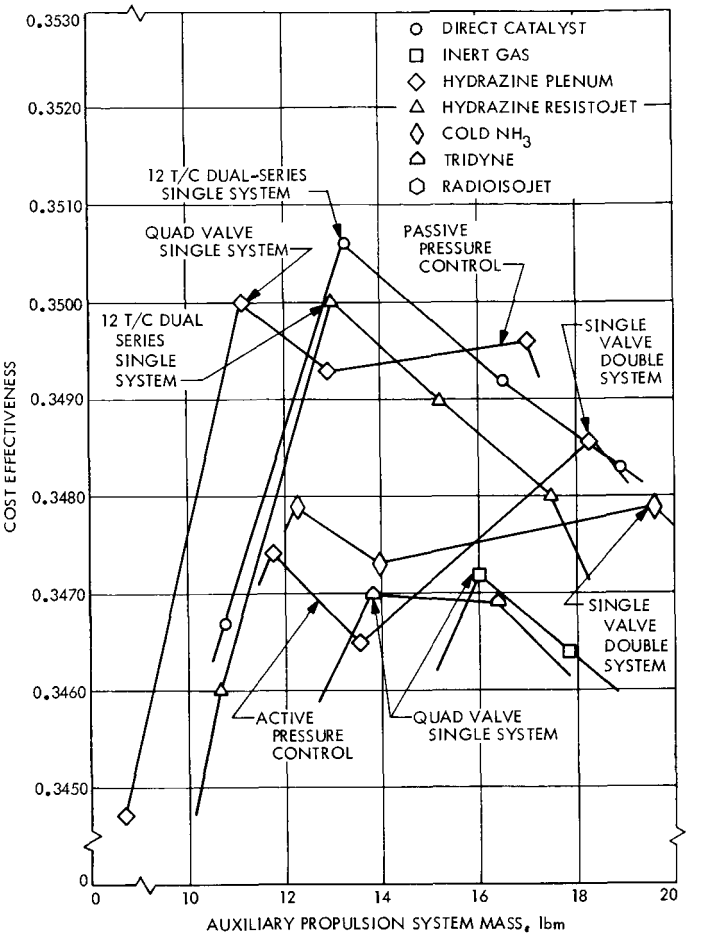

Fig. 23. Auxiliary propulsion system cost effectiveness for TOPS mission

to this feed system was arbitrary since no data has been generated. One point that should be stressed is that depending on the duty cycle, a passive pressure control type hydrazine plenum system or a hydrazine resistojet in the low millipound (on the order of 10 to 30 mlbf) thrust level is potentially more favorable than a hydrazine direct catalyst system.

The most favorable redundancy concept varied from system to system. The gas feed systems (Tridyne and inert gas) maximize with the quad valve-single system configuration. The hydrazine direct catalyst and resistojet systems peak with the 12 T/C dual-series valve single system configuration. The relatively low reliability of the valve-thruster arrangement is most greatly enhanced in the 12 T/C dual-series valve single system. Finally, the hydrazine plenum and vaporizing ammonia systems reach a maxima at the single-valve double system configuration. It is noted that the reliability of the two feed systems is low due to the plenum-control valve loops in both systems; thus, the 12 T/C dual series valve single system is favorable. The ammonia radioisojet system favors the quad-valve single system configuration. The reliability parameter is dwarfed by mass consideration in this system. In summary, the auxiliary-propulsion tradeoff applied to the TOPS mission results in the following system ranking:

(1) Hydrazine direct catalyst, 12 T/C dual series valve, single system.

(2) Hydrazine resistojet, 12 T/C dual series valve, single system.

(3) Hydrazine plenum, passive feed, quad valve, single system.

(4) Hydrazine plenum, single valve, double system.

(5) Vaporizing ammonia, single valve, double system.

(6) Inert gas, nitrogen, quad valve, single system.

(7) Tridyne, quad valve, single system.

(8) Radioisojet.

VI. Conclusions

The usefulness of cost effectiveness as a comparison tool must be stressed. Since system comparison or tradeoff must be preformed in the light of a particular mission, the mission requirements will influence the tradeoff in a variety of ways. Cost effectiveness becomes the method by which systems can be compared. The exact agreement with the results of Sections III, IV, and V is not necessary to acknowledge the usefulness of this methodology. If other system inputs are preferred or other mission profiles are under consideration, then the application of cost-effectiveness techniques to these new system inputs and missions is strongly encouraged. It is felt that this report provides a useful tradeoff technique which can be applied to any auxiliary-propulsion system selection.

The mission analyses provide several interesting and noteworthy results. The subsynchronous (ERTS) mission tradeoff results in the following system ranking:

(1) Combined systems:
   (a) Hydrazine plenum (6T) and hydrazine catalyst (2T).
   (b) Inert Tridyne (6T) and Tridyne (2T).
   (c) Vaporizing NH_3 (6T) and resistojet, NH_3 (2T).
   (d) Inert gas (6T) and inert gas resistojet (2T).

(2) Single systems:
   (a) Hydrazine direct catalyst (8T).
   (b) Vaporizing NH_3 (8T).
   (c) Hydrazine plenum (8T).
   (d) Hydrazine resistojet (8T).
   (e) Inert gas (8T).
   (f) Tridyne (8T).

The synchronous (*Intelsat IV*) mission tradeoff results in the following system ranking:

(1) 10-mlbf resistojet, NH_3.

(2) Hydrazine catalyst.

(3) Water electrolysis.

(4) 50-mlbf resistojet, NH_3.

The planetary (TOPS) mission tradeoff results in the following system ranking:

(1) Hydrazine catalyst.

(2) Hydrazine resistojet.

(3) Hydrazine plenum.

(4) Vaporizing NH_3.

(5) Inert gas.

(6) Tridyne.

For the ERTS mission, the use of combined systems seems to give rise to the maximum value of cost effectiveness. The mutual feed system acts to reduce the total system mass and cost. The combination of high-performance, high-level thrusters with low-level thrusters will also act to reduce system mass. The combination of hydrazine plenum low-level thrusters with hydrazine catalyst high-level thrusters appears to provide the optimum configuration.

The *Intelsat IV* mission has several interesting results. The 10 mlbf NH_3 resistojet system seems to be the optimum system assuming its response time (thrust level dependent) and power usage can be accepted. The hydrazine catalyst system is second behind the ammonia resistojet. The hydrazine catalyst system, however, does not suffer from duty cycle limitations.

The TOPS mission results in a tradeoff between two top contenders. The hydrazine catalyst system is preferred over a hydrazine resistojet system. Due to the high penalty for power on the TOPS mission, the hydrazine resistojet system was severely penalized for the power required for its operation. With more advanced development (decreased development cost), this system will become more attractive. If the passive pressure control is implemented in the hydrazine plenum system, then it becomes a close contender to the catalytic system. The thrust level selected was 50 mlbf. If this thrust level is decreased by future mission criteria, the hydrazine plenum system will surpass the catalytic system (at approximately 10 to 30 mlbf) in cost effectiveness.

VII. Recommendations

Several systems should be studied in greater detail. The hydrazine catalyst system was found to be favorable in all three missions to a varying degree. It was found to be the most favorable auxiliary-propulsion system in the planetary mission. Although considerable effort has gone into the development of the hydrazine catalytic thrusters in higher thrust levels (>0.5 lbf), low-thrust (0.05 lbf) catalytic hydrazine technology to date is somewhat limited. Increased effort in this area is warranted.

The hydrazine plenum system ranked third in the planetary mission example and first (when coupled with catalytic high level thrusters) in the subsynchronous mission. The passive plenum system is attractive and should be

explored more deeply. The hydrazine plenum-hydrazine catalyst thrust level tradeoff point should be redefined for a passive plenum system.

The hydrazine resistojet thruster is constrained by a large development cost. With increased development (hence decreased cost), this system will surpass a catalytic hydrazine system (at 50 mlbf) provided a low duty cycle ($<1\%$) total impulse in excess of 300 lbf-s is required. For any mission with these requirements, a close look at the hydrazine resistojet system is warranted.

The inert gas system will see continual use in systems with low total impulse requirements and small mass influence coefficients (OGO, *Nimbus*, and *Mariner*). The combination of inert gas low-level thrusters with inert gas resistojet high-level thrusters was found favorable in the subsynchronous mission.

The Tridyne system was found to be favorable for orbit correction when the attitude-control thrusters are inert (nonreacting) low-level thrusters (ERTS mission). With decreased system cost, the Tridyne system will become even more attractive. Development of the Tridyne thruster into a flight-qualified system is suggested.

The ammonia resistojet (10 mlbf) system was found to be the optimum auxiliary-propulsion system for the large impulse, synchronous satellite under consideration. The careful definition of allowable thrust levels and response times is necessary before an ammonia resistojet system is selected. The potential for these systems is great and they should see increased use in the following years.

The water electrolysis system was found to be the third most preferred auxiliary-propulsion system for the *Intelsat IV* mission. This was based on O_2/H_2 spark thruster predictions provided by the Marquardt Corporation. This system has not been developed into flight hardware yet, although the feed system has been demonstrated. Present thruster technology tends to limit this system to a less than optimum maximum specific impulse. With improved thruster performance at high fuel–oxidizer mixture ratios, this system will become more attractive.

The following systems did not appear to be competitive in these three mission tradeoffs: hydrazine electrolysis, subliming solid, "cap pistol," "honeycomb," and radioisojets.

Tables of component mass, tank mass, component reliability, system reliability equations, redundancy reliability equations, and system costs are provided in the Appendixes. They may be modified if other more pertinent data are available or preferred. The component and system data provided are averaged over several designs, and exact system data will probably differ from those values presented herein.

This report has not considered electric propulsion systems in its detailed parameterization. It is recommended that this study be expanded to include ion thrusters, pulsed plasma thrusters, and colloid thrusters. A more complete survey of auxiliary-propulsion system costs is recommended. Parameterization of system characteristics should be expanded to include volume, momentum wheel interactions, position error, and flexibility of operation. The system reliability equations should be expanded to include more sophisticated redundancy concepts.

Nomenclature

C_i mission cost ($ million) where $\sum_i C_i$ = total mission cost

CE cost effectiveness, $\left(\frac{\text{units}}{\$\,\text{million}}\right)$

CE_{baseline} baseline cost effectiveness, $\left(\frac{\text{units}}{\$\,\text{million}}\right)$

P_i mission probability of success, where i refers to a time increment

R_{BL} reliability of the baseline auxiliary propulsion system

R_{MS_i} mission probability of success including modified subsystem reliability, where i refers to a time increment

R_{NS} increased reliability of a comparative subsystem

$RWSP\,(X)$ relative worth of scientific payload at a payload mass of X lbm, (units)

$RWSP$ (baseline mass) relative worth of scientific payload at the baseline payload mass, (units)

T minimum number of thrusters required to control spacecraft

T/C actual number of thrusters in the auxiliary propulsion system

W_i worth of mission, where i refers to a time increment, (units)

$\frac{\Delta CE}{\Delta \text{cost}}$ cost influence coefficient, $\frac{\left(\frac{\text{units}}{\$\,\text{million}}\right)}{\$\,\text{million}}$

$\frac{\Delta CE}{\Delta \text{mass}}$ mass influence coefficient, $\frac{\left(\frac{\text{units}}{\$\,\text{million}}\right)}{\text{lbm}}$

$\frac{\Delta CE}{\Delta \text{reliability}}$ reliability influence coefficient, $\frac{\left(\frac{\text{units}}{\$\,\text{million}}\right)}{\text{increase in reliability}}$

Δcost difference in comparative subsystem cost and the baseline subsystem cost, where increases in cost above baseline cost are positive, ($ million)

Δmass difference in baseline subsystem mass and comparative subsystem mass, where increases in mass above baseline mass are negative, (lbm)

Δreliability difference in comparative subsystem reliability and the baseline subsystem reliability, where increases in reliability above baseline reliability are positive

Appendix A

Available Thruster Systems

Described herein is an outline of the various system configurations and development status of various auxiliary propulsion systems. These systems can be divided into four categories: liquid propellant, solid propellant, gaseous propellant, and electric. These categories can be further subdivided as shown in Fig. A-1. Thermal heaters are also included in Fig. A-1. These devices can be considered as subsets of the liquid, solid, or gas system headings. Both electrical and nuclear heating sources are included. Not all the systems in Fig. A-1 will be discussed herein. Because of the scope of this report (satellite and space probe attitude propulsion selection criteria), high-thrust (>5 lbf) (auxiliary propulsion systems) have not been included. For thrust levels below 5 lbf with mission total impulse requirements below 75,000 lbf-s bipropellant liquid systems become undesirable.

I. Gas Systems: Inert Monopropellant

The inert monopropellant, or cold gas system has flown on all *Ranger*, *Mariner*, and *Surveyor* spacecraft, *Orbiting Astronomical Observatory* (OAO), *Nimbus*, *Orbiting Geophysical Observatory* (OGO), *Pioneer*, *Vela*, and many more. As a result of its extensive use, the *Mariner* inert gas system has been chosen as a datum for system comparisons in this study. The inert gas control system will continue its wide use on future missions whose mass influence coefficients are low, since the inert gas system is both inexpensive and highly reliable.

If ideal gases are compared for total impulse delivered from a given tankage and propellant mass, nitrogen is found to have the optimum molecular weight. This is due to the increase in density with molecular weight, which leads to reduced tankage weight. Although hydrogen, with its low molecular weight, has a higher specific impulse than nitrogen, its low density leads to excessively heavy tanks. When heavy gases such as Freon 14 (nonideal gas) are considered, the effect of compressibility becomes important. Freon 14 provides a larger total impulse per pound of system than nitrogen.

A typical inert gas system is diagrammed schematically in Fig. A-2. A demonstration system is shown in Fig. A-3. Gas storage pressures range from 1000 to 4500 psia, taking advantage of compressibility where possible.

The typical system consists of a propellant tank, fill valve, start valve, filter, regulator, low-pressure relief valve, two pressure transducers, control valves, and nozzles. The fill valve is capped after filling to provide higher reliability. The relief valve may be protected by a burst disk, at a pressure slightly higher than the relief valve. This will prevent loss of gas caused by small relief valve leaks. System activation occurs with the firing of the squib start valve. A filter is employed downstream of the start valve to remove any contaminants which may have originated during squib firing. Line pressures are monitored by pressure transducers, the high pressure reading indicating the quantity of remaining propellant. Solenoid valves are provided for flow control.

Some flight systems may not contain all the components described in the typical system. The *Mariner* inert gas system has a tank, regulator, control valves, and nozzles. The control valves act as built-in relief valves.

Table A-1. Characteristics of several inert gas systems

Spacecraft	Propellant	System weight, lbm	Storage pressure, psia	Thrust level, lbf	Specific impulse, $\frac{\text{lbf-s}}{\text{lbm}}$	Total impulse, lbf-s
Pioneer	nitrogen	9.6	3250	0.20	72	72
OGO A, B, C	argon	37.0	4000	0.050	52	880
OGO D	krypton	60.0	4000	0.050	37	1300
Vela III	nitrogen	9.6	4000	0.20	72	190
Nimbus D	Freon 14	275.0	2000	0.2-0.5	45	300
Discos	Freon 14	13.0	3000	0.001	45	200

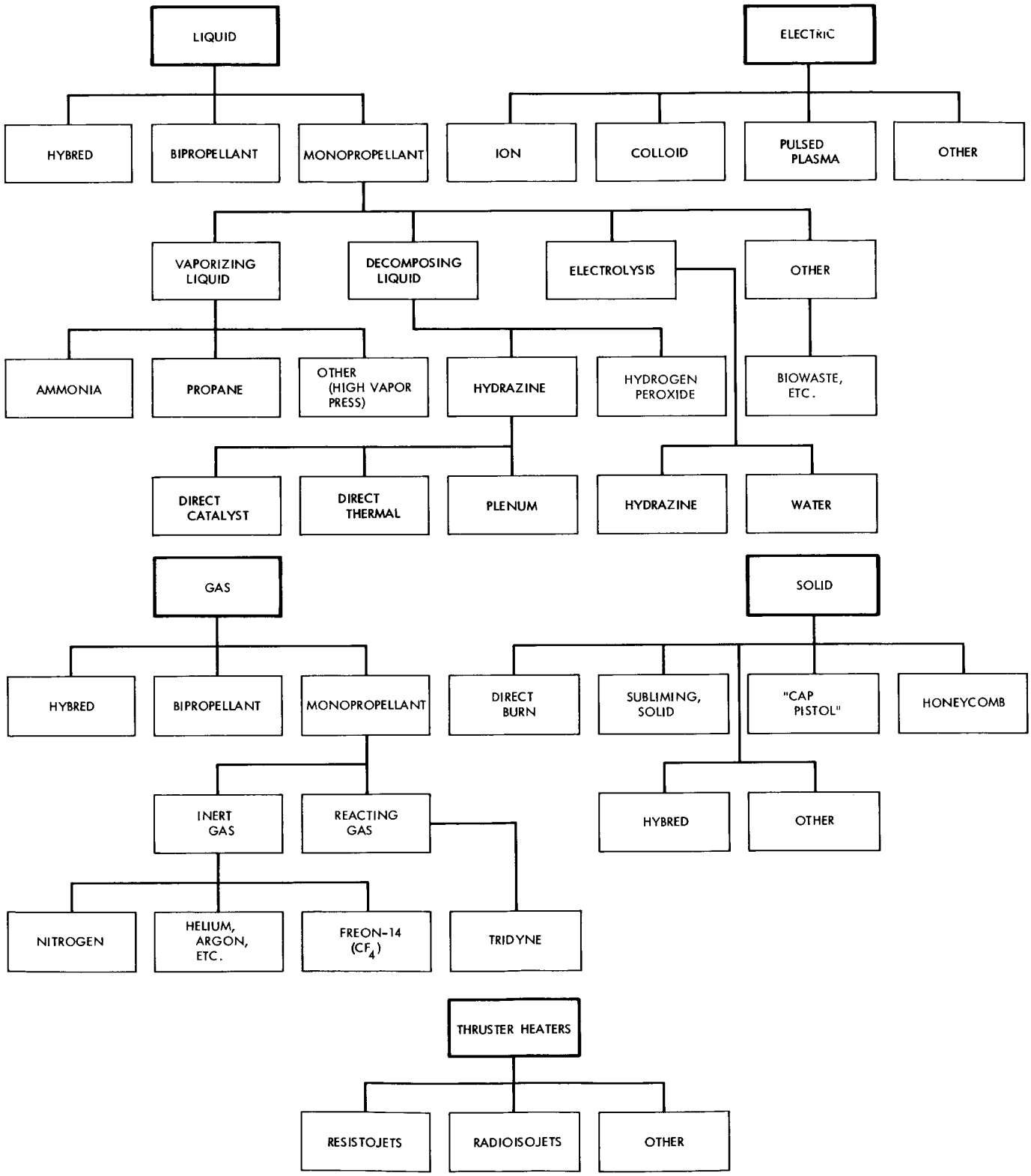

Fig. A-1. Thruster systems

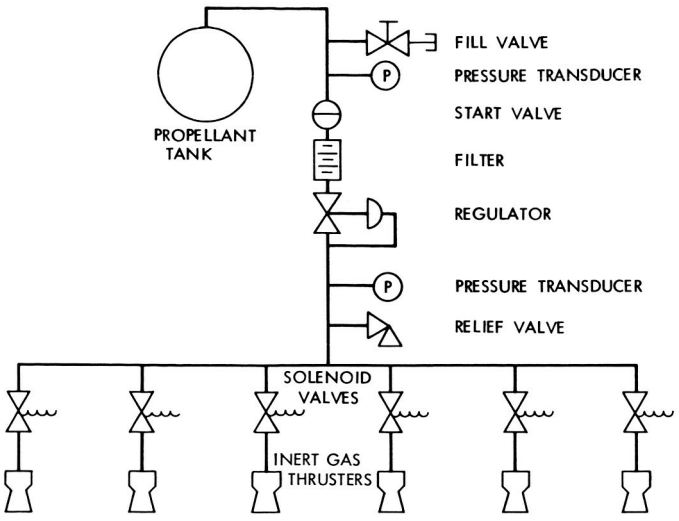

Fig. A-2. Typical inert gas auxiliary propulsion system

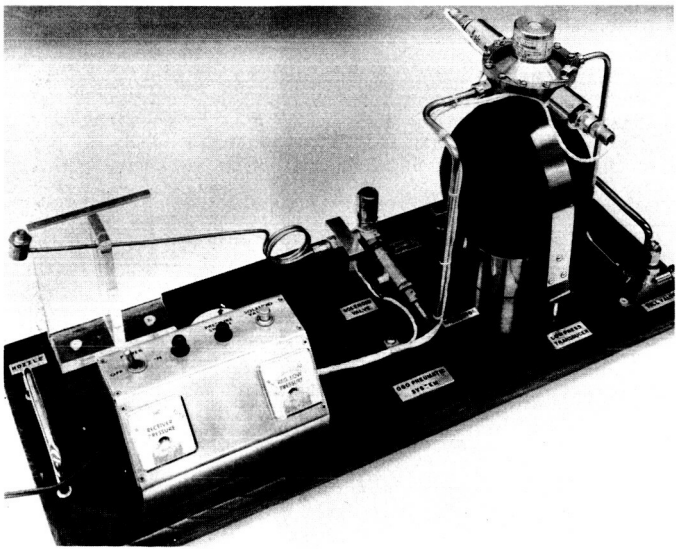

Fig. A-3. OGO pneumatic system demonstrator (photo courtesy of TRW Systems)

Some of the propellants which have been considered are: hydrogen, helium, neon, nitrogen, argon, krypton, xenon, Freon 14, and methane. System mass and performance are presented in Appendix B. The only power requirement is that for instrumentation and valve actuation. Appendixes C and D present reliability and cost considerations, respectively.

The vast number of flight inert gas systems prohibits a complete list of system characteristics. Some system characteristics are presented in Table A-1. Many inert gas systems have several years of flight experience. The *Mariner* type system has been in use for nearly 10 yr.

Areas for future development are restricted to component reliability improvements. Valve leakage rates of 2 to 10-cc/h are considered typical. The *Mariner* system is designed with an expected 5 cc/h leakage rate. Brazed-in-place connections are currently state of the art and will be used widely in the future. System and component redundancy concepts will undergo increased exploration.

II. Gas Systems: Tridyne

One of the serious drawbacks of the inert gas system is its low specific impulse, which results in large quantities of propellant and excessive tankage. The Tridyne concept was conceived during an attempt to reduce the required tankage mass. The specific impulse of the Tridyne gas mixture will greatly exceed that of cold nitrogen, while the gas density is almost the same as that of nitrogen. The Tridyne mixture (patented by Rocketdyne, Division of North American Rockwell Corp.) is 85% nitrogen, and the remaining 15% a stoichiometric mixture of hydrogen and oxygen. The feed system utilized in the Tridyne system is the same as the inert gas system. The Tridyne thruster contains a catalyst that causes the hydrogen and oxygen to combine exothermically. In order to minimize thrust buildup time and reduce thermal losses, it is desirable to maintain the catalyst bed at approximately 600°F. This can be accomplished through the use of a 1.5-W heater. Theoretically, the temperature of the gas mixture in the chamber should be approximately 1500°F. However, due to unavoidable heat losses, the actual temperature is approximately 1300°F.

The Tridyne mixture is favorable for the following reasons:

(1) Mixture will not allow propagation of a detonation wave.

(2) Mixture has near-optimum ideal gas molecular weight for a gas system.

(3) The ignition of the hydrogen-oxygen mixture is well known from past programs.

(4) Gas mixture is compatible with spacecraft materials.

(5) Adiabatic flame temperature is moderately low to prolong catalyst life.

The typical Tridyne system is shown in Fig. A-4. The feed system components are exactly the same as those discussed in the inert gas system. The Tridyne thruster is under development at Rocketdyne, Division of North

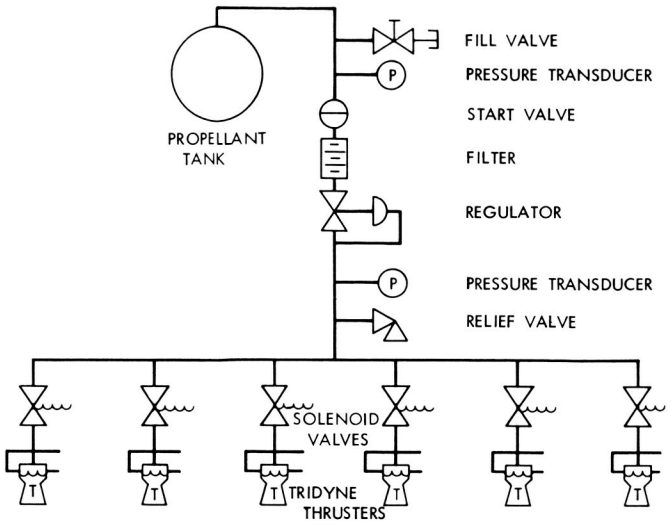

Fig. A-4. Typical Tridyne auxiliary propulsion system

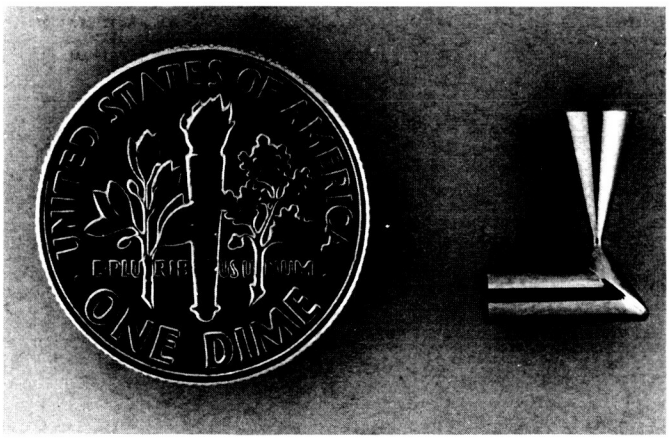

Fig. A-5. Tridyne thruster

American Rockwell. This thruster is shown in Fig. A-5. The design requirements are listed in Table A-2 (Ref. 11).

Since this system is presently under development, finalized thruster performance data are not yet available. The system has not yet been flight qualified. System integration will rapidly follow completion of the preliminary thruster development phase.

Completion of testing on the preliminary design will be essential to development of this concept. A design which features a cluster of three nozzles has been proposed. Its fabrication and testing are a large factor in system development. The problems of catalyst selection and thruster configuration have been solved; however,

Table A-2. Tridyne system data

Parameters	Requirement
Vacuum thrust, lbf	0.01 ± 0.002
Expansion area ratio	100:1
Chamber pressure, psia	15-30
Specific impulse, lbf-s/lbm	143
Impulse bit, lb-s × 10^4	2.0 ± 0.4
Valve excitation time, ms	20
Thrust response time, ms	
From signal to 2% chamber pressure	6
From signal to 90% chamber pressure	8
Nominal pulse width	20
Thrust decay times, ms	
Off signal 10% chamber pressure	8
Power, W/cluster	1.5

additional experimental work will be necessary to refine the heater power requirements in various thermal environments.

III. Liquid Systems: Vaporizing Liquid

The vaporizing liquid system is characterized by a liquid propellant pressurized by its own equilibrium vapor pressure and the expulsion of this vapor through a nozzle. While no great improvements over inert gas specific impulse can be obtained, considerable savings in tank mass result from the propellant's high density and low pressure. Thermal storage heat transfer is the preferred method of liquid vaporization, since the addition of heat by electrical or radioisotope sources results in an increased system mass and complexity. The required duty cycle and thrust level may exceed the thermal storage heat transfer rate and fix an upper limit on thrust level and impulse bit.

The mass advantages of the vaporizing liquid systems over the inert gas systems are realized at the expense of increased complexity. Zero-g feed systems must be capable of providing completely vaporized and regulated gas. A typical zero-g 3-axis stabilized system is presented in Fig. A-6. Since the propellant is selected for its high vapor pressure, it acts as its own pressurant. The propellant is fed to the vaporizer, which is designed to operate in a zero-g environment. The vaporizer is designed to accommodate liquid, gas, or mixed phase flow. Flow into the vaporizer and plenum is regulated by a pressure switch and control valve. The thruster-valve configuration is similar to that of the inert gas system. Again, variations on this baseline will exist from system to system. For example, the Avco feed system consists of a preplenum

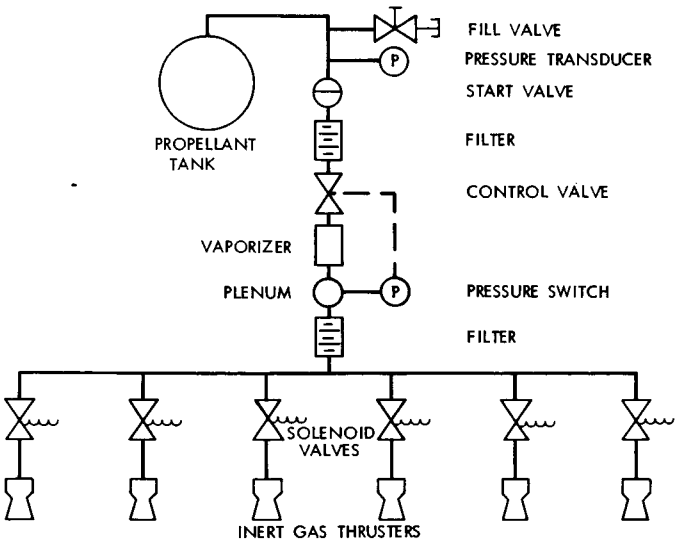

Fig. A-6. Typical vaporizing liquid auxiliary propulsion system

and plenum combination, whereas the TRW system has a plenum only.

Propellant selection is more complex for vaporizing liquid systems than for inert gas systems. The following points must be balanced:

(1) Liquid vapor pressure must be sufficiently high to allow plenum pressure in excess of 10 psia, yet low enough to allow light propellant tankage (500 psia or less).

(2) Vapor should have low molecular weight.

(3) Low heat of vaporization is necessary to minimize the requirement for additional heater mass.

(4) Compatibility of propellant and spacecraft structure materials is required.

(5) High heat capacity of liquid is required to allow high thermal storage capability of liquid.

To date ammonia is the most widely used propellant for vaporizing liquid systems. It has a high vapor pressure, low vapor molecular weight (high I_{sp}), and high heat capacity. It is compatible with most spacecraft materials and has a relatively low heat of vaporization. Ammonia undergoes a dissociation at 1500°F, and when a cold ammonia feed system is coupled with a propellant heater, large improvements in system performance can be realized. Propane, however, has a more favorable heat of vaporization, requiring one third the heat to vaporize the liquid. In a system seriously constrained by duty cycle and thrust level, propane may be an improvement over ammonia. System mass and performance, reliability, and cost are considered in Appendixes B, C, and D, respectively.

Several vaporizing ammonia systems have been designed, including a variety of systems developed by Avco, TRW, GE, and Philco Ford.

General Electric has developed two vaporizing ammonia systems: one was developed under contract to the Naval Research Laboratory (NRL). This system (Ref. 12) vaporizes the liquid from a flat wick interface (Fig. A-7). The wicking action is incorporated for zero-*g* service. Low temperature gradients across the tank wick interface result in low heat transfer rates. The other system was developed under contract to JPL. This system (Ref. 13) was designed in an effort to increase feed system heat transfer rates and system efficiency (Fig. A-8). It was later modified for an *Applications Technology Satellite* (ATS) proposal effort. This feed system employs an orifice to reduce feed temperature and pressure. The NRL sponsored feed system has been flight-qualified and flown. The JPL sponsored system has not been tested in flight but its system capability has been proven. This feed system can provide an ammonia flow rate of 5×10^{-3} lbm/s (70°F).

The TRW concept (Fig. A-9 and Ref. 14) is similar to the GE feed system developed for JPL. The GE orifice and coil heat transfer unit is replaced by a capillary tube heat exchanger attached to the tank wall. System thrust level and duty cycle or required heat transfer rate dictate the required number of capillary tubes. This system has also not been flight-tested. A flow rate of 1 mlbm/s for 300 to 400 s (70°F) has been demonstrated.

Philco Ford and NRL jointly developed a system for use on the NRL *Explorer 30,* which was launched in November 1965. The spacecraft was spin-stabilized and vapor was extracted from the vapor ullage cavity in each tank. A more complete system description is presented in Table A-3.

Avco has devoted considerable effort to the vaporizing ammonia system technology. Five zero-*g* vaporizing ammonia systems (Figs. A-10 and A-11) have been flight-qualified and flown (Refs. 15 and 16). Four of the five systems have been coupled with resistojet thrusters, one flew with an empty fuel tank, and the last of the five systems flew with cold ammonia (i.e., no resistojet thrusters). The inert ammonia system *Lincoln Lab. Experimental Satellite* (LES 6) was launched in September

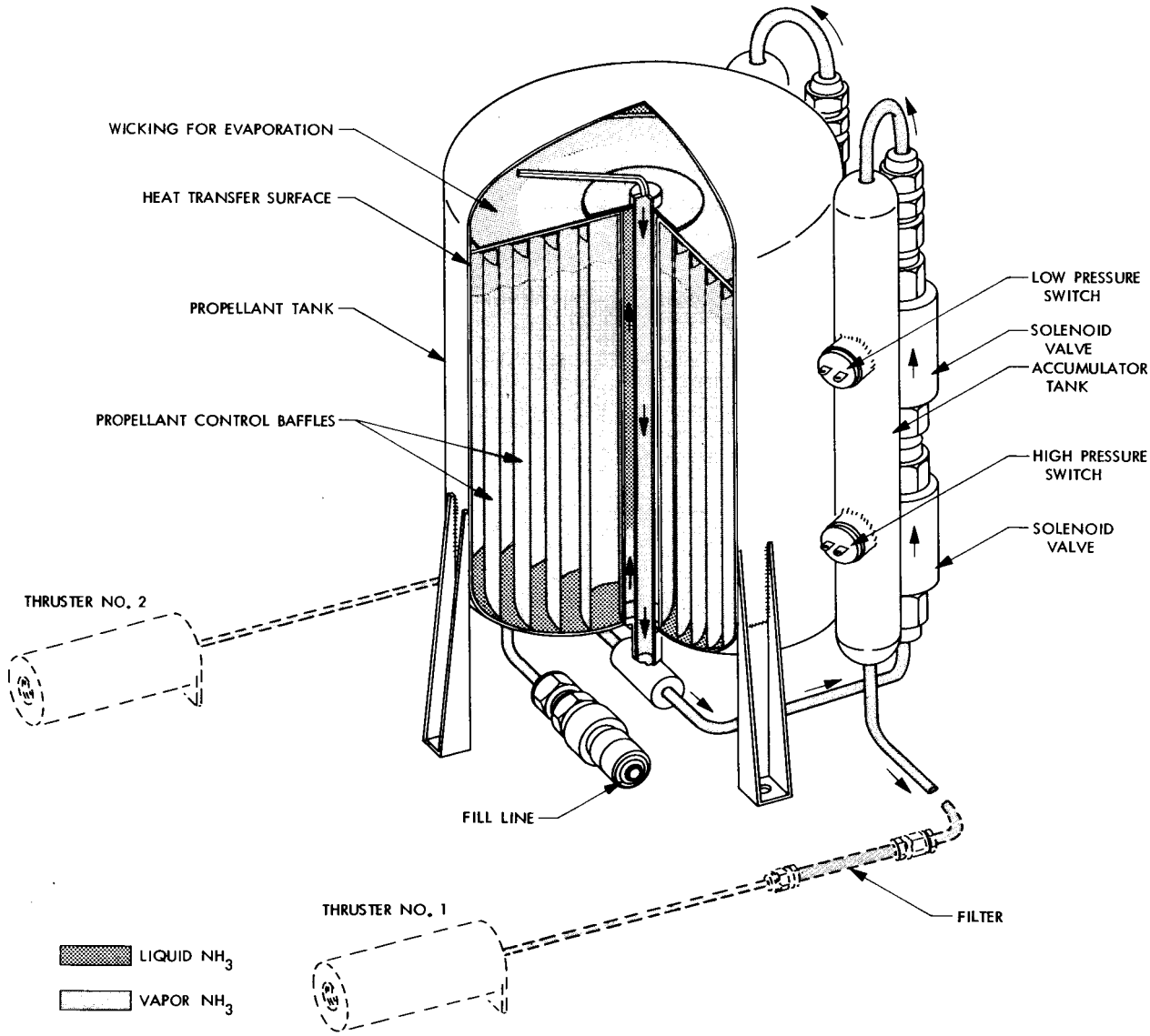

Fig. A-7. Schematic of NRL microthruster system

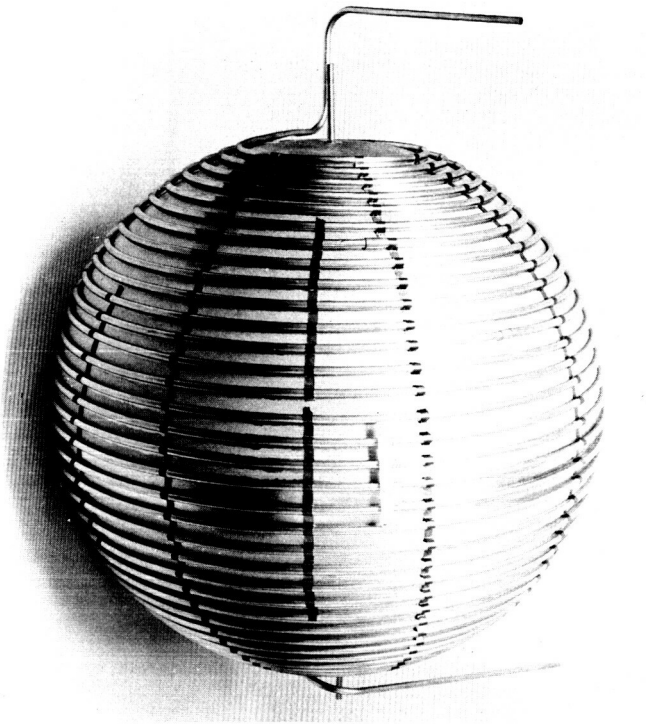

Fig. A-8. Feed system storage tank with vaporizer brazed to exterior surface (photo courtesy of GE)

Table A-3. NRL vaporizing ammonia system[a] requirements

Parameters	Requirements
Propellant	Anhydrous ammonia
Thrust level, lbf	0.020 to 0.070
Specific impulse, $\frac{\text{lbf-s}}{\text{lbm}}$	70 to 90
Total impulse, lbf-s	~ 1000
Power requirements, W	3 (max)
Total system weight, lbm	15

[a]Developed by Philco Ford, Newport Beach, Calif.,for NRL.

1968. It performed its orbital pulse-mode station-keeping job satisfactorily. After one year of space storage, the system was reactivated and resumed station-keeping activity. The system had 12 lb of propellant and delivered a specific impulse of 105 lbf-s/lbm. In addition to these six flight systems, another three are under qualification for future application.

The technology of liquid ammonia propulsion systems can be considered state of the art. Possible areas of improvement could be in the areas of optimum system packaging and zero-g heat transfer.

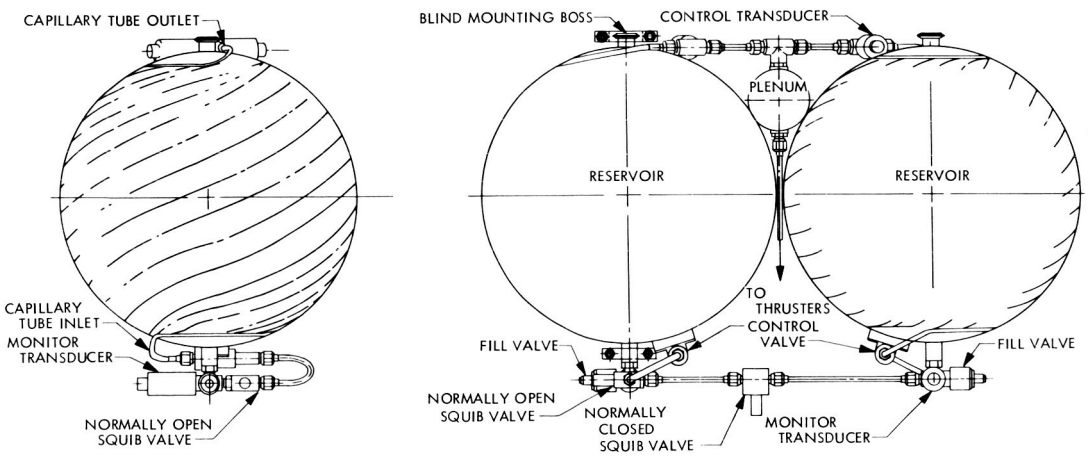

Fig. A-9. TRW Systems vaporizing liquid feed system

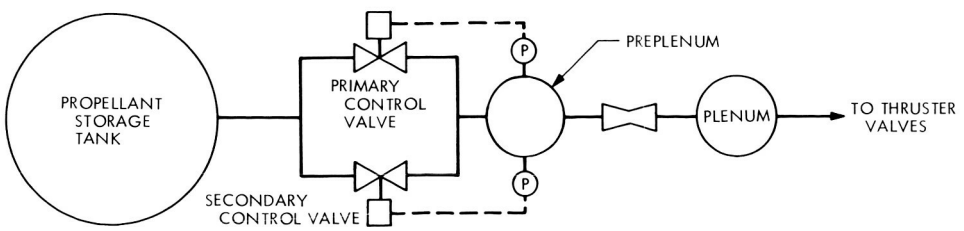

Fig. A-10. Avco ammonia feed system

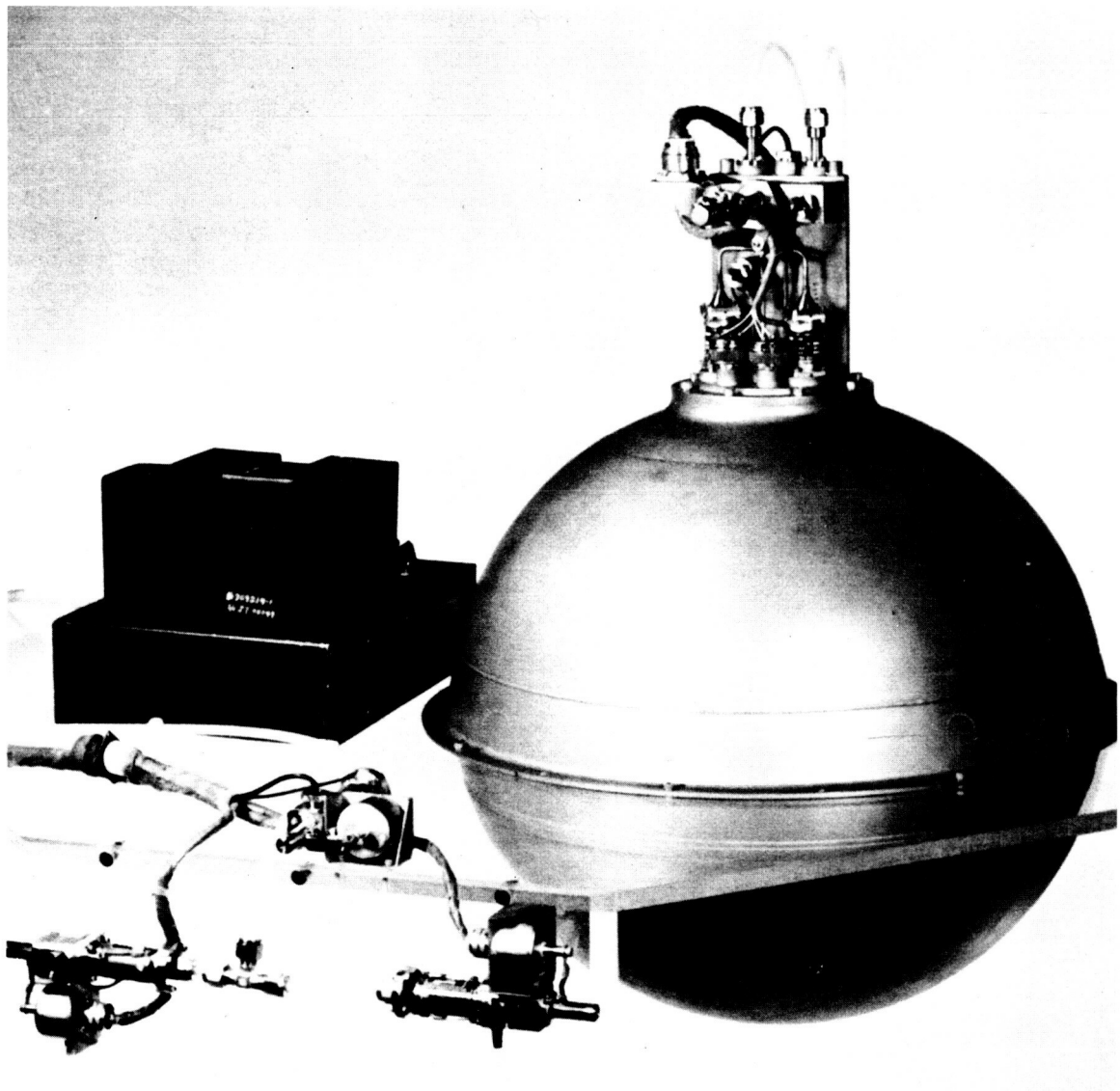

Fig. A-11. Three thruster assemblies shown with propellant storage and feed system and system electronics (photo courtesy of Avco)

IV. Liquid System: Monopropellant Hydrazine

There are three distinct and different concepts of monopropellant hydrazine thrusting systems: expulsion of gases from direct thermal decomposition, expulsion of gases from direct catalytic decomposition, and plenum storage of the decomposition products for later gas expulsion. All three utilize an exothermic chemical reaction to aid the decomposition of hydrazine. The cause of initial chemical decomposition differentiates between the resistojet and catalytic systems. Early hydrazine thrusters relied on heaters to initiate decomposition and heat the H-7 catalyst. Thereafter, the heated H-7 catalyst caused the spontaneous decomposition of the fuel. A reappraisal of this technique of hydrazine decomposition is under way. The rapid growth of hydrazine as a monopropellant fuel results from the development of the Shell 405 catalyst, which spontaneously and repeatably initiates the decomposition of the fuel (Ref. 17). The Shell 405 catalyst is used in both the direct catalytic and plenum systems. The combustion products are expelled from the catalyst bed to space in the direct catalytic system, while the gases are stored in a plenum chamber in the hydrazine plenum system. Hydrazine is attractive as an auxiliary propulsion system propellant for the following reasons:

(1) Combustion gas has low molecular weight (10 to 18).

(2) Decomposition is exothermic.

(3) Decomposition temperature is low enough to prolong catalyst and thrust chamber life (adiabatic gas temperature of 1100 to 2500°F).

(4) Relatively high-density liquid minimizes tankage mass.

(5) Compatible with most spacecraft structure materials.

(6) Not shock-sensitive.

(7) Decomposition may be initiated by spontaneous catalyst (e.g., Shell 405), or thermal heater.

The resistojet and direct catalytic systems have identical feed systems consisting of a pressurization system, propellant tank, expulsion device, start valve, filter, control valve, and fill valve. In spinning spacecraft, expulsion devices are not necessary.

Two modes of propellant tank pressurization are commonly used. The first mode utilizes the storage of a high-pressure gas in a tank external to the propellant tank. Upon demand, the gas is fed from the storage vessel through a regulator to the propellant tank. The other common method stores all of the pressurant gas (at a preselected but relatively low storage pressure) in the propellant tank. In this mode, commonly referred to as the blow-down mode, the propellant tank pressure varies with propellant usage. This system eliminates the use of separate pressure tanks and regulators; however, the propellant pressure is no longer fixed. The selection of ullage volume will fix the pressure decay, and thus, the thrust decay. For purposes of this report, an ullage volume of 50% has been selected (volume propellant = volume pressurant). The operating pressure range is, therefore, initial pressure to one half initial pressure. The direct catalytic system is characterized by either a pressure-regulated or "blow-down" hydrazine feed system and a catalytic (e.g., Shell 405) thrust chamber assembly (Fig. A-12). The resistojet system is similar, with the catalytic thrust chamber being replaced by a modified resistojet (lower heater temperature). Typical direct hydrazine systems are schematically shown in Fig. A-13. The hydrazine plenum system is different from the direct systems (Fig. A-14). The hydrazine flow is regulated into a catalytic bed, where the decomposition gases are exhausted into a plenum. Hydrazine flow is regulated by the plenum pressure. Either capillary tube pressure drop (passive), or pressure switch-control valve (active) techniques may be used for plenum pressure control. The flight systems may not contain all the components described in the baseline system. Performance and mass, reliability, and cost are covered in Appendixes B, C, and D, respectively.

A large number of hydrazine systems have been flight-qualified and flown. Both Hamilton Standard and Rocket Research have flight-qualified spectrums of low-thrust catalytic engines. TRW, Marquardt, and Aerojet-General each have developed several low-thrust catalytic thrusters. Rocket Research and TRW have worked on hydrazine plenum systems. Avco and TRW are presently developing thermal decomposition thrusters.

Hamilton Standard has developed a number of low-thrust catalytic thrusters, some of which are shown in Fig. A-15. Table A-4 describes some of their typical hydrazine/Shell 405 monopropellant flightweight rocket engines (Ref. 18). Figure A-16 presents the effect of pulse mode operation on performance on a 5-lbf thruster. The 5-lbf engines have been flight-qualified and successfully operated in space onboard the ATS III and IV. The development of the Hamilton Standard 0.1 lbf engine was initially for a classified project, and no flight data are available.

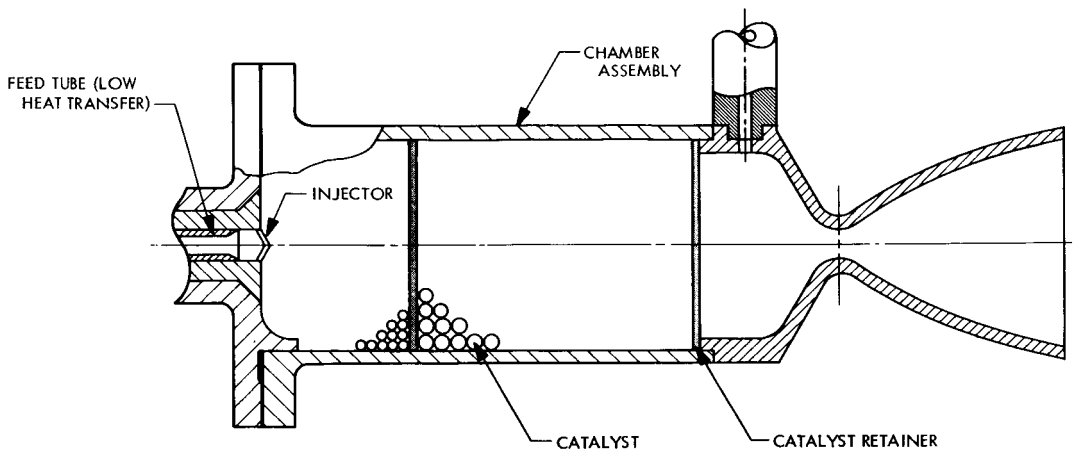

Fig. A-12. Typical catalytic thrust chamber

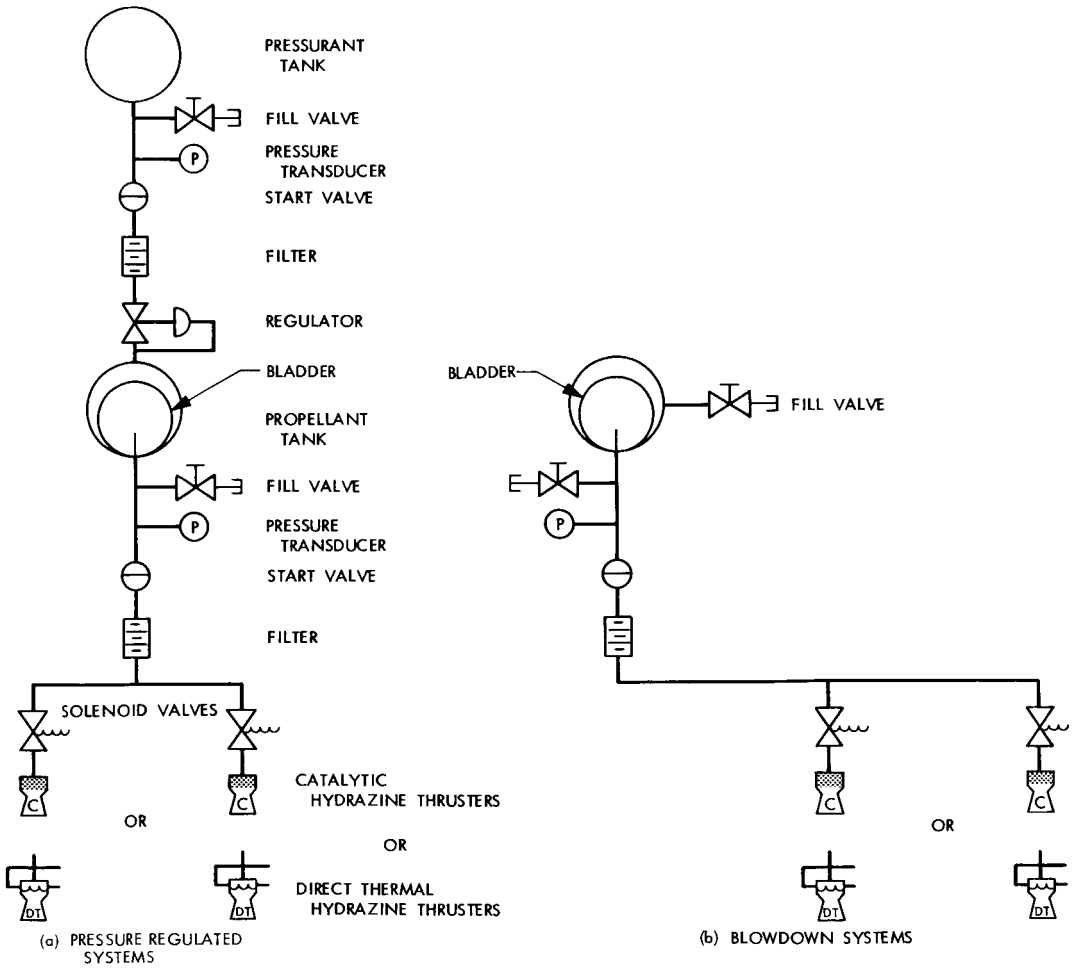

Fig. A-13. Typical direct hydrazine auxiliary propulsion systems

Table A-4. Hamilton standard hydrazine/shell 405 thruster data

Thrust, lbf	Designation	Chamber pressure, psia	Expansion area ratio, ϵ	Specific impulse, $\frac{\text{lbf-s}}{\text{lbm}}$	Valve and thruster weight, lbm	Status
0.05		150	sea level	195	0.4	
0.1	REA-10	140	sea level	200	0.49	34,573 s and 130,603 pulses
1.0	REA-17	160	40	215	0.7	4,150 s and 215,000 pulses
2.0	REA-6	150	sea level	217	0.8	
3.3	REA-6	150	30	219	0.85	
5.0	REA-16	110	55	225	0.76	—[a]
5.0	REA-16	110	55	225	0.98	Initial Defense Communication Satellite Program (IDCSP)
5.0	REA-18	110	55	225	0.76	
5.0	REA-21	68	50	225	0.98	—[b]

[a]ATS III—5 min steady state and 20,000 pulses in space; ATS IV—41 min steady state in space.
[b]Intelsat IV—600,000 pulses and 650 min steady state during endurance test.

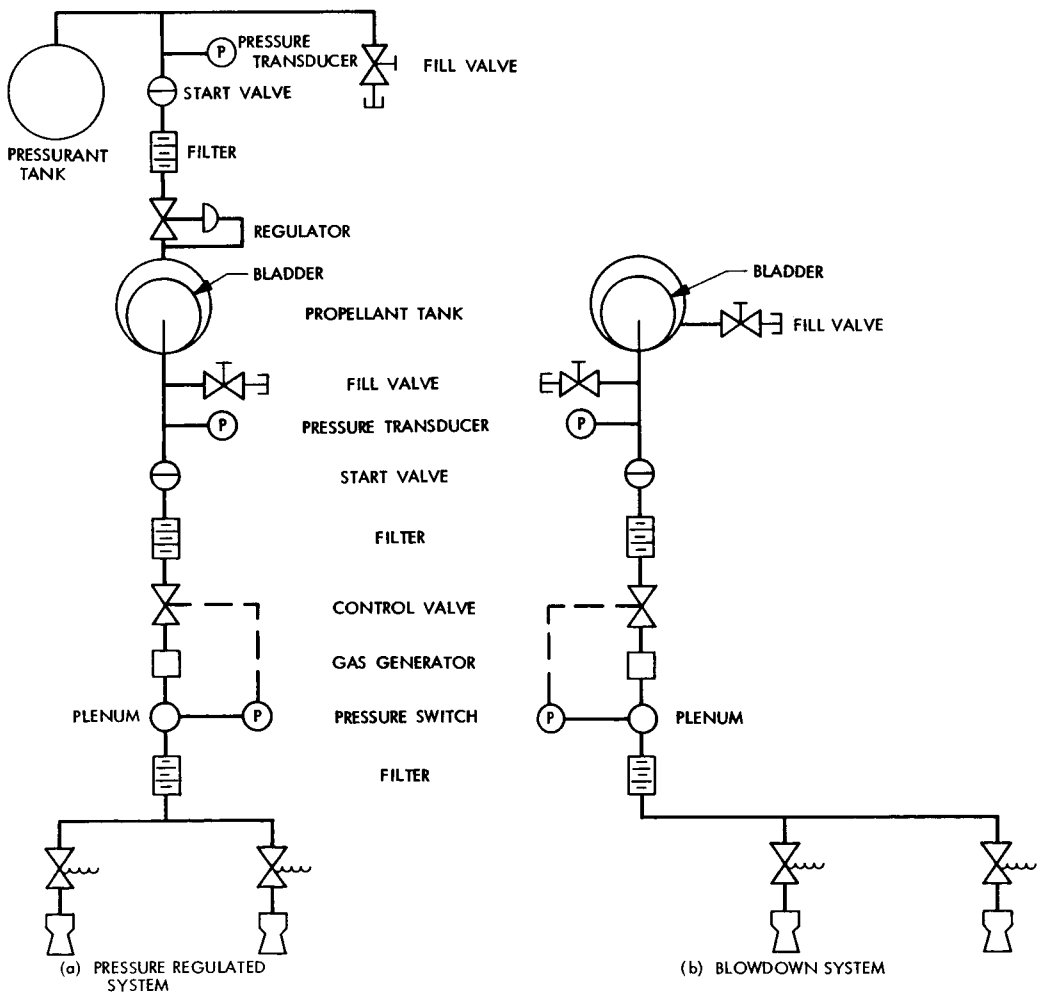

Fig. A-14. Typical hydrazine plenum auxiliary propulsion systems

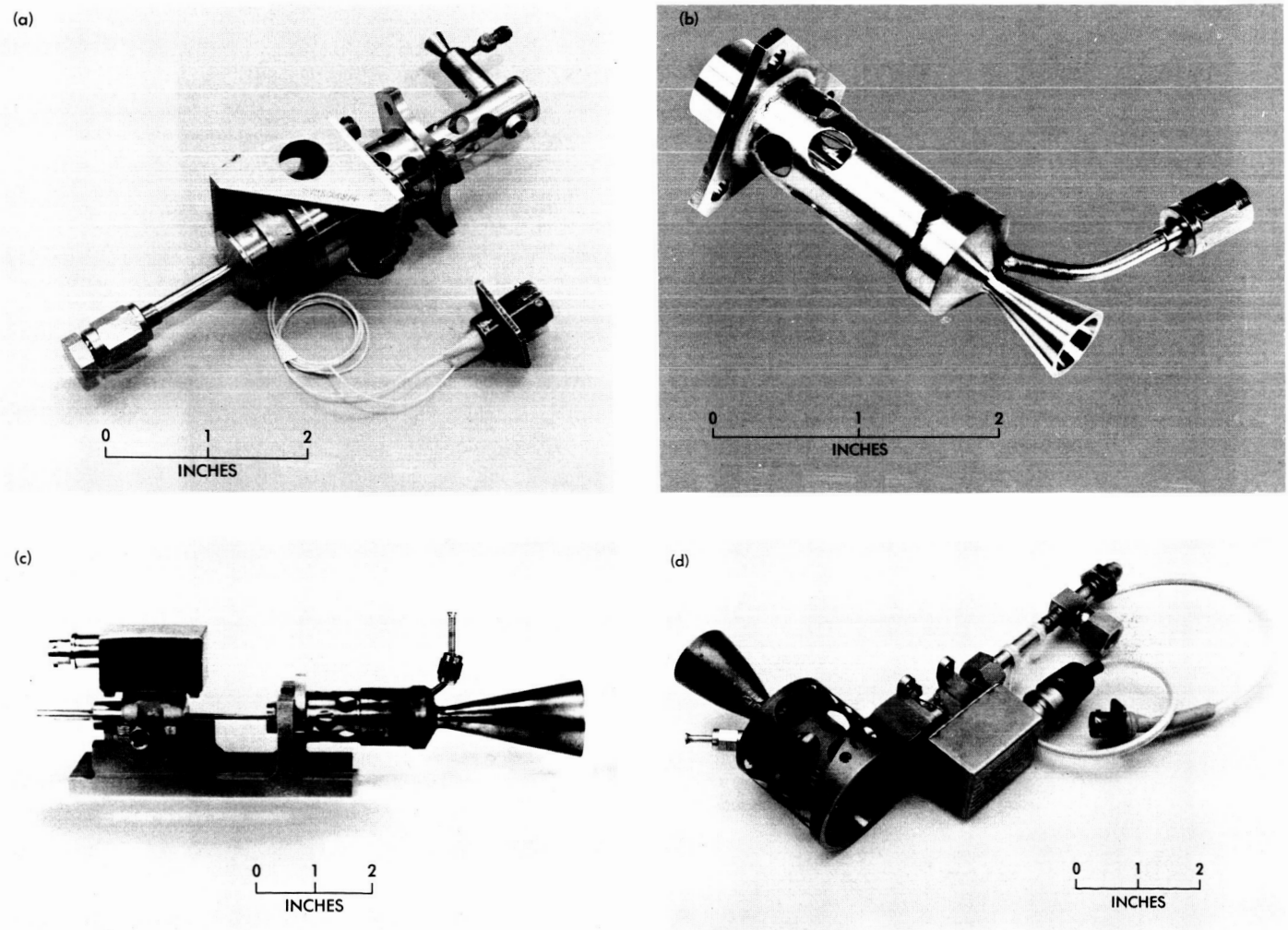

Fig. A-15. Typical Hamilton Standard flight weight catalytic hydrazine thrusters; (a) 0.1 lbf, (b) 1.0 lbf, (c) IPCSP/A and NATOSAT 5 lbf, (d) *Intelsat IV* 5.8 lbf (photos courtesy of Hamilton Standard)

Rocket Research has also developed a number of low-thrust catalytic thrusters, some of which are shown in Fig. A-17. Rocket Research monopropellant hydrazine engine performance and mass numbers are presented in Table A-5.[6] The data in Table A-5 are, again, considered representative of the Rocket Research technology status. The development of the hydrazine propulsion module (MR-6A) has led to the delivery of at least 39 engines to a classified project. No flight data are available; the continued delivery, however, of flight units with little comment implies successful operation.

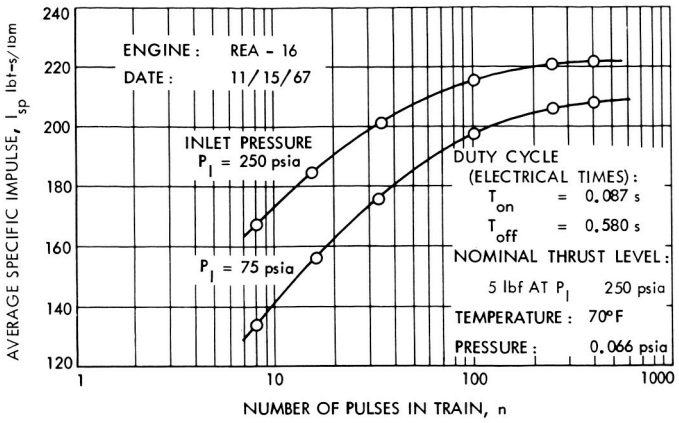

Fig. A-16. Average vacuum specific impulse vs number of pulses

The Marquardt Corporation has developed three low-thrust catalytic engines with thrust levels of 0.1, 1, and 5 lbf, respectively. These engines are shown in Figs. A-18 and 19. Performance data are listed in Table A-6 (Refs. 19 and 20). None of these thrusters have flown yet; however, the 5-lbf engine has undergone life testing in excess of 1,000,000 cycles.

The TRW has developed several low-thrust monopropellant hydrazine engines. Two of them are the 0.5-lbf

[6]Data supplied by B. Schmidt, Rocket Research, Redmond, Wash.

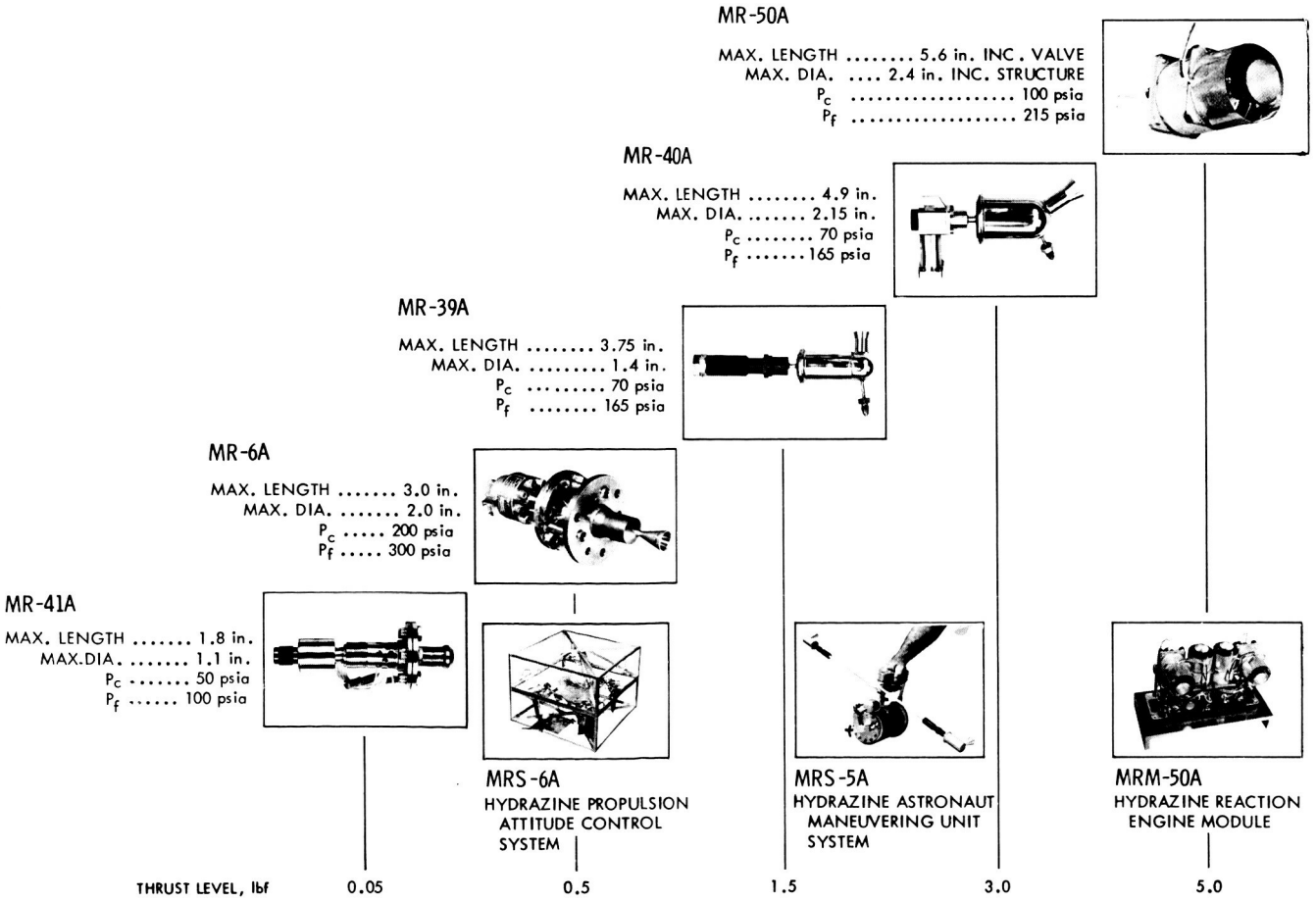

Fig. A-17. Rocket Research Corp. monopropellant hydrazine engines and propulsion systems (photos courtesy of Rocket Research Corp.)

and *Intelsat III* thrusters shown in Figs. A-20 and A-21. The performance of these thrusters is presented in Table A-7 (Refs. 21 and 22). Included in Fig. A-22 is the effect of cold bed pulsing on performance. The ½-lb engine has been cycled 1,000,000 times during life testing. The *Intelsat III* engines have performed well on all the satellites in orbit. East-west station keeping is done by pulsed mode operation of these engines.

Table A-5. Rocket Research catalytic hydrazine thruster data

Thrust, lbf	Designation	Chamber pressure, psia	Expansion area ratio, ϵ	Specific impulse, $\frac{\text{lbf-s}}{\text{lbm}}$	Valve and thruster weight, lbm	Status
0.05	MR-41A	50	50	195	0.498	100,000 cycles; 50,000 s
0.1	MR-74	40	4	218.4	—	After 25,000 pulses no change in pulse shape; 16.5 h SS
0.5	MR-6A	200	100	228.9	0.70	
0.5-0.25	MRS-6A	200-100	100	228.9-227.6	0.70	Flight qualified, class flight
1.5	MR-39A	70	30	130[a]	—	
3.0	MR-40A	70	30	130[a]	—	
5.0	MR-50A	100	50	228	1.0	
5.0	MR-26A	200	60	233	1.24	
5.0	MR-34A	200	100	233	0.88	
5.0	MR-13A	200	1.5	175[b]	—	Delivered to LTV

[a]50% hydrazine, 50% water mixture.
[b]Sea level.

Table A-6. Marquardt hydrazine thruster data

Thrust; lbf	Designation	Chamber pressure, psia	Expansion area ratio, ϵ	Specific impulse, $\frac{\text{lbf-s}}{\text{lbm}}$	Valve and thruster weight, lbm	Status
0.1	R 25 A	100	50	220	0.45	
1	—	100	50	225	0.66	
5	R 13 D	100	50	225	1.6	1,000,000 cycles

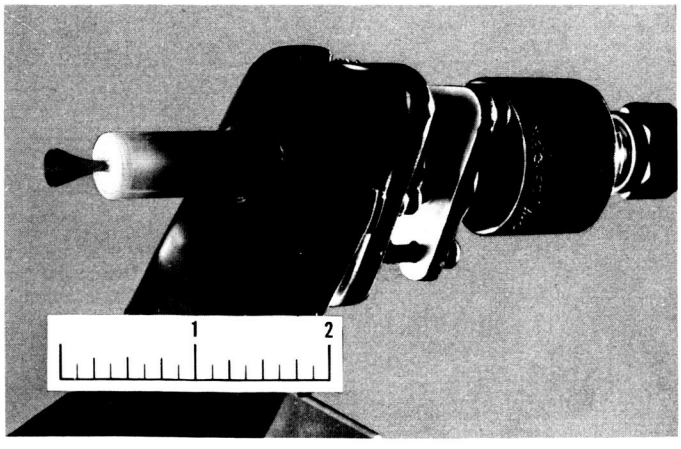

Fig. A-18. Monopropellant rocket engine (1/10 lb thrust) on test (photo courtesy of the Marquardt Corp.)

Table A-7. TRW catalytic hydrazine thruster data

Thrust, lbf	Designation	Chamber pressure, psia	Expansion area ratio, ϵ	Specific impulse, $\frac{\text{lbf-s}}{\text{lbm}}$	Valve and thruster weight, lbm	Status
0.5	Half-pound	100	50	220	1.7	1,000,000 cycles
4.0-0.8	*Intelsat*	275 (max)	50	229 (max)	0.62	Flight proven on *Intelsat III*

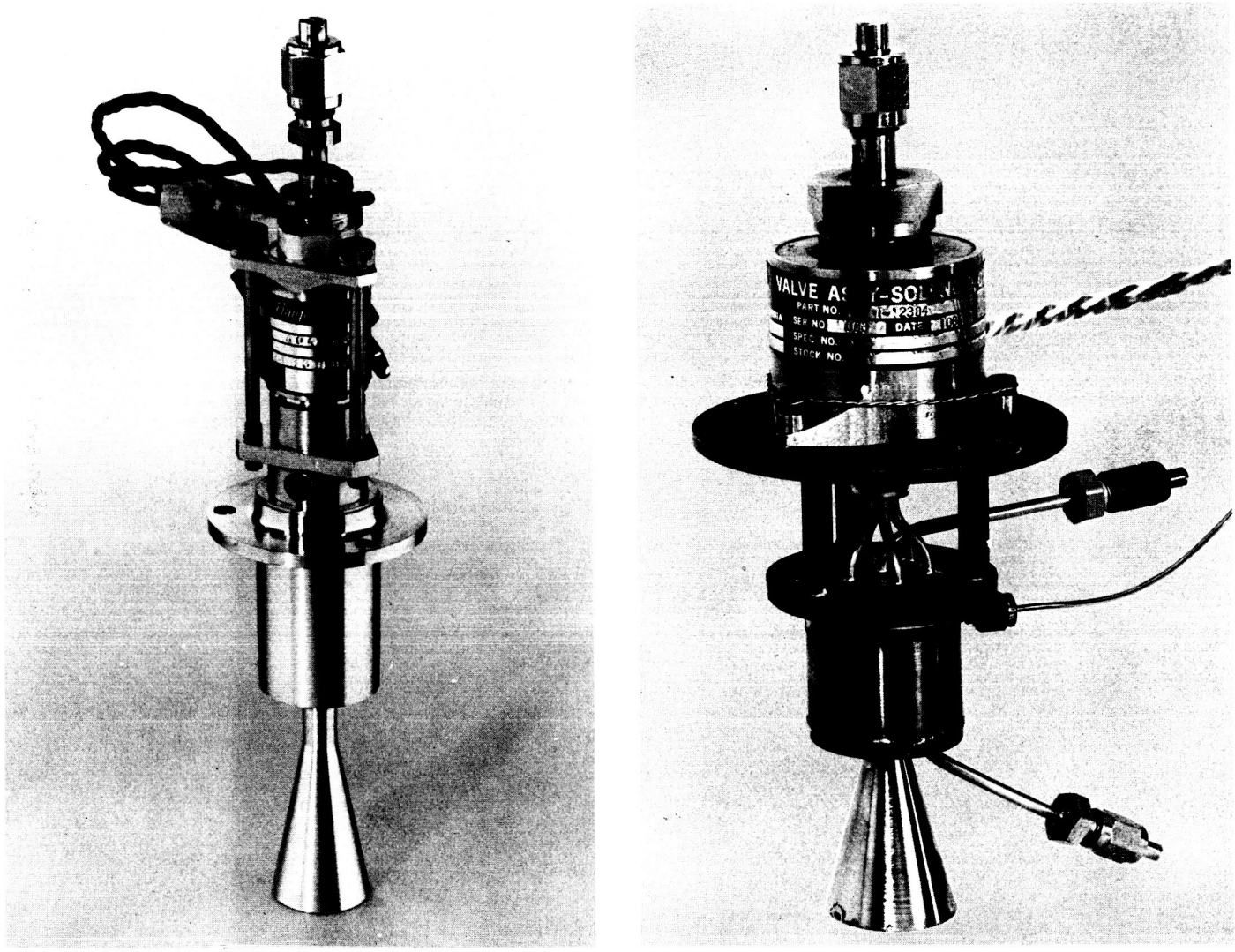

Fig. A-19. Marquardt 5-lbf catalytic hydrazine thrusters (photos courtesy of the Marquardt Corp.)

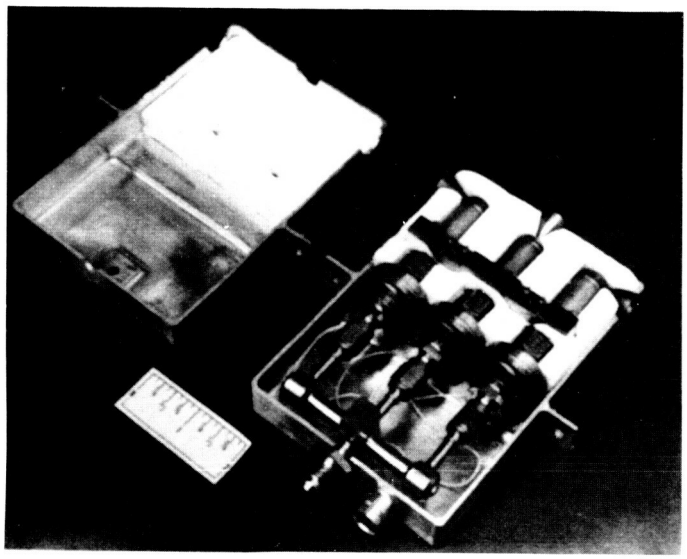

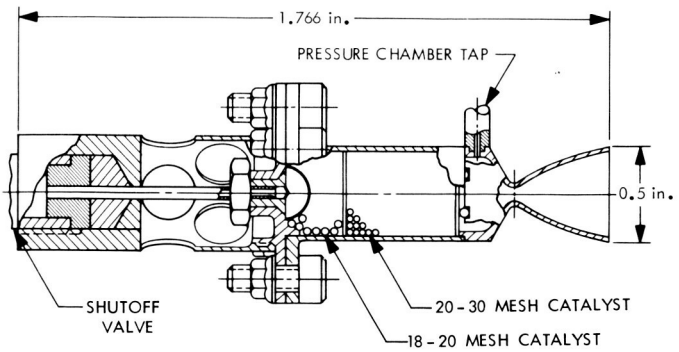

Fig. A-20. TRW Systems 0.5-lbf catalytic hydrazine thruster (photo courtesy of TRW Systems)

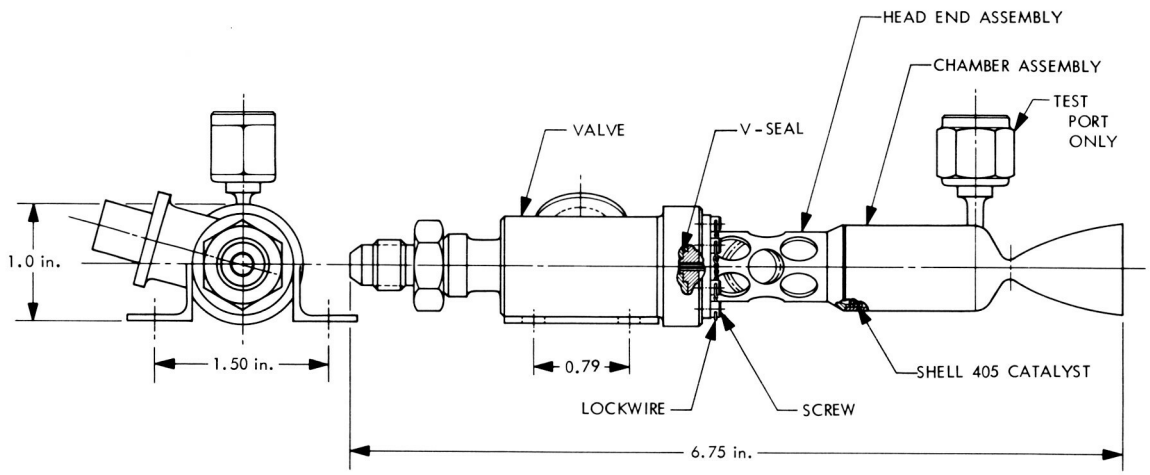

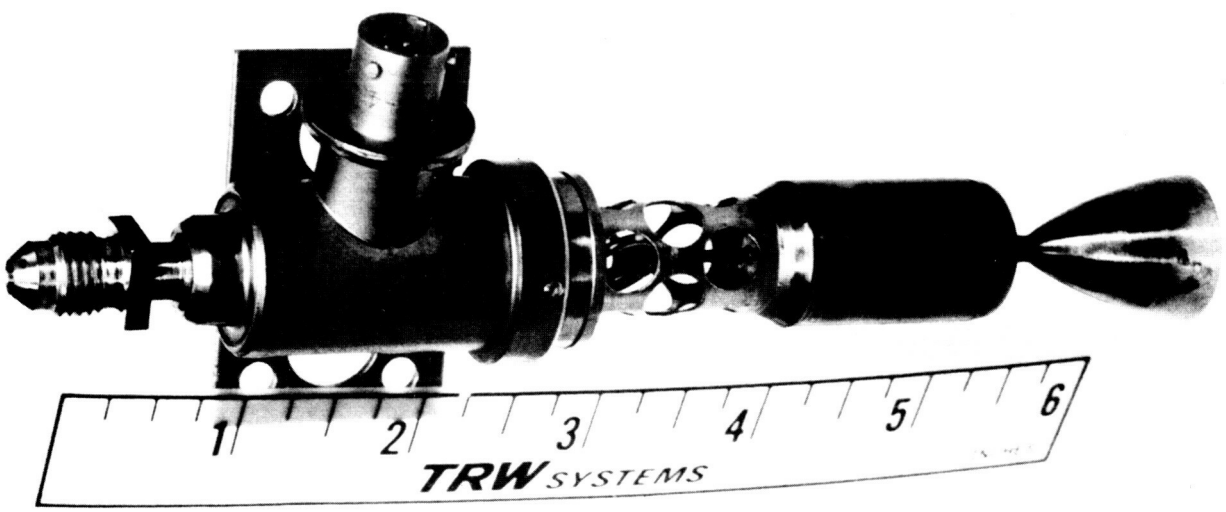

Fig. A-21. TRW Systems Intelsat III catalytic hydrazine thruster (photo courtesy of TRW Systems)

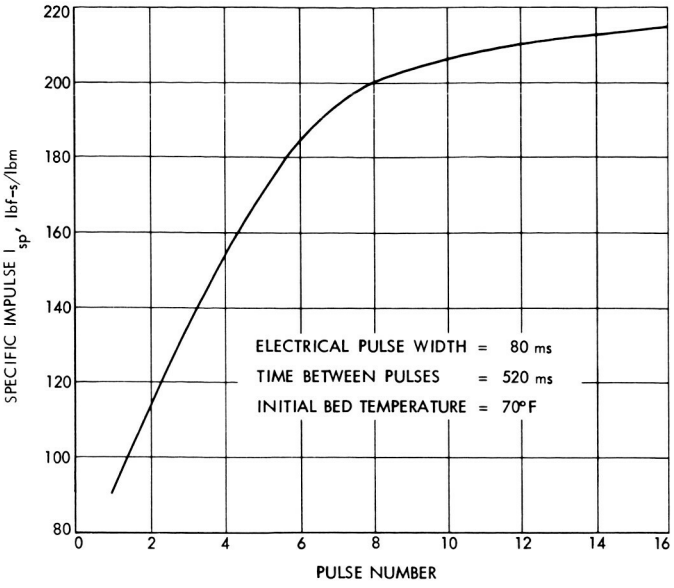

Fig. A-22. Average specific impulse per pulse as a function of pulse number

Aerojet-General has entered the low-thrust hydrazine field with a 5-lbf catalytic thruster design (Fig. A-23) (Ref. 23). The performance of this thruster is listed in Fig. A-24. This engine has undergone 204,000 pulses with little pulse degradation or shape change.

Walter Kidde and Co., Inc., an experienced company in early hydrogen peroxide monopropellant systems, has a low-thrust (5 lbf) catalytic hydrazine thruster (Fig. A-25). The performance of this thruster is presented in Table A-8. This thruster is a contender for use aboard the Radio Astronomy Explorer-B Satellite.

The hydrazine resistojet (or hybrid) is currently under development at Avco (Ref. 24) and TRW.[7] In an early investigation of their concept, Avco selected a porous ceramic injector configuration presented in Fig. A-26. Performance of this thruster is also provided in Fig. A-27.

[7]Murch, C. K., TRW Systems, private communication, 1970.

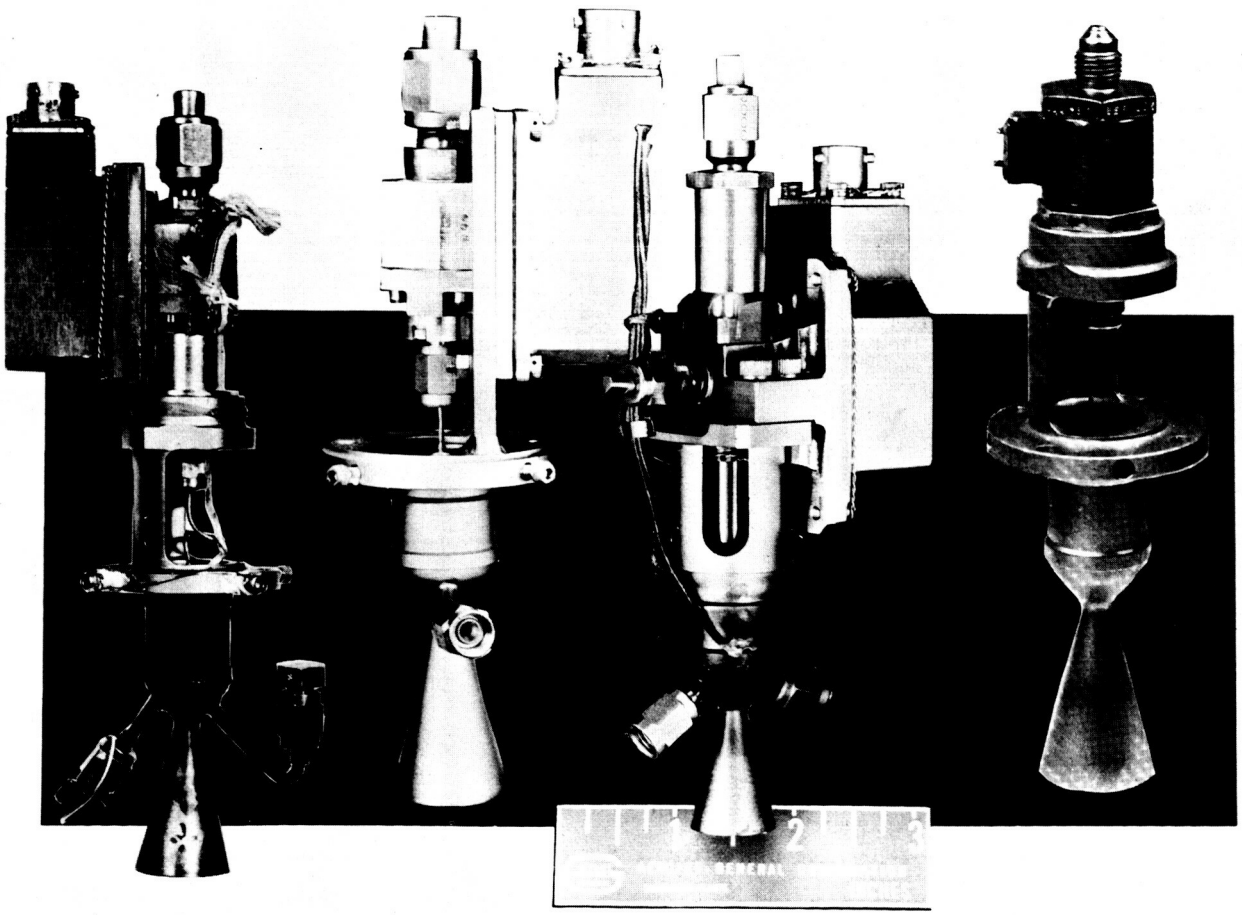

Fig. A-23. Aerojet-General 5-lbf catalytic hydrazine thrusters (photo courtesy of Aerojet-General)

THRUST (VAC)	5 lbf
P_c	150 psia
A_c/A_t	50:1
SPECIFIC IMPULSE	227 s
CATALYST	SHELL 405
PROPELLANT	N_2H_4
BED LOADING	0.05 $lb/in.^2$-s

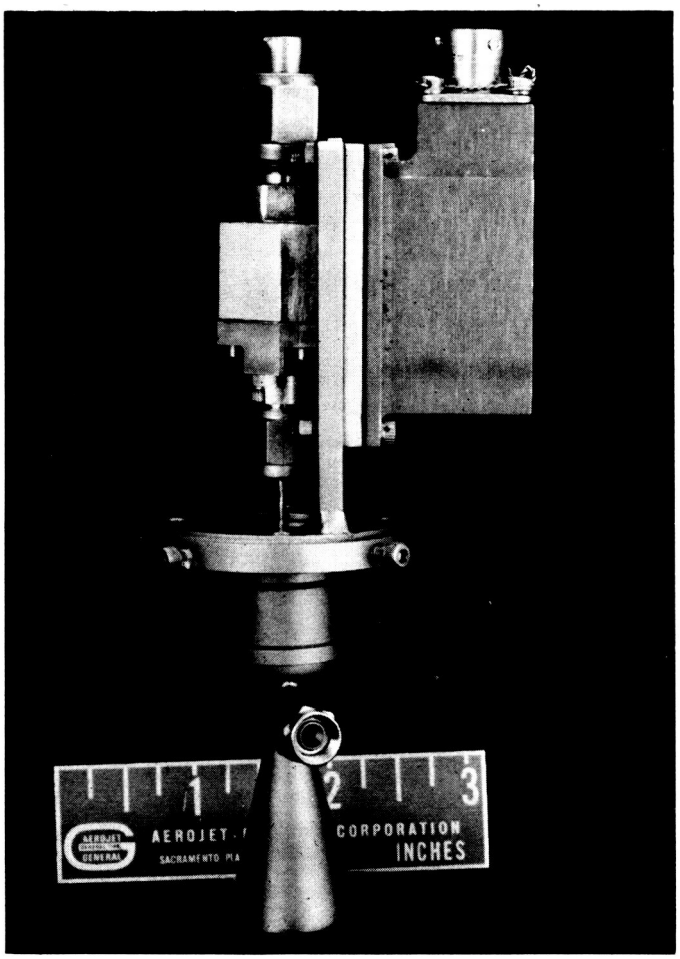

Fig. A-24. Aerojet-General 5-lbf catalytic hydrazine thruster (photo courtesy of Aerojet-General Corp.)

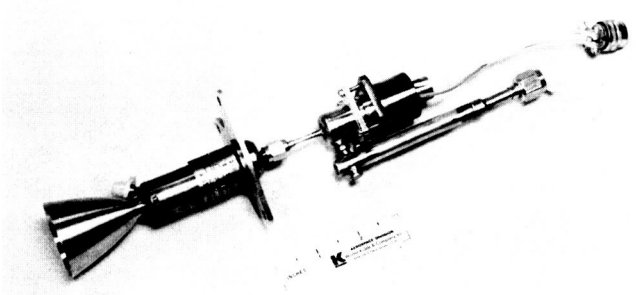

Fig. A-25. NASA-Lewis 5-lb thrust hydrazine engine (photo courtesy of Walter Kidde and Co., Inc.)

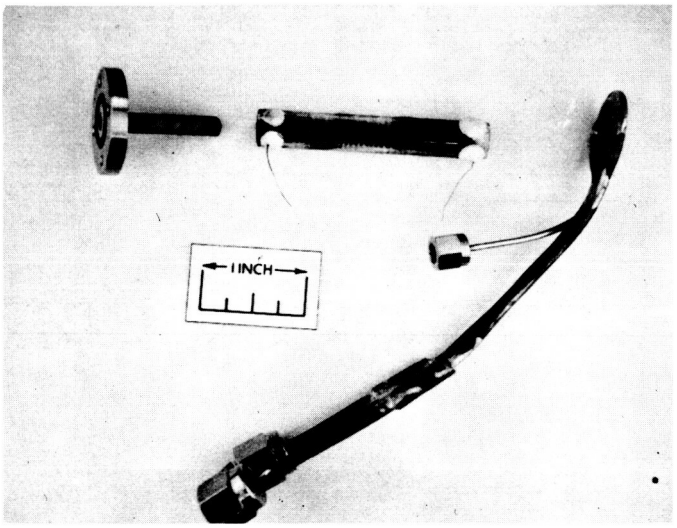

Fig. A-26. Wire coil thruster (porous ceramic injector) (upper left) (photo courtesy of Avco)

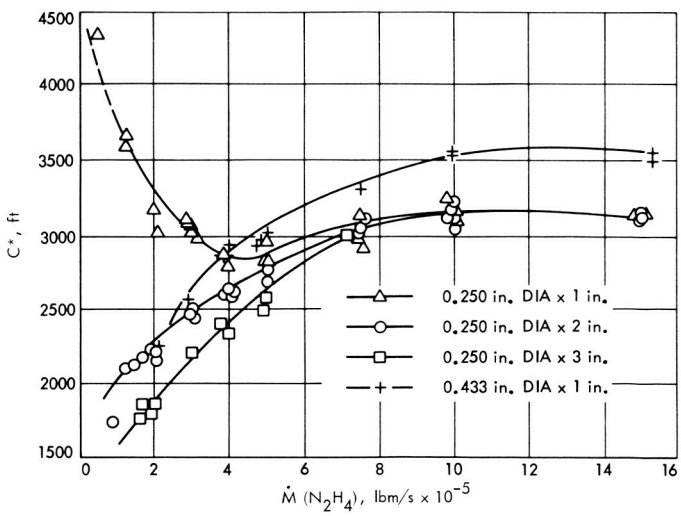

Fig. A-27. Avco thruster performance (unpowered)

Improvements in performance were noted with the addition of ¾ in. of quartz felt to the quartz chamber. Table A-9 presents the performance of the 1-in. quartz chamber. In a followon contract with NASA-Goddard, Avco has investigated this system in greater detail. The most recent results suggest a sustained steady state specific impulse of 210 lbf-s/lbm with no power addition (17 mlbf) and a specific impulse of 193 lbf-s/lbm at a power to thrust ratio of 2 W/mlbf (10 mlbf). This thruster has also undergone pulse tests with a 1 second on time at 10, 20, and 50% duty cycles.

Table A-8. Walter Kidde hydrazine thruster data

Thrust, lbf	Designation	Chamber pressure, psia	Expansion area ratio, ϵ	Specific impulse, $\frac{\text{lbf-s}}{\text{lbm}}$	Status
5	5-lb	80	50	225	5 h SS

Table A-9. Avco hydrazine resistojet performance data

Thrust, mlbf	$\dot{m}$, lbm/s	Chamber pressure, psia	Power, W	Specific impulse, $\frac{\text{lbf-s}}{\text{lbm}}$	c*	C_F
3.53	1.90×10^{-5}	9.6	0	186	3830	1.56
3.70	1.90×10^{-5}	10.1	12	195	4020	1.56
3.85	1.90×10^{-5}	10.5	12	202	4180	1.56

TRW has completed the preliminary development of a hydrazine resistojet thruster for both pulsed and steady state operation. In order to obtain short, reproducible impulse bits, a concept which utilizes hydrazine vapor as the propellant was developed. This concept employs a propellant vaporizer upstream of the thruster valve for pulsed operation. For steady-state operation, the vaporizer cools sufficiently to allow liquid hydrazine operation of the thruster. Tests have shown that the transition from vapor to liquid hydrazine is both smooth and stable. Development activity has been concentrated in the range of 0.005–0.015 lbf. A 0.010-lbf thrust hydrazine thruster has been demonstrated which provides reproducible impulse bits for command pulses as short as 0.020 s. The pulsed mode specific impulse is 180 lbf-s/lbm; steady-state operation results in a delivered specific impulse of 200 lbf-s/lbm. The total power input for a 0.010-lbf thrust system is less than 5 W excluding the valve power.

Hydrazine plenum systems have been developed and flight-qualified by Rocket Research and TRW (Refs. 22 and 25). An early plenum/"sublex" system was designed at Rocket Research for use on a classified project. This system utilized a bed of subliming solid material to cool the decomposition products. The system was flight-qualified, but information on its performance is not available. In a later program, a monopropellant hydrazine plenum system was developed and sent to NASA-Goddard. A diagram of this test module is shown in Fig. A-28. The complete system is shown in Fig. A-29. The pressure control is passive. When the plenum pressure drops lower than a pre-determined value, the pressure difference across the capillary tube upstream of the catalyst bed increases, thus allowing hydrazine to flow into the catalyst. When the pressure in the catalyst bed increases, flow is again restricted. Although this system was not flown, extensive ground tests have proved its capabilities. Plenum systems are, however, limited in their steady-state operation. During a simulation of an ATS F and G mission profile, thermal control problems were encountered. The addition of ammonia to the plenum was required to maintain a cool plenum temperature during a long pulse duty cycle.

TRW has been working on a high-level and low-level thrust system for use on a classified project. The low-level thrusters comprise a hydrazine plenum system, with individually heated thrusters. A diagram of this system is presented in Fig. A-30. A pressure level of 35 ± 1.5 psia is maintained in the plenum with a pressure switch control valve loop. Thruster performance is presented in Table A-10. This system (Model 35 low-level thrusters) is presently under flight qualification.

The field of hydrazine thruster technology has grown rapidly in the past few years. Direct catalytic thrusters have received a great deal of attention and can be considered state of the art. Hydrazine direct thermal (hybrid resistojets) thrusters are still in the early stages of development. Increased effort in the area of pulsed mode operation of these thrusters is needed. Hydrazine plenum

Table A-10. TRW hydrazine plenum system data

Thrust, lbf	Specific impulse, $\frac{\text{lbf-s}}{\text{lbm}}$	Propellant	Catalyst	Plenum pressure, psia
0.029	114-132	N_2H_4	Shell 405	35 (nominal)

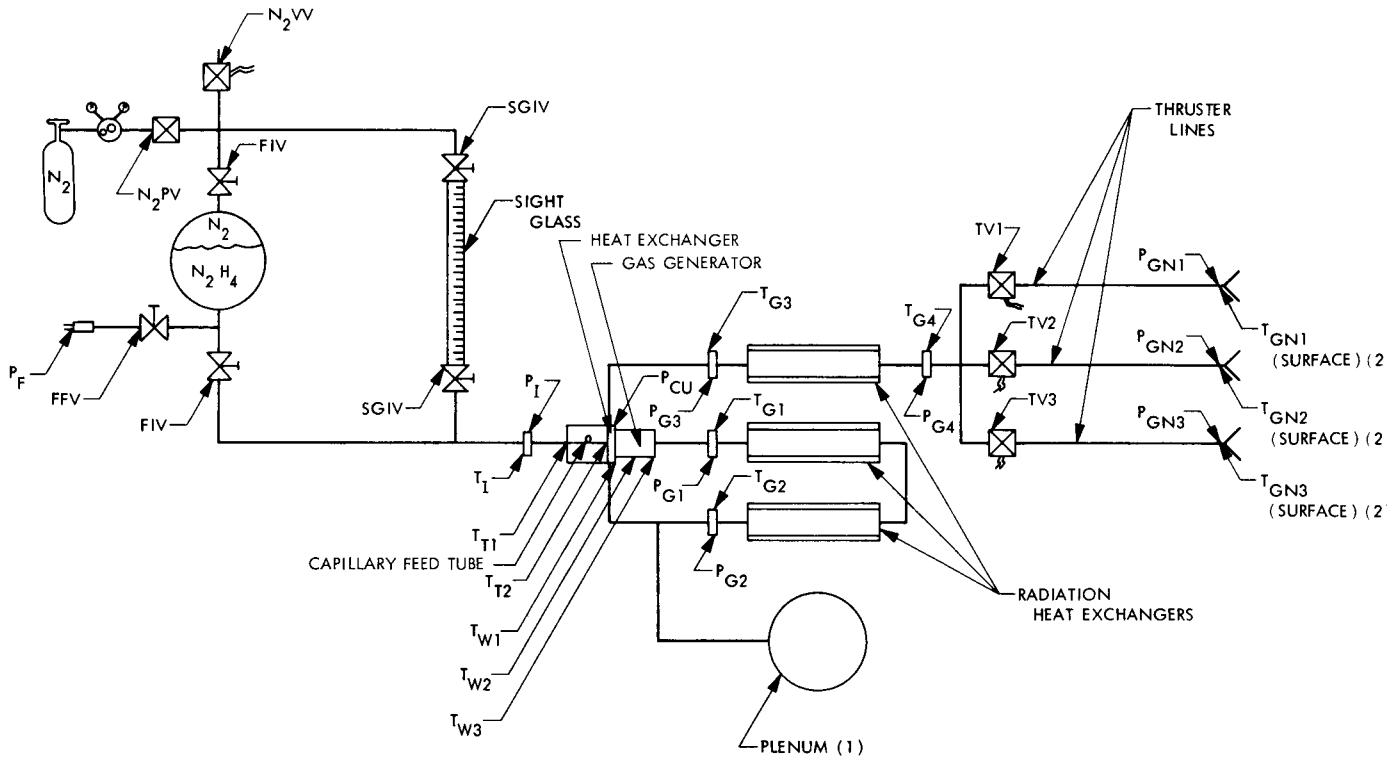

(1) GAS SAMPLE BOTTLE REPLACES PLENUM DURING GAS SAMPLE TESTS

(2) SYSTEM IS PLACED ON MICROTHRUST BALANCE TO MEASURE THRUST DURING FORCE MEASUREMENT PERFORMANCE TESTS

Fig. A-28. Schematic of rocket research hydrazine plenum test module

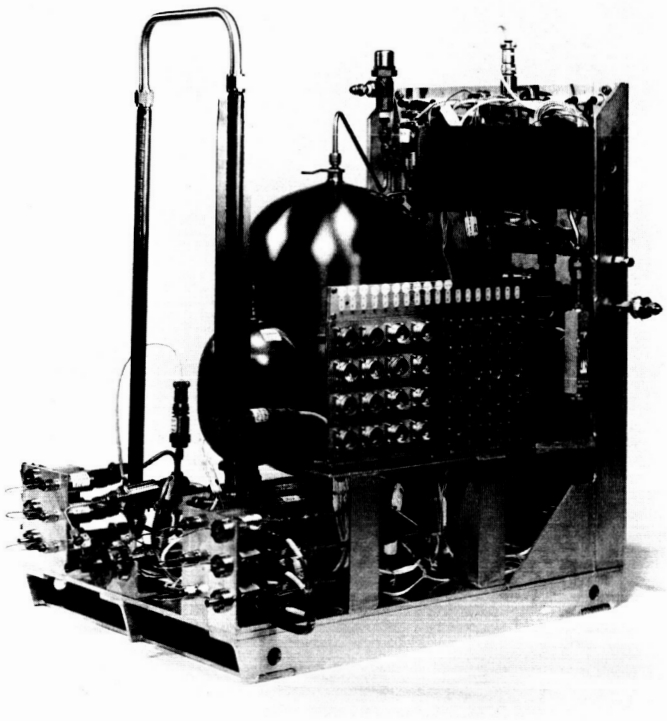

Fig. A-29. Rocket Research passive hydrazine plenum system (photo courtesy of Rocket Research Corp.)

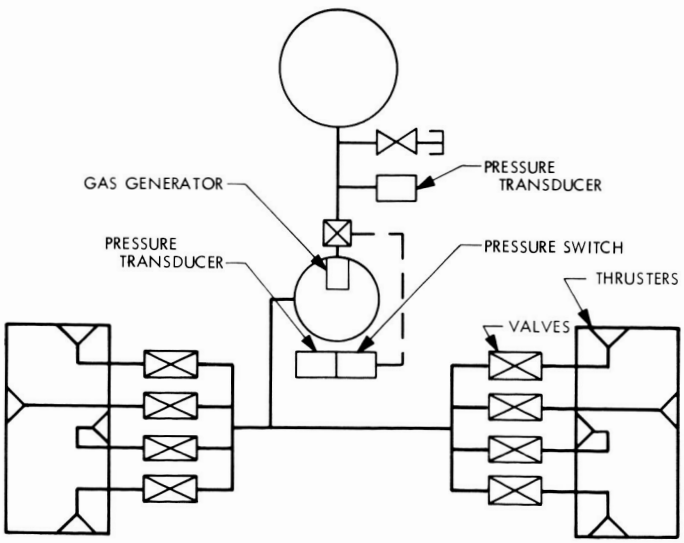

Fig. A-30. TRW Systems low-level Model 35 thruster system (hydrazine plenum)

systems have received considerable development effort and can be considered in the flight-ready state. Thermal control of plenum systems seems to be the largest single area of system improvement.

V. Liquid Systems: Electrolysis System

Electrolysis auxiliary propulsion systems produce a low-molecular weight, gaseous propellant by the electrolysis of a suitable liquid. Water and hydrazine are applicable candidates for such a system. The hydrogen-oxygen mixture produced by this electrolysis of water may be expelled at ambient temperature, or ignited and utilized in a hot gas mode. Hydrazine electrolysis products are expelled at ambient temperatures.

The storage of a high-density liquid, and the conversion of that liquid into a low-molecular weight gas, results in low-tankage mass and high-specific impulse. The ignition of hydrogen and oxygen leads to an extremely high theoretical specific impulse (375 lbf-s/lbm). For systems with large total impulse requirements, large quantity of fuel, electrolysis systems can look attractive. Zero-g operation of electrolysis cells presents problems. Several types of zero-g electrolysis cells are presented in Fig. A-31. The separation of hydrogen and oxygen is essential if hot gas operation is desired (prevent flashback). Also, the liquid/gas separation is essential.

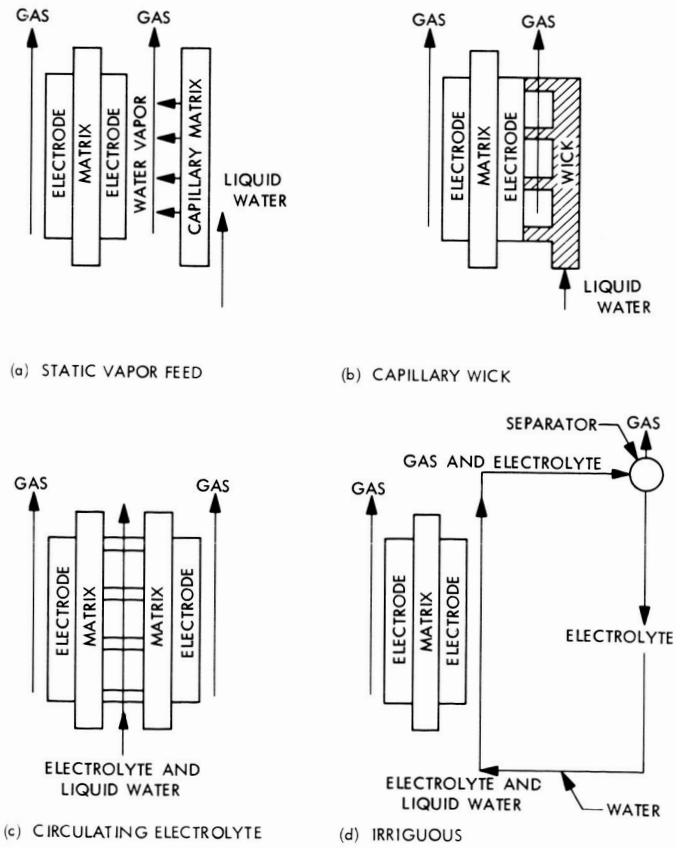

Fig. A-31. Water feed system concepts

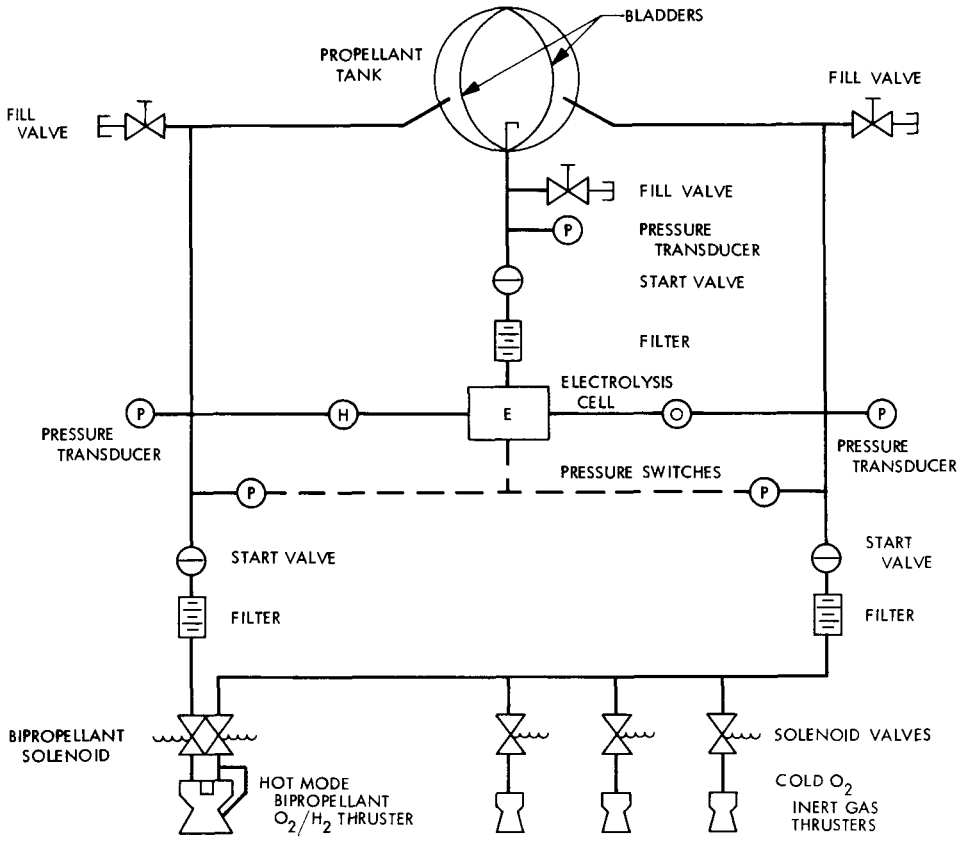

Fig. A-32. Typical water electrolysis thruster system

Although both hydrazine and water have been proposed as propellants for electrolysis systems, water is preferred because it results in the generation of hydrogen and oxygen in separate streams, with possible hot and cold mode operation. A typical system is presented in Fig. A-32. Again, hydrazine may be substituted for water with separated mixtures of nitrogen and hydrogen resulting. The water electrolysis system consists of a triad tank which serves to provide passive pressure control. The stream of water to the electrolysis cell is regulated by a pressure switch-control-valve arrangement. The separate streams of hydrogen and oxygen are fed to a bipropellant solenoid valve that may be actuated on the oxygen side only (ambient oxygen), or simultaneous hydrogen-oxygen actuation (2.5:1 hot O_2/H_2 mixture). The components for this system are available, but modification of these components would be necessary for system integration. Mass, performance, reliability, and cost of such a system are discussed in Appendixes B, C, and D, respectively.

Electrolysis systems have been studied at several companies (e.g., Hughes Aircraft Co., Allis-Chalmers, and Life Systems). Early work in this field was initiated at Hughes using water (Ref. A-26). As a result of further studies, work with hydrazine was initiated. After chemical testing of various electrolytes, oxalic acid was selected. Aluminum was selected as cathode material. The zero-g cell was designed to generate a mixture of hydrogen and nitrogen. The tank and electrolysis cell were an integral unit, see Fig. A-33. The generated gas is fed to the central chamber, which contains several retention screens (Fig. A-34). These screens act to restrict the flow of liquid into the gas phase during zero-g operation. This cell was operated in a -1-g environment. The hydrogen and nitrogen gas mixture contained a large amount of liquid hydrazine vapor (aerosol). In later tests of this cell under extremely abnormal operating conditions the formation of local hot spots in the cell matrix led to the rupture of the tank and destruction of the electrolysis cell (Ref. 27). Problems encountered with the handling of hydrazine in electrolysis cells have led to a reduction in development efforts.

An electrolysis cell was developed for NASA-GSFC by HAC to confirm the zero-g operation and vapor gas

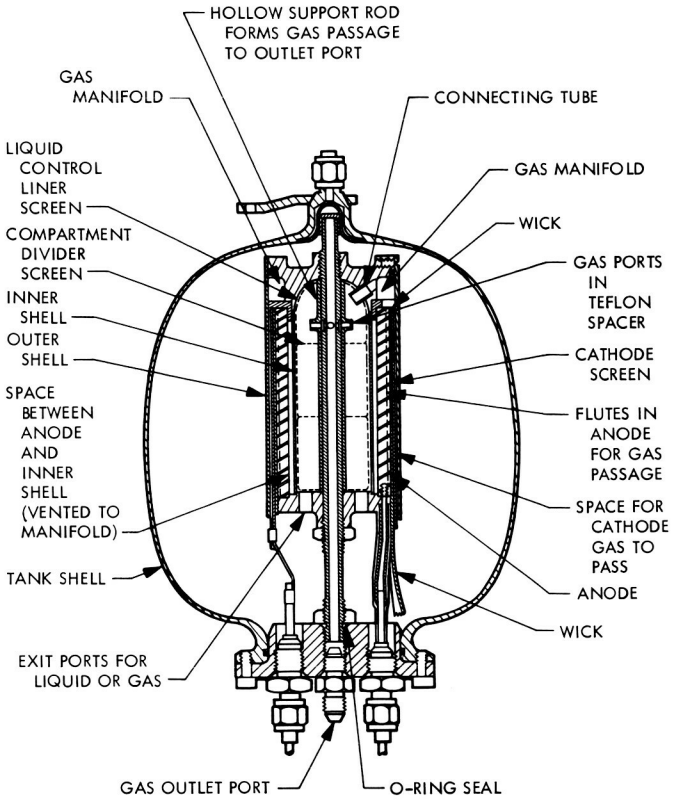

Fig. A-33. Hughes hydrazine electrolysis system (drawing courtesy of Hughes Aircraft Co.)

separation.[8] The cell is shown in Figs. A-35 and A-36. It was designed as an experiment with no weight limitation and, consequently, does not look like a flight-weight package. This test cell has been re-scheduled for a later flight date because of system pressure excursions prior to launch. These excursions are thought to be caused by hydrazine-electrolite interaction.

Life Systems, Inc., has approached the design of an electrolysis thruster from the life-support electrolysis cell field (Ref. 28). This system is centered around a life-support electrolysis cell which generates separate streams of hydrogen and oxygen gas. A schematic of this cell is presented in Fig. A-37. This cell has undergone extensive testing, and the problems of water aerosol and migration of water vapor have been solved. Propellant generation rate is shown in Fig. A-38. An exact system configuration has not been studied in detail; however, several methods of propellant management have been considered.

Allis-Chalmers entered the electrolysis propulsion field in a manner similar to that employed by Life Systems, Inc. (Ref. 29). During the early stages of the Hughes Aircraft Company work on electrolysis cells, a survey of existing technology (November 1966) concluded that the Allis-Chalmers cell was best-suited for spacecraft propulsion.

[8]Mahaffney, D., Goddard Electrolysis Cell, Hughes Aircraft Co., Jan. 1970.

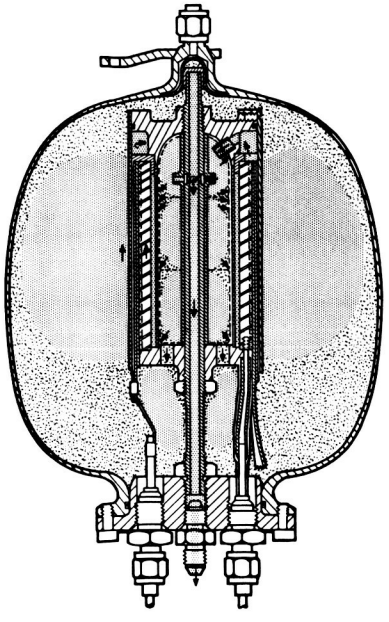

Fig. A-34. Zero-gravity gas-liquid separation in the Hughes hydrazine electrolysis system (drawing courtesy of Hughes Aircraft Co.)

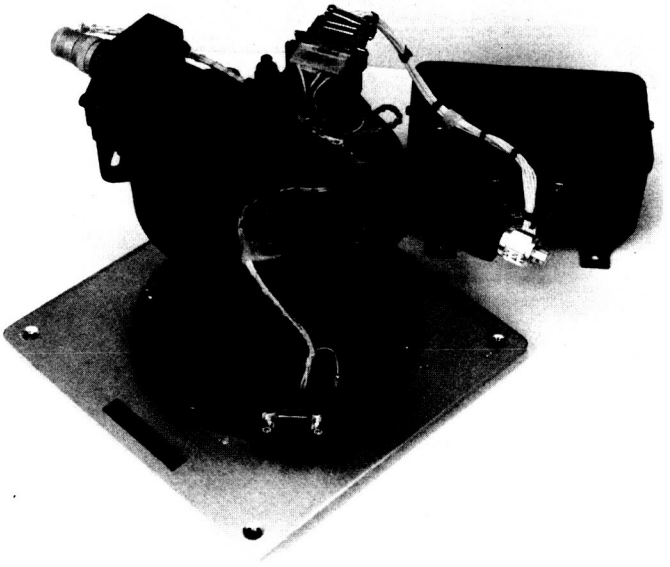

Fig. A-35. Hughes NASA Goddard hydrazine electrolysis system (photo courtesy of Hughes Aircraft Co.)

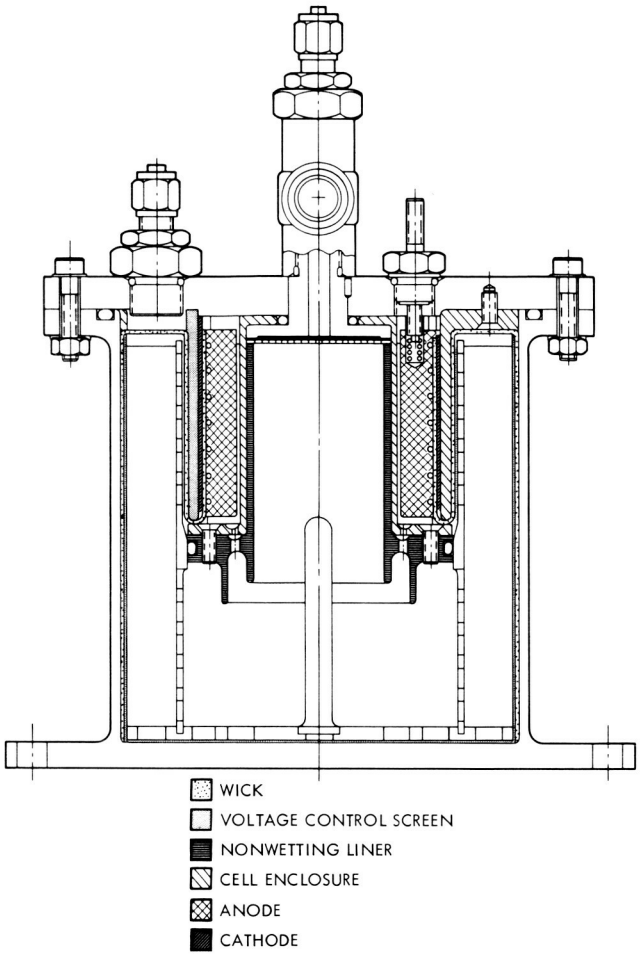

Fig. A-36. Hughes hydrazine electrolysis tank/cell subassembly

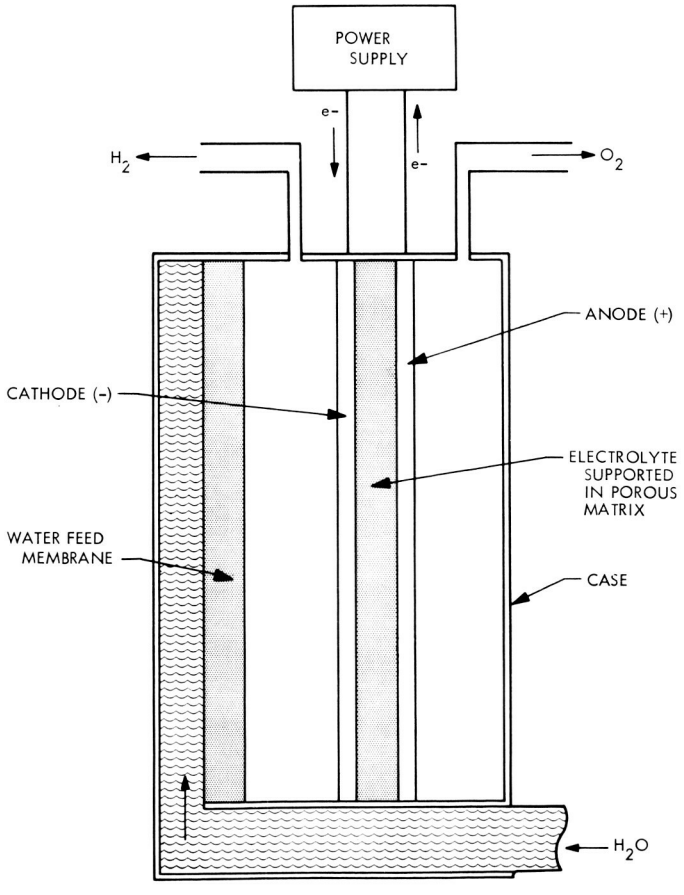

Fig. A-37. Life Systems, O_2/H_2 electrolysis cell schematic

The Hughes Aircraft Co. desired a hydrazine electrolysis cell, while Allis-Chalmers continued with development of a zero-g life-support electrolysis cell for the NASA Langley Research Center. The Allis-Chalmers zero-g concept is shown in Figs. A-39 and A-40. The performance of this cell, which is quite similar to the Life Systems cell, is presented in Fig. A-41. In the feasibility study, several candidate designs were investigated; the final selection was the passive pressure-control design shown in Fig. A-42. An investigation of several bipropellant O_2/H_2 thrusters provided several candidates. A bipropellant 20-lbf catalytic thruster designed for reaction control operation has been studied at the NASA Lewis Research Center (Ref. 29). Performance data are presented in Table A-11. Although this thruster was designed for operation at 20 lbf, the thrust level can realistically be brought down to 5 lbf. An integration of these two systems could lead to a functional water electrolysis system.

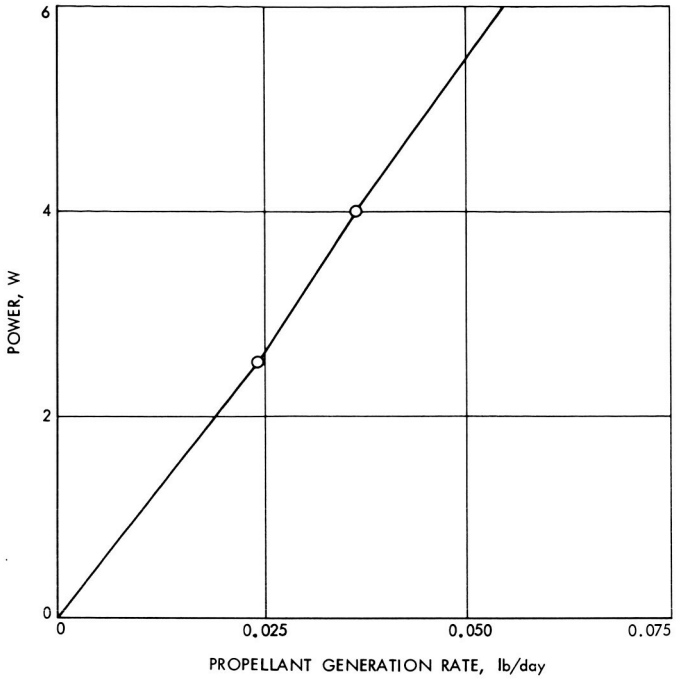

Fig. A-38. Propellant generation rate vs power, Life Systems electrolysis cell

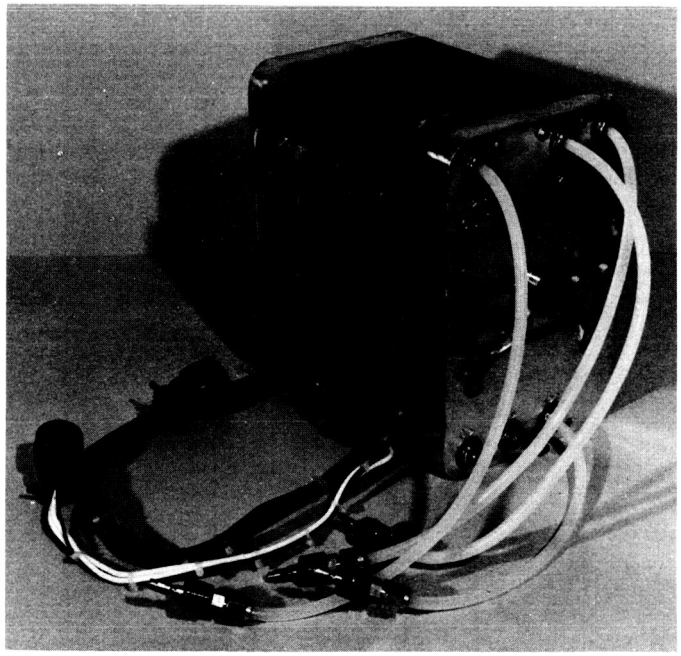

Fig. A-39. Allis-Chalmers zero-gravity life support electrolysis cell (photo courtesy of Allis-Chalmers)

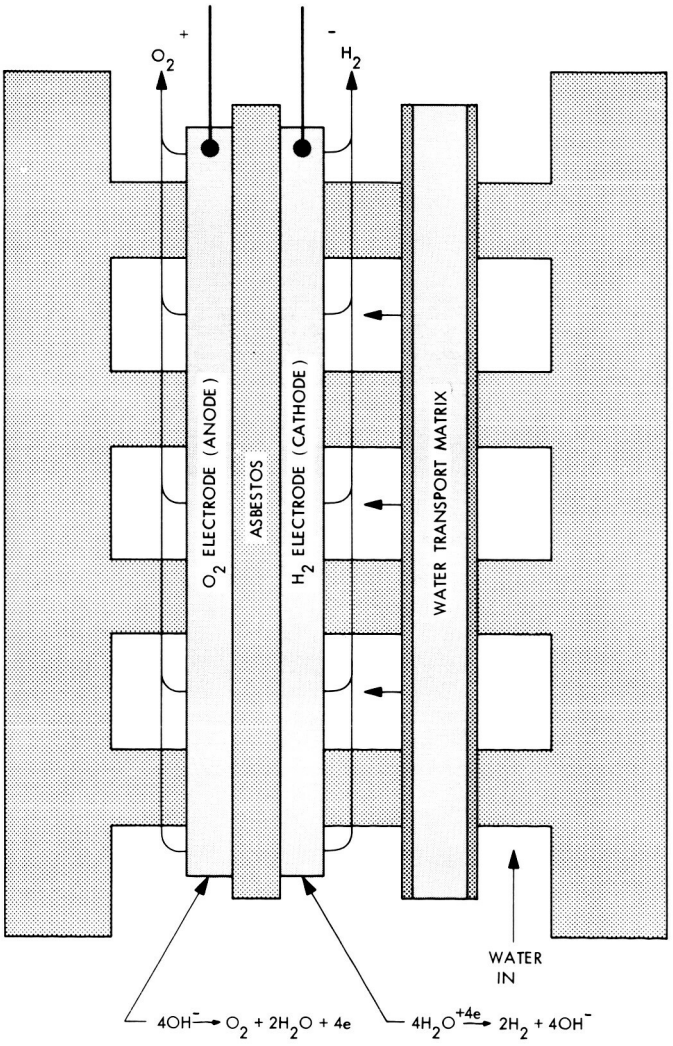

Fig. A-40. Allis-Chalmers electrolysis cell schematic diagram (drawing courtesy of Allis-Chalmers)

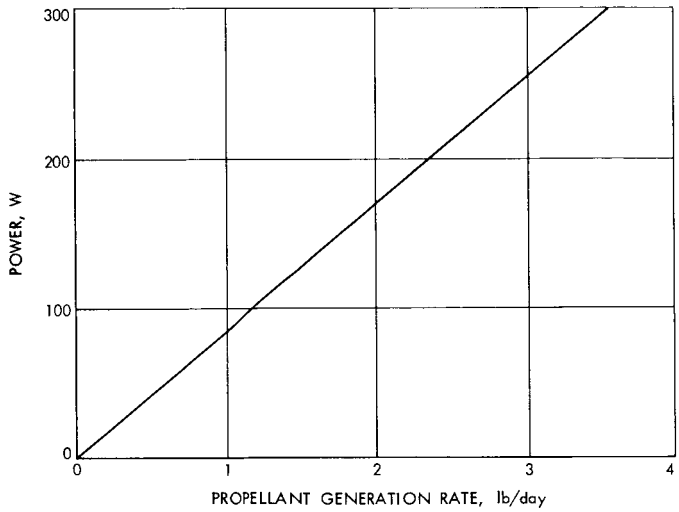

Fig. A-41. Propellant generation rate vs power

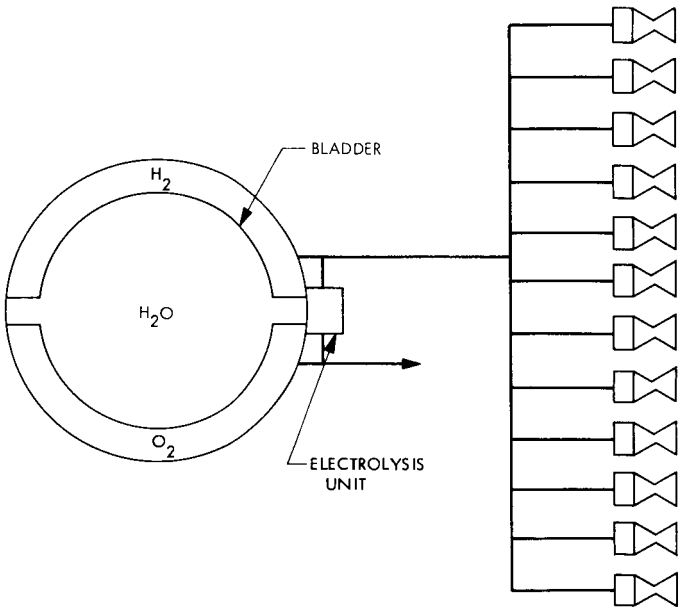

Fig. A-42. Allis-Chalmers water electrolysis attitude control thruster system concept

A Marquardt O_2/H_2 spark thruster is also available. The technology of high-thrust (1000 lbf) O_2/H_2 engines has been extrapolated to 1–5 lbf thrust. Theoretical calculations on a 1-lbf thruster operating at a mixture ratio of 8 to 1 (hydrogen film cooling) reveal a delivered specific impulse of approximately 250 lbf-s/lbm. This engine is designed to operate at a low (2000°F) chamber wall temperature to prolong thruster life. At a 2500°F chamber wall temperature a specific impulse of 310 lbf-s/lbm (5-lbf)

Table A-11. NASA Lewis Research Center gaseous O_2/H_2 attitude control thruster performance data

Parameters	Performance data
Thrust (Vac), lbf	20
Chamber pressure, psia	10, 100, 290
Specific impulse, $\frac{\text{lbf-s}}{\text{lbm}}$	390
Propellants	Gaseous O_2/H_2
Propellant temperature, °F	Ambient to −250
Ignition	Pilot bed/catalytic
Overall thruster mixture ratio, O/F	1.0 to 3.5 (2.5 max performance)
Duty cycle	Steady-state, pulse mode

can be realized. The thruster is suited for auxiliary propulsion due to its pulse mode operation characteristics. Breadboard operation of an Allis-Chalmers electrolysis cell and a Marquardt 5-lbf O_2/H_2 pilot spark chamber has been demonstrated. Further system functional tests should be conducted to determine if any system integration problems exist (thermal or pressure control).

Water electrolysis life-support system technology has advanced considerably in the last few years. A demonstration integration of life-support systems into a water electrolysis attitude control system is recommended. This system is presently restricted by thruster technology. Operation of O_2/H_2 thrusters at mixture ratios of 3 to 1 are preferred over mixture ratios of 8 to 1. High temperatures are resultant at these high mixture ratios. To compensate for these high temperatures, thrust chamber walls must be cooled. If hydrogen is used as a film coolant, then a decrease in specific impulse results. This decrease is quite large in small 1-lbf thrust engines ($\approx$230 to 250 lbf-s/lbm). If the thruster is operated at the preferred 3 to 1 mixture ratio, only 4 lbm per 9 lbm of generated propellant are combusted. The remaining 5 lbm of cold oxygen must be expelled cold (I_{sp} 70 lbf-s/lbm). This results in an even lower specific impulse. Although this system has been demonstrated, improvements in propellant-delivered specific impulse are necessary to make this a competitive system. In an attempt to improve the specific impulse of the propellant, a mixture of hydrazine and water may be substituted. The resulting products will contain a larger percentage of hydrogen and a smaller percentage of oxygen. The addition of nitrogen to the mixture will act to cool the combustion gases. Further development in the area of hydrazine electrolysis technology is required. Additional effort in electrolite selection and gas-liquid phase separation is required.

VI. Solid Systems: Subliming Solid

The subliming solid system is characterized by a solid propellant, which when heated, is pressurized by its own vapor pressure and this vapor is expelled through a nozzle. While no great improvement in specific impulse can be obtained, considerable savings in tank mass result from the high-density and low-vapor pressure of the propellant. Passive heat transfer is the preferred method of sublimation of the solid. Early subliming solid thrusters utilized high-vapor pressure solids, which could supply the required heat of sublimation from spacecraft thermal energy. The propellant vapor may be contained by either a solenoid control valve, or a "valveless" control valve. The valveless concept utilizes propellant condensation in the feed lines to act as a valve. A porous plug is inserted in the line and the propellant is condensed on this plug to restrict the flow. To begin the flow, the plug is heated to vaporize the entrained solid material. Thrust level sets the required propellant heater power in a valveless system. The mass advantages of this system are noted in the low tank pressure. Zero-g propellant problems are nearly nonexistent, since the propellant is formed under high pressure into its flight configuration, and migration of the solid in large pieces is nonexistent. Propellant migration due to thermal gradients is an important problem; however, proper thermal design and selection of propellant can help to eliminate this problem. A typical valveless design is presented in Fig. A-43. The propellant tank is usually made of light-weight aluminum designed to survive buckling and external launch forces. A propellant heater is integral with the tank. Thermal shielding is provided to improve propellant heater performance. The valveless valve, as previously mentioned, consists of a porous plug inserted in a feed line surrounded by a line heater. Additional line heaters are provided to compensate for propellant migration and additional propellant condensation. Inert gas thrusters are included to complete the system.

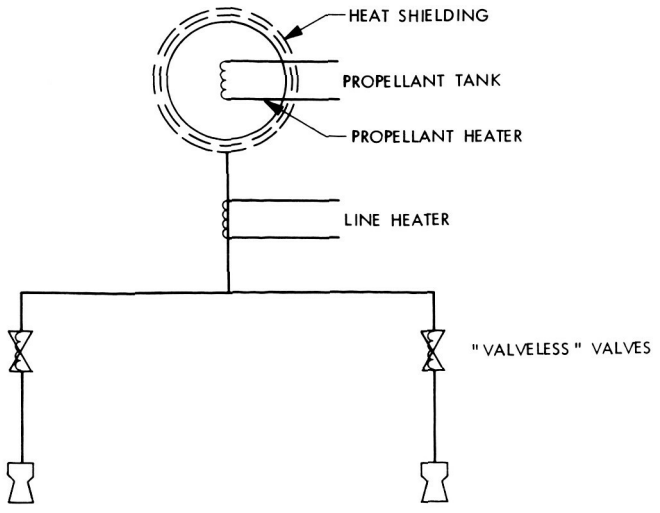

Fig. A-43. Typical subliming solid attitude control thruster system

Propellant selection is a tradeoff of duty cycle requirements, thrust level, and system design. Some of the important points for selection of propellants are as follows:

(1) Low molecular weight vapor.

(2) High solid density.

(3) Low heat of sublimation.

(4) High equilibrium vapor pressure.

(5) High thermal heat capacity.

Several propellants have been used in the past. Ammonium bisulfide (hydrosulfide) has a very high equilibrium vapor pressure at room temperatures (10 psia at 80°F) and a low heat vaporization. This propellant has been used by Rocket Research in their valves subliming solid system. The high vapor pressure of this propellant limits its use to valved systems, since the continual sublimation of propellant would be too great in a valveless system.

Table A-12. OV 2-1 subliming solid rocket system

Parameters	Data
Thrust, lbf	10^{-2}
Propellant	Ammonia bisulfide
Specific impulse, $\frac{\text{lbf-s}}{\text{lbm}}$	75
Lifetime, years	1
Environment, °F	70
Type	Valved

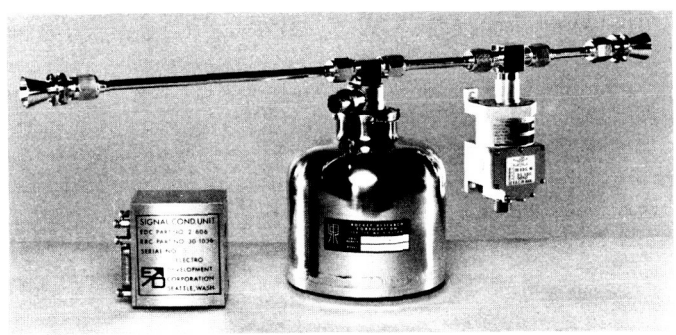

Fig. A-44. OV2-1 sublex respin rocket system (photo courtesy of Rocket Research Corp.)

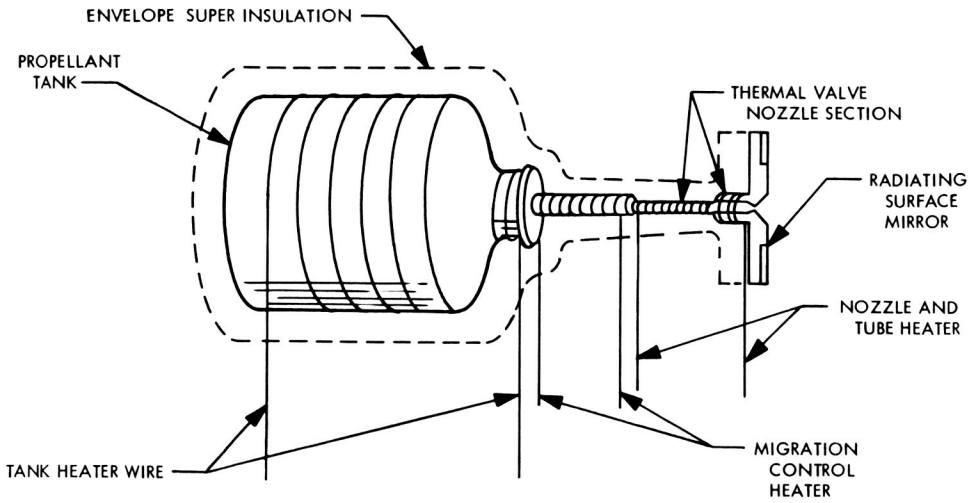

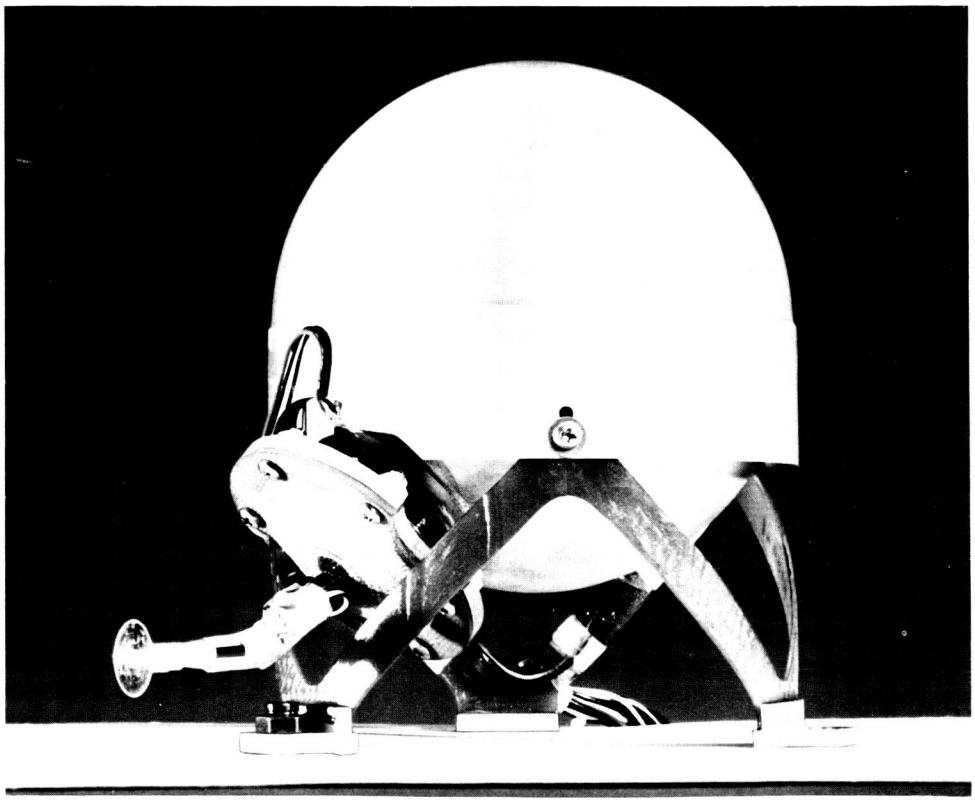

Fig. A-45. Rocket Research NRL "valveless" subliming solid thruster system (photo courtesy of Rocket Research Corp.)

Subsequent valveless designs utilizing ammonium carbamate, monomethylamine carbamate, and ammonium sulfite have been designed by Lockheed and Rocket Research. A more complete coverage of subliming solid system design aspects is given in Ref. 30. Performance and mass, reliability, and cost of subliming solid systems are outlined in Appendixes B, C, and D, respectively.

The first flight system constructed was of the valved design. This system, designed for the *OV* 2-1 satellite (Ref. 31), was the culmination of several years of research at Rocket Research. The system is presented in Fig. A-44. The system was designed to spin up the spacecraft and restore any lost spin. Performance data of this system are presented in Table A-12. Several problems which occurred during the development of this engine led to the addition of thermal control heaters.

Thermal control of the system is important and, prior to launch, problems with recondensation of propellant were encountered. Ground tests of the engine confirmed its performance characteristics; unfortunately, the *OV* 2-1 satellite was not ejected into orbit, because of a failure of the transtage booster. No flight data are available.

Rocket Research designed two valveless subliming solid systems. One system was designed for the AIMP-E, but a decision to use inert gas Freon 14 stopped this program. The second system was designed for a NRL satellite (Ref. 32) which is shown in Fig. A-45. Its performance characteristics are prescribed in Table A-13. This system was flight-qualified and flew on a classified spacecraft. It functioned well in pre-flight tests. Data on the flight performance are not available.

Lockheed has designed a subliming solid system for the ATS program (Ref. 33). This system is shown in Fig. A-46. The cross-section diagram shown in Fig. A-47 helps to illustrate the system design. The porous plug is cooled by a partially silvered reflector. Thermal control is ensured by line heaters and heat shielding of components. System design parameters are presented in Table A-14. A trace of system dynamic response data obtained from pre-flight testing is presented in Fig. A-48. This system has flown on several ATS spacecraft; unfortunately, none of the spacecraft upon which it was installed achieved proper orbit. Operation of the system in space is confirmed by the flight reproduction of pressure response data simulated in Fig. A-48, but the thrust level

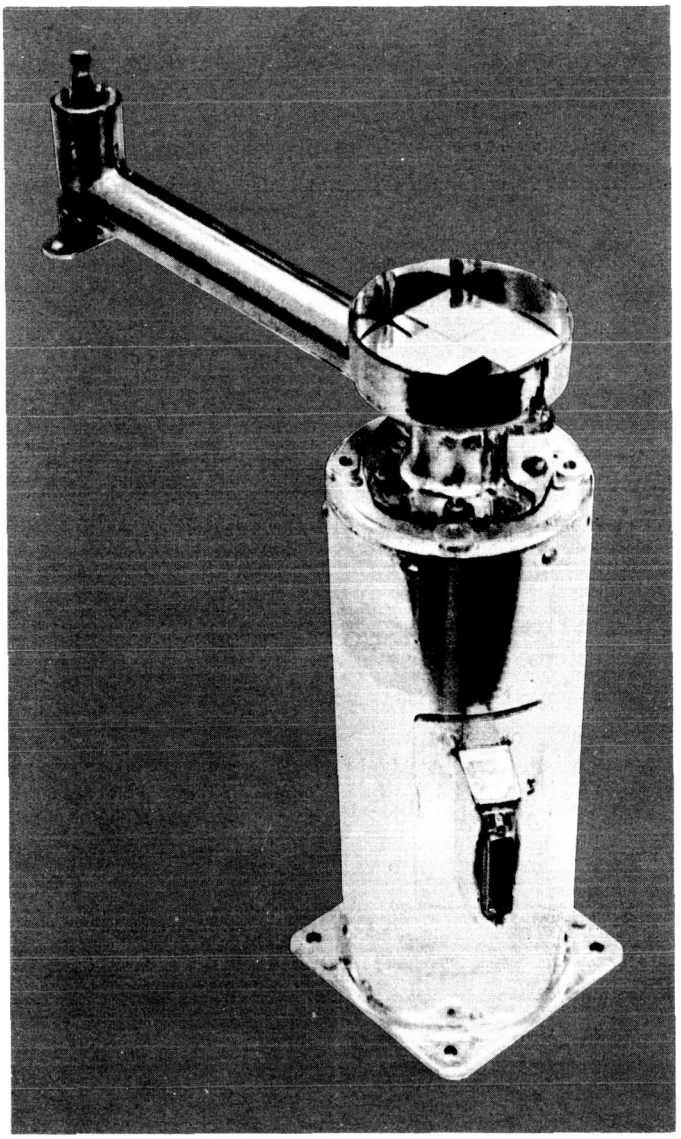

Fig. A-46. Lockheed ATS "valveless" subliming solid thruster system (courtesy of Lockheed Missiles and Space Co.)

Table A-13. Rocket Research NRL subliming solid-rocket system

Parameters	Data
Thrust, lbf	9×10^{-6}
Propellant	Ammonia bisulfide
Specific impulse, $\frac{\text{lbf-s}}{\text{lbm}}$	40
Lifetime, years	1
Environment, °F	(0–130)
Type	Valveless
Response time, in min	
On	120
Off	120

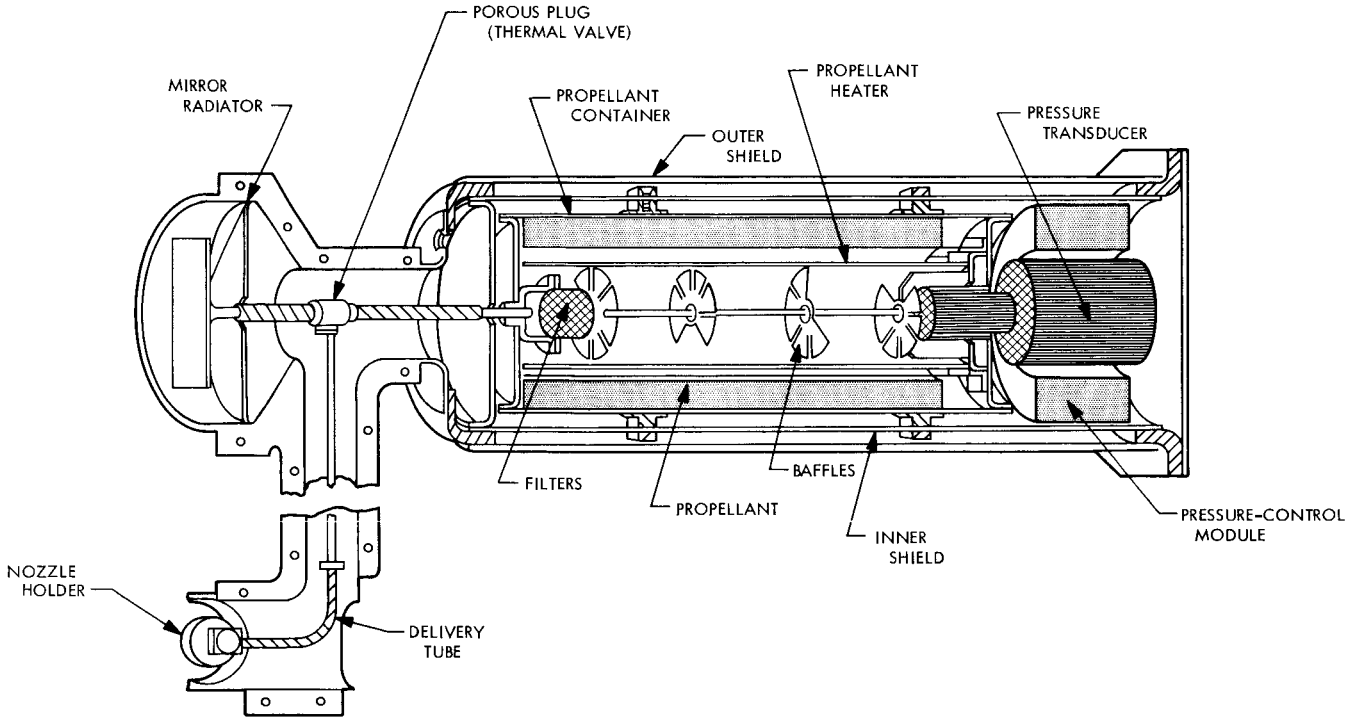

Fig. A-47. Cross-sectional view of Lockheed "valveless" subliming solid thruster system

of the thrusters cannot be determined from spacecraft movement.

Valveless flight systems can be considered state of art. Careful thermal design is necessary to overcome problems of propellant migration. Theoretical calculations of performance differ greatly from actual delivered performance at the low-thrust levels. The problem of poor performance in the low Reynolds number regime (less than 1000) is not well understood, and further research in this area is warranted.

Table A-14. Lockheed valveless subliming solid rocket

Parameters	Data
Thrust, lbf	5.4×10^{-5}
Propellant	Monomethylamine carbamate
Specific impulse, $\frac{\text{lbf-s}}{\text{lbm}}$	50
Lifetime, years	3
Environment, °F	40–100
Type	Valveless
Response time, in min	
On	60
Off	60

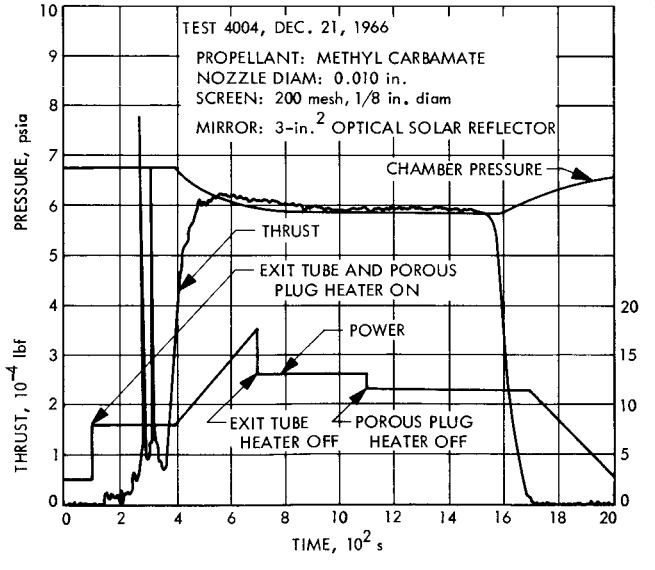

Fig. A-48. Thrust startup and termination for the "valveless" ATS subliming solid reaction control system

VII. Solid Systems: "Cap Pistol"/"Honeycomb"

Two devices have been proposed to meet an anticipated requirement for a limited number of repetitive

impulse bits. One of these devices is the Curtiss-Wright "Cap Pistol," which is a number of miniature solid-propellant rocket motors bonded to a tape (Ref. 34). The motors are fed into a thrust chamber and fired as needed. This device suffers from low-volume efficiency and mechanical complexity. Residue from the motors contaminates the mechanism. The other device is the Lockheed Missile and Space Company (LMSC)/Talley Industries "Honeycomb," which consists of a honeycomb section of insulating material filled with solid propellant with each cell having its own igniter (Refs. 35 and 36). This device suffers from variable location of thrust application.

Unless some mission demands the use of the "Honeycomb," costs for development and qualification of these devices render this concept prohibitive. There may be some potential application, however, since the Air Force has classified some of the performance data. Table A-15 lists the known performance data.

Table A-15. Performance data—"cap pistol" and "honeycomb" solid systems

Parameters	Data
"cap pistol"	
Manufacturer	Curtiss-Wright
Impulse/unit propellant, lbf-s	0.1; WSR-2[a]
	0.1; WSR-4
	(Classified) WSR-101
Rate of fire, units/s	0–40
Size, $in.^3$/1000 lbf-s	200
τ, ms	$1 \rightarrow 5$
"honeycomb"	
Manufacturer	LMSC; Talley Industries
Impulse/unit propellant, lbf-s	$0.1 \rightarrow 2$; 0.01
Specific impulse, lbf-s/lbm	150–250

[a]WSR-2 was to be used on *TIROS*.

VIII. Electric System: Ion Thruster

Two basic engines which are grouped under this classification: (1) the electron bombardment ion engine (Kaufman engine) and (2) the contact ion engine. The electron bombardment engine uses an anode-cathode arrangement to ionize a propellant such as mercury or cesium. The ions are accelerated in an electrostatic field and neutralized as they are emitted to avoid the limitations of space charge flow. Usually, an electromagnet or permanent magnet is used in combination with the anode-cathode to improve the ionization efficiency. The contact engine uses a heated porous tungsten plug to ionize the flow of cesium propellant vapor through it. It is heated electrically, but can also be heated with a radioisotope. The ions thus produced are then handled in exactly the same way as those in the electron bombardment ion engine.

A major limitation of either of these ion engines is the electrode erosion caused by ion bombardment. The ions which cause most of the damage are those formed from neutral particles which pass through the ionizer, and have subsequently undergone charge exchange collision with fast positive ions. Therefore, a high-ionization efficiency is important in extending electrode life.

The contact ionization thruster (Ref. 37) has a power-to-thrust characteristic as shown in Fig. A-49. As specific impulse decreases below 5000 lbf-s/lbm, the required power to thrust begins to raise. This is due to the constant power loss (radiation at 1200°F) of the ionizer. It is for this reason that contact ionization engines operate at specific impulses above 5000 lbf-s/lbm. A good feature of the cesium contact ionization thruster is its high propellant ionization efficiency (99 to 100%). Cesium is stored in a reservoir and fed by wick to a vaporizer. Cesium vapor is fed to the heated ionizer.

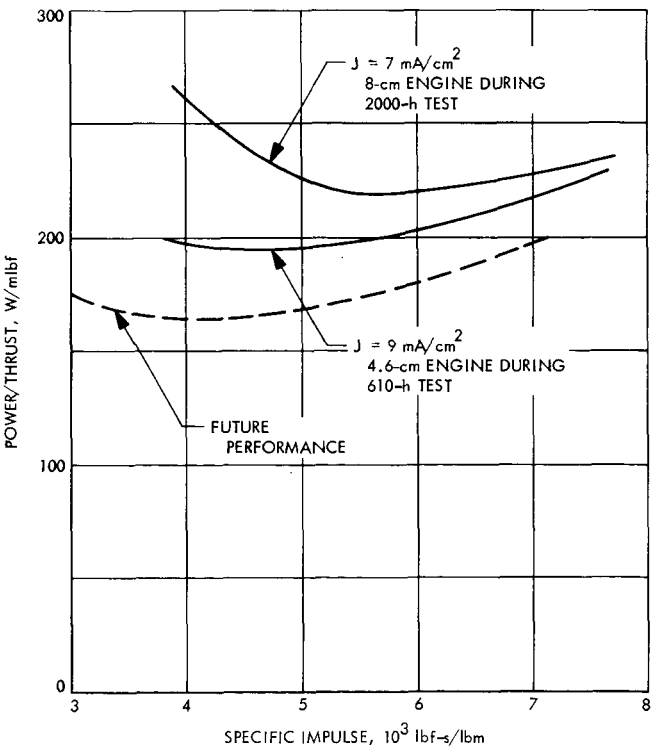

Fig. A-49. Power-to-thrust vs specific impulse for single-strip ion thrusters

The bombardment ionization thruster has slightly different characteristics. Specific impulses of 3000 to 4000 lbf-s/lbm are preferred (see Fig. A-50 and Ref. 38). The propellant ionization efficiency is less than that of a contact ionization thruster. If the efficiency of the ionization process is plotted as in Fig. A-51, it is noted that the desired ionization efficiency is near the knee of the curves (Ref. 39), usually from 85 to 95% efficiency. Propellant feed systems for bombardment systems are similar to those of the contact ionization thruster. Two propellants have been used: mercury, and cesium. The ionization potential for cesium is less than that of mercury; however, the cross section for electron-atom interactions for mercury are greater than for cesium. The result is that it is about as easy to ionize both propellants. Mercury with its larger molecular weight will have the advantages of increased thrust and decreased tankage weight.

The electrostatic engines are presently available at thrust levels of 10 to 20,000 μlbf and specific impulses of 2700 to 7500 lbf-s/lbm have been realized. Some representative performance data are given in Table A-16 for

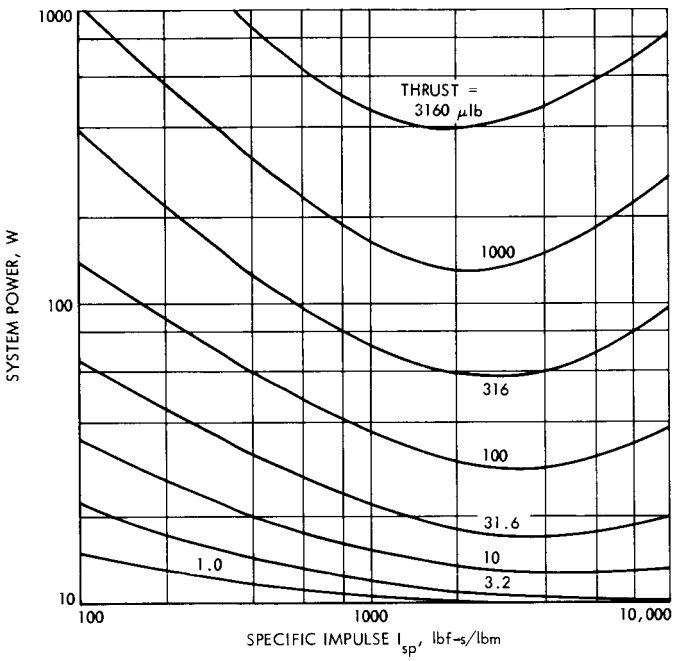

Fig. A-50. Effect of specific impulse on thruster system power

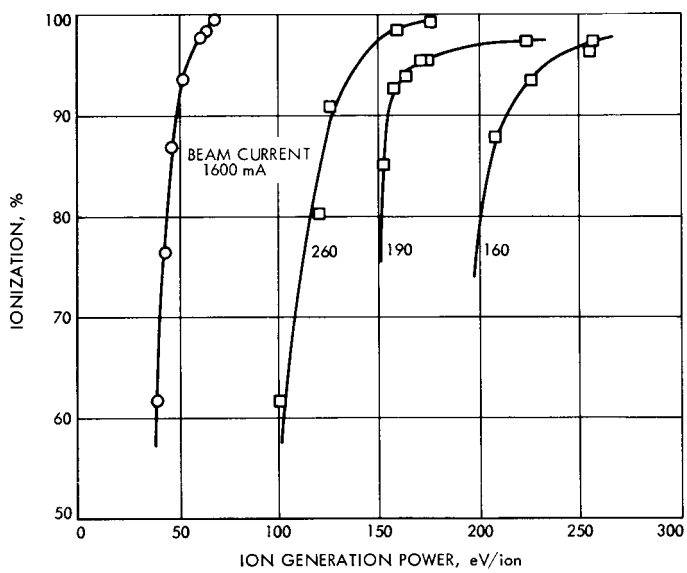

Fig. A-51. Efficiency of selected cesium plasma sources

Table A-16. Ion thruster performance data

Manufacturer	Thrust, μlbf	Power, W	Specific impulse, lbf-s/lbm	Power/thrust, kW/lbf	Efficiency	
					Overall, %	Propellant, %
NASA Lewis	1000	250	4000	250	35	70
NASA Lewis	650	144	3000	220	30	50
NASA Lewis	650	171	4000	260	33	66
NASA Lewis	520	128	3300	250	30	30
Hughes	700	133	5500	190	64	99
Hughes	560	126	5500	225	54	~100
Hughes	300	60	5000	200	55	~100
Hughes	10	8	5200	820	14	~100
NASA Lewis	350	118	7000	336	43	~99
EOS	24	25	7300	1050	15	~100
EOS	10	13	6700	1290	11	

electrostatic engines (Refs. 37, 40, and 41). The bombardment ionization thrusters are those with low propellant efficiency (<98%) and low specific impulse.

Ion engine experiments have flown on three early ballistic trajectories. Two were on Blue Scout vehicles (EOS). The second flight was successful and data on the EOS cesium contact ionization thruster were returned. The third early flight was SERT-I. The payload consisted of a mercury bombardment thruster and a cesium contact thruster (Hughes Aircraft). The mercury bombardment thruster was successfully operated for 40 min. An EOS cesium contact ion thruster was launched onboard SNAP-10; operation of its engine was unsuccessful. A later cesium contact thruster was flown as an experiment on ATS-D, and operated successfully. The SERT-II is presently flight-qualified and, at the time of this writing, awaiting launch.

IX. Electrical Systems, Pulsed Plasma

The general mode of operation is for a propellant to be ionized by a high-voltage discharge and accelerated by the interaction of the discharge current with its own magnetic field.

Early work in plasma propulsion centered around high-power, high-temperature steady-state plasma thrusters. Recent work has centered around pulsed plasma thrusters, which require lower average power.

The specific impulse and minimum impulse bit can be varied over a wide range by proper choice of discharge voltage, discharge energy, and quantity of propellant flow. Efficiency is generally low. Four pulsed plasma thrusters have flown and operated in space in excess of 3500 h aboard LES-6. These thrusters were built by Fairchild Hiller. The GE SPET has been demonstrated in flight prototype. Some typical performance parameters of pulsed plasma thrusters are given in Table A-17 (Ref. 42).

X. Electrical System: Colloid

The colloid engine utilizes a very strong electric field to charge the droplets in a propellant spray. Although the masses of the charged droplets vary, they are generally greater than the mass of ions produced in ion engines. In some engines, these charged droplets are handled from this point just like the ion engines; however, in other engines it is possible to produce plus and minus charges simultaneously. This negates the need for a neutralizer.

The colloid engine suffers from the randomness of the particle formation and the manner of inducing the charge. It alone, of the electrostatic engines, has the most efficient formation of charged particles. The colloid engine is adaptable to a specific impulse range between the chemical and the ion engines.

The TRW system colloid data are presented in Table A-18.[9] The colloid system was flight-qualified for the DODGE-M satellite. The program was cancelled and the thruster system was not flown.

[9]Cohen, E., TRW Systems, letter to Comsat Corp., April 1969.

Table A-18. Colloid thruster characteristics[a]

Item	Type	1968 state of art	1970 projection
Thrust element	Needle	2 μlb/needle	5 μlb/needle
	Slit[b]	25 μlb/linear in.	75 μlb/linear in.
Packing density	Needle	33 needles/in.^{2}	33 needles/in.^{2}
	Slit	3/in.	4/in.
Thrust density, μlb/in.^{2}	Needle	66	165
	Slit	75	300
Basic elements/mlbf thrust	Needle	500	200
	Slit	30	10
Vectoring ability, deg	Needle	±15	±15
	Slit	±15	±15
Continuous testing, h	Needle	2400	10,000
	Slit	120	10,000

[a]Propellant 20% NaI/80% Glycerol (by weight).
[b]Projected.

Table A-17. Pulsed plasma performance data

Manufacturer	Thrust, μlbf	Power, W	Specific impulse, lbf-s/lbm	Power/Thrust, kW/lbf	Efficiency, %	Weight, lbm	Life, yr
Republic Division, Fairchild Hiller	6	3	300	500	9	~12	2 (flight)
GE	1-10	2-5	1000/4000	2000/500	10-20	~2	3 (projected)

XI. Thruster Heater: Resistojets

The resistojet is the simplest of all electrical propulsion systems. Cold fluid is increased in temperature by passing through an electrical resistance heater. The performance of inert gas, vaporizing liquid, hydrazine plenum, and subliming solid systems can be substantially improved by heating the propellant prior to expulsion through the nozzle, since the specific impulse of a gas is proportional to the square root of temperature. Maximum gas temperature is limited by two important factors: power, and materials. Each additional degree of temperature added to a propellant by a resistojet requires more heater power. Power available to resistojets is usually limited. Thermal cycling and high-temperature operation of the resistojet requires special high-temperature material technology, which sets a practical limit on maximum temperature.

A resistojet should be perceived as a subsystem rather than a complete thruster system. The feed system can be inert gas, subliming solid, hydrazine plenum, or vaporizing liquid mentioned elsewhere in Appendix A. Propellants which are especially attractive are those that undergo dissociation (lowering in molecular weight) below 2000°F. Ammonia, ammonium hydrosulfide, and ammonium carbamate are a few propellants that undergo a dissociation at 1400 to 1800°F. Also, low molecular weight gases are especially attractive. Performance of several candidate working fluids are plotted in Fig. A-52. Tradeoffs in power, performance, and heat loss must be made. Heat loss and power requirements become extremely large as temperatures are increased above 3000°F. As a consequence, most resistojets are not designed to operate above 3000°F.

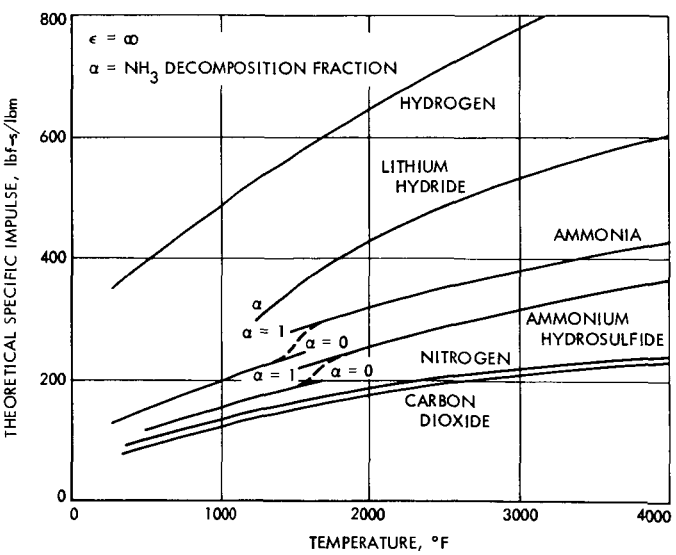

Fig. A-52. Theoretical performance of heated propellants

There are two types of resistojets: fast heat up, and thermal storage. The difference between these may be expressed in a time constant. If it takes less than 10 min to heat up the resistojet to operating temperature, it is called a fast heat up resistojet. If much longer times are required to heat up the resistojet, then it is called a thermal storage resistojet. The advantage of a fast heat up resistojet is a reduction in average power required; however, thermal cycling is greater in this type of system. Performance and mass, reliability, and cost are presented in Appendixes B, C, and D, respectively.

Avco has flown four ammonia resistojet systems. The thrusters operate on the fast heat-up philosophy. The fluid flows through a single-pass rhenium heat exchanger tube with an integral nozzle. The heater tube/nozzle is nitro brazed to a stainless steel inlet mount. Four platinum leads complete electrical continuity to the heater shroud. The shroud acts as a combination electrical conductor and radiation shield. Alumina insulating rings isolate the mounting flange and shroud. The ammonia-fueled ATS III thrusters were placed in orbit in November 1967 as an experiment (Ref. 15). The Avco resistojet performed well; however, valve problems were encountered. Extensive valve qualification tests were conducted to improve valve reliability (Ref. 43). The ATS IV system was placed in orbit in August 1968. The system performed well for 750 h of operation (Ref. 16). The ATS V has been placed in orbit, but due to injection and spin error, operation of these thrusters has been restricted. Three additional flight units are under flight qualification for classified payloads. The Avco resistojet has been proven on several flight projects, both as experiment and prime attitude-control system. Examples of the thrusters and performance data are presented in Fig. A-53 and Table A-19.

TRW has also contributed a great deal to resistojet technology. The following information is extracted from Ref. 44 with the permission of TRW Systems.

"The Vela 3 thruster system, utilizing N_2 gas, provides an orbital velocity increment of up to 20 ft/s for each of two satellites placed in a near-circular 60,000-mi orbit. The thruster configuration is shown in Fig. A-54 and an external view in Fig. A-55. The thruster consists of a helical resistance heater and a helical propellant flow tube brazed onto a metal core and nozzle assembly. The brazed assembly is insulated by a jacket of molded Min-K

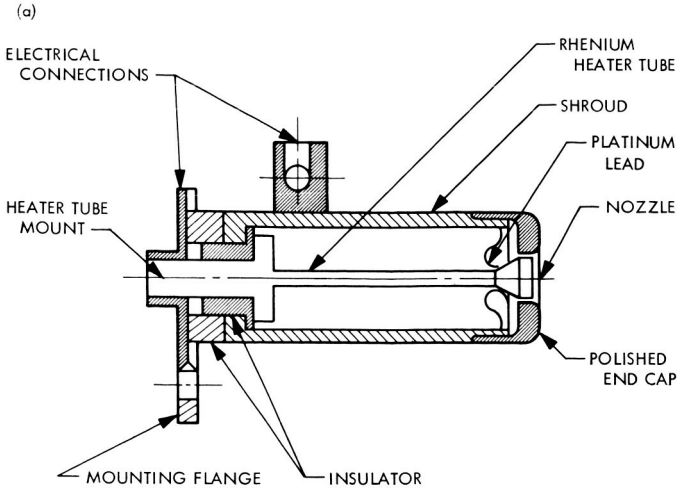

Fig. A-53. Avco ammonia thrusters: (a) assembly, (b) millipound prototype, (c) ATS-D/E micropound (photos courtesy of Avco)

Table A-19. ATS III Avco ammonia resistojet performance data

Operating conditions	Cold (~70°F)	Hot
Orbital test of thruster 1		
Thruster pressure,[a] psia	0.46	0.86
Plenum pressure,[b] psia	14.7	14.7
Thruster mass flow,[a] lbm/s	0.31×10^{-6}	0.29×10^{-6}
Thruster heater current, A	—	7.5
Thruster heater voltage, V	—	0.33
Thruster heater power, W	—	2.5
Thrust (laboratory), lbf	28×10^{-6}	41×10^{-6}
Thrust (flight), lbf	33×10^{-6}	38×10^{-6}
Specific impulse (lab), $\frac{\text{lbf-s}}{\text{lbm}}$	81	135
Specific impulse (flight),[a] $\frac{\text{lbf-s}}{\text{lbm}}$	105	132
Orbital test of thruster 2		
Thruster pressure,[a] psia	3.12	4.65
Plenum pressure,[b] psia	15.0	15.0
Thruster mass flow,[a] lbm/s	2.77×10^{-6}	2.64×10^{-6}
Thruster heater current, A	—	8.0
Thruster heater voltage, V	—	0.45
Thruster heater power, W	—	3.6
Thrust (laboratory), lbf	255×10^{-6}	430×10^{-6}
Thrust (flight), lbf	238×10^{-6}	417×10^{-6}
Specific impulse (lab), $\frac{\text{lbf-s}}{\text{lbm}}$	90	150
Specific impulse (flight),[a] $\frac{\text{lbf-s}}{\text{lbm}}$	86	158

[a]Calculated
[b]Determination of regulated plenum pressure (Ref. 15).

insulation. The entire assembly is encased in fiberglass. Characteristic data are presented in Table A-20.

"The Vela 3 thrusters were placed into orbit in July 1965, and were first successfully operated on September 19, 1965, when a thruster was fired for approximately 1800 s and changed the velocity of the spacecraft by approximately 8 ft/s. The thruster on the second spacecraft was fired in December 1965, to provide a reverse correction of 4 ft/s, and again in March 1966, to provide a correction of 4.75 ft/s. Total firing time to date is approximately 1 h.

"A diagram of the Vela advanced spacecraft thruster is shown in Fig. A-56. The thruster is shown in Fig. A-57. Characteristic data are given in Table A-21. The heater and propellant tubes are supported by plastic standoffs which sublime when the thruster is heated, thus improving thermal efficiency. This design provides thermal performance about equal to that of the Vela 3 thruster in a more compact package.

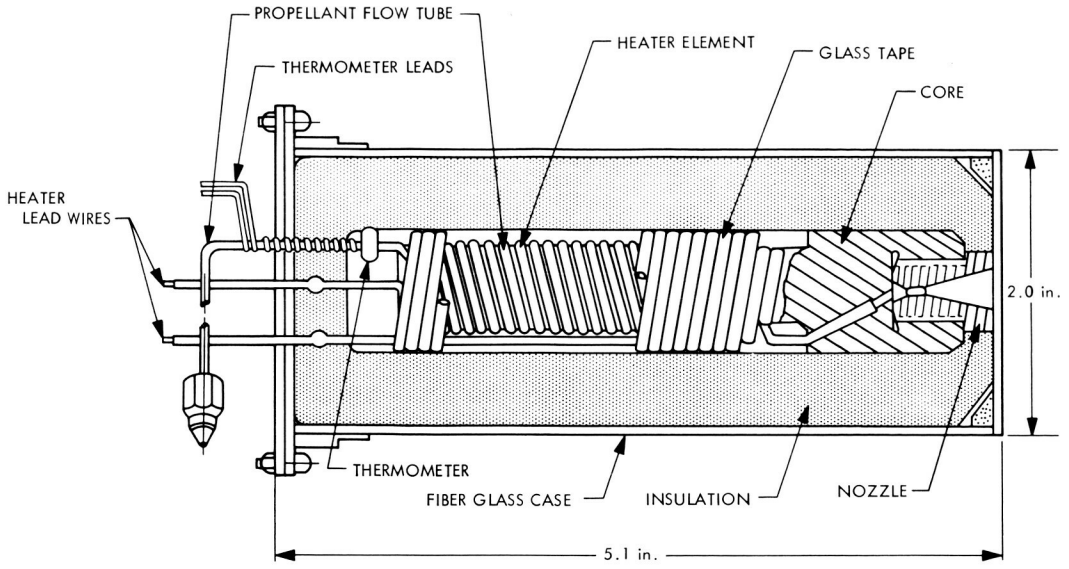

Fig. A-54. Electrothermal thruster, Vela-3

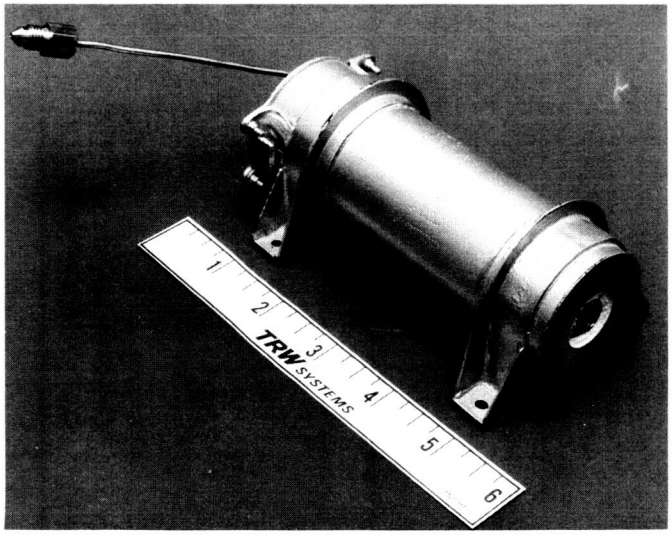

Fig. A-55. Electrothermal propulsion Vela-3 thruster (photo courtesy of TRW Systems)

Table A-20. TRW Systems propulsion data sheet—characteristics of electrothermal reaction control thruster, model *Vela 3*

Parameters	Characteristics
Thrust, lbf	0.042 (single nozzle)
Specific impulse, $\frac{\text{lbf-s}}{\text{lbm}}$	123
Propellant	Nitrogen gas with 2% argon (vol)
Power requirement, W	92
Duty cycle capability	Continuous
Chamber pressure, psia	15
Operating temperature, °F	1000 (nominal)-1200 (max)
Thermal operating efficiency, %	93
Nozzle expansion ratio	100
Thruster weight, lbm	0.65
Thruster size envelope	See Fig. A-54
Demonstration service function	Velocity correction, *Vela 3*
Service total impulse requirement	200 lbf-s (80 min)

"The design of the heater and flow tubes for the advanced Vela thruster is similar to that of the Vela 3 thruster, except that three nozzles are employed to allow three-axis thrusting. Each nozzle is controlled by a separate valve upstream of the thruster.

"Two Vela advanced spacecraft were placed in orbit in April 1967. Each of the four thrusters has been successfully operated for approximately 13 h to date.

"The ACSKS (Attitude Control and Station Keeping Subsystem) thruster using ammonia as the propellant is shown in Fig. A-58. The assembly consists of a metallic core around which are wrapped and brazed redundant sheathed electrical heating elements and four propellant flow tubes. These tubes are sized to provide the heat transfer area necessary to raise the propellant to 1500°F. The flow tubes also provide the catalytic surface necessary for decomposition of the ammonia. A nozzle is brazed to each of the four propellant flow tubes and the aft end.

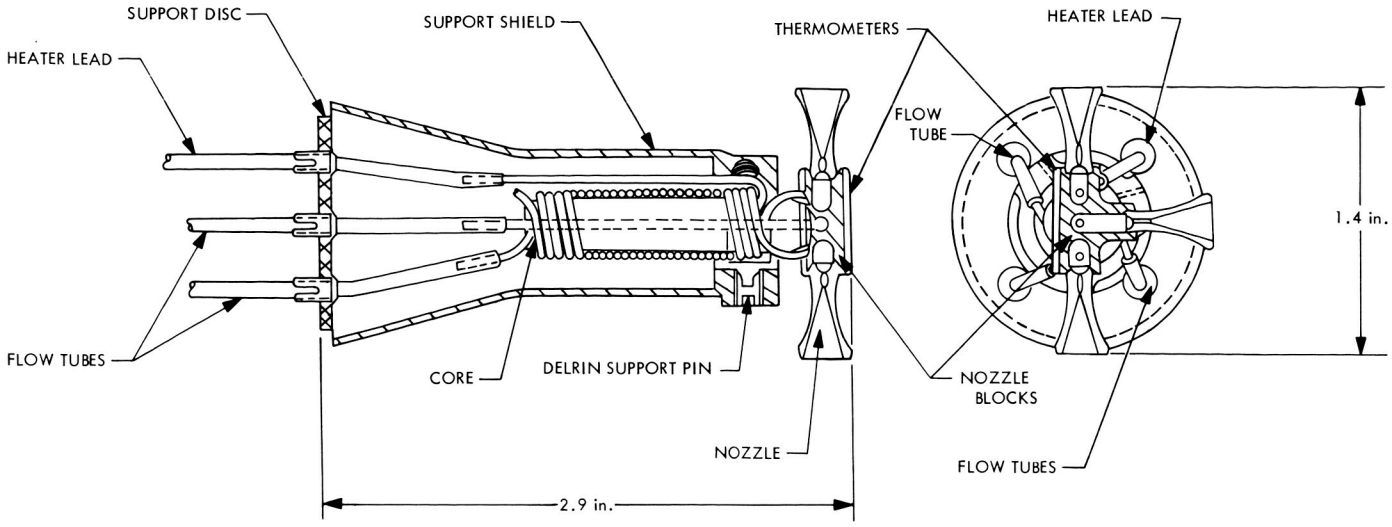

Fig. A-56. Electrothermal thruster, advanced Vela

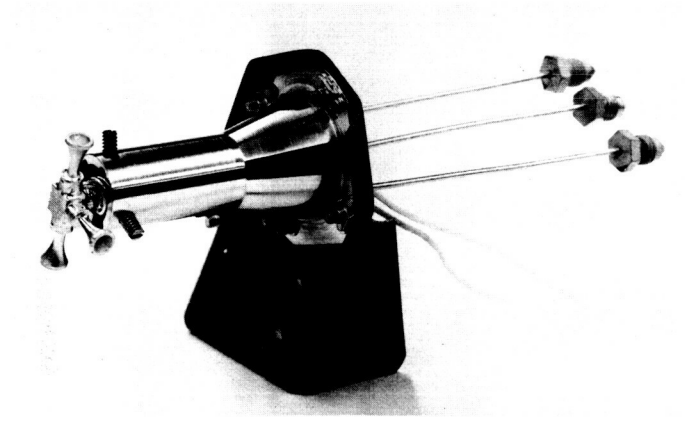

Fig. A-57. Electrothermal thruster, advanced Vela thruster (photo courtesy of TRW Systems)

A combination of refractory foil and ceramic fiber (Refrasil) provides thermal insulation. The entire assembly is packaged within a thin metal container or outer shield. The core assembly is supported by the propellant flow tubes, which are brazed to the outer shield at the inlet end. Thermal separation of the core from the outer shield is accomplished, when the heater is activated in space, by sublimation of plastic support pins.

"Characteristic data are presented in Table A-22 and the thruster is shown in Fig. A-59."

TRW Systems has developed an electrothermal thruster that uses a vortex heat exchanger. A coaxial wire-wound heater element is contained within a cylindrical cavity.

Table A-21. TRW Systems propulsion data sheet—characteristics of electrothermal reaction control thruster, model Advanced Vela

Parameters	Characteristics
Thrust, lbf	0.02 (each of 3 nozzles)
Specific impulse, $\frac{\text{lbf-s}}{\text{lbm}}$	132
Propellant	Nitrogen gas with 2% argon (vol)
Power requirement, W	30 W (steady state) 17 W, pulsing, 10% duty cycle
Duty cycle capability	Continuous
Chamber pressure, psia	30
Operating temperature, °F	1250 (nominal)-1425 (max)
Thermal operating efficiency, %	Greater than 90
Nozzle expansion ratio	67
Thruster weight, lbm	0.30
Thruster size envelope	See Fig. A-56
Demonstrated service function	Spin, attitude and velocity control, advanced Vela
Service total impulse requirement	1250 lbf-s

The propellant is injected tangentially and spirals radially inward with high tangential, but low radial velocity. The propellant is heated by passing around and through the heater element prior to expulsion through a conventional nozzle. Very high thermal efficiencies can be achieved without the use of thermal insulation because the small physical size of the heater limits radiative losses to the thruster walls. The tangential propellant injection maintains the wall temperature at a low value. The basic

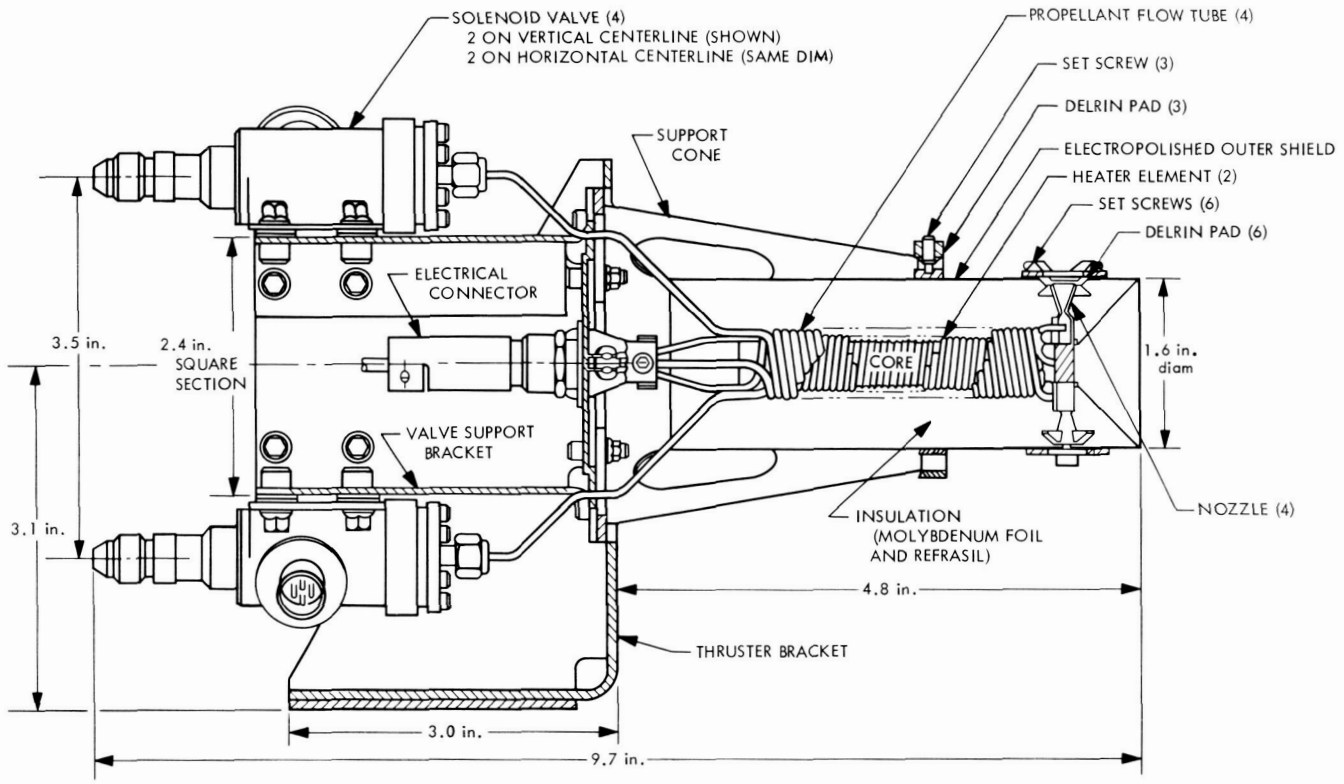

Fig. A-58. Electrothermal thruster ACSKS

Table A-22. TRW Systems propulsion data sheet—characteristics of electrothermal reaction control thruster, model ACSKS

Parameters	Characteristics
Thrust, lbf	0.020 (each of 4 nozzles)
Specific impulse, $\frac{\text{lbf-s}}{\text{lbm}}$	240–260
Propellant	Ammonia (NH_3) vapor feed-liquid stored
Power requirements, W	14
Duty cycle capability	0.0200–4.5-s pulse length, 2.0% duty cycle
Chamber pressure, psia	15
Operating temperature, °F	1550–1750
Nozzle expansion ratio	50
Thruster weight, lbm	0.5
Thruster size envelope	See Fig. A-58
Demonstrated service	5 mo at 1575°F

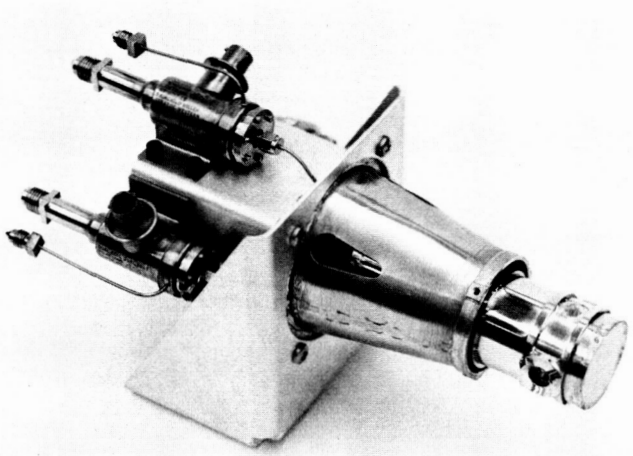

Fig. A-59. Electrothermal propulsion, ACSKS thruster (photo courtesy of TRW Systems)

thruster configuration has been tested with ammonia, nitrogen, hydrogen, Freon-14, anhydrous hydrazine, and several biowaste propellants.

The 0.003-lbf thrust unit is shown in Figs. A-60 and A-61. The unit is fabricated entirely from refractory materials. At the design point, the thruster produces 224 lbf-s/lbm specific impulse with ammonia with a power input of 28 W. The operating voltage is 26 Vdc; the inlet pressure is 20 psia. Performance data on this thruster is included in Table A-23.

Table A-23. TRW vortex resistojet performance data

Parameters	Characteristics
Thrust, lbf	0.003
Power, W	28.0
Voltage, V	19.7
Current, A	1.42
Flow rate, lbm/s	1.34×10^{-5}
Specific power, W/mlbf	9.33
Specific impulse, lbf-s/lbm	224.0

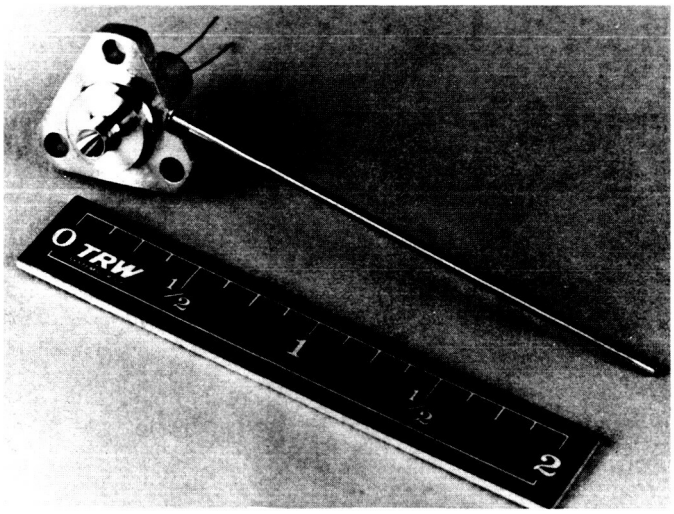

Fig. A-60. TRW vortex thruster (photo courtesy of TRW Systems)

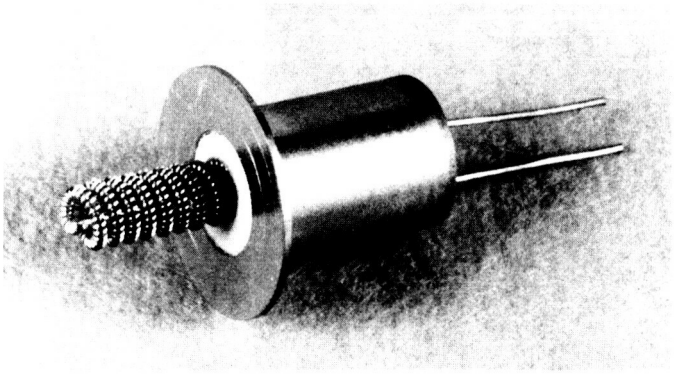

Fig. A-61. Exposed heater element of TRW vortex thruster (photo courtesy of TRW Systems)

A 0.010-lbf thrust resistojet under development at Marquardt, operates on either ammonia or hydrogen and is shown in Figs. A-62 and A-63. The R-100 resistojet consists of concentric vapor-deposited rhenium tubes that are fused into a one-piece series connected structure.

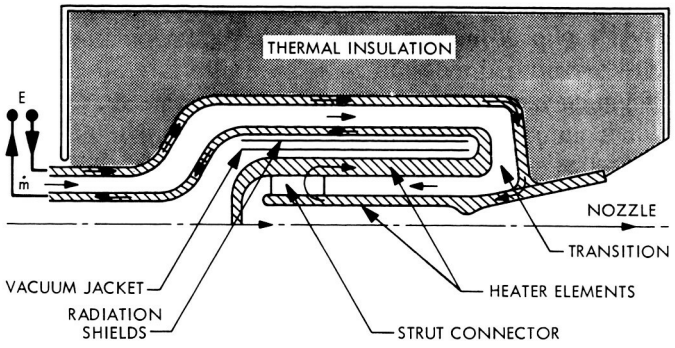

Fig. A-62. Evacuated-concentric tubular resistojet concept

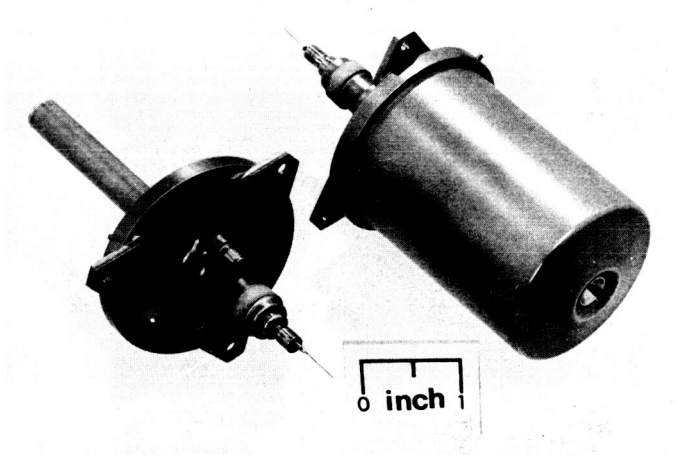

Fig. A-63. 10-mlbm resistojet thruster (photo courtesy of the Marquardt Corp.)

The nozzle is integral with the innermost tube. The outside tubes are thermally insulated from the central tube by a vacuum jacket and radiation shields. A bellows relieves axial thermal stresses. The entire assembly is insulated with metallic radiation shields, min-K, and a layer of dyna quartz. Life tests of six high-temperature resistojets have been conducted. Examination of four ammonia and two hydrogen resistojets running in a vacuum chamber for 11 mo revealed no degradation and resulted in the speculation that this design could very well run for several years. The test cycle used was 30 min *on* and 30 min *off*. Performance data with hydrogen and ammonia service are presented in Table A-24 (Ref. 45).

The GE thruster shown in Figs. A-64 and A-65 consists of three components: (1) an insulation package, (2) a thruster body, and (3) an electrical heater unit. The insulation package is comprised of a series of 40 concentric nichrome shells (0.003-in. wall thickness) separated by

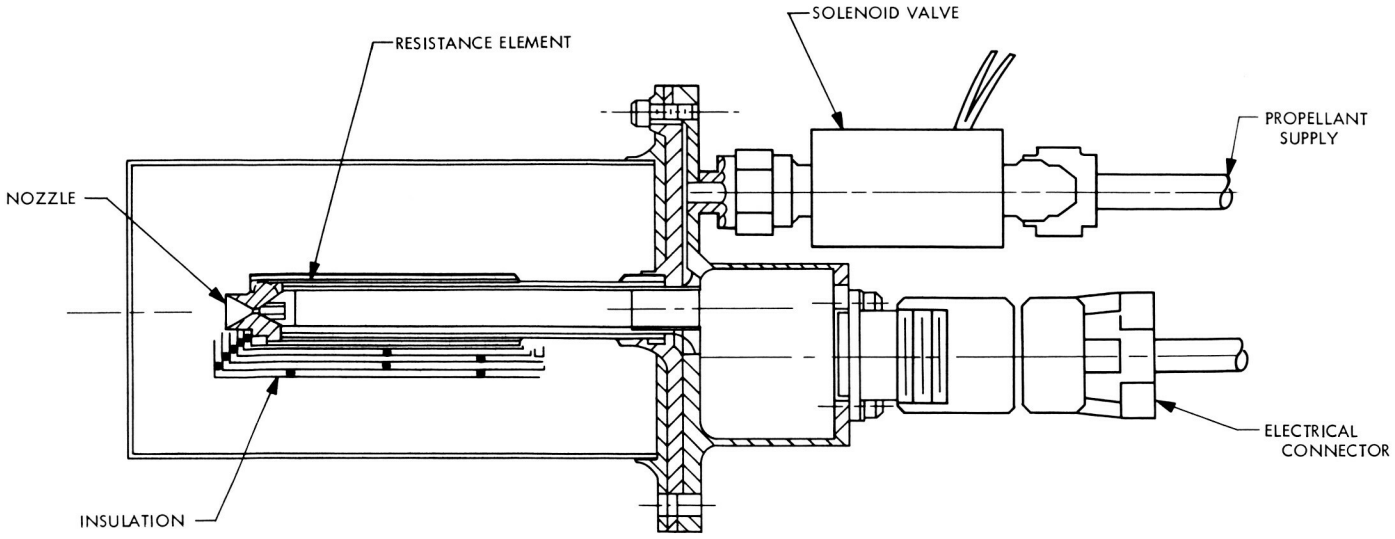

Fig. A-64. GE single jet thermal storage resistojet

Table A-24. Marquardt MORL resistojet performance data

Parameters	Ammonia	Hydrogen
Thrust level, mlbf	10	10
Power, W	175	230
I_{sp}, lbf-s/lbm	300	500
Mass, g	264	204
Duty cycle	Continuous	Continuous
Gas temperature, °K	2200	2200
Status	Excess of 8000 h of life test	Excess of 8000 h of life test

Table A-25. GE resistojet performance data

Parameters	Laboratory demonstration	NRL satellite
Thrust, mlbf	20	0.01
Propellant	Ammonia	Ammonia
Power, W	30	2
I_{sp}, lbf-s/lbm	230	110
Mass, lbm	1.75	0.55
Duty cycle	$<2\%$	$<2\%$
Gas temperature, °R	2300	2300

nichrome wire (0.014 in. diam). The shells are contained by a Hastelloy X outer shell. The heater module is a swaged unit consisting of a platinum filament on a magnesia core contained in a Hastelloy X sheath. The thruster body contains a sonic nozzle. Performance data for this thruster were extracted from Ref. 46 and are presented in Table A-25. Also included in this report is a low-power

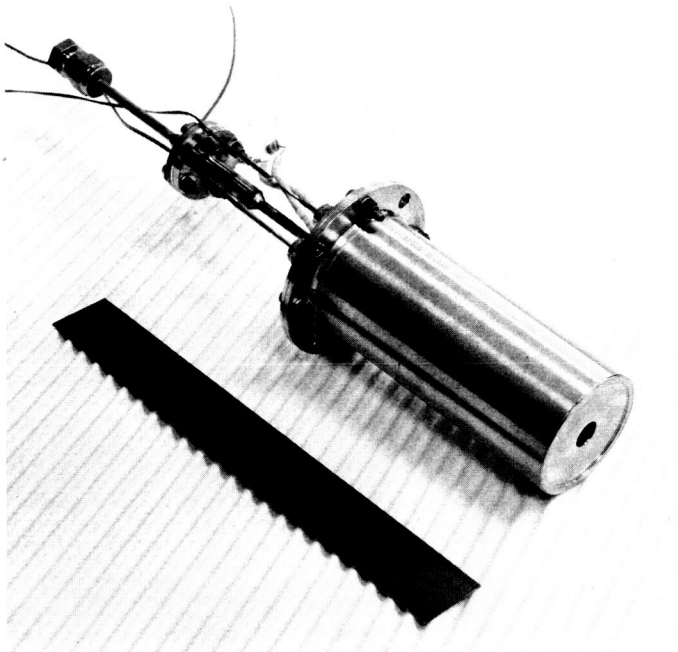

Fig. A-65. GE single jet thermal storage thruster (photo courtesy of GE)

NRL resistojet. These two resistojets were flight-qualified. The NRL system was placed in orbit; the classified nature however of the satellite restricts release of performance data.

The primary problem areas in the development of heated fluid reaction control systems relate to the thrusters. Electrothermal thrusters operating at temperatures below 2000°F have been flight-qualified and flown.

Long-term demonstration tests of higher-temperature (2500°F) thrusters have indicated that the reliability goals applicable to mission durations greater than 2 yr can be realized. Reliability of high-temperature (4000°F) and high-performance thrusters remains essentially undetermined and considerable effort is still required before these thrusters can be flight-qualified.

XII. Thruster Heater: Radioisojet

The radioisojet is similar to the resistojet; cold fluid increases in temperature by passing over a nuclear heater source. Performance of the working fluid can be substantially improved by an increase in expulsion temperature. The selection of radioisotope and its configuration will define the source temperature. A temperature around 2000°F is usually chosen to reduce material and heat-shielding problems and still maintain a temperature sufficient to dissociate ammonia and ammonia base propellants.

This system should be thought of as a subsystem rather than a complete thruster system. The feed systems can be inert gas, subliming solid, hydrazine plenum, or vaporizing liquid systems mentioned in other sections of Appendix A. Propellants which are especially attractive are those which undergo a dissociation (lowering of molecular weight) below 2000°F. Ammonia, ammonium hydrosulfide, and ammonium carbamate are a few of the propellants which undergo a dissociation at 1400 to 1800°F. Low molecular weight gases are also especially attractive.

The selection of the radioisotope is influenced by several factors:

(1) Power density (both weight and volume).

(2) Availability and cost.

(3) Half-life.

(4) Specific activity and shielding requirements.

Spacecraft integration, launch-handling, and shielding requirements tend to eliminate isotopes having significant external radiation fields, such as cobalt-60 and strontium-90. Isotopes receiving considerable attention for propulsion applications include plutonium-238, promethium-147, and polonium-210. Characteristics of these isotopes are presented in Table A-26. Polonium-210 is the least expensive, and presents only minor shielding problems. Unfortunately, its short half-life eliminates it from long-life missions. Both promethium-147 and plutonium-238 have been used in radioisojet development programs.

Table A-26. Characteristics of radioisotope heat sources

Isotope	Pm-147	Po-210	Pu-238
Half-life	2.6 yr	138 days	89 yr
Power density, W/gm	0.361	641.3	0.56
Gamma dose rad/h-W at 1 m	1×10^{-3}	1.5×10^{-4}	5.5×10^{-6}
Neutron dose rad/h-W at 1 m		2.5×10^{-7}	8.0×10^{-6}
Shielding requirements	Minor	Minor	Minor
Availability	Limited, prop	Good	Good
Future cost, $/W	91	10	890

The AEC requirements for launch safety (launch explosions, aborted launches, inadvertent reentry from orbit, and ground impact) impose strict capsule design restraints. As a result, capsule design represents a critical aspect of radioisotope thruster development. In addition, considerable thermal design is necessary to minimize heat loss and to optimize the required heat source configuration. Radioisotope thrusters attain maximum performance under low-flow conditions. The thermal storage efficiency of the heat source and the duty cycle will define the performance delivered.

TRW Systems has done considerable work in radioisojet development. The following several paragraphs and diagrams are extracted from Ref. A-34 with the permission of TRW Systems.

"The decomposed ammonia radioisotope thruster (DART), shown in Fig. A-66, consists of a plutonium fuel form encapsulated in a cylindrical, refractory metal capsule, around which four propellant flow tubes are coiled. Each tube is connected to a separate propulsive nozzle. Thermal insulation, in the form of refractory metal radiation shields, surrounds the entire assembly. Aerodynamic fins aid in achieving intact reentry into the atmosphere by causing the thruster to spin, thereby producing a uniform distribution of the aerodynamic heat flux. A coolant limits maximum temperature prior to launch so as to prevent oxidation of the insulation. The DART is designed to provide thrust either continuously or in a pulsed mode of operation. The minimum operating temperature in space, dictated by the requirement for complete decomposition of the ammonia propellant, is 1500°F. The maximum temperature is limited to a safe level when no propellant is flowing by proper thermal

insulation design. Constant thrust over the entire temperature range is ensured by sizing of the pneumatic components. The thruster was operated at the AEC Mound Laboratory during 1967. Technical data are given in Table A-27 and the thruster is shown in Fig. A-67. Characteristic data for a similar thruster operating on hydrogen propellant are presented in Table A-28.

"The POODLE thruster shown in Fig. A-68 was designed for primary upperstage propulsion. The thruster uses polonium-210 fuel to heat gaseous hydrogen.

"The cylindrical isotope containment capsules were fabricated from a tungsten-rhenium alloy. The hydrogen propellant flows around a thin helical annulus surrounding the capsules and then is expelled through a nozzle. The entire assembly is surrounded with a cooling water jacket (to remove the heat during ground operations) and high-temperature insulation comprised of refractory radiation shields. The entire package is then enclosed within a finned reentry module. The POODLE concept has been demonstrated at subscale power levels at the AEC Mound Laboratory. Data for this thruster are given in Table A-29."

Table A-27. TRW Systems propulsion data sheet—characteristics of decomposed ammonia radioisotope thruster, model Dart

Parameters	Characteristics
Thrust, lbf	0.005-0.10 each nozzle (can be multi-nozzle)
Specific impulse, $\frac{\text{lbf-s}}{\text{lbm}}$	230-280
Propellant	Ammonia (NH_3) vapor feed-liquid stored
Duty cycle	Continuous (thrust 0.01 lbf or lower) pulsing (thrust 0.01–0.10 lbf)
Radioisotope compound	Pu-238
Chamber pressure, psia	15
Operating temperature, °F	Above 1500
Nozzle expansion ratio	50 minimum
Thruster size envelope	See Fig. A-66
Thruster weight, lbm	Classified
Demonstrated service	Tested at AEC Mound Lab., January 1967
Potential applications	Attitude control, station keeping, drag makeup

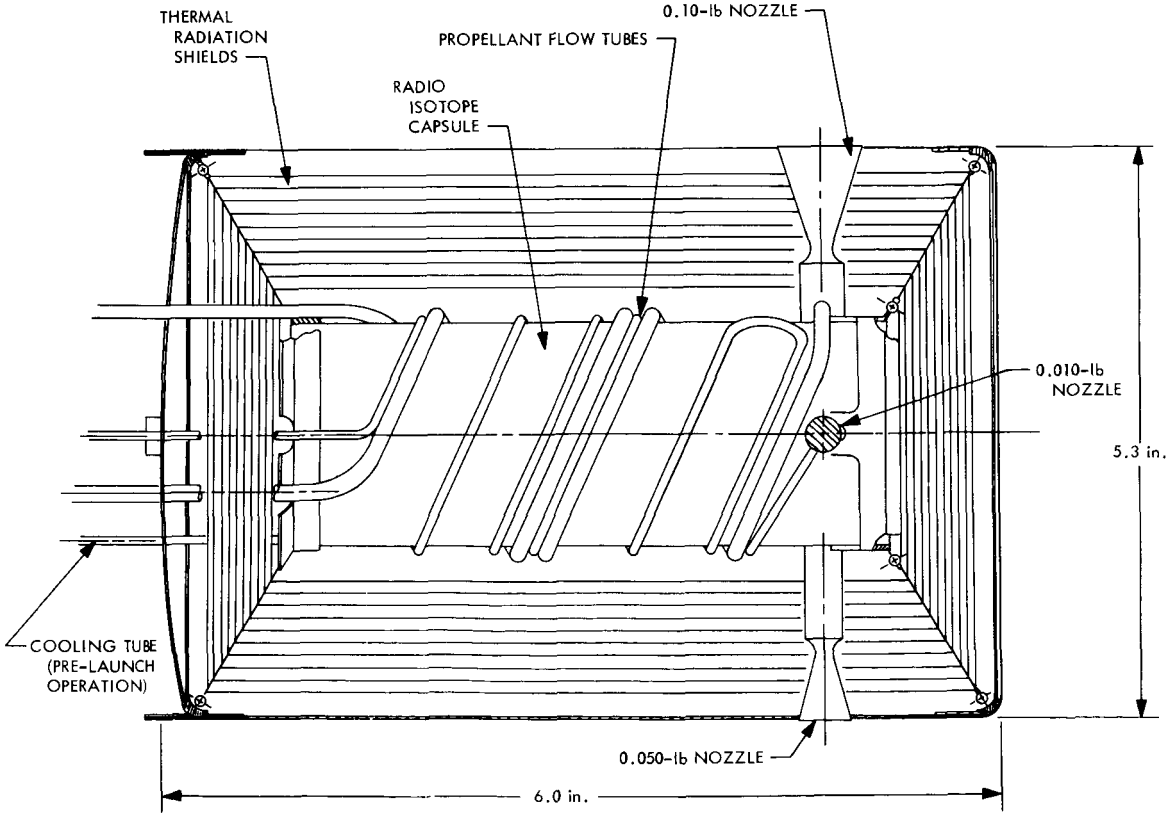

Fig. A-66. Radioisotope thruster, Dart

General Electric, along with Monsanto (Mound Laboratories), has developed a radioisojet system utilizing promethium-147 as fuel (Ref. 47). The thermal design was refined by the use of simulated electrical heaters (this method is often used in nuclear technology). The thruster has the same basic design as the GE thermal storage resistojet, previously discussed in Appendix A. The electrical heater is replaced by a radioisotope heat source (see Fig. A-69). Characteristics of this thruster are presented in Table A-30. This thruster has been demonstrated at the AEC Mound Laboratory.

Table A-28. TRW Systems propulsion data sheet—characteristics of radioisotope heated reaction control thruster, model HRT

Parameters	Characteristics
Thrust, lbf	0.005-0.10
Specific impulse, $\frac{\text{lbf-s}}{\text{lbm}}$	485-545
Propellant	Hydrogen (H_2) liquid feed gaseous feed
Duty cycle	Pulsed, or continuous below 0.0075 lbf
Radioisotope compound	Pu-238
Chamber pressure, psia	15
Operating temperature, °F	1500-2000
Nozzle expansion ratio	50 minimum
Thruster weight, lbm	4.5
Demonstrated service	In development (key components same status as model Dart)
Potential applications	Attitude control, station keeping, drag makeup

Table A-29. TRW Systems propulsion data sheet—characteristics of radioisotope heated thruster, model POODLE

Parameters	Characteristics
Thrust, lbf	0.25
Specific impulse, $\frac{\text{lbf-s}}{\text{lbm}}$	710
Propellant	Hydrogen
Duty cycle	Continuous
Radioisotope compound	Po-210
Operating temperature, °F	3600
Thruster size envelope	See Fig. A-63
Thruster weight, lbm	Approximately 45
Demonstrated service	Ground demonstration with subscale fuel loading

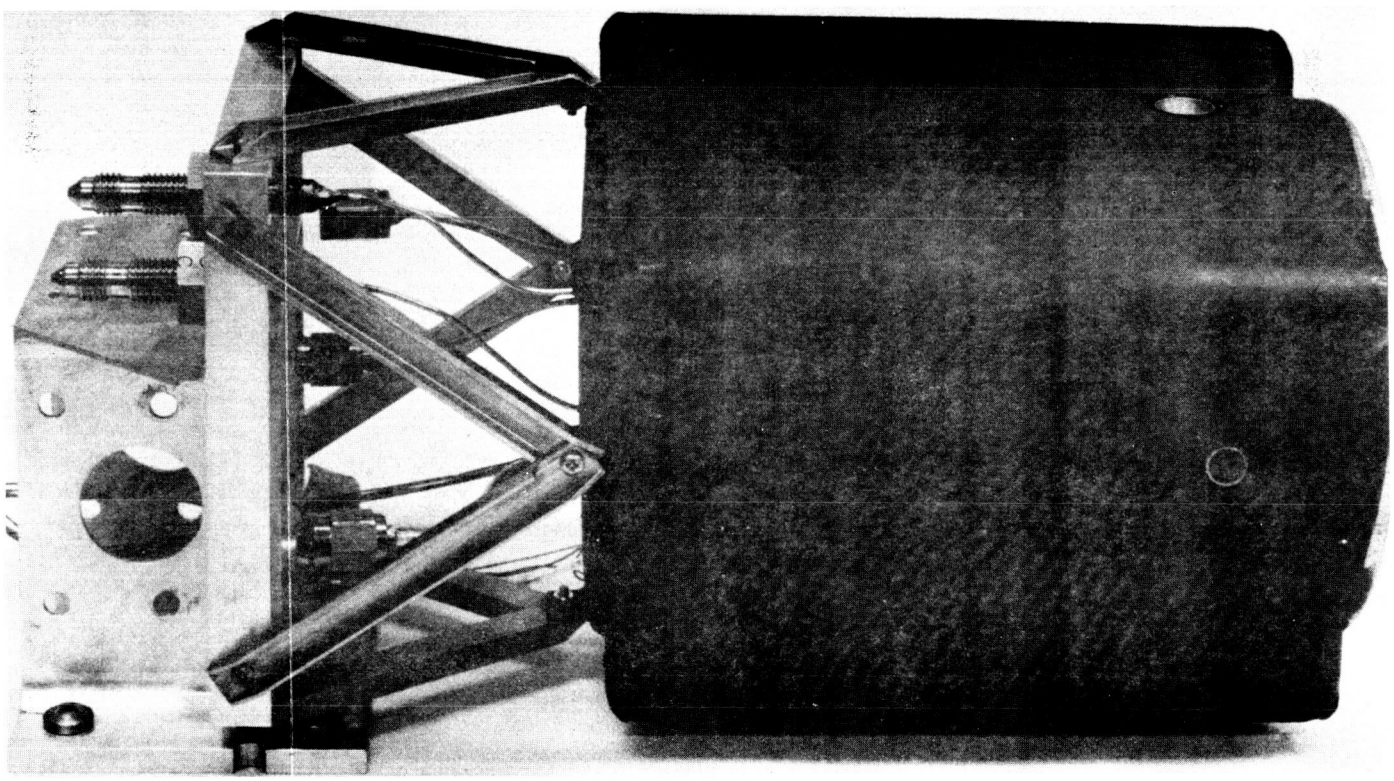

Fig. A-67. Radioisotope heated propulsion decomposed ammonia thruster (photo courtesy of TRW Systems)

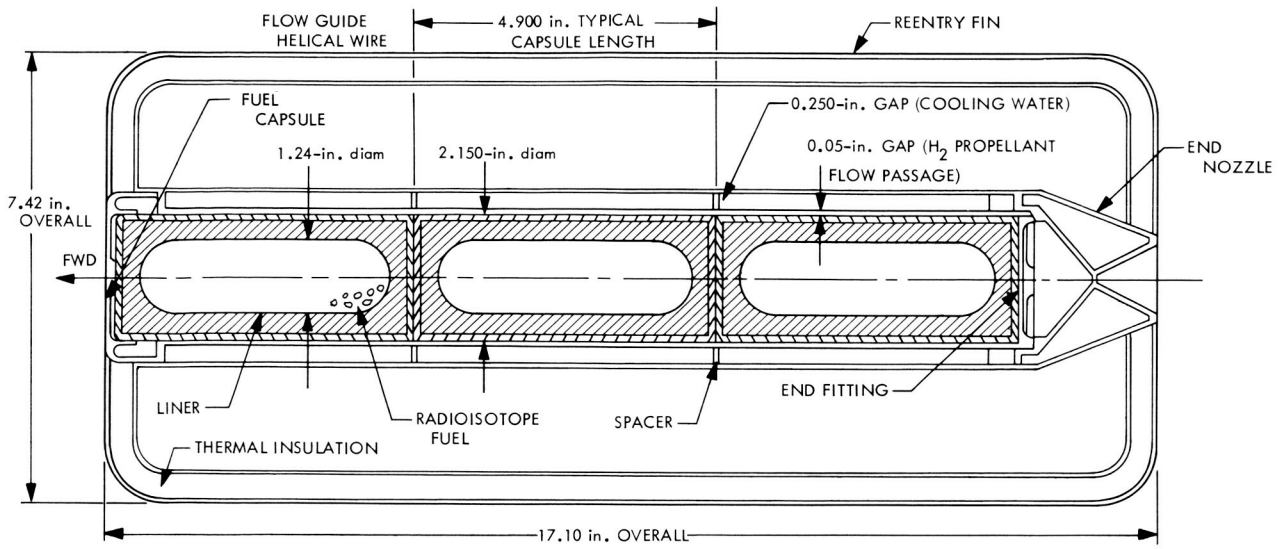

Fig. A-68. Radioisotope thruster Poodle

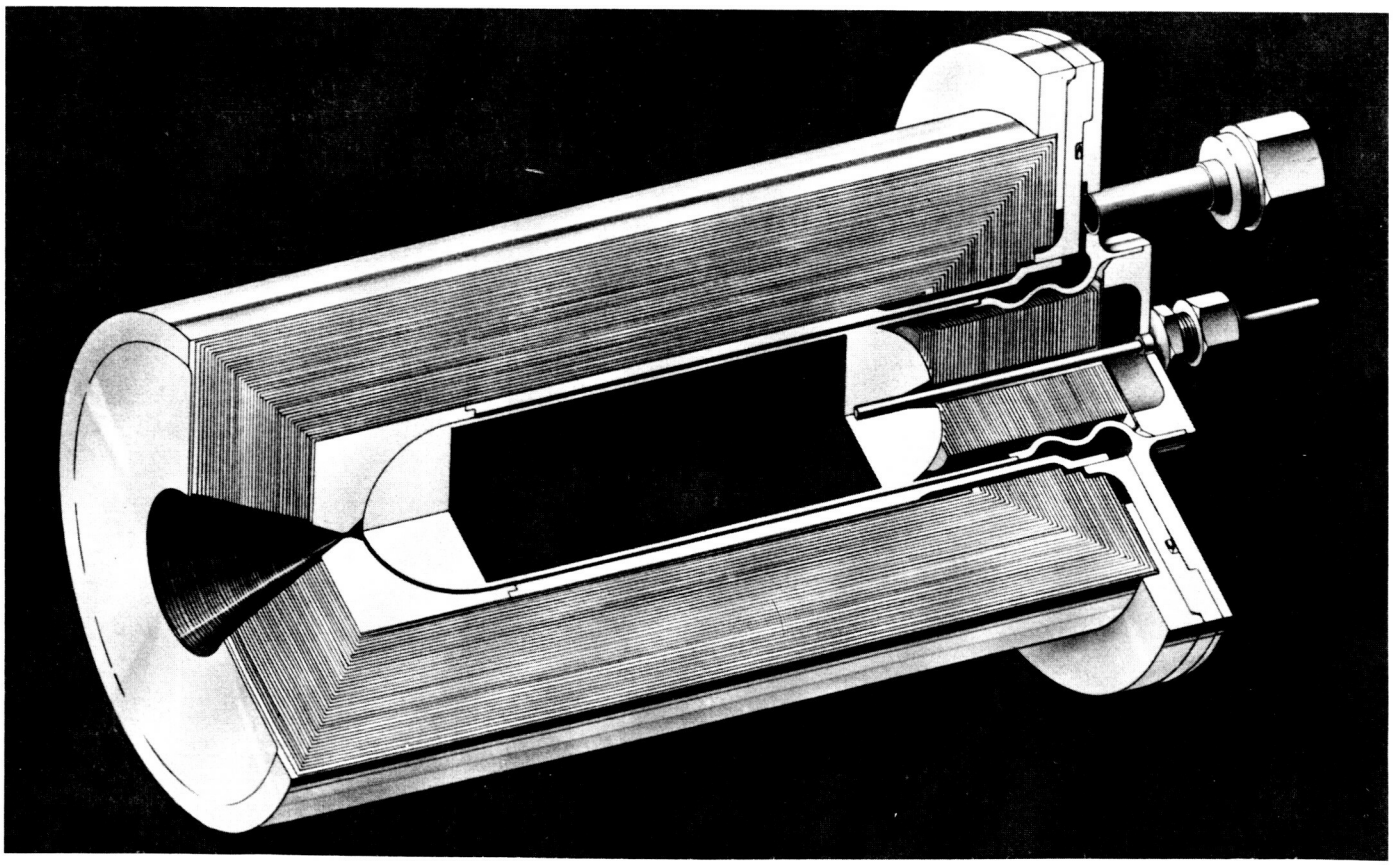

Fig. A-69. Cross-sectional view of TSK 2000-IRE simulated radioisojet thruster

Table A-30. GE radioisojet performance data

Parameters	Data
Propellant	Ammonia
Radioisotope fuel	Pm-147
Thrust fuel, lbf	0.02
Operating temperature, °F	1750
Duty cycle	Variable
Specific impulse, $\frac{\text{lbf-s}}{\text{lbm}}$	Variable; 232 at 1660°F
Power, W	60 (thermal)
Mass, lbm	5.0

Radioisotope-heated thrusters not only have many of the materials problems as electrothermal resistojets (reliability for long-duration, high-temperature performance, and thermal cycling effects), but these materials must satisfy the additional design constraints primarily imposed by nuclear safety considerations. Plutonium-238 or promethium-147 thrusters operating at temperatures of 2000 to 2500°F can be expected within the next decade. Operating temperatures of the order of 2900°F can be expected for polonium-210 heat sources (short mission life) within the same period.

Appendix B

System Mass and Performance

I. Introduction

The assigned system mass is an integral part of subsystem comparisons. For any given mission, a penalty must usually be paid for excess mass. For most missions, a ceiling is set on overall system mass by the launch vehicle; however, in the past, some system design masses have been below launch vehicle capabilities (*Voyager*). Before any system mass calculation can be initiated, the required mass of propellant must be determined. It is for this reason that performance has been considered along with mass in this appendix.

Thruster total impulse requirements can be determined from mission requirements. After selection of a thrust range, propellant performance can be calculated. The mass of propellant is determined by dividing total impulse by specific impulse. Propellant feed system mass is a function of required propellant mass. Component mass is tabulated so combinations of components may be altered to correlate with various redundancy concepts.

II. Performance

Spacecraft ambient temperature is set at 80°F. Table B-1 presents performance characteristics of the systems considered. Whenever possible, the performance values were selected from actual test data. The inert gas-delivered specific impulse was assumed from 90 to 92% theoretical. This assumption was also used for the hydrazine plenum, cold hydrazine and water electrolysis, and vaporizing liquids calculations. Resistojet and radioisojet performance data were based on a propellant temperature of 2000°F along with actual flight and test data (Refs. 14, 15,

Table B-1. Performance characteristics of systems studied

Systems	Thrust level, lbf	I_{sp} (vac), lbf-s/lbm	I_{min}, lbf-s
Inert gas (80°F)			
H_2	0.0001–1.0	272	10^{-6}
He	0.0001–1.0	165	10^{-6}
Ne	0.0001–1.0	75	10^{-6}
N_2	0.0001–1.0	72	10^{-6}
A	0.0001–1.0	52	10^{-6}
Kr	0.0001–1.0	37	10^{-6}
Xe	0.0001–1.0	28	10^{-6}
CF_4	0.0001–1.0	45	10^{-6}
CH_4	0.0001–1.0	105	10^{-6}
Tridyne (T = 1300°F)	0.1	143	10^{-3}
Hydrazine direct catalyst			
Steady state	0.05–0.10	200	5×10^{-4}
Cold pulse	0.05–0.10	100	5×10^{-4}
Hot (50th) pulse	0.05–0.10	170	5×10^{-4}
Steady state	0.5–5	225	5×10^{-3}
Cold pulse	0.5–5	110	5×10^{-3}
Hot (50th) pulse	0.5–5	210	5×10^{-3}
Hydrazine resistojet			
Initial pulse and steady state	10^{-2}	175	10^{-4}
Initial pulse and steady state	10^{-1}	200	10^{-3}
Initial pulse	0.1–5	210	10^{-3}

Systems	Thrust level, lbf	I_{sp} (vac), lbf-s/lbm	I_{min}, lbf-s
Hydrazine plenum			
Cold (80°F)	0.010–0.060	100	10^{-4}
Electrolysis			
Hot O_2/H_2 gas	0.05–5	350	5×10^{-2}
Hot O_2/H_2 gas (Marquardt)	0.05–5 (2500°F)	310	5×10^{-2}
Cold H_2O gas (80°F)	100×10^{-6} to 1.0	109	10^{-6}
Hydrazine cold (80°F)	100×10^{-6} to 1.0	116	10^{-6}
Vaporizing liquid (80°F)			
NH_3	10×10^{-6} to 50×10^{-3} lbf	97	10^{-7}
Freon	10×10^{-6} to 50×10^{-3} lbf	52	10^{-7}
Butane	10×10^{-6} to 50×10^{-3} lbf	84	10^{-7}
Propane	10×10^{-6} to 50×10^{-3} lbf	89	10^{-7}
Resistojets (2000°F)— Radioisojet (2000°F)			
NH_3	10×10^{-6} (3 W)	130	10^{-7}
	100×10^{-6} (3 W)	160	10^{-6}
	10×10^{-3} (10 W/mlbf)	230	10^{-4}

Table B-1. (contd)

Systems	Thrust level, lbf	I_{sp} (vac), lbf-s/lbm	I_{min}, lbf-s
NH_3 (radioisojet)	5 to 20 × 10^{-3}	250	10^{-4}
H_2 (gas)	100 × 10^{-6} to 1 (20 W/mlbf)	550	10^{-7}
N_2 (gas)	100 × 10^{-6} to 1 (3.5 W/mlbf)	150	10^{-7}
Subliming solids (80°F)			
Ammonium hydrosulfide	10^{-2}	78	20
	10^{-3}	75	2.0
	10^{-4}	45	0.2
Ammonium carbamate	10^{-2}	78	20
	10^{-3}	74	2.0
	10^{-4}	45	0.2
Monomethyl ammonium carbamate	10^{-2}	73	20
	10^{-3}	70	0.2
	10^{-4}	42	0.02
Superheated subliming solid (2000°F)			
Ammonium carbamate	10^{-2} to 10^{-4} (10 W/mlbf)	195	0.2

16, 45, and 46). Figures B-1–B-3 present the effect of power and efficiency on resistojet (NH_3, N_2, and H_2) performance; also several existing designs are plotted to define efficiencies that have been obtained (5–20 mlbf thrust). The direct catalytic hydrazine decomposition performance data were extracted from many papers (Refs. 14, 19, 20, 48, 49, and additional data[10]). Numbers thought to be representative were selected. Specific impulse during the pulse mode is a function of duty cycle and pulse number. Between 90 to 95% of steady-state specific impulse will be reached after 50 pulses of a 100 ms *on* and 1 s *off* duty cycle. In a steady-state mode, 90 to 95% theoretical specific impulse is achieved after 10 to 20 s of firing. Figures A-16 and A-22 present a more complete picture of the effect of temperature and pulse width on thruster performance. Hydrazine/resistojet performance characteristics were taken from Ref. 24. Initial pulse specific impulse is high due to the absence of heat losses. Figure B-4 presents the effect of power and efficiency on hydrazine resistojet performance, and two designes are plotted to define efficiencies that have been obtained. Subliming solid performance values were calculated from Ref. 30. Delivered specific impulse for the Tridyne system were extracted from Ref. 11. Electrolysis cell performance for the hot gas mode was extracted from present work on hydrogen-

[10]Data supplied by B. Schmitz, Rocket Research, Redmond, Wash.

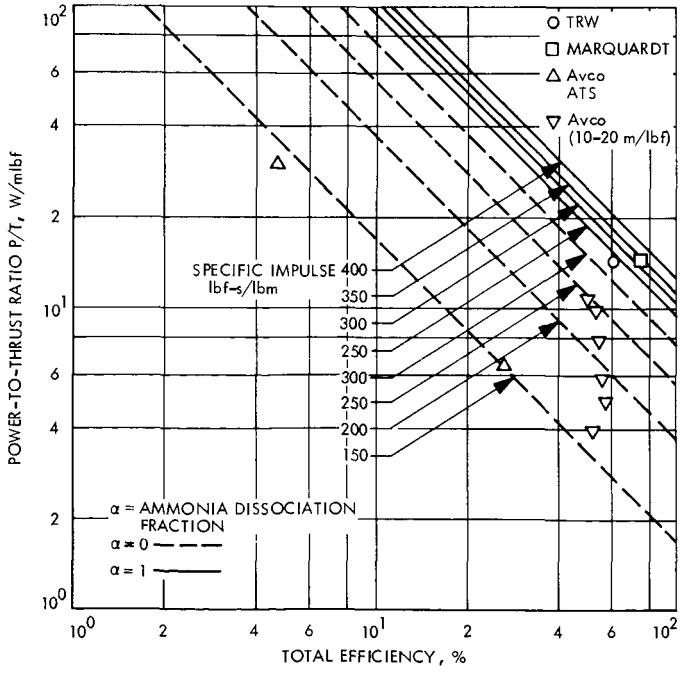

Fig. B-1. Ammonia resistojet efficiency as a function of specific impulse and power-to-thrust ratio

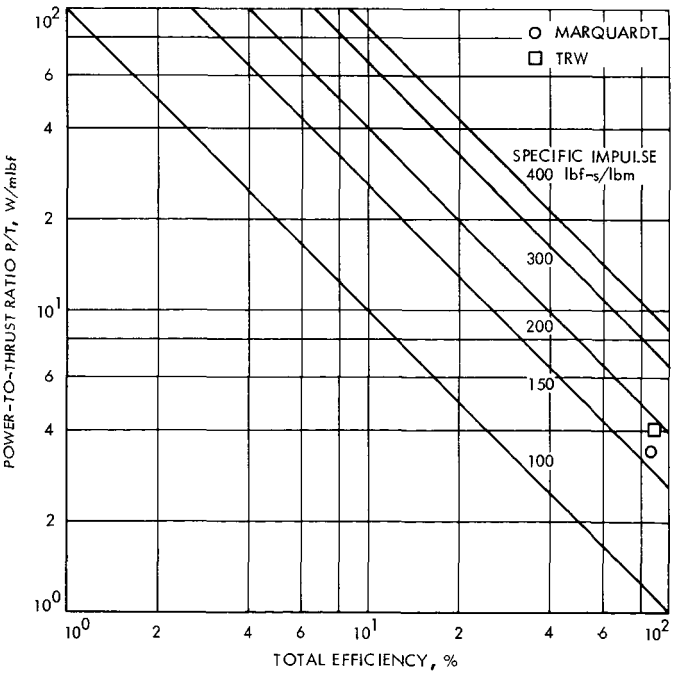

Fig. B-2. Nitrogen resistojet efficiency as a function of specific impulse and power-to-thrust ratio

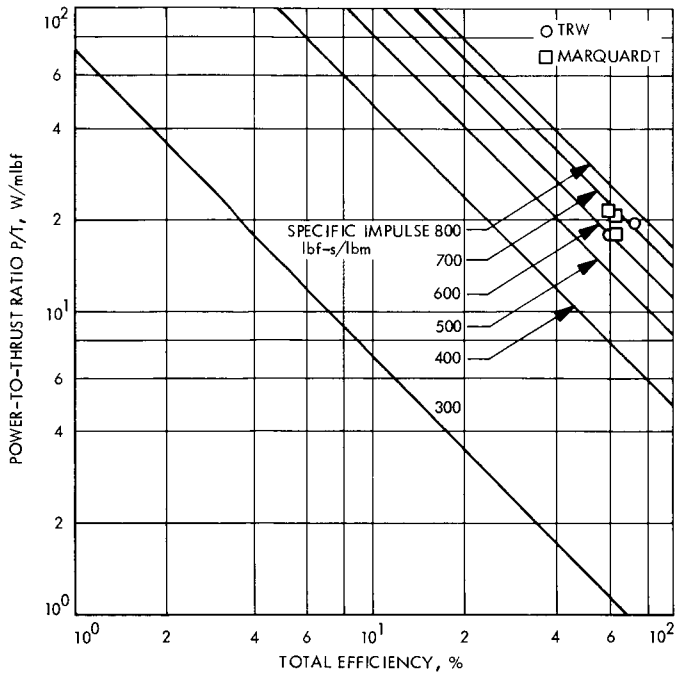

Fig. B-3. Hydrogen resistojet efficiency as a function of specific impulse and power-to-thrust ratio

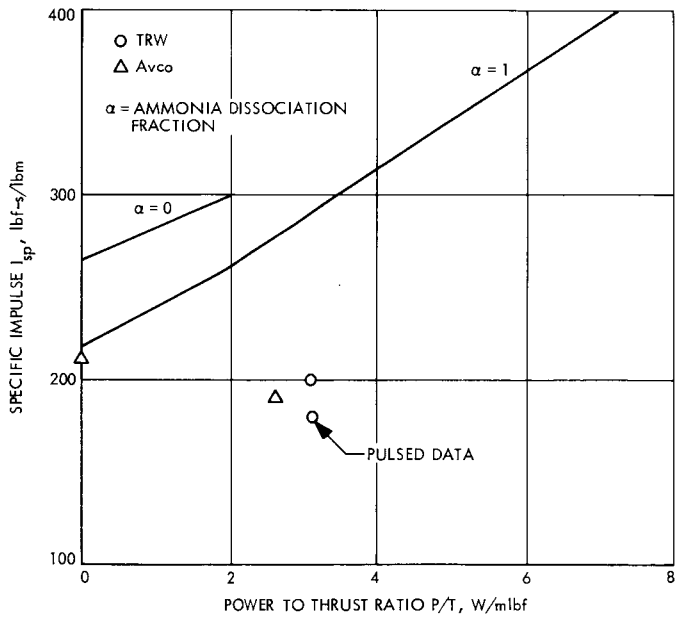

Fig. B-4. Specific impulse of a hydrazine resistojet vs power-to-thrust ratio (solid curves represent 100% total efficiency)

oxygen catalytic thruster design. A hydrogen-oxygen catalytic thruster under development at NASA-Lewis (Ref. 50) will provide a specific impulse of 350 lbf-s/lbm at a 3.5 to 1 mixture ratio. Pulse mode operation of this thruster is quite limited since ignition delay times on the order of 1 sec have been observed. Also included is a Marquardt spark ignited thruster. The performance presented is for an 8 to 1 mixture ratio with hydrogen acting as a film coolant. This is a predicted delivered specific impulse.

Satellite parameters such as mass, moment arms, and moments of inertia, along with design requirements of tipoff rate reduction, spinup, reference acquisition, momentum wheel unloading, and limit cycle operation define thruster size and duty cycle. Each design operation will require a specific duty cycle which will establish the delivered specific impulse (Table B-1). Propellant mass is then calculated for each operation and the result is summed. Although many missions will require only one level of thrust, a few may require two thrust levels. Systems mass sizing is included in the following sections.

III. System Sizing

Spherical tanks were assumed for all systems. Aluminum and titanium were selected as candidate materials. Although fracture mechanics is the best method of tankage calculation, the variety of propellants considered in this report vastly exceed available fracture mechanics data. As a result of insufficient data, the rib stress method of tank calculation was used. A safety factor of 2.2 was selected for all systems. In addition, two design criteria were imposed on the calculations. These two criteria required a minimum working thickness of 0.020 in. to allow tankage handling and machining along with a maximum diameter-to-wall thickness ratio of 850 for aluminum and 1000 for titanium to alleviate buckling during a vacuum purge.

Feed and thruster systems are considered separately. This is done to aid in redundancy calculations. A mass penalty of 0.3 lbm/W of electrical power is imposed on all systems.

IV. Inert Gas and Tridyne

The typical system consists of a pressure vessel, start and fill valves, lines, filter, regulator, solenoid valve, and thruster. The feed system is displayed in Fig. B-5. The pressure vessel is set at 3500 psia and will blow down to 200 psia. This defines a requirement of 5.7% propellant residual. If filament-wound epoxy composites are considered, considerable reductions in tank mass can be

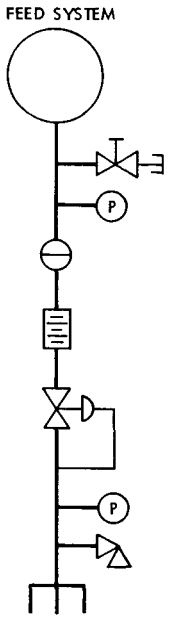

COMPONENT	MASS, lbm
FILL VALVE	0.25
PRESSURE TRANSDUCER	0.25
START VALVE	0.25
FILTER	0.35
REGULATOR	0.40
PRESSURE TRANSDUCER	0.25
RELIEF VALVE	0.30
MISC. LINES	0.20
	2.15

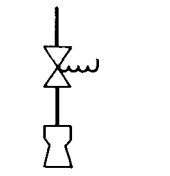

COMPONENT	MASS, lbm
SOLENOID CONTROL VALVE	0.20
LINES (1 PER THRUSTER)	0.20
THRUSTER (0.01 TO 0.10 lbf)	0.10
THRUSTER (0.20 TO 1.0 lbf)	0.20

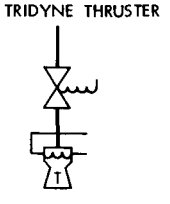

COMPONENT	MASS, lbm
SOLENOID CONTROL VALVE	0.20
LINES (1 PER THRUSTER)	0.20
THRUSTER (0.10 lbf) [CLUSTER OF 3]	0.20
POWER (1.5 W PER CLUSTER IN CLUSTER OF THREE)	0.45

Fig. B-5. Inert gas system

achieved. Filament-wound vessels require metallic liners because the shell is very permeable to most gases; also, water absorption of the liner becomes a problem which can leäd to tank rupture at high altitude. Titanium was selected as the tankage material because of its favorable past performance on many programs. Figure B-6 presents propellant related feed system mass as a function of propellant mass. The Tridyne system is included since its propellant is essentially an inert gas mixture.

Thruster mass numbers are presented in Fig. B-5. Tridyne thruster mass is also included, and a penalty of 0.3 lbm/W is imposed on the Tridyne thrusters.

V. Hydrazine Direct Catalyst, Resistojet, and Plenum

The typical system consists of a pressure vessel containing a bladder, pressurized by either a regulated gaseous nitrogen supply or a blowdown concept utilizing the propellant tank as shown in Fig. B-7. Surface tension retention screens have been proposed for replacement of bladders (Ref. 51). Slow permeation of bladders by gas and propellant presents problems, which do not have screens. Retention screens have been used by Lockheed in the Agena feed system and are being actively studied for general propellant tank applications. Spinning craft require no vapor-liquid separation device. Mass estimates for hydrazine systems included a small adjustment for bladder mass. Errors arising from the addition of this mass to a spinning tank or a tank with retention screens can be ignored.

Titanium was selected as tankage material and ethylene propylene rubber as bladder material. The pressurized and blowdown feed systems are presented in Fig. B-7. For the pressurized system, initial gas pressure was set at 3500 psia and regulated to 300 psia. A 200 psia pressure differential was required for proper pressure regulation, thus defining the required pressurant gas. Pressurant tank mass was calculated as in the inert gas system. One half of the propellant tank was allocated for pressurant gas in the blowdown system. Thus, the system operational pressure was 300 psia to 150 psia. A filter, start and fill valves, a pressure transducer, and lines are downstream of the tank. Figure B-8 presents feed system mass as a function of propellant mass. Both blowdown and regulated pressure supply concepts are included.

Thruster mass values are also provided in Fig. B-7. Hydrazine resistojet thruster mass is also included in this figure along with the required power penalty. The feed system for the hydrazine resistojet thruster is identical to that of the direct catalyst.

A typical hydrazine plenum system is presented in Fig. B-9. Propellant tankage mass for the hydrazine plenum system is identical to that of the direct hydrazine thrusters; however, additional feed system mass must be added for plenums, gas generators, and plenum pressure control hardware. Feed system mass is presented in Fig. B-10 as a function of propellant mass. Again, both blowdown and regulated pressure supply concepts are included. Thruster mass values are also provided in Fig. B-9.

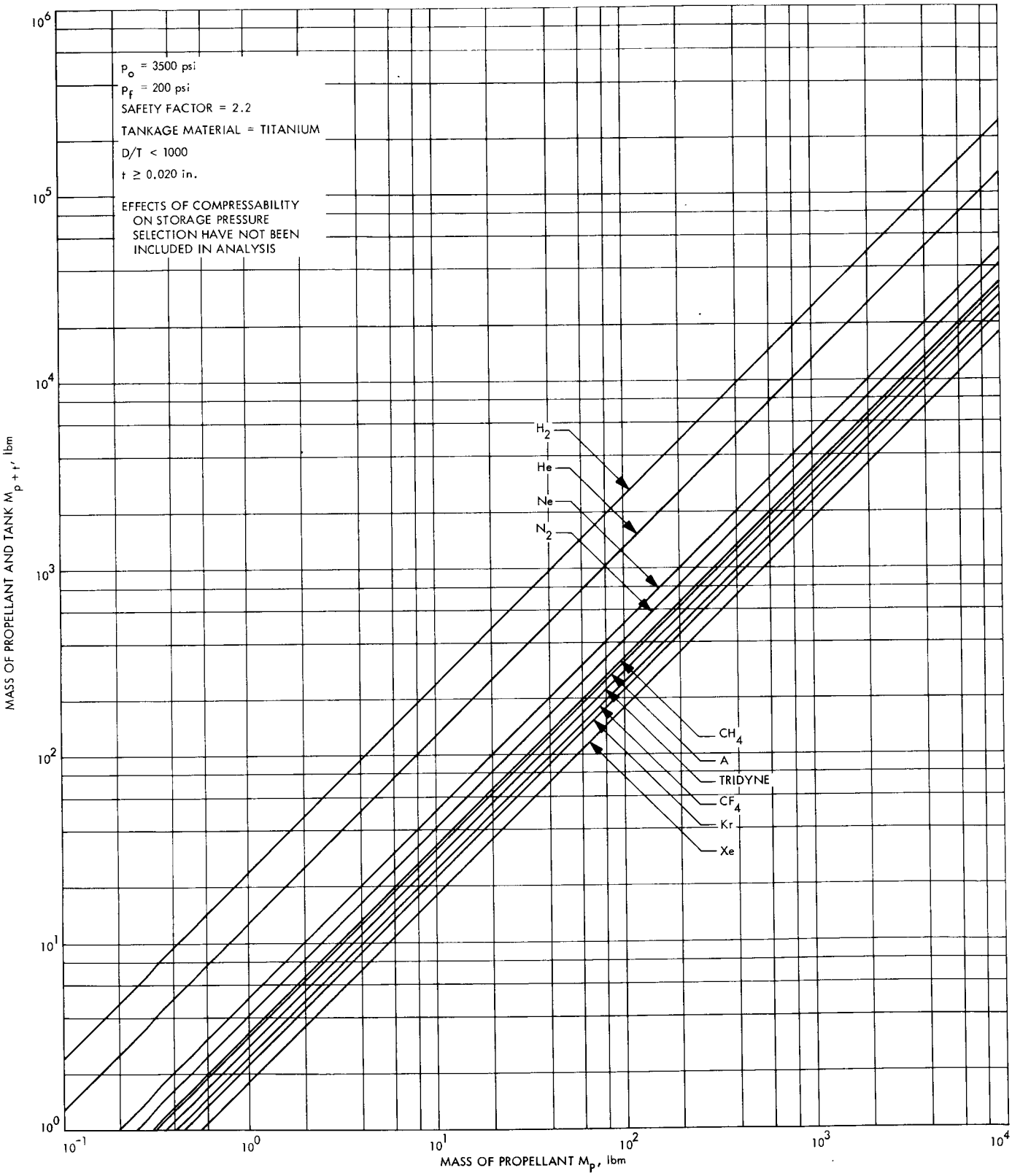

Fig. B-6. Inert gas and tankage mass

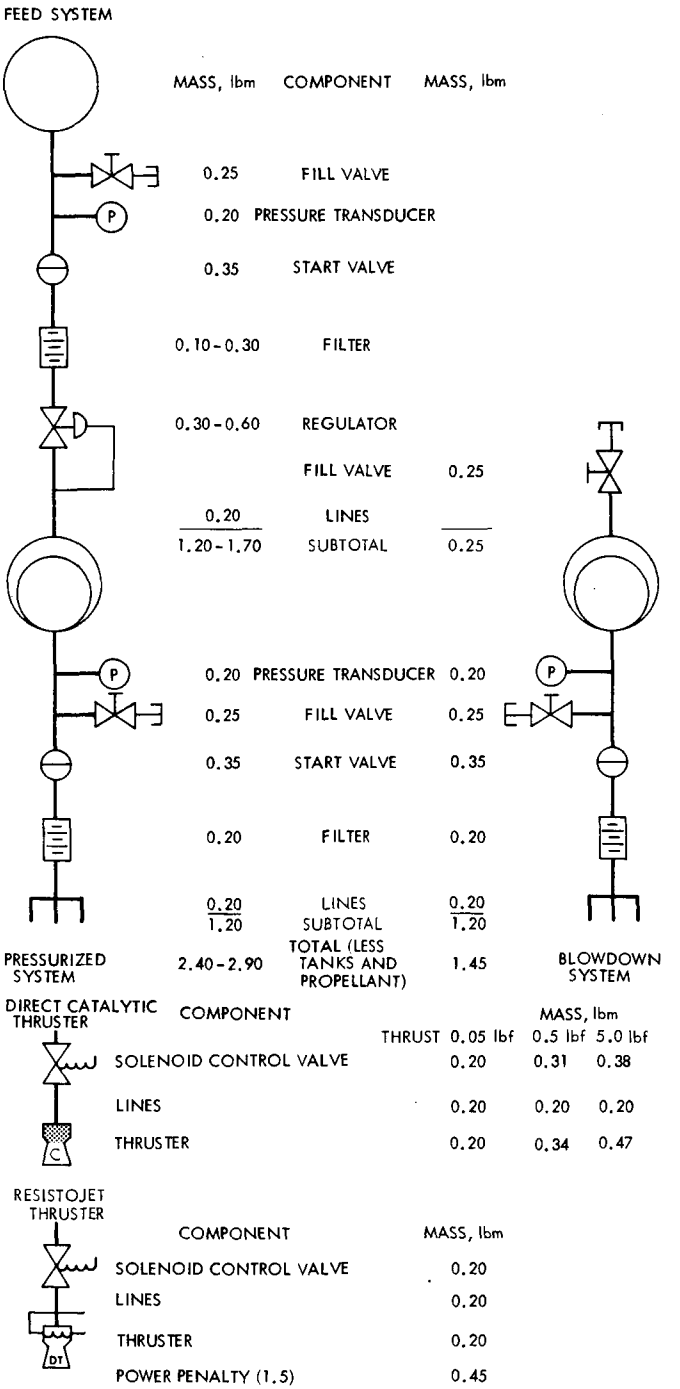

Fig. B-7. Hydrazine direct (liquid feed) system

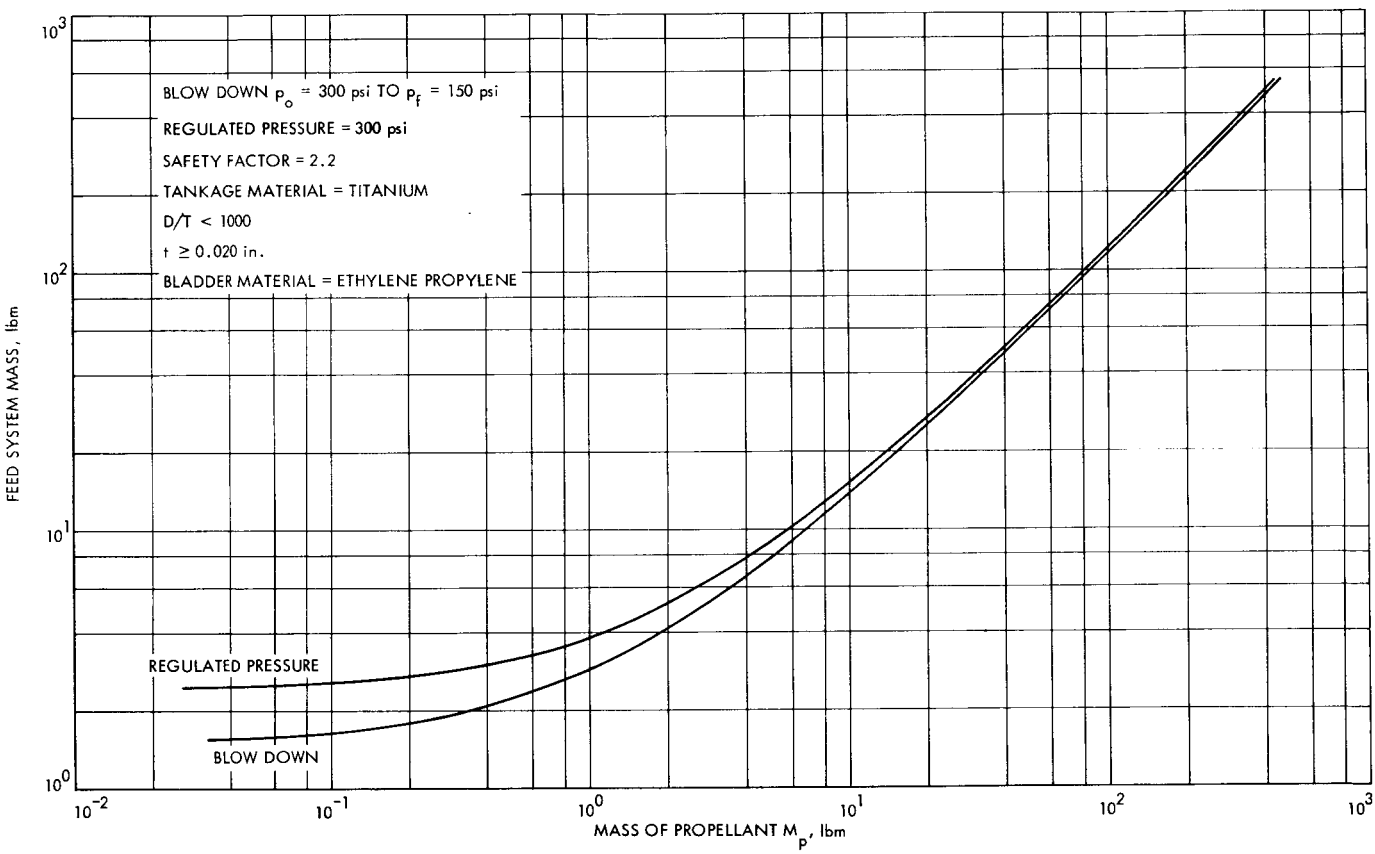

Fig. B-8. Hydrazine resistojet and direct catalytic feed system mass

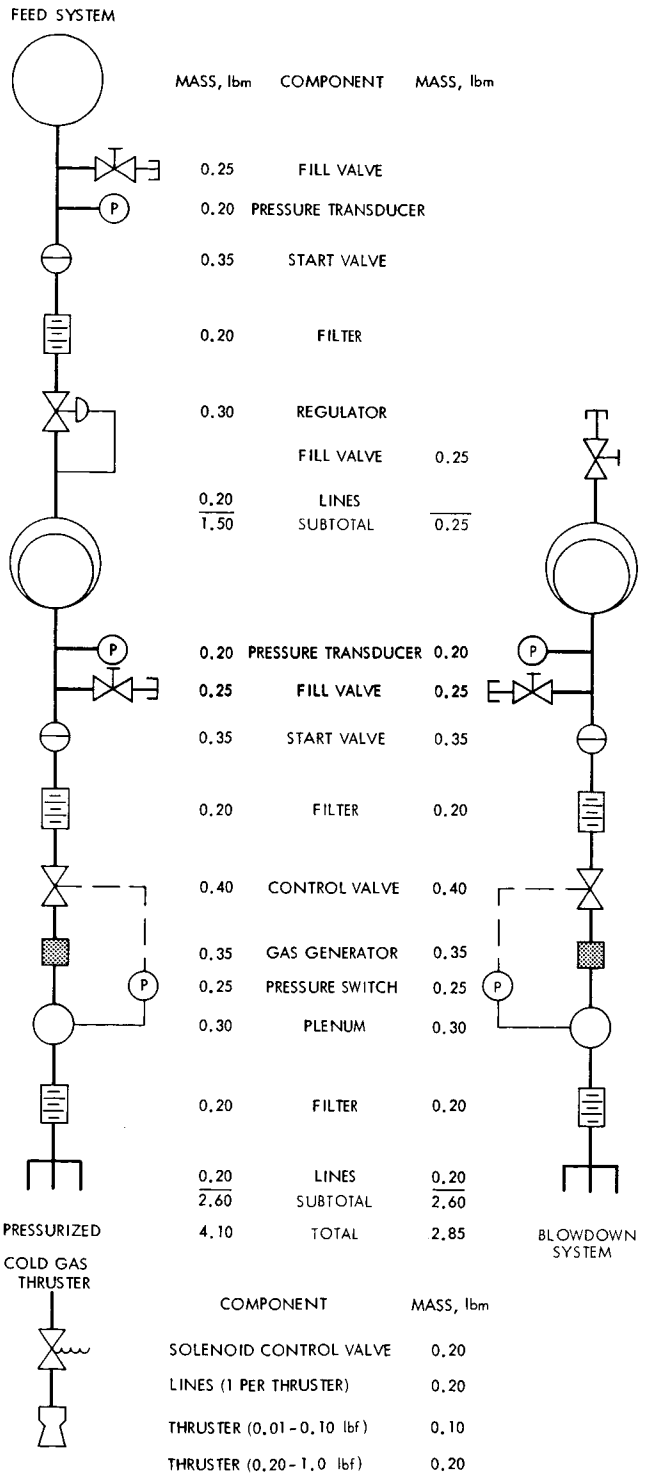

Fig. B-9. Hydrazine plenum system

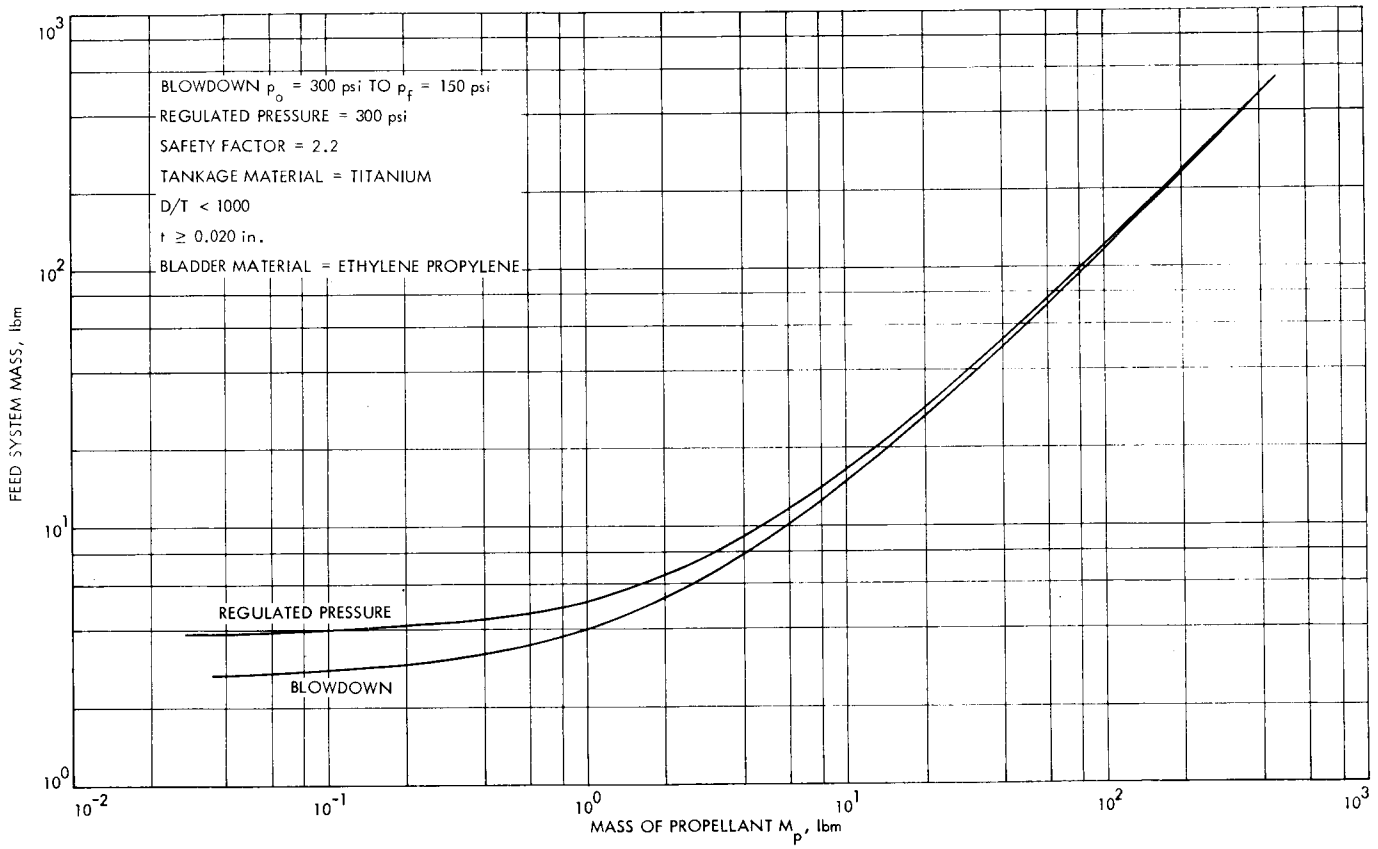

Fig. B-10. Hydrazine plenum feed system mass

VI. Vaporizing Liquid

The typical feed system consists of a tank, pressure transducer, fill valve, start valve, vaporizer (heat exchanger), pressure control device, and plenum tank. Mass values are presented in Fig. B-11. No bladder is required since either liquid or vapor may pass into the heat exchanger; however, system design must consider the possibility of either vapor or liquid passing through the heat exchanger. Since tank pressurization is only from the vapor pressure of the liquid propellants, the minimum wall thickness influenced the selection of tankage material. Aluminum is found to have lowest tankage mass for total system propellant mass below 5 lbm. Feed system mass as a function of propellant mass is presented in Fig B-12, where titanium is used for tankage material. Inert gas thruster mass is presented in Fig. B-11.

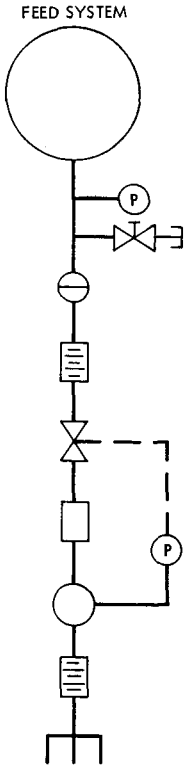

FEED SYSTEM	COMPONENT	MASS, lbm
	PRESSURE TRANSDUCER	0.20
	FILL VALVE	0.25
	START VALVE	0.35
	FILTER	0.10
	CONTROL VALVE	0.40
	VAPORIZER	1.00
	PRESSURE SWITCH	0.25
	PLENUM	0.30
	FILTER	0.10
	LINES	0.20
		3.05

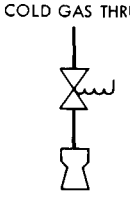

COLD GAS THRUSTER	COMPONENT	MASS, lbm
	SOLENOID CONTROL VALVE	0.20
	LINES (1 PER THRUSTER)	0.20
	THRUSTER (0.01 - 0.10 lbf)	0.10
	THRUSTER (0.20 - 1.0 lbf)	0.20

Fig. B-11. Vaporizing liquid system

VII. Resistojet and Radioisojet

The typical feed systems for the resistojet systems are inert gas (N_2, H_2), vaporizing liquid (NH_3), or liquid hydrogen. Feed system mass can be obtained from the previous sections. Liquid hydrogen feed system mass is not included here since a liquid hydrogen supply is available on large LOX-LH_2 propulsion systems (e.g., SIV-B). Separate LH_2 tankage for the attitude control system would be heavy and would require excessive insulation. Thruster mass and power penalties are included in Fig. B-13. Radioisojets are also included. The exact mass of shielding required is a function of AEC and launch safety requirements for that specific thruster. If the thruster must survive a reentry and crash, a heavy heat shield is required. In the low millipound thrust level, however, shielding may be minimized to less than 5 lbm.

VIII. Electrolysis

A typical system is outlined in Fig. B-14. The system consists of a triad tank containing two bladders with hydrogen, oxygen, and water compartments. These compartments act to provide passive pressure control, and all three will equilibrate to a common pressure. Downstream of the propellant (water or hydrazine, typically) tank the system contains three start valves, three fill valves, electrolysis unit, two pressure transducers, two pressure control devices (switches), and three filters. Initial tipoff rate reduction and orientation maneuvers require that some pressurized gas be stored initially onboard the spacecraft. This requirement can become the predominant contributor to tank mass in small total impulse systems.

The propellant is initially pressurized to 300 psia and undergoes a blowdown to 150 psia. Gas production is controlled by control devices like pressure-actuated switches in the propellant tank. Strain gauges may be substituted for the pressure switches in a passive control system. The resistance across the strain gauge devices is a function of the rib stress in the propellant tank. Power to the electrolysis cell can be regulated when these devices are connected in series with the cell and propellant tank.

The buckling and minimum thickness criteria suggest that aluminum is a more favorable tankage material than titanium for a total system propellant mass below 0.03 lbm;

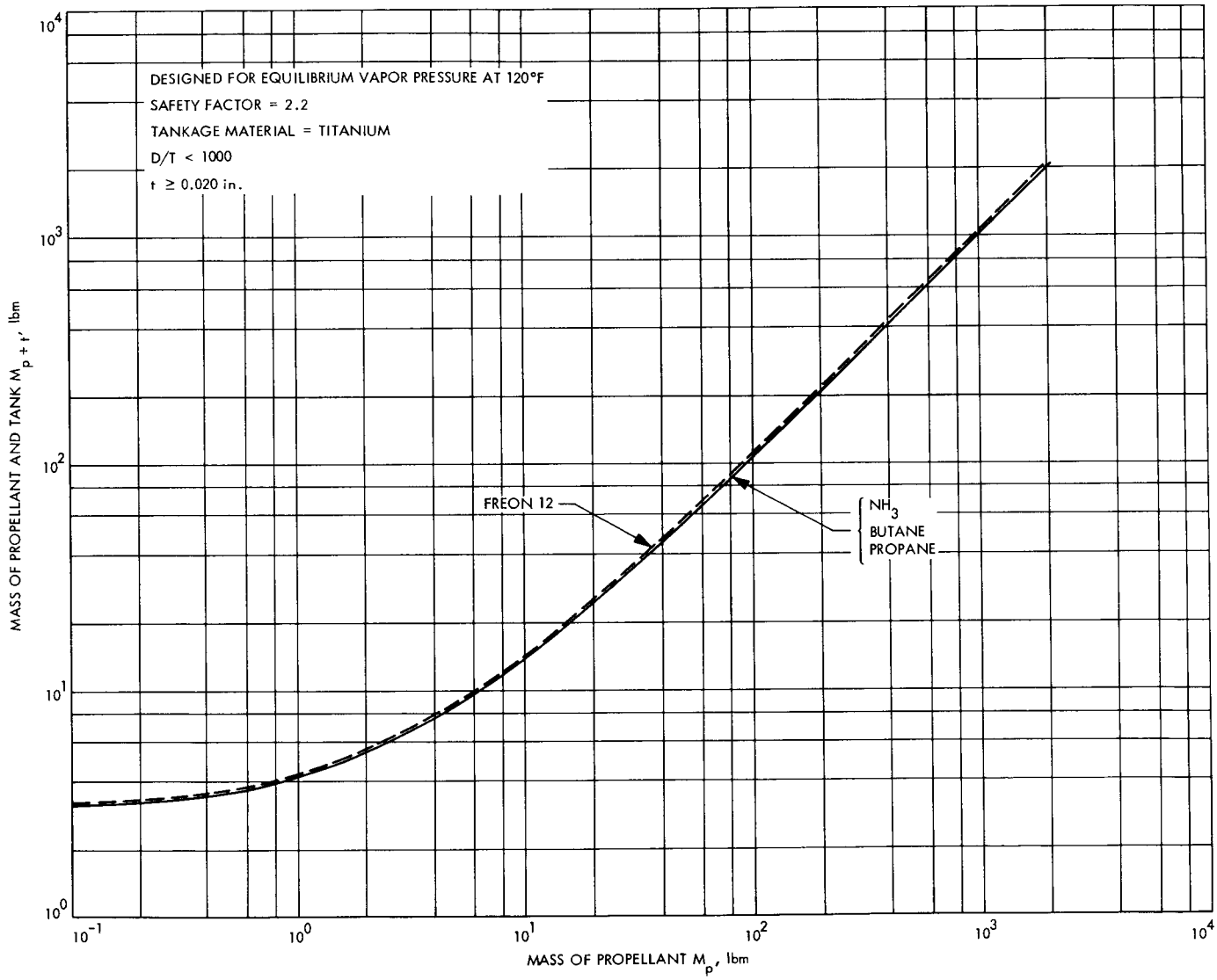

Fig. B-12. Vaporizing liquid and tankage mass

FEED SYSTEM

SEE VAPORIZING LIQUID, OR INERT GAS

THRUSTER SYSTEMS

COMPONENT	MASS, lbm
SOLENOID CONTROL VALVE	0.20
LINES (1 PER THRUSTER)	0.20

THRUSTER

PROPELLANT	THRUST LEVEL, lbf	POWER, W	MASS, lbm	MASS TOTAL + POWER PENALTY, lbm
NH_3	10×10^{-6}	2	0.50	1.3
NH_3	100×10^{-6}	10	0.50	3.5
NH_3	3×10^{-3}	30	0.50	9.5
N_2	10×10^{-3}	35	0.50	11.0
H_2	10×10^{-3}	280	0.50	84.5

RADISOJET:

NH_3	$5-20 \times 10^{-3}$	5.4/CLUSTER 3-4 THRUSTERS

Fig. B-13. Resistojet and radioisojet systems

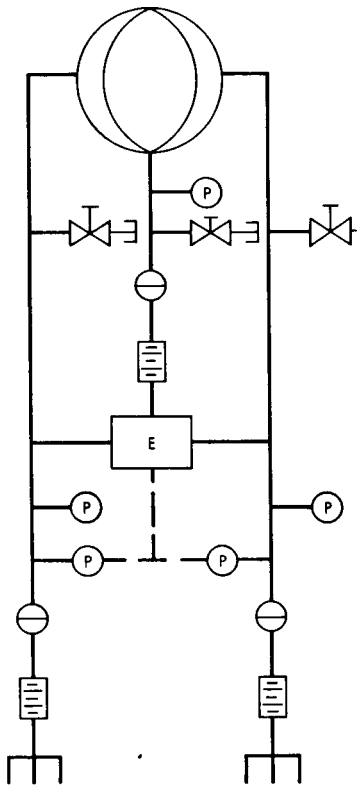

COMPONENT	MASS, lbm
PRESSURE TRANSDUCER	0.20
FILL VALVE (3)	0.75
START VALVE	0.35
FILTER	0.20
ELECTROLYSIS CELL	(SEE BELOW)
PRESSURE TRANSDUCER (2)	0.40
PRESSURE SWITCH (2)	0.25
START VALVE (2)	0.70
FILTER (2)	0.40
LINES (2)	0.40
	7.95

ELECTROLYSIS CELL

MASS = 4.3 lbm + 0.7 (X) lbm X = NUMBER OF CELLS

HOT H_2 O_2 THRUSTER

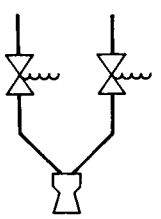

COMPONENT	LEWIS CATALYTIC MASS, lbm	MARQUARDT SPARK
LINES (2)	0.40	0.40
SOLENOID CONTROL VALVE (2)	0.40	0.40
THRUSTER (3-5 lbf)	1.0	5.0

COLD O_2 THRUSTER

COMPONENT	
LINE (1)	0.2
VALVE	0.2
THRUSTER	0.2

Fig. B-14. Electrolysis system

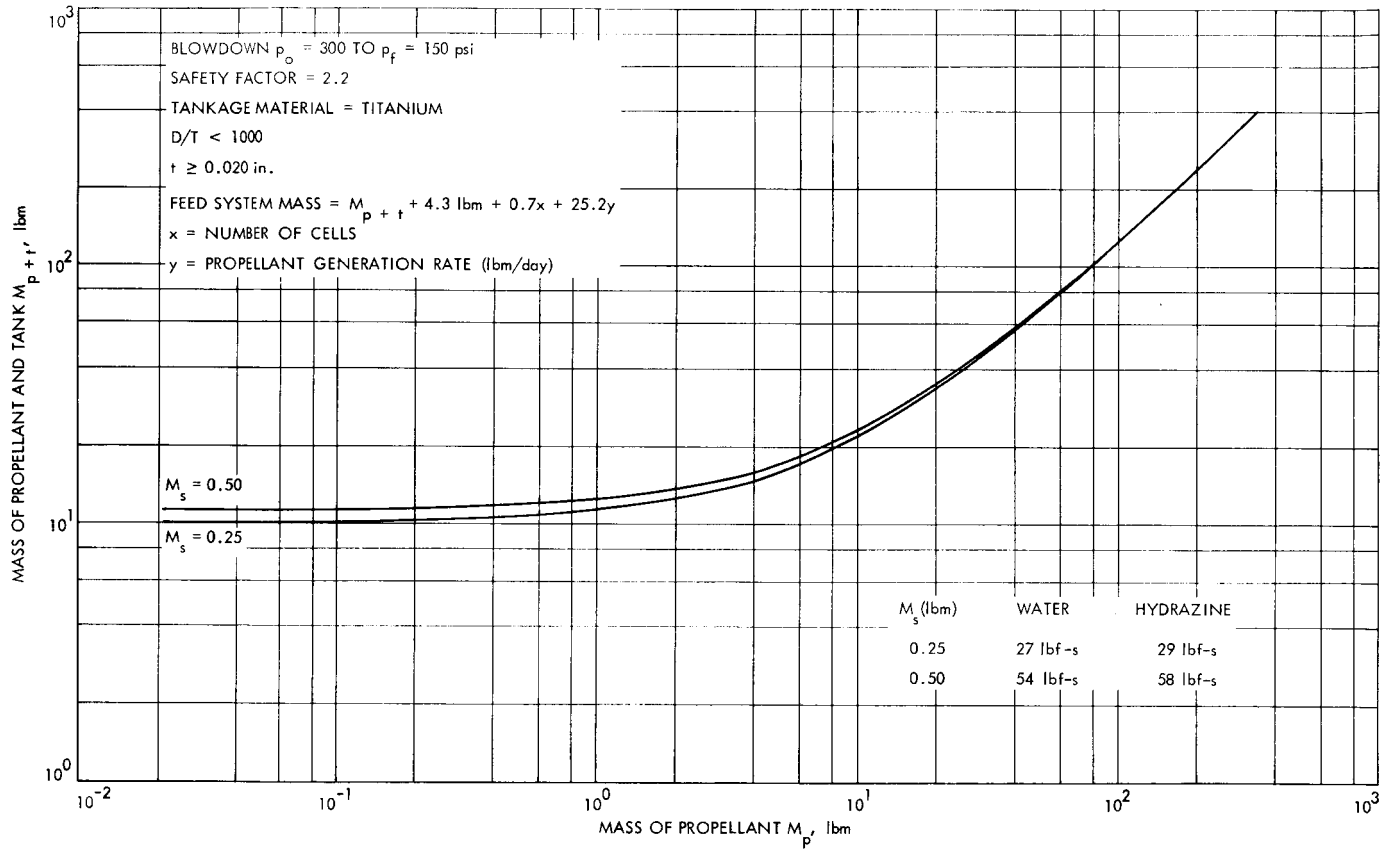

Fig. B-15. Electrolysis feed system mass (hydrazine and water)

however, titanium is the lightest tankage material for most systems under consideration. Feed system mass is plotted as a function of propellant mass in Fig. B-15. Since the density of water and hydrazine are about equal, hydrazine electrolysis cell feed system mass will be approximately that of water. The lighter elements present in the hydrazine decomposition products leads to a slightly higher specific impulse, resulting in a slight reduction in required propellant (water electrolysis in the cold gas mode).

Thruster systems for water electrolysis may be of two types, cold gas or hot O_2/H_2. Cold gas mass characteristics have been outlined in previous sections. Mass characteristics for the catalytic hot thrusters designed at NASA-Lewis and Marquardt are included in Fig. B-14.

IX. Subliming Solid

The typical feed system consists of a propellant tank encased in an insulation, propellant lines surrounded by heating coils, a propellant heater, and a "valveless" valve. The "valveless" valve is a porous plug encased in a heating coil. The very low vapor pressure of the propellant suggests that aluminum is the best material for tankage. A comparison of aluminum density to that of a super insulation (e.g., min-k) reveals that an insulation mass of about 75% tankage mass is required for adequate thermal protection. Propellant heater power is a function of mass flow rate or thrust level.

Representative subliming solid and superheated subliming solid feed systems, along with thruster mass data, are presented in Fig. B-16. Feed system mass is presented as a function of propellant mass in Fig. B-17.

FEED SYSTEM

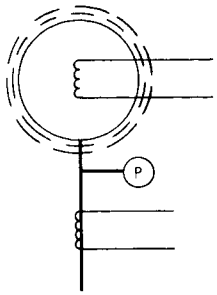

COMPONENT	MASS, lbm
PROPELLANT HEATER	0.10
PRESSURE TRANSDUCER	0.20
LINE HEATER	0.05
	0.35

THRUST, lbf	PROPELLANT HEATER POWER, W	MASS PENALTY, lbm
10^{-2}	100	30
10^{-3}	10	3
10^{-4}	1	0.3
SUPERHEATED		
10^{-2}	40	12
10^{-3}	4	1.2
10^{-4}	0.4	0.12

THRUSTER DATA:	COMPONENT	MASS, lbm	POWER, W	TOTAL MASS, lbm (MASS PLUS PENALTY)
	"VALVELESS" VALVE	0.55	5	0.70
	LINES	0.20	0	0.20
	COLD THRUSTER	0.10	—	0.10
	SUPERHEATED THRUST 10^{-2}	0.50	100	5.2
	10^{-3}	0.50	10	3.7
	10^{-4}	0.50	5	2.2

Fig. B-16. Subliming solid systems

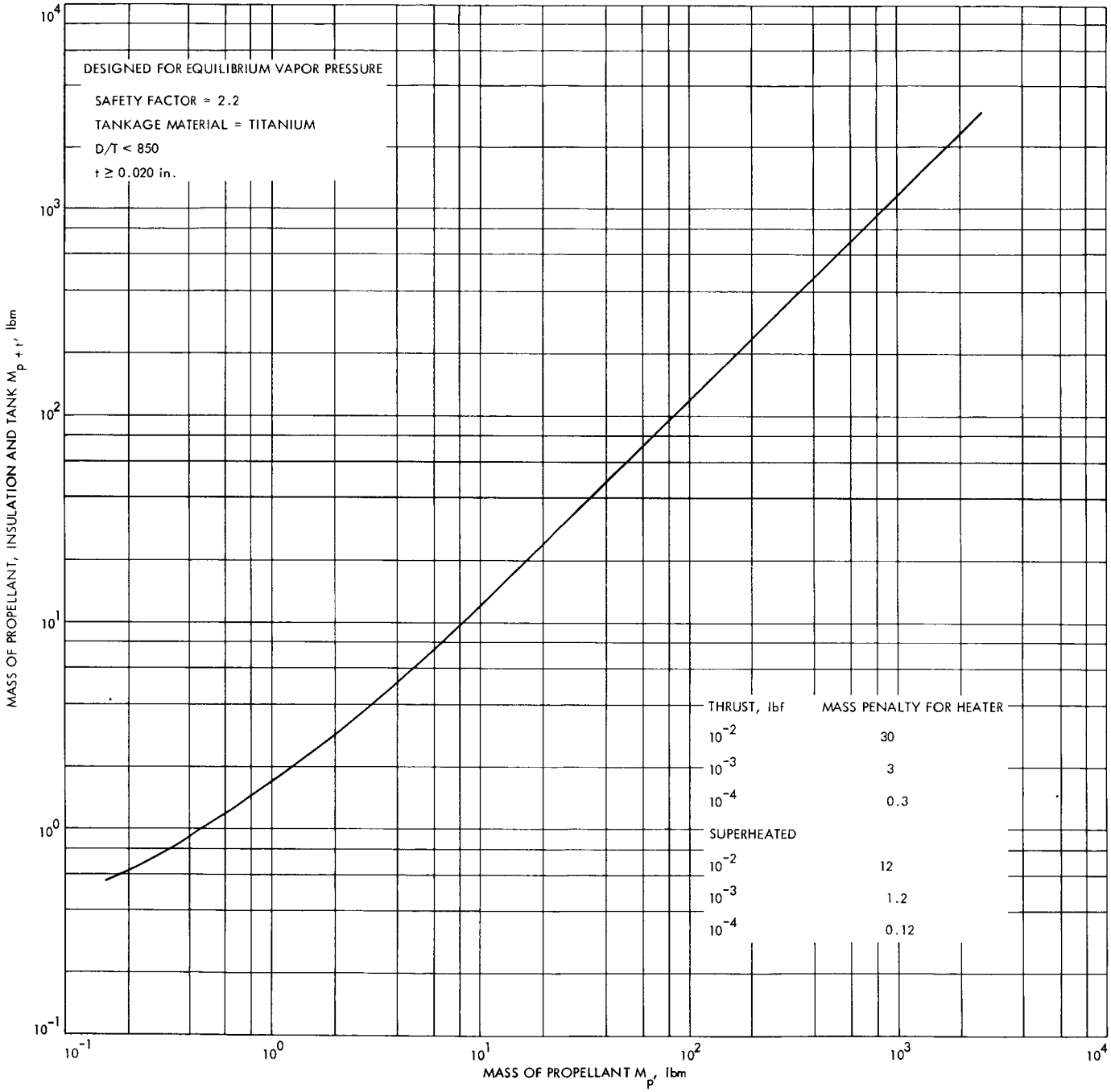

Fig. B-17. Subliming solid propellant related mass

Appendix C

Reliability

Reliability is one of the most essential elements in cost effectiveness evaluations of competitive system concepts or design options. Recommendations based on comparisons of *relative reliabilities* (qualitative ranking) are useful in concept comparisons, but are not sufficient for a conclusive selection of component designs or subsystem redundancy requirements.[11]

Reliability magnitude becomes important when systems are compared by cost effectiveness techniques. The magnitude of system mass and cost can be determined with reasonable accuracy. This is not the situation with reliability numbers for propulsion components which do not have the extensive statistical failure rate data typical of electronic components. Unless quantitative component reliabilities can be determined, the tradeoff of mass, cost, and reliability becomes erroneous and can, at best, be only bracketed.

I. Reliability Theory

An essential ingredient in the calculation of mission reliability for a component or system is component failure rate data. The failure rate of a component may be expressed as failures per cycle or failures per unit time. Reported failure rates of electrical components have proven to be fairly consistent (resistors: one order of magnitude). Mechanical failure rates vary widely from source to source (solenoid values: four orders of magnitude). A comparison of mechanical and electrical failure rates is presented in Figs. C-1 and C-2. The wide variation of mechanical component failure rates has lead to a skeptical view of mechanical reliability calculations. Electrical components are usually uniform in construction and failure mechanism; mechanical components are not. It becomes important to consider failure modes and effects of a specific mechanical design. The detailed design elements of a particular mechanical component will dictate the devices failure modes and rates of failure.

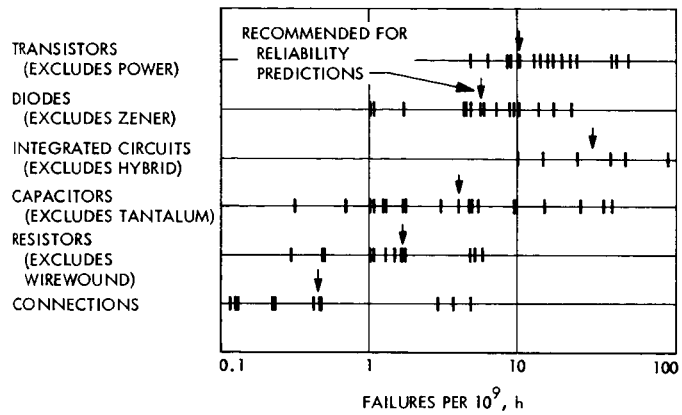

Fig. C-1. Operating failure rates for screened electronic parts

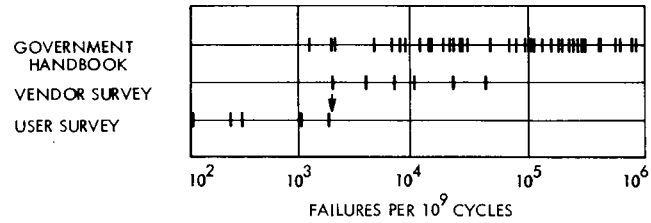

Fig. C-2. Solenoid valve failure rate data

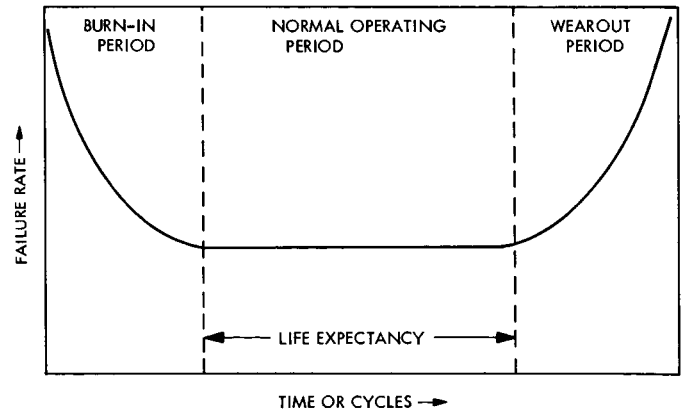

Fig. C-3. Classical "bathtub" failure rate curve

The classical "bathtub" failure rate time curve is presented in Fig. C-3. The initial "burn-in" or "debugging" period can be effectively eliminated by extensive system testing. Many times during the course of development of a system, the cost of testing prohibits extensive qualification. The result is a system with "bugs" which can lead to premature failure of the system. The large number of

[11] R. F. Miles, Jr., Internal Document, Sept. 15, 1969.

system design criteria requires that two or three constraints be imposed on a system test simultaneously. This can act to mask failures and lead to erroneous corrective measures. The wearout portion of the "bathtub" curve can also be defined by extensive testing; in the case of long-life (for example 5 yr) components, however, life testing also becomes expensive and constrained by schedules.

The proposed Grand Tour Mission will have a nominal 10-yr life and must be launched by October 1978. Conventional life testing of components for this mission becomes impossible since mission life exceeds the total time remaining prior to launch. Two methods of accelerated life testing have been proposed: overstress, and controlled testing. Overstressing a component may lead to accelerated failure. This method is applicable to failure mechanisms of the chemical or nuclear type, where increased concentration, temperature, voltage or particle flux will act to accelerate reactions. Care must be taken to avoid side effects. An increased temperature may accelerate additional failure modes. A second type of testing, called controlled testing, relies on extremely fine measurements. A part is placed in its normal operating environment and periodic measurements are made. If the failure mode is assumed to be O-ring shrinkage, then the size of the O-ring is measured to extremely fine accuracy during a short test period. This rate is then extrapolated to increased times. A problem may occur when a part undergoes a dual mode of failure. The O-ring in question may expand for 6 mo and contract for the remaining 10 yr. A short duration test of 6 mo would therefore reveal incorrect information. Both methods suffer from problems, and both rely on an accurate description of the failure mechanism. Controlled testing and accelerated testing along with the accumulation of failure rate data based on such testing is of value and should be encouraged. It is hoped that during the engineering development phase of system design that initial "burn-in" has occurred and the wearout time has been identified. Components can then be designed to operate in the constant failure rate portion of the failure/time curve.

The "largest flaw" concept will result in a constant or generic failure rate. Other theories have been proposed to account for a failure rate time increase. These theories take the form of failure rate time distributions which incorporate the constant and wear out portion of the failure rate curve. Some of these distributions are Weibull, Log-Normal, Gamma, Gompertz-Markseham, and others.

In mathematical terms, the probability distribution of time to failure of a part with constant failure rate is given by $p(t) = \lambda \exp - \lambda t$, where the failure rate λ may be statistically estimated by experiment. Reliability is usually given by $R = \exp - \lambda t$. In practice, some parts appear to fail exponentially with time, while others are assigned a fixed reliability (pyro valves). If components are assumed to fail exponentially with time, long duration missions result in extremely low values of calculated reliability. It appears reasonable that parts which cycle extensively will fail with greater probability with time (cycles), while parts which do not cycle extensively (pyro valves, only one cycle) will have a constant probability of failure with time. For purposes of this study, noncyclic component reliabilities were calculated based on a constant failure rate and exponential failure over a 1-yr life.

The time or cyclic dependence of reliability is important when moving components are considered. Failure rates for moving or cyclic components are often expressed as failures per cycle. Each actuation of a valve may be followed by a cycling of regulators, catalyst beds, electrolysis cells, thrust chambers, pressure switches, spark generators, and other active components. If failure rates are expressed as failures per cycle, then the duty cycle (number of total cycles) of the system will determine the active mission reliability of these components.

Environmental factors are applied to failure rates to account for actual observed stress levels. For purposes of this study, system reliability comparisons have ignored the launch stress environment since the auxiliary propulsion system is dormant during this period. Ground failure rates are usually projected to space dormancy periods

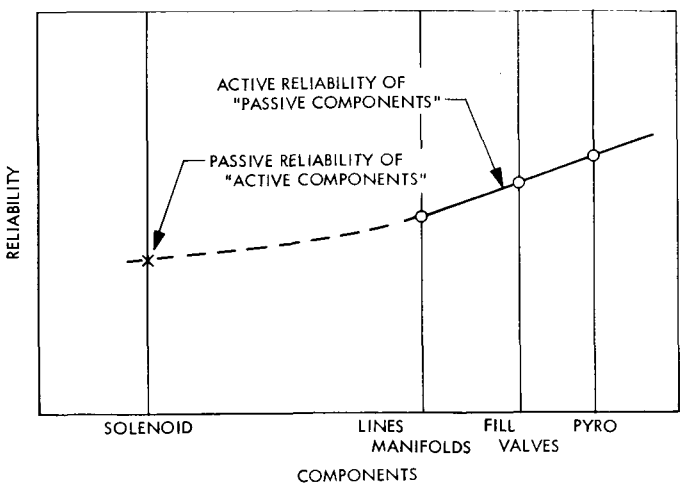

Fig. C-4. Skewed line dormancy correction for cyclic mechanical components

with an environmental factor (1/10 to 1/1000). This, however, does not seem like a satisfactory method to apply across the board. For example, tanks have similar failure modes and failure rates whether the thruster is being fired or not, while a solenoid valve has different failure mechanisms in the dormant and active states. The predominant failure mechanism of a valve in the dormant state is deterioration by chemical and nuclear action. Failure mechanisms of lines and manifolds ("passive components") in an active state are similar to failure mechanisms of solenoids and regulators ("cyclic components") in the dormant state. Rather than use a constant correction factor (K_E) for all components, a "skewed line" approximation seems to be a more appropriate dormancy correction for cyclic components (see Fig. C-4).

II. Component Reliabilities

In order to get a qualitative component reliability ranking, an averaging technique was employed. Previous reliability studies were reviewed and component reliability and failure rate values were extracted (Refs. 52–58 and three internal communications[12]). Data points which varied greatly from the average were explored. Those which were based on bad initial data or on a limited data sample were removed. Components were listed in order of reliability (or failure rate) magnitude. Each list was numbered and normalized by the total number of components. Then, these lists were averaged and a new list was obtained. This was done primarily to set the relative ranking of components. Biases were generally removed, or smoothed out, by this technique; some components were given a relative ranking by value judgments when no data were available for that specific component. The design of a mechanical component as discussed before had direct bearing on its reliability. One company may rate a fill valve high and another company may rate it low, due to differences in their fill valve design. An effort has been made to obtain data on similar components (size, usage, and design). The resulting list of components is expressed in descending order on the bottom of Fig. C-5.

Quantitative ranking of the components becomes difficult. Since there were differences in qualitative component ranking, vast differences exist in component reliability magnitudes. As was mentioned earlier, reliabilities for noncyclic components were based on a 1-yr mission duration. Items 6 through 14 in Fig. C-5 are noncyclic components. The data points for these non-cyclic components were taken from several references (Refs. 52–56) and the three communications just listed. The solid line through these data points was used to approximate the reliability values of the non-cyclic components. No correction factor is applied to these data for a passive environment.

The four profiles above the cyclic components in Fig. C-5 represent four duty cycles (1,000, 5,000, 10,000 and 100,000 cycles). Cyclic failure rate data were used to set the end points of these curves. Two representative component failure rates were selected from previously tested auxiliary-propulsion components. It must be stressed that if a reliability value is to be accepted for a component, failure rates used must be extracted from similar mechanical designs. Auxiliary-propulsion solenoid failure rates may not correlate well with midcourse propulsion solenoid failure rates. The failure rate for solenoid valves was based on life testing of seven valves. There were three Carlton, one Sterer, and three Kidde valves.[13] These valves may be pessimistic in view of the Avco, and NRL Wright valve life tests, but they were considered representative. This results in an average failure rate of 1.3 failures per million cycles with a 90% confidence level using a Poisson frequency distribution. The failure rate for catalytic thrusters was based on life testing of seven thrusters (Refs. 59–61). These seven thrusters accumulated nearly 2,450,000 cycles with no apparent catalyst failure. This failure rate corresponds to approximately 0.57 failures per million cycles, with a 90% confidence level.

The "skewed line" concept is applied to compute dormant failure rates of cyclic components. The mode of dormant failure of cyclic components (valves) is similar to the failure mode of passive components (propellant line or manifold) in the active mode. The skewed line will not become parallel, that is, dormant valve reliability will always be less than a sealed-off manifold connection. The actual slope of this line may be questionable, but the concept of cyclic component dormant failure rate approaching that of lines and manifolds seems reasonable. Cyclic components must undergo both dormant and active modes of failure.

The failure rates presented in all the above discussion and referenced figures were adjusted to account for only

[12]Young, Don to Lance, T., Interoffice Memorandum, Dec. 13, 1965; Groudle, Tom, JPL internal document, 1969; and Jennings, C. N. to Baughman, L. E., Interoffice Memorandum, Sept. 5, 1969.

[13]Ferraera, John, JPL internal document, 1969.

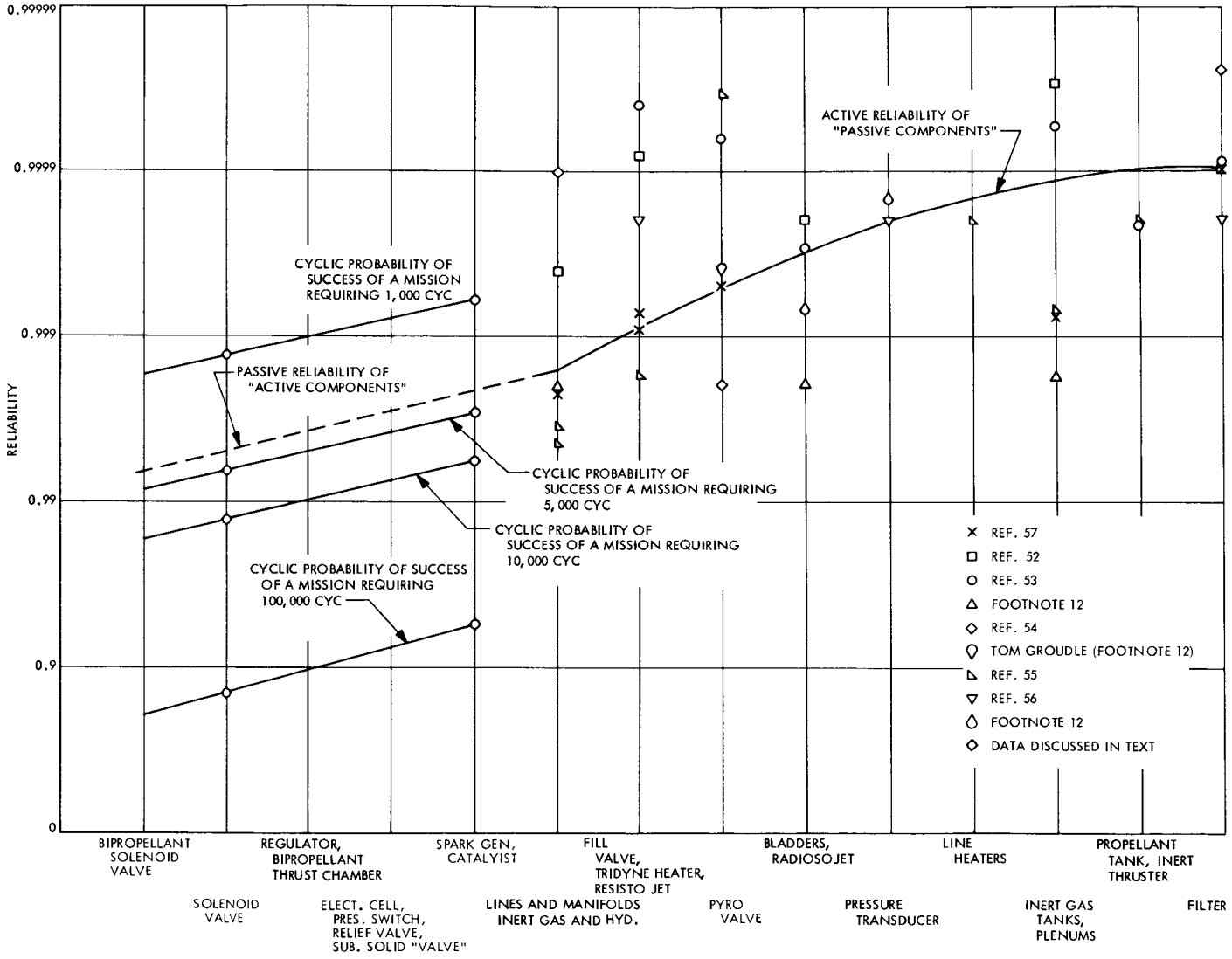

Fig. C-5. Component reliabilities

Table C-1. Component reliability data

Component	Cyclic mode				Passive mode
	Cycles				
	1,000	5,000	10,000	100,000	
Bi-prop solenoid	0.9983	0.9915	0.983	0.830	0.9934
Solenoid valve	0.9987	0.9935	0.9871	0.871	0.9950
Regulator	0.999	0.996	0.990	0.900	0.9963
bi-prop thrust chamber					
Electrolysis cell	0.9992	0.996	0.9925	0.925	0.997
pressure valve					
relief valve					
subliming solid "valve"					
Spark generator	0.9994	0.9981	0.9942	0.942	0.998
catalysis thrust chamber					
direct thermal thrust chamber					
Lines and manifolds					0.9985
Fill valve (capped)					0.9991
Tridyne resistojet					
Pyro					0.9995
Bladders					0.99968
radioisojet source					
Pressure transducer					0.9998
Line heaters (low T)					0.99985
Inert gas (pressurized)					0.99988
plenum tanks					
Propellant tank					0.9999
inert gas thrust chamber					
Filter					0.9999

those modes that lead to system failure. That is, the failure of a pressure transducer to measure pressure accurately will not necessarily affect the mission success. Only those transducer failure modes (leaks) which lead to mission failure were counted. If observed component failures which lead to system failure are only 10% of part failure modes, then the overall failure rate must be corrected to include only 10% of the total failure rate.

Table C-1 presents a tabulated record of reliabilities selected for auxiliary-propulsion system components.

III. Redundancy Concepts

Application of redundancy is the most direct method of increasing system reliability. Component reliabilities are usually fixed by present design technology; however, new basic design concepts may improve component reliability substantially. The weakest link in auxiliary-propulsion systems is the solenoid valve. Four commonly used valve redundancy configurations are: dual series, dual parallel, quad, and quad connected (see Fig. C-6). The selection of a valve configuration is dependent on the predominant valve failure mode. Most valves tend to favor the fail open mode. A value of 75% failures in the open mode has been selected for purposes of this study. The seven valves used to determine failure rate experienced four failures: one closed, and three open. The dual series is favored over dual parallel, and the quad is favored over the quad connected when the fail open mode is predominant. Valve redundancy equations are presented in Fig. C-7. Regulators are the second least reliable component in the considered systems. Parallel regulators with squib (pyro) isolation valves is one method of improving reliability. The predominant failure mode of regulators is the fail open position (e.g., 90% fail open). The parallel regulator concept and math model are presented in

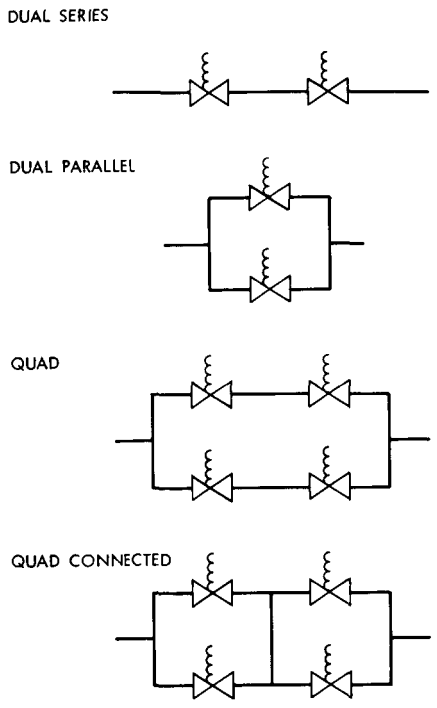

Fig. C-6. Most-used valve redundancy configurations

Fig. C-8. A more complete redundancy study is included in an internal communication by R. R. Bowman[14].

System equations are presented on a summary page (Table C-2). The six thrust chamber single system has no preference to valve failure mode. Both an open and a closed failure will lead to system failure. The total valve-thruster reliability is raised to the sixth power. In the twelve thruster single system, the valve system failure mode becomes important. If the failure of a valve system is in the open position, the system fails; but, if a valve system fails closed, a second thruster-valve unit will still be available. Since the probability of a thruster to fail open (not restrict flow) is nearly one, only the closed failure mode incorporates thruster reliability. The double system concept is portrayed in Fig. C-9. In order to protect against the open failure, three times the required fuel is necessary. Should the plus roll jet (1) fail open, the two minus roll jets (2 and 8) would counter with equal thrust to balance the leaking jet. Thus, the plus jet (1) would use twice the fuel of the minus jet (2) from system A. If the open failure occurred at launch, two-thirds of system A fuel would leak out the plus jet and one third out each of the two minus jets, leaving two-thirds of the

[14]Bowman, R. R., Interoffice Memorandum, July 1969.

R_{SV_o} = PROBABILITY OF NO OPEN FAILURE

R_{SV_c} = PROBABILITY OF NO CLOSED FAILURE

$P_{SV_o} = 1 - R_{SV_o}$ = PROBABILITY OF OPEN FAILURE

$P_{SV_c} = 1 - R_{SV_c}$ = PROBABILITY OF CLOSED FAILURE

VS = VALVE SYSTEM COMBINATION

SINGLE VALVE

$$P_{VS} = P_{VS_o} + P_{VS_c}$$

$$R_{VS} = 1 - P_{VS} = 1 - \left(1 - R_{VS_o}\right) - \left(1 - R_{VS_c}\right) = R_{VS_o} + R_{VS_c} - 1 = R_{SV_o} + R_{SV_c} - 1$$

DUAL SERIES

$$P_{VS} = P_{VS_o} + P_{VS_c}$$

$$P_{VS_o} = P_{SV_o}^2$$

$$P_{VS_c} = 1 - \left(1 - P_{SV_c}\right)^2$$

$$P_{VS} = P_{SV_o}^2 + 1 - \left(1 - P_{SV_c}\right)^2$$

$$R_{VS} = 1 - P_{VS} = R_{SV_c}^2 - \left(1 - R_{SV_o}\right)^2$$

DUAL PARALLEL

$$P_{VS} = P_{VS_o} + P_{VS_c}$$

$$P_{VS_o} = 1 - \left(1 - P_{SV_o}\right)^2$$

$$P_{VS_c} = P_{SV_c}^2$$

$$P_{VS} = P_{SV_c}^2 + 1 - \left(1 - P_{SV_o}\right)^2$$

$$R_{VS} = 1 - P_{VS} = R_{SV_o}^2 - \left(1 - R_{SV_c}\right)^2$$

QUAD

$$P_{VS} = P_{VS_o} + P_{VS_c}$$

$$P_{VS_o} = 1 - \left(1 - P_{SV_o}^2\right)^2$$

$$P_{VS_c} = \left[1 - \left(1 - P_{SV_c}\right)^2\right]^2$$

$$R_{VS} = 1 - P_{VS} = \left[1 - \left(1 - R_{SV_o}\right)^2\right]^2 - \left(1 - R_{SV_c}^2\right)^2$$

QUAD CONNECTED

$$P_{VS} = P_{VS_o} + P_{VS_c}$$

$$P_{VS_c} = 1 - \left(1 - P_{SV_c}^2\right)^2$$

$$P_{VS_o} = \left[1 - \left(1 - P_{SV_o}\right)^2\right]^2$$

$$R_{VS} = 1 - P_{VS} = \left[1 - \left(1 - R_{SV_c}\right)^2\right]^2 - \left(1 - R_{SV_o}^2\right)^2$$

Fig. C-7. Valve redundancy equations

Table C-2. System calculations summary

Single systems:

A. Six thrusters (six required for operation):

$R_{system} = R_F R_{VS}^6 R_{TH}^6$

R_F: feed system reliability

R_{VS}: solenoid valve system reliability (single, dual series, quad) for all systems; electrolysis cells, this is a bipropellant valve system.

R_{TH}: thruster reliability, inert gas, spark generator, resistojet. . .

B. N-thrusters (N-required for operation):

$R_S = R_F R_{VS}^N R_{TH}^N$

R_F: reliability of feed system

R_{VS}: reliability of valve system

R_{TH}: thruster reliability, systems may be used as auxiliary propulsion systems for spin up (N = 2), gravity gradient inverter (N = 2), or station keeping on a 3-axis stabilized craft (N = 4).

C. Single system with 12 thrusters (six required for operation):

$R_{system} \cong R_F [R_{VS_o}^2 - (1 - R_{VS_c} R_{TH})^2]^6$

R_F: reliability of feed system

R_{VS_o}: reliability of valve system open

R_{VS_c}: reliability of valve system closed

R_{TH}: reliability of thruster

Double systems:

A. Three times required propellant active systems:

$R_{system} = i - (1 - R_{SS})^2$

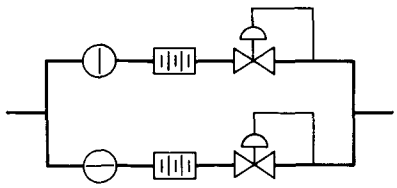

$$P_{PRS_o} = \left(1 - R_{R_o}\right)^2 = P_{R_o}^2$$

$$P_{PRS_c} = \left(1 - R_{R_c}\right)^2 = P_{R_c}^2$$

$$P_{PR_S} \cong \left[1 - \left(P_{R_o}^2 + P_{R_c}^2\right)\right] R_S^2$$

WHERE THE START VALVE RELIABILITY IS ADDED TO CORRECT FOR SENSING AND SWITCHING.

SINCE $P_{R_o} \gg P_{R_c}$

$$P_{PR_S} \approx \left[1 - R_R^2\right] R_S^2$$

Fig. C-8. Parallel regulator concept and mathematical model

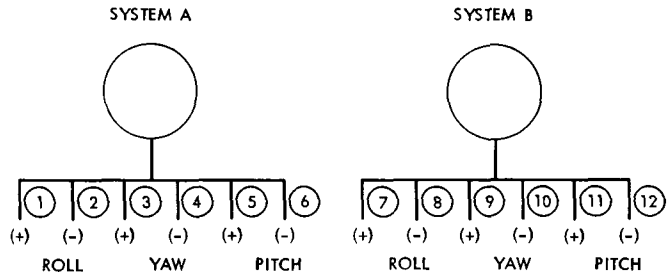

Fig. C-9. Double system

initial fuel in tank B. The amount of fuel loaded (tanks A and B) is therefore three times the required fuel. The redundancy equation for double systems is included in Table C-2.

The concepts of standby redundancy, system isolation by latching valves, and other more sophisticated redundancy concepts have not been included in this appendix. These are important concepts and should be included in future work.

IV. System Calculations

The system calculations have been broken into three segments: feed systems, valve-thruster configurations, and system integration. For rapid selection of system reliabilities, a table of total system reliability is included at the end of this appendix. This table is an incorporation of the feed and valve-thruster reliabilities. If different initial reliabilities are preferred to those presented in this appendix, then the modeling equations presented can be used to calculate new system reliabilities.

The basic feed system reliabilities are presented in Figs. C-10 through C-15. Baseline systems consist of the diagrammed components. The cyclic dependence of these systems is assumed to correspond to the thruster duty cycle. To improve the reliability of regulators, dual parallel squib isolated regulators have been included in the modified feed systems. Four thruster-valve configurations have been considered. Since the predominant failure mode for solenoid valves is open, the two preferred redundant valve configuration are dual series and quad. The single valve configuration has also been included. Single thruster-valve configurations with twelve active and no standby redundant thrusters present several interesting ramifications. Twelve thrusters with single valves have a very low reliability, since only one of the twelve valves in the open position leads to a failure ($R_{VS_o}^{12}$). The reliability of the twelve T/C dual series valve single system is high.

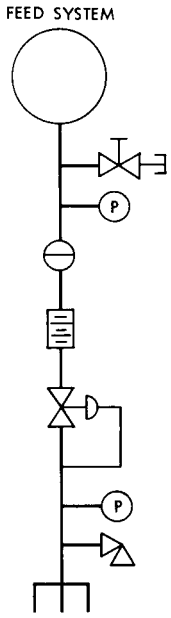

$$R_F = R_T R_{FV} R^2_{PT/D} R_R R_F R_L$$

	BASELINE SYSTEM	BASELINE WITH PARALLEL REGULATOR
$R_{F_{1,000\ cyc}}$	0.9887	—
$R_{F_{10,000\ cyc}}$	0.9834	0.9871
$R_{F_{100,000\ cyc}}$	0.894	0.9765

Fig. C-10. Inert gas system

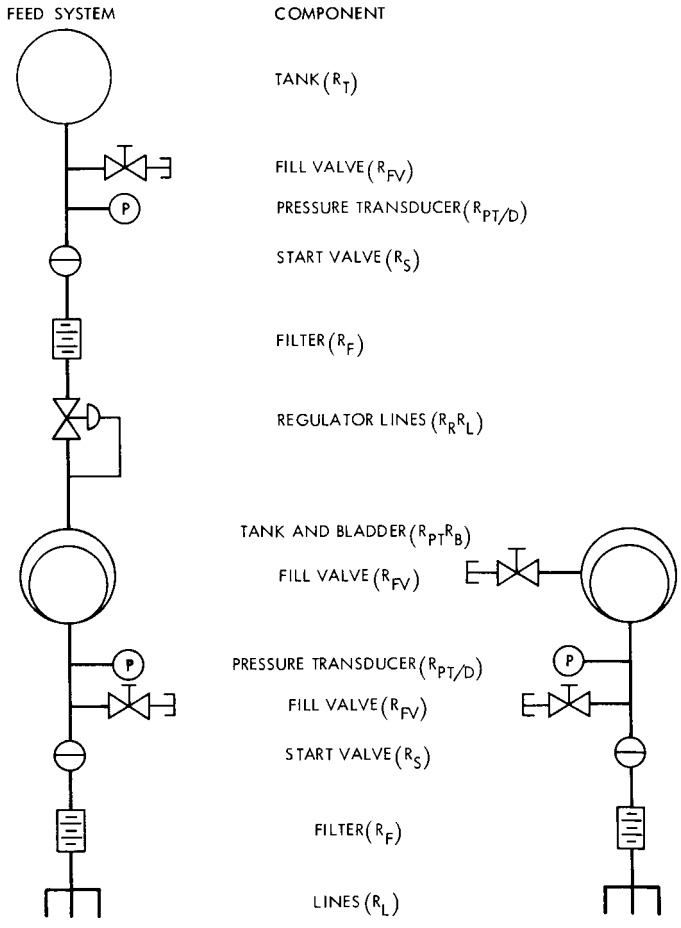

$$R_{F_{PR}} = R_T R^2_{FV} R^2_{PT/D} R^2_S R_R R^2_L R_B R^2_F R_{PT}$$

$$R_{F_{BD}} = R_{PT} R_B R^2_{FV} R_{PT/D} R_S R_F R_L$$

	BASELINE SYSTEM	BASELINE WITH PARALLEL REGULATOR
$R_{F_{PR\ 1000\ cyc}}$	0.9885	—
$R_{F_{PR\ 10,000\ cyc}}$	0.9796	0.9833
$R_{F_{BD\ 1000\ cyc}}$	0.9954	—
$R_{F_{BD\ 10,000\ cyc}}$	0.9954	—

Fig. C-11. Hydrazine direct systems

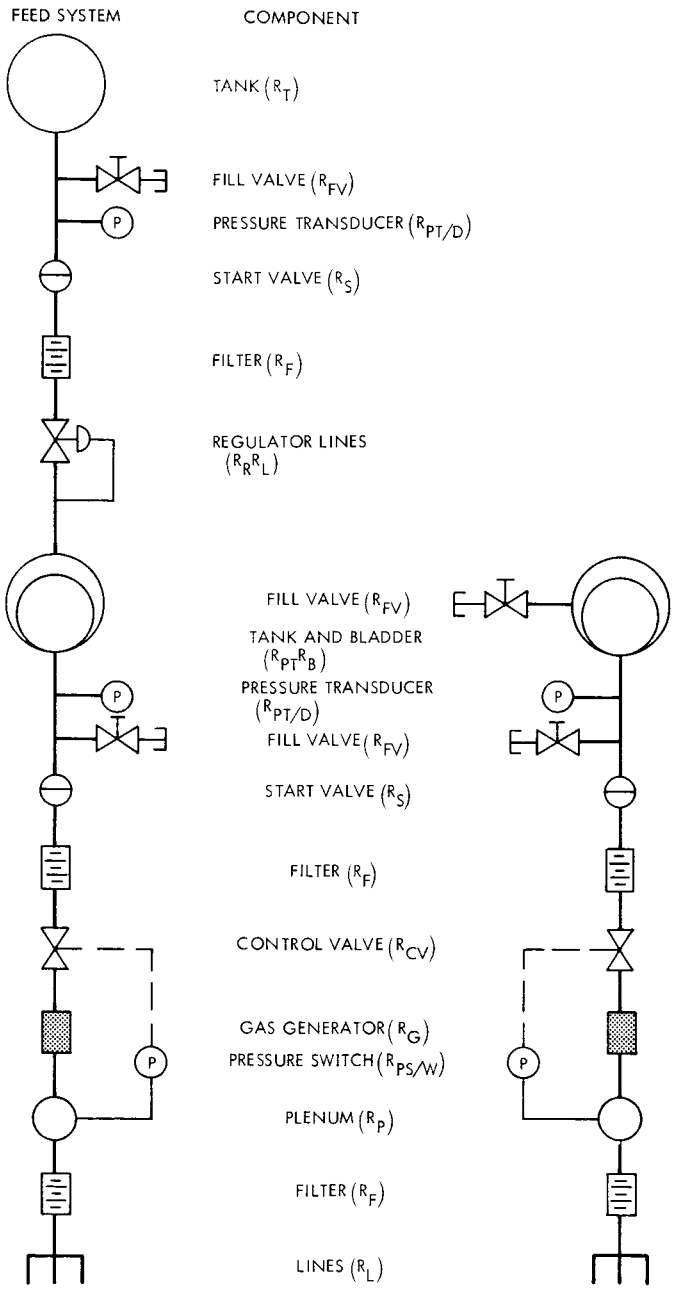

$$R_{F_{PR}} = R_T R_{FV}^2 R_{PT/D}^2 R_S^2 R_F^3 R_R R_L^2 R_{PT} R_B R_{CV} R_G R_P R_{PS/W}$$

$$R_{F_{BD}} = R_{PT} R_B R_{FV}^2 R_{PT/D}^2 R_S R_F^2 R_L R_{CV} R_G R_P R_{PS/W}$$

	BASELINE SYSTEM	BASELINE WITH PARALLEL REGULATOR
$R_{F_{PR\ 1000\ cyc}}$	0.9757	—
$R_{F_{PR\ 10,000\ cyc}}$	0.9443	0.9478
$R_{F_{BD\ 1000\ cyc}}$	0.9835	—
$R_{F_{BD\ 10,000\ cyc}}$	0.9606	—

Fig. C-12. Hydrazine plenum system

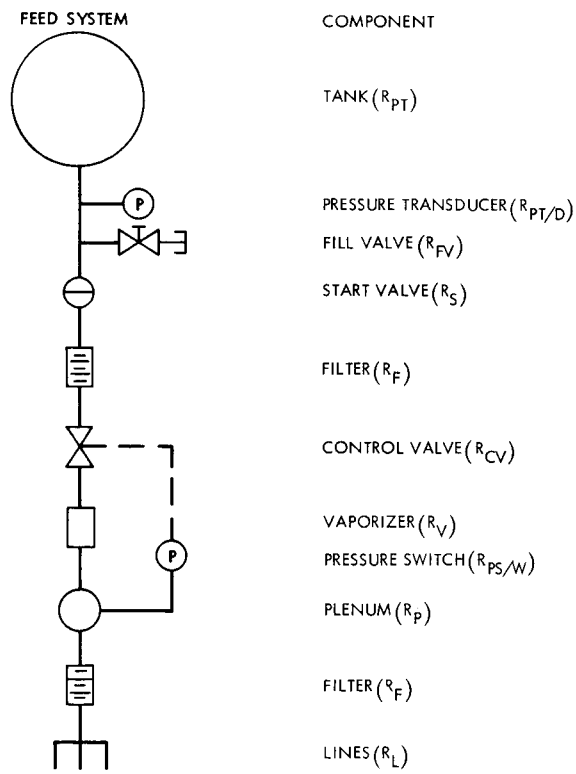

$$R_F = R_{PT} R_{PT/D} R_{FV} R_S R_F^2 R_{CV} R_V R_P R_{PS/W} R_L$$

	BASELINE SYSTEM
$R_{F_{1000\ cyc}}$	0.9863
$R_{F_{10,000\ cyc}}$	0.9683

Fig. C-13. Vaporizing liquid system

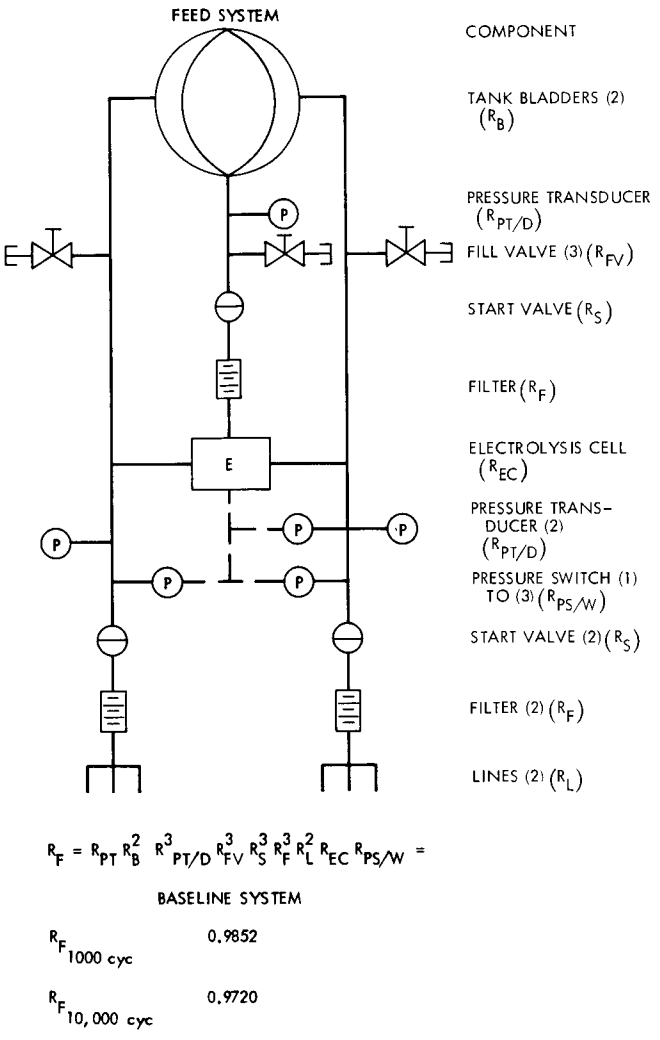

Fig. C-14. Electrolysis system

This is due to the low probability of two valves failing in the open position. By going to a twelve T/C quad redundant valve single system, the reliability of the system is slightly reduced. The probability of a fail open is greater in a quad redundant valve scheme than a dual series valve arrangement (twice the number of paths to an open failure). Therefore, the increased mass of a quad redundant system over a dual series system will not increase the overall system reliability. Only the dual series valve in the twelve T/C single system scheme has been included in this study. Valve-thruster reliabilities are presented in Table C-3. Various thrusters along with a water electrolysis system (bipropellant) are included in this table.

Auxiliary-propulsion system reliability is summarized in Table C-4. From a baseline system standpoint the reliability ranking (high to low) of the feed systems alone that were considered in this study is as follows:

(1) Subliming solid

(2) Hydrazine blowdown

(3) Inert gas

(4) Hydrazine pressurized

(5) Vaporizing liquid

(6) Electrolysis cell

Table C-3. Valve-thruster reliability

Type	Cycles	
	1,000	10,000
Inert gas:		
Single	0.9622	0.8973
Dual series	0.9802	0.9455
Quad	0.9991	0.9964
12 T/C dual series	0.9997	0.997
Hydrazine thruster:		
Single	0.9479	0.8566
Dual series	0.9656	0.9027
Quad	0.9842	0.9513
12 T/C dual series	0.9996	0.9958
Resistojet-tridyne:		
Single	0.9576	0.8941
Dual series	0.9755	0.9422
Quad	0.9943	0.993
12 T/C dual series	0.9997	0.997
Radioisojet:		
Single	0.9609	0.8960
Dual series	0.9789	0.9442
Quad	0.9978	0.995
12 T/C dual series	0.9997	0.9976
Electrolysis:		
Single	0.9297	0.8272
Dual series	0.9523	0.8869
Quad	0.9762	0.9512
12 T/C dual series	0.9994	0.9960

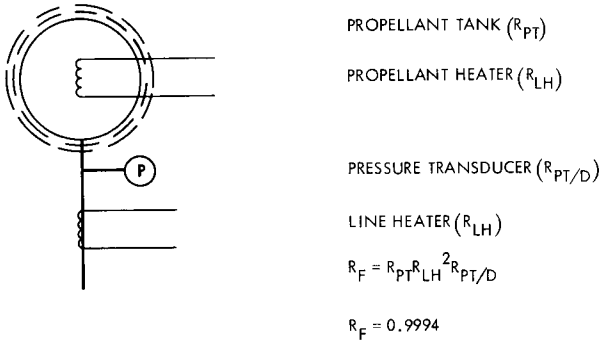

Fig. C-15. Subliming solid systems

(7) Hydrazine plenum blowdown

(8) Hydrazine plenum pressurized

The single valve, six thruster, reliability (1000 action cycles) ranking is:

(1) Inert gas thruster-valve

(2) Radioisojet thruster-valve

(3) Resistojet thruster-valve

(4) Hydrazine thruster-valve (direct thermal and catalyst)

(5) Electrolysis thruster-valve (hot gas bipropellant)

Table C-4. Auxiliary-propulsion system reliability

Parameters	Single systems				Double systems		
	Single	Dual series	Quad	12 T/C dual series	Single	Dual series	Quad
Inert gas							
1,000	0.9513	0.9691	0.9878	0.9884	0.998	0.999	0.9998
10,000	0.8822	0.9295	0.980	0.980	0.986	0.995	0.9996
Hydrazine							
BD[a] 1,000	0.944	0.961	0.980	0.995	0.997	0.998	0.9996
BD 10,000	0.853	0.899	0.947	0.991	0.978	0.980	0.997
PRS[b] 1,000	0.937	0.955	0.973	0.988	0.996	0.998	0.999
PRS 10,000	0.8391	0.884	0.932	0.9755	0.974	0.987	0.995
Hydrazine plenum							
BD 1,000	0.946	0.964	0.983	0.983	0.997	0.999	0.9997
BD 10,000	0.8619	0.908	0.957	0.958	0.981	0.992	0.998
PRS 1,000	0.939	0.956	0.9748	0.9759	0.996	0.998	0.999
PRS 10,000	0.8473	0.8928	0.9409	0.9415	0.977	0.989	0.997
Vaporizing, NH_3							
1,000	0.949	0.9668	0.985	0.986	0.997	0.999	0.9998
10,000	0.8689	0.9155	0.9648	0.965	0.983	0.993	0.999
Resistojet							
NH_3[c] 1,000	0.944	0.962	0.981	0.986	0.997	0.999	0.9996
NH_3 10,000	0.866	0.912	0.962	0.965	0.982	0.992	0.999
GN_2[d] 1,000	0.9468	0.964	0.983	0.988	0.997	0.999	0.9997
GN_2 10,000	0.8793	0.9266	0.977	0.980	0.985	0.995	0.9996
Radioisojet							
NH_3 1,000	0.948	0.9656	0.984	0.986	0.997	0.999	0.9997
NH_3 10,000	0.868	0.914	0.963	0.966	0.983	0.993	0.999
Electrolysis							
CGM[e] 1,000	0.948	0.966	0.984	0.985	0.997	0.999	0.9997
CGM 10,000	0.872	0.919	0.969	0.969	0.984	0.993	0.999
HGM[f] 1,000	0.916	0.938	0.962	0.985	0.993	0.996	0.999
HGM 10,000	0.804	0.862	0.925	0.968	0.962	0.981	0.994
Subliming solid							
(2T)[g] 1,000	0.9918				0.9999		
(2T) 10,000	0.9784				0.9995		

[a]Blowdown system.
[b]Pressure regulated system.
[c]Ammonia feed system.
[d]Gaseous feed system.
[e]Inert gaseous expulsion system.
[f]Ignited propellant expulsion system.
[g]System containing only two thrusters.

Appendix D

System Cost

As implied by its definition, cost is an integral part of cost effectiveness. The impact of an auxiliary-propulsion system cost on overall mission cost is diminished as total mission cost increases. System costs should be broken into recurring and non-recurring cost. The development status of an auxiliary-propulsion system is perhaps the largest factor associated with non-recurring costs. A large portion of development cost is expended for flight qualification. Most systems studied in this report can be considered developed; the low development costs shown assume qualification for a new mission, not development of an entirely new size or configuration. The electrolysis cell, the Tridyne concept, and the thermally decomposed hydrazine thruster are not in the developed and flight qualified stage, and consequently they are charged with high development costs.

The enclosed system cost figures summarized in Table D-1 must be considered only as estimates and should not be taken as exact. These figures were derived by examining earlier cost estimates, development and flight qualification costs, and component costs. One factor affecting cost variation is the rate of inflation. At an 11%/yr inflationary rate, a baseline system of $100,000 will grow to nearly $170,000 in 5 yr. The system costs depicted in Table D-1 are expressed in 1969 dollars.

I. Inert Gas Systems

The inert gas system consists of 6 unheated thrusters and 6 valves. The required quantity and species of gas will affect system hardware cost. Valve redundancy will also affect hardware cost. Development and qualification costs would be approximately $300,000 for a typical system in the 10- to 500-millipound thrust range with representative hardware cost would be $200,000.

II. Tridyne Systems

The Tridyne system is similar to the inert gas system. The 6 thrusters will be consolidated into 2 modules containing 3 thrusters each, with a 1.5-W heater for each cluster. The feed system would be quite similar to that of the gaseous nitrogen system, since the Tridyne gas mixture is a gaseous monopropellant.

Although the Tridyne concept has never been flight qualified, the feed system, which is essentially identical to that of an inert gas system, will not greatly affect development costs.

A system development and qualification program will cost around $600,000, which includes approximately $400,000 hardware acquisition cost.

III. Unheated Vaporizing Liquid Systems

The vaporizing liquid system again is more complex than the inert gas system since the vaporizing liquid feed system contains additional components like a plenum, vaporizer, and pressure control valve. The thrusters,

Table D-1. Summary of system costs

System	System development and flight qualification, $	Single system				Double system		
		Single valve system, $	Dual-series valve system, $	Quad-valve system, $	12 T/C dual-series valve, $	Single valve, $	Dual-series valve, $	Quad valve, $
Inert gas	300 K	200 K	220 K	260 K	270 K	400 K	440 K	520 K
Tridyne	600 K	400 K	420 K	460 K	550 K	800 K	840 K	920 K
Cold ammonia	500 K	300 K	320 K	360 K	370 K	600 K	640 K	720 K
Hydrazine catalyst	600 K	400 K	420 K	460 K	550 K	800 K	840 K	920 K
Resistojet	1.4 M	400 K	420 K	460 K	550 K	800 K	840 K	920 K
Plenum	500 K	300 K	320 K	360 K	370 K	600 K	640 K	720 K
Resistojet ammonia	600 K	400 K	420 K	460 K	550 K	800 K	840 K	920 K
Inert gas	500 K	400 K	420 K	460 K	550 K	800 K	840 K	920 K
Radioisojet	3.5 M	900 K	920 K	960 K	1.05 M	1.8 M	1.84 M	1.92 M
Electrolysis	2.7 M	700 K	730 K	780 K	980 K	1.4 M	1.46 M	1.56 M
Subliming solid	500 K	300 K	—	—	—	600 K	—	—

however, are the same as those used in the inert gas system. Since this system has previously been flight qualified and flown, development costs are lower than undeveloped systems. System development and qualification will cost approximately $500,000, which includes $300,000 expended on hardware acquisition.

IV. Resistojet

A resistojet is an electrically heated thruster which can be implemented to any gas generation source. An inert gas feed system concept has been flight qualified and flown. Again, as in the Tridyne concept, thrusters may be consolidated into clusters thus reducing heater costs. Development and flight qualification of an electrically heated gas system will cost around $500,000. Included in this are the recurring system hardware costs, which will be on the order of $300,000.

An ammonia resistojet system has been flight qualified and flown. Since the baseline system was used only for station keeping maneuvers, it consequently had only thruster pairs. Clustering thrusters in a module, a 6-thruster or 2-thruster system would result in nearly equal hardware cost. Development and flight qualification for a 6-thruster system would be on the order of $600,000 with $400,000 attributed to non-recurring hardware costs.

V. Radioisojet

AEC nuclear safety considerations are exacting, although interpretation of these rules may vary from system to system. The incorporation of a re-entry capsule which will assure that the radioisotope fuel remains contained becomes extremely expensive. The approximate cost of development and qualification of a flight system will be approximately $3,500,000. About $900,000 in system hardware can be expected.

VI. Liquid Hydrazine Systems

There are three hydrazine systems considered in this report. These are resistojet decomposition, direct catalytic decomposition, and catalytic plenum. The resistojet and catalytic systems are similar except for the thruster itself. The direct catalytic thruster employs a bed made of a spontaneous type catalyst such as Shell 405, which costs over $2,000 a pound. These thrusters have been flight qualified and have flown; consequently, their development costs are considerably less than the resistojet decomposition thruster. The resistojet decomposition thruster is presently under advanced development; however, a flight hardware hydrazine resistojet thruster with a high cyclic reliability (heater coil) is not available. A considerable amount of effort is necessary to develop this thruster. On the other side of the hydrazine system spectrum is the catalytic plenum system, which has been flight qualified and delivered to a classified project.

From present system status, development and qualification costs of the direct catalytic, resistojet, and plenum systems are, respectively, $600,000, $1,400,000, and $500,000. Similarly, the recurring hardware costs are, respectively, $400,000, $400,000, and $300,000.

VII. Electrolysis

The electrolysis system in this study utilizes water as the stored propellant and consists of 6 bipropellant thrusters which may operate in the cold oxygen or hot hydrogen-oxygen mode. Implementation of a hydrazine and water mixture will result in a negligible cost perturbation. Gas generation will occur with an electrolysis cell of the separated gas (life support type) configuration. The electrolysis cell has been flight qualified, and a 20-lb thrust bipropellant catalytic thruster is under development. The development of a dual mode 1 to 5 lbf bipropellant hydrogen oxygen thruster is the most expensive element in a flight development and qualification program. Implementation of the electrolysis cell as a semipassive feed system will also require considerable funding. A total system flight development and qualification program should cost approximately $2,700,000, of which hardware costs will be approximately $700,000.

VIII. Subliming Solid

The subliming solid configuration consists of a valveless feed system and 2 thrusters. The use of this system is restricted to station keeping, gravity gradient inversion, and spin-up maneuvers which do not require high thrust or extremely accurate impulse bits.

System development and qualification costs are around $500,000 of which $300,000 is attributed to hardware.

IX. Summary

A summary of system costs is presented as Table D-1. The first column is the cost of development and flight

qualification of a system. The second column presents the hardware cost of the given system. The difference between columns one and two is the non-recurring cost associated with system development. If more than one flight is considered, then this cost may be divided into the total number of flights. The single valve system hardware cost is modified in the remaining columns to accommodate different redundancy concepts. With the exception of the subliming solid system (2 thrusters), all the other systems presented are in a 6-thruster baseline configuration. Total impulse of the systems considered is in the range of 50–2000 lbf-s.

References

1. Wanger, R. F., *Application of Cost Effectiveness Criteria as a Basis for Attitude-Control System Selection,* Report PIR 9752-033, General Electric Corp., Spacecraft Department, New York, N.Y., April 1, 1964.
2. Jennings, C. N., *Design Criteria for Spacecraft Propulsion Systems,* Report No. 1069 FR-1, Space General Corp., Los Angeles, Calif., Oct. 1967.
3. Fosdick, G. E., *Launch Vehicle Cost Parameter Study,* Martin Company, NASA CR 62357, Jan. 1965.
4. Lifson, M. W., "Value Theory," in English, J. M., *Cost Effectiveness,* John Wiley, New York, 1968, pp. 79-112.
5. English, J. M., "Concepts of System Resource Requirements," in English, J. M., *Cost Effectiveness,* John Wiley, New York, 1968, pp. 64-78.
6. Congressional Record, October 3, 1966, pp. A-5088-A-5089.
7. Quade, E. S., "Cost-Effectiveness: Some Trends in Analysis," in English, J. M., *Cost Effectiveness,* John Wiley, New York, 1968, pp. 242-254.
8. Leventhal, Abraham, and Bloomquist, C. E., "Spacecraft Mission Effectiveness," *Annals of Reliability and Maintainability,* Spring Issue, 1968.
9. Strauss, R., *Success Criteria for Intelsat IV on a per Channel Basis,* Comsat Task 211-4019, TCLP 112, Comsat Corporation, Washington, D.C., Sept. 11, 1968.
10. *Proposal for Intelsat IV Satellite and Associated Equipment,* Document No. PFP 68-3, Vol. IV, Hughes Aircraft Co., Los Angeles, Calif., 1968.
11. Iacobellis, S. F., *Tridyne Attitude Control Thruster Investigation,* Report No. R-7743P, Rocketdyne, Jan. 1969.
12. Kamin, J., *Ammonia Vapor Microthruster System,* Final Technical Report for NRL under Contract No. N00014-66-C0129, General Electric Missile and Space Division, Sept. 1966.
13. *ATS F and G Prototype Ammonia Feed System Program Description,* Report No. SPDS 8-100, General Electric Missile and Space Division, dated Mar. 1968.
14. Grossman, Jones, and Lee, *Auxiliary Propulsion Survey, Part III,* Technical Report No. AFAPL-TR-68-67, Sept. 1968.

References (contd)

15. Pugmire, T. K. and Lund, W., "ATS-III, Resistojet Thruster System Performance," AIAA Paper 68-553, June 1968.

16. Pugmire, T. K., Shaw, R. and Callens, R., "Ammonia Resistojet Station Keeping Subsystem Aboard Applications Technology Satellite (ATS)-IV," AIAA Paper 69-296, March 1969.

17. Price, T. W., "Hydrazine Monopropellant Provides 0.5-600 lb Thrust," *Space Aeronautics,* Oct. 1969, p. 70.

18. *Monopropellant Hydrazine Rocket Engine Technical Information,* Report No. HSPC 691202, Hamilton Standard, prepared for JPL, May 1969.

19. *Basic Data Package Flight Weight Hydrazine Monopropellant REA, Model R12D 5-lb Thrust,* Propulsion Division, The Marquardt Corporation, Van Nuys, Calif., Aug. 1969.

20. *Basic Data Package Flight Weight Hydrazine Monopropellant REA, Model R25A 0.1-lb Thrust,* Propulsion Division, The Marquardt Corporation, Van Nuys, Calif., Aug. 1969.

21. *Half-Pound Monopropellant Hydrazine Thruster,* Report, TRW Systems Group, Redondo Beach, Calif., Dec. 1968.

22. *Monopropellant Spacecraft Maneuvering and Attitude Control System,* Report TRW Systems Group, Redondo Beach, Calif., Dec. 1968.

23. *Monopropellant Rocket Engines,* Report, Propulsion Division, Aerojet-General Corp., Sacramento, Calif., June 1969.

24. Schreib, R. R., Pugmire, T. K., and Chapin, S. G., "The Hybrid (Hydrazine) Resistojet," *AIAA* Paper 69-496, June 1969.

25. *Monopropellant Hydrazine Plenum System,* First Quarterly Report under Contract No. NAS 5-10389 (67-R-117), Rocket Research Corp., Seattle, Wash., Aug. 24, 1961.

26. Butcher, W. W., *Hydrazine Electrolysis for Spacecraft Propulsion,* Report for JPL Contract No. 951720 ISS080316R, Hughes Aircraft Company, Space Systems Division, Aug. 1968.

27. Morgan, N. E., *Hydrazine Electrolysis Cell Safety Limits Tests, Tasks VII and VIII,* Report for JPL Contract No. 951720, Hughes Aircraft Company, Space Systems Division, June 1969.

28. Picciotti, E., Rouch, K., and Pax, C., *A Study of the Feasibility of a Separated O_2-H_2 Electrochemical Propulsion System,* Report, Allis-Chalmers, Sept. 1969.

29. Rodewald, N., Falkenstein, G., Herr, P., and Provo, E., *Evaluation and Demonstration of the Use of Cryogenic Propellants (O_2/H_2) for Reaction Control Systems,* Report No. NASA CR-72244 (R-6838-2), June 1968.

30. Owens, W., "Design Aspects of Subliming Solid Reaction Control Systems," AIAA Paper 68-516, June 1968.

31. *Development of the Subliming Solid Control Rocket Phase II,* Report No. NASA CR-712, prepared under Contract No. NAS 5-9070 by Rocket Research Corp., Seattle, Wash., Mar. 1967.

References (contd)

32. *Application of the Valveless Subliming Solid Control Rocket to the NRL Gravity Gradient Satellite*, Report No. RRC-66-R-59, Rocket Research Corp., Seattle, Wash., May 1966.

33. *Subliming Solid Reaction Control System*, Final Report No. LMSC-679102, Missile & Space Company, Lockheed Aircraft Corp., Sunnyvale, Calif., Oct. 1967.

34. *Encapsulated Solid Propellant Rockets*, Report No. WAD R831, Curtiss-Wright, Aug. 1966.

35. *Repetitive Impulse Generator (Rig)*, Report No. LMSC/677084-R, Missiles & Space Company, Lockheed Aircraft Corp., Sunnyvale, Calif., Sept. 1968.

36. Suddreth, D., and Blackwood, D., *A Solid-State Pulse Motor System for Spacecraft Attitude Control*, Report, Talley Industries, Mesa, Arizona.

37. Anderson, J., and Thompson, S. A., "Development and Long-Life Performance of Ion Engines for Satellite Control," AIAA Paper 66-234, Mar. 1966.

38. Sohl, G., Fosnighi, V. V., Goldner, S. J., and Speiser, R. C., "Cesium Electron-Bombardment Ion Microthrusters," AIAA Paper 67-81, Jan. 1967.

39. Free, B. A., and Mickelsen, W. R., "Plasma Separator Thruster," AIAA Paper 66-598, June 1966.

40. Worlock, R. M., Caplinger, E., and Eilenberg, S. L., "Characteristics of Micropound Range Ion Thrusters," AIAA Paper 66-212, Mar. 1966.

41. Kerslake, W. R., Wasserbauer, J. F., and Margosian, P., "Experimental Mercury Bombardment Thruster at $\sim 13\mu$ Millipound Thrust," AIAA Paper No. 4, Vol. 5, April 1967, pp. 683–691.

42. Guman, W., *Pulsed Plasma Microthruster Propulsion System Application Notes*, Report No. PCD-TR-69-1, Fairchild-Hiller, Jan. 1969.

43. *Solenoid Valve Qualification Test Report ATS-D/E Auxiliary Propulsion System*, Report No. AVSSD-0165-68-CR, for Contract No. NAS 5-10394, Avco, Aug. 1968.

44. *Electrothermal and Radioisotope Heated Propulsion for Spacecraft Reaction Control*, Report, TRW Systems Group, Redondo Beach, Calif., Feb. 1968.

45. Page, R. J., Short, R. A., and Ownby, M. L., *Resistojet Thruster Life Test*, First Quarterly Report for Contract No. NAS-1-8090, Rocket Systems Division, The Marquardt Corp., Van Nuys, Calif., July 1968.

46. Cygnarowicz and Gibson, "Design and Performance of a Thermal Storage Resistojet," AIAA Paper 67-662, Sept. 1967.

47. Viventi, R., and Usley, W. C., "Design and Demonstration of a Radioisojet," AIAA Paper 67-425, July 1967.

48. Hamilton Standard, *0.1 lb_f 15-Hour Continuous Mode Firing Test Results*, Proposal, Hamilton Standard.

49. Hamilton Standard, *Monopropellant Hydrazine Rocket Engine*, Hamilton Standard Report HSPC 69R02, prepared for JPL, May 1969.

References (contd)

50. Rodewald, N., Falkenstein, G., Herr, P., and Prono, E., *Evaluation and Demonstration of the Use of Cryogenic Propellants (O_2/H_2) for Reaction Control Systems, Volume II—Experimental Evaluations and Demonstrations*, Report CR-72244 (R-6838-2) The National Aeronautics and Space Administration, June 1968.

51. DeBrock, S. C., "Spacecraft Capillary Propellant Retention and Control for Long-Life Missions," AIAA Paper 68-465, Apr. 1968.

52. Jennings, C. N., *Procedure for the Design and Optimization of Liquid Rocket Propulsion Systems*, Vol. II-B, Report SGC 837 FR-1, Space General Corp., El Monte, Calif., Apr. 1966.

53. Jennings, C. N., *Design Criteria for Spacecraft Propulsion Systems*, Vol. V, Report 1069 FR-1, Space General Corp., El Monte, Calif., Oct. 1967.

54. *Voyager Studies*, Report FR-22-103, Vol. II, Sect. I, Martin-Marietta Corp., Denver, Colo., 1967.

55. *Voyager '71 Program (Reliability Analysis)*, Report D2-23834-1. Boeing Aircraft Co., Seattle, Wash., Apr. 1965.

56. Paulson, R. A., *Bi-Propellant, Mono-Propellant Reliability Study*, Contract Report No. 95254, TRW Systems, Inc., Redondo Beach, Calif., Aug. 1969.

57. Butcher, W. W., et al., *Spacecraft Attitude Control Gas System Analysis*, Report SS07017212, Hughes Aircraft Co., El Segundo, Calif., Apr. 1967.

58. *Low-Thrust Solid and Hybrid Propulsion Systems (Phase II)*, Report No. LMSC-685070, Lockheed Missiles and Space Co., Sunnyvale, Calif., Feb. 1968.

59. Allen, R. C., *Propulsion Division Newsletter*, Marquardt Corp., Van Nuys, Calif., Oct. 1969.

60. Schmitz, Bruce, *MR-74 Rocket Engine Test Report*, Report No. 69-R-194, Rocket Research Co., Redmond, Wash., Aug. 1969.

61. Beauregard, W., *Final Report on 0.1 lb_f Valve/Thruster Evaluation Testing*, Hamilton Standard Report SVHSER 5447, Hamilton Standard Div., United Aircraft Corp., Windsor Locks, Conn., Vol. I, July 1969.

Bibliography

Survey Papers

Burnstein, A., and Dicristina, H., "Position and Orientation Propulsion Systems For Unmanned Vehicles", Paper P 37, 19th Congress of the International Astronautical Federation, New York, Oct. 1968.

A broad survey of hydrazine, hydrogen peroxide, cold nitrogen, electrolyzed hydrazine, subliming solid, resistojets, and ion propulsion systems is included. Spin-stabilized, gravity gradient, and three-axis stabilized spacecraft are examined.

Butcher, W. W., *Hydrazine Electrolysis for Spacecraft Propulsion*, Hughes Final Report SSD 80316R (JPL Contract 951710), Aug. 1968.

A good general attitude control system analysis reference. Stored cold gas, vaporizing liquid, hydrazine plenum, water electrolysis, hydrazine electrolysis, and dual mode hydrazine (electrolysis and monopropellant hydrazine) systems were considered. A wealth of reliability and redundancy analysis is included.

Final Report: ATS-4, prepared by Fairchild Hiller Space Systems Division for NASA-Goddard, Dec. 1966, NASA CR-81562.

A comparison of several candidate reaction jet types for application to the ATS-4 spacecraft. Cold gas, ion engines, and hypergolic bipropellants were eliminated from the detailed study. Ammonia resistojets and hydrazine monopropellants were compared in depth, with hydrazine monopropellants being selected for the mission.

Goodman, M., "Low Thrust Propulsion for the MORL", AIAA Paper 66-226, Mar. 1966.

The application of resistojet (H_2, NH_3 and CO_2) arcjet, ion engines, radioisotope, monopropellant hydrazine, and a bipropellant liquid propulsion system to MORL mission requirements is explored. Low thrust propulsion using resistojets or radioisotope thrusters appears to be feasible and to offer lower weight (conclusion of report).

Grossman, I., Jones, I. R., and Lee, D. H., *Auxiliary Propulsion Survey Part III Survey of Secondary Propulsion and Passive Attitude Control Systems for Spacecraft*, Technical Report APAPL-TR-68-67, Sept. 1968.

Excellent system technology survey of monopropellant chemical, bipropellant chemical, cold gas mass expulsion, vaporizing liquid, subliming solid, electrolysis, heated fluid, and non-mass expulsion systems for satellite attitude control.

Hahn, H. T., and Kindsvater, H. M., "Analysis of Future Missions Which Require Low Thrust Solid and Hybrid Propulsion Systems", AIAA Paper 68-517, ICRPG/AIAA 3rd Solid Propulsion Conference, Atlantic City, N.J., 1968.

Low Thrust Solid and Hybrid Propulsion Systems (Phase II), Final Report, LMSC-685070, Lockheed Missiles and Space Company (prepared under Contract NAS 7-573), Feb. 1968.

A wide variety of low-thrust solid and hybrid propulsion systems were investigated. Four mission profiles were selected: ATS-4, *Voyager*, ATM, and EVA. Systems were defined in terms of mass and reliability.

Bibliography (contd)

Neufeld, M. J., and Angel, B. M., "Synchronous Satellite Station-Keeping" AIAA Paper 66-304, May 1966.

Study of station keeping requirements of an advanced synchronous satellite. The use of a water electrolysis system, for a 3-axis stabilized communications satellite is explored. Other systems mentioned were cold gas, hydrogen peroxide, hydrazine, and storable bipropellants.

Nunz, G., "Candidate Low Thrust Devices For the Space Station Reaction Control System", Report No. TOR-0066 (5759-03-1), (Contract F04701-69-C-0066), Aerospace Corp., May 1970.

Survey of low-thrust propulsion devices suitable for the space station. Included in survey were cold gas, heated gas (catalytic, electrothermal, and nuclear-thermal), liquid monopropellant (N_2H_4 and H_2O_2), gaseous bipropellant (O_2/H_2), and electric (ion, colloid, and pulsed plasma).

Nunz, G., and Oberstone, J., *Propulsion Systems for Advanced Geosynchronous Satellites*, Air Force Report No. SAMSO-TR-70-171, Aerospace Corp., May 1970.

A broad survey of low-thrust propulsion systems for use on post-1975 SYNCSATs. Of the general conclusions a hybrid system employing a catalytic monopropellant (N_2H_4) and a low-thrust–high-performance system was found to be a good compromise system. The utilization of electrostatic propulsion may be mandatory for ambitious future missions.

Pujes, J. P., "The Development of Microthrusters in France under the C.N.E.S. Authority," Paper 70-617, AIAA 6th Propulsion Joint Specialist Conference, San Diego, Calif., June 1970.

Survey paper describing the thruster systems under investigation in France. Included in the survey are inert gas, subliming solids, ammonia resistojets, hydrazine catalyst, dual mode hydrazine, and ion engines.

Roberson, R. E., *Methods for Control of Satellites And Space Vehicles*, Vol. I, WADD Technical Report 60-643, Wright Air Development Division, July 1960.

Early Study of expelled momentum devices. Included are solid propellant, hydrogen peroxide, and gaseous nitrogen. Reliability and weight are studied. Momentum storage devices are also included.

Survey of U. S. Programs Related to Satellite Propulsion, Orientation and Station Keeping Devices (Contract F 33615-67-C-1854), Electro-Optical Systems, May 1967.

This broad survey of 65 U. S. Organizations and 140 persons contains a wealth of information on satellite propulsion work in the U. S.

Shattuck, R., *Auxiliary Propulsion Survey, Part I Electric Thrusters Survey, EOS*, Technical Report AFAPL-TR-68-67, Part I, Sept. 1968.

General description of cesium bombardment, mercury bombardment, contact ion, colloid, thermal arc jets, ALPHA MHD arc jets, and pulsed electromagnetic thrusters.

Study of Spacecraft Attitude Control Propulsion Devices, Report No. 8214-933001, Bell Aerosystems Co., Dec. 1962 (Confidential).

A very broad survey of the auxiliary propulsion field. Included in early report are solids, bipropellants, monopropellants N_2H_4 and H_2O_2, cold gas, and ion pulsed plasma thrusters. Reaction wheels are also discussed.

Sutherland, G. S., and Maes, M. E., A Review of Micro-Rocket Technology: 10^{-6} to 1 lb_f Thrust," AIAA Paper 65-620, June 1965.

This early (1965) survey of solid propellant ("Cap Pistol," subliming solid), liquid propellants (vaporizing liquid, monopropellant hydrogen peroxide, hydrazine, hydrazine plenum, liquid bipropellant), gaseous propellants (inert gas, gaseous bipropellants), resistojets, radioisojet, and electrolysis systems, gives a brief description of each system. The problems of low Reynolds number flow and back pressure effects on low thrust (10^{-4} lbf) nozzles are brought to light.

Gas Systems, Inert Monopropellant

Analysis of a Cold Gas Thruster Subsystem for the Anchored Interplanetary Monitoring Platform Attitude Control System, SSD-165.0, Fairchild Hiller Corporation, Space and Electronic Systems Division, Maryland, Dec. 1966.

Broadhurst, R. H., *Reliability of the Cold Gas Attitude Control System*, Bird Engineering-Research Associates, Inc., Vienna, Virginia, May 1967.

Dolder, F. D., *Final Report and Technical Manual S-16 Orbiting Solar Observatory*, Ball Brothers Research Corporation, Boulder, Colorado.

Ferrera, J. D., and Roselli-Lorenzini, F. G., "Viking Reaction Control Gas System Weight Reduction Analysis Phase I," Engineering Memorandum 344-222FGR-L, Jet Propulsion Laboratory, Pasadena, Calif., April 1969.

Discussion of weight and performance of the Viking inert gas system.

Ferrera, J. D., and McKown, P. M., *A Method For Calculating Steady-State Thrust and Flow-Rate Levels for Mariner IV Type Attitude Control Nitrogen Gas Jets*, Technical Report 32-1353, Jet Propulsion Laboratory, Pasadena, Calif., Dec. 1968.

A technique for estimating the performance of inert gas monopropellant thrusters is provided in this reference. Nozzle performance loss is included in thruster performance calculations.

Greer, H., and Griep, D. J., *Dynamic Performance of Low Thrust Cold Gas Reaction Jets in a Vacuum*, Report No. TR-669(6230-33)-1, Aerospace Industries, El Segundo, Calif., Aug. 1966.

The propulsive performance of various gases are analytically derived and are correlated with vacuum experiments.

Greer, H., and Griep, D. J., "Dynamic Performance of Low-Thrust, Cold Gas Reaction Jets in a Vacuum," *AIAA Journal of Spacecraft*, Vol. 4, No. 8, p. 983, Aug. 1967.

Pulsed propulsive performance of low-thrust reaction jets, typical of those used for attitude control of small spacecraft, is analyzed and compared with laboratory experiments.

Bibliography (contd)

Haloulakos, V. E., "Thrust and Impulse Requirements for Jet Attitude-Control Systems," *AIAA Journal of Spacecraft*, Vol. 1, No. 1, p. 84, Jan. 1964.

Requirements of attitude propulsion systems are investigated in this paper. The selection of thrust level is studied.

Hendel, F. J., "Attitude Control With Hydrogen Microthrusters," Paper 70-613, AIAA 6th Propulsion Joint Specialist Conference, San Diego, June 1970.

Description of an inert monopropellant hydrogen thrusting system utilizing boil-off hydrogen from the main propulsion system of a Lunar Logistics Vehicle.

Mariner Mars 1964 Project Report: Mission and Spacecraft Development, Volume I, Technical Report 32-740, Jet Propulsion Laboratory, Pasadena, Calif., Mar. 1965.

A description of the Mariner gas actuator system is presented. System performance and component technology is presented.

McCarthy, D. K., and Corter, R. H., *AIMP-E Attitude Control System*, Report X-723-68-410, Goddard Space Flight Center, Greenbelt, Md., Nov. 1968.

Description of AIMP-E inert gas monopropellant system, utilizing Freon 14 propellant. Component test data is included.

Robertson, V. S., and Weaver, J. J., "Spacecraft Attitude Control," British Interplanetary Society, 1st Annual Meeting, University of Southampton, Released from Elliott Brothers (London) Limited, Space and Guided Weapons Division, Chobham Road, Frimley, Camberley, Surrey, England, April 1968.

Description of the inert gas actuator system for the Black Arrow satellite.

Gas Systems, Reacting Tridyne

Barber, H. E., et al., "Microthrusters Employing Catalytically Reacted Gas Mixtures, Tridyne," AIAA 6th Propulsion Joint Specialist Conference, San Diego, June 1970.

Description of the tridyne program including experimental performance data. The fabrication techniques used for construction of this thruster are discussed. System concepts such as three-thruster module construction are discussed.

Iacobellis, S. F., *Tridyne Attitude Control Thruster Investigation*, Report No. R-7743P, Rocketdyne, Jan. 1969.

Results of an early look at the Tridyne concept. Thruster configuration, predicted performance, and system studies are presented.

Liquid Systems, Vaporizing Liquid

ATS F & G Protype Ammonia Feed System Description, Report SPPS-8-100, General Electric, Space Power and Propulsion Section, Mar. 1968.

Proposal for an Ammonia feed system for the ATS F & G spacecraft. The feed system is similar to the system discussed in GE Report GESP-236, July, 1968.

Briscoe, H. M., "The Choice of Propellant for a Cold Gas Propulsion System for a Satellite," *Journal of the British Interplanetary Society*, Vol. 20, p. 72, 1965-66.

A broad survey of more than 15 vaporizing liquid propellants suitable for spacecraft auxiliary propulsion is presented. Propellant characteristics are explored.

Cromwell, R., and Viventi, R., *Spacecraft Attitude Control System Prototype and Test*, Report GESP-236 (Contract 951895), General Electric, Nuclear Systems, July 1968.

This document is the final test report on the design, development, fabrication, and test of a laboratory prototype, passive vaporizing liquid ammonia attitude control system for JPL.

Flight Prototype Ammonia Storage and Feed System, Final Report, Report AVSSD-0100-67-RR (Contract NAS5-10128), Avco Missiles, Space and Electronics Group, Jan. 1967.

Discussion of the Avco ammonia feed system which has flown on ATS A, C, D, and E.

Griep, D. J., *Experimental Performance of Anhydrous Ammonia*, Report No. TDR-469 (5230-33)-1 (Contract No. AF 04 (696) 469), Aerospace Corporation, Oct. 1964.

Kanning, G., *Measured Performance of Water Vapor Jets for Space Vehicle Attitude Control Systems*, NASA TND-3561, Aug. 1966.

Krieve, W. F., Merritt, F. L., and Grobbi, R., "Zero Gravity Ammonia Propellant System," Paper 70-1151, to be presented at the AIAA 8th Electric Propulsion Conference, Stanford, Calif., Sept. 1970.

Discussion of the TRW capillary tube ammonia feed system.

Kamin, J. and Bromberg, M. L., *NRL Ammonia Vapor Microthruster System*, (Contract N00014-66-C0129), General Electric, Space Power and Propulsion Section, Sept. 1966.

Discussion of the NRL ammonia system. This system was flight-qualified and flown. Just prior to launch additional power was allotted to the thrusters, which led to the adoption of resistojets to the system.

Tinling, Bruce E., *Measured Steady-State Performance of Water Vapor Jets for Use in Space Vehicle Attitude Control Systems*, NASA TND-1302, May 1962.

Liquid Systems, Hydrazine

Catalytic Thrusters

Basic Data Package Flight Weight Hydrazine Monopropellant REA, Model R12D 5-lb Thrust, Propulsion Division, The Marquardt Corporation, Van Nuys, Calif., Aug. 1969.

Description of The Marquardt Company 5 lbf thrust monopropellant hydrazine thruster. Life testing data are also provided.

Basic Data Package Flight Weight Hydrazine Monopropellant REA, Model R25A. 0.1-lb. Thrust, Propulsion Division, The Marquardt Corporation, Van Nuys, Calif., Aug. 1969.

Description of The Marquardt Company 0.1 lbf thrust monopropellant hydrazine thruster.

Bibliography (contd)

Eggers, R. F., "Microthrust Monopropellant Hydrazine Propulsion System Technology," Paper 68-556, AIAA 4th Propulsion Joint Specialist Conference, Cleveland, Ohio, June 1968.

Discussion of monopropellant hydrazine systems with thrust levels of 100 mlbf and less. Hydrazine catalytic, hydrazine electrolysis, and hydrazine plenum systems are discussed.

Final Report, 0.1 lbf Valve/Thruster evaluation Testing, Volume 1 Valve/Thruster Performance, Report SVHSER 5447, Hamilton Standard Corp., Windsor Locks, Conn., July 1969.

This report presents test results from the 0.1-lbf valve/thruster evaluation program. Four propellant valves were tested. Life testing data is presented along with thruster performance.

Half-Pound Monopropellant Hydrazine Thruster, TRW Systems Group, Redondo Beach, Calif., Dec. 1968.

Performance data of a half-pound catalytic hydrazine thruster.

Long Life 5 lbf Hydrazine Engines For Endurance Requirements, Report SP13R68, Hamilton Standard Corp., Windsor Locks, Conn., Aug. 1968.

Monopropellant Rocket Engines, Propulsion Division, Aerojet-General Corp., Sacramento, Calif., June 1969.

Description of Aerojet-General 5 lbf hydrazine monopropellant thruster.

Monopropellant Spacecraft Maneuvering and Attitude Control System, TRW Systems Group, Redondo Beach, Calif., Aug. 1969.

Description of the TRW Model 35 hydrazine system, which includes a 5-lbf catalytic thruster.

MR-50A Rocket Engine Assembly Design and Description, Report 69-R-183, Rocket Research, Redmond, Wash., Nov. 1969.

Design aspects and performance of the Rocket Research 5-lbf thrust catalytic hydrazine thruster.

MR-74 Rocket Engine Test Report, Report 69-R-794, Rocket Research, Redmond, Wash., Aug. 1969.

Description of a 0.10-lbf Rocket Research thruster, with steady-state and pulse mode operation test results.

Price, T. W., and Evans, D. D., *The Status of Monopropellant Hydrazine Technology*, Technical Report 32-12271, Jet Propulsion Laboratory, Pasadena, Calif., Feb. 1968.

A comprehensive review of hydrazine monopropellant technology. Included in this report is an extensive survey of past and current status of the technology. This report has a rather extensive bibliography of early work in this field, this is an excellent report for an introduction to hydrazine monopropellant technology.

Bibliography (contd)

Hydrazine Resistojets

Schreib, R. R., Pugmire, T. K., and Chapin, S. G., "The Hybrid (Hydrazine) Resistojet," AIAA Paper 69-496, June 1969.

This early paper presents some initial experiments with hydrazine resistojets.

Hydrazine Plenum

Eggers, R. F., "Microthrust Monopropellant Hydrazine Propulsion System Technology," Paper 68-556, AIAA 4th Propulsion Joint Specialist Conference, Cleveland, Ohio, June 1968.

Discussion of hydrazine plenum systems. Included is the Rocket Research passive pressure control system.

Final Report for Monopropellant Hydrazine Plenum Study, Rocket Research, Redmond, Washington, Dec. 1969.

Summary report on the passive control hydrazine plenum system. Included are performance data.

Monopropellant Spacecraft Maneuvering and Attitude Control System, Report, TRW Systems Group, Redondo Beach, Calif., Aug. 1969.

Description of the Model 35 hydrazine system, which employs a hydrazine plenum system.

Liquid Systems, Electrolysis Systems

Bell, L. R., and Picciotti, E. F., "Electro Chemical Propulsion System," to be presented at the 12th Liquid Propulsion Meeting, New Technology Session, Las Vegas, Nev., Nov. 1970.

A discussion of a combined electrolysis cell and bipropellant O_2/H_2 thruster system.

Butcher, W. W., *Hydrazine Electrolysis for Spacecraft Propulsion*, Report SSD 80316R (JPL Contract 951710), Hughes Aircraft Co., Aug. 1968.

This report discusses the design, fabrication, and test of a breadboard propulsion system. The report also includes the design of a dual-mode hydrazine propulsion system.

In-Flight Bipropellant Generator for Attitude Control, Life Systems Inc., Cleveland, Ohio, June 1969.

Discussion of a water electrolysis system which provides separated streams of oxygen and hydrogen.

Morgan, N. E., *Hydrazine Electrolysis Cell Safety Limits*, report on Tasks VII and VIII (JPL Contract No. 951720), Hughes Aircraft Co., El Segundo, Calif., June 1969.

The hydrazine electrolysis cell was operated at extreme conditions to test its safety limits. A hot spot developed, which led to cell destruction.

Picciotti, E., Rouch, K., and Pox, C., *A Study of the Feasibility of a Separated O_2H_2 Electrothochemical Propulsion System*, Allis Chalmers, Advanced Electrochemical Products Division, Milwaukee, Wis., Sept. 1969.

A study was made to determine the feasibility of an electrochemical oxygen-hydrogen propulsion system wherein the propellant gases are generated in high purity, separated streams.

Rodewald, N., Falkenstein, G., Herr, P., and Prono, E., *Evaluation and Demonstration of the Use of Cryogenic Propellants (O_2/H_2) for Reaction Control Systems*, Volume II, NASA CR-72244 (R-6838-2), June 1968.

Discussion of a 20-lbf catalytic O_2/H_2 (gaseous) thruster. Several thrusters are discussed.

Rollubler, J. R., *Experimental Performance of a Water-Electrolysis Rocket*, NASA TM X-1737, Feb. 1969.

An experimental stociometric hydrogen/oxygen spark thruster was demonstrated to deliver 325 lbf-sec/lbm steady-state specific impulse. Flashback of the propellants was observed (premixed gas).

Solid Systems, Subliming Solids

Berkopec, F. D., *Performance of Two Subliming Solid-Propellant Thrustor Systems for Attitude Control of Spacecraft*, NASA TN D-3841, Feb. 1967.

Two subliming-solid-propellant systems were investigated: a 10^{-2} lbf thrust system utilizing ammonium hydrosulfide (NH_4HS) and a 2×10^{-4} lbf thrust system utilizing ammonium carbonate ($NH_4CO_2NH_2$) as propellant. Both systems were of the valved type.

Eggers, R. F., "Subliming Solid Propulsion System Technology," presented at ICRPG IAIAA Solid Propulsion Conference, Anaheim, Calif., June 6–8, 1967.

Federline, F., *Development of the Subliming Solid Control Rocket—Contributions From the Explorer XXXV (AIMP-E) Satellite Program*, Document X-723-68-227, NASA Goddard Space Flight Center, June 1968.

Forsythe, R. W., *Impulse and Thrust Test of a Subliming Solid Micropropulsion System*, TN D-3245, NASA Goddard Space Flight Center, March 1966.

Greer, H., and Griep, D. J., *Dynamic Performance of a Subliming Solid Reaction Jet*, Report No. TR-1001 (2230-33)-1, Aerospace Industries, Dec. 1966.

Performance and design relationships of a valved subliming solid jet reaction system are analytically derived and correlated with results of sea level and vacuum experiments. The propellant was ammonium carbonate.

Hardt, A. P., Foley, W. M., and Brandon, R. L., "The Chemistry of Subliming Solids For Micro Thrust Engines," AIAA Paper 65-595, June 14–18, 1965.

Vapor pressure and kinetic data of several propellants suitable for subliming solid microthrusters is presented.

Kindevater, H. M., "Simplified Space Mechanisms Using Subliming Solids", Proceedings of the First Aerospace Mechanisms Symposium, University of Santa Clara, Santa Clara, Calif., May 19–20, 1966.

Kindevater, H. M., "Design Criteria for Subliming Solid Applications", presented at ICRPG/AIAA Solid Propulsion Conference, Anaheim, Calif., June 6–8, 1967.

Bibliography (contd)

Final Report, Subliming Solid Reaction Control System", Lockheed Missiles and Space Company Report LMSC-5A102 (Hughes Aircraft Company Purchase Order 44-819904), Oct. 1967.

Discussion of the design, construction, testing, qualification, and acceptance of a subliming solid system for use on the ATS spacecraft.

Owens, W. L., "An Experimental Study of Superheated Subliming Solid Thruster Performance," AIAA Paper 70-210, 8th Aerospace Science Meeting, Jan. 1970.

Comparison of experimental and analytical performance of a subliming solid resistojet system.

Owens, W. L., Jr., "Design Aspects of Subliming Solid Reaction Control Systems," AIAA Paper 68-516, June 1968.

This paper attempts to formalize the design aspects of subliming solid reaction control systems. Included are the topics: Propellant Selection, Nozzle Performance, Propellant Sublimation Area, Power, Capillary Pressure Drop, Dynamic Response, and Valveless Design.

Application of the Valveless Subliming Solid Control Rocket to the NRL Gravity Gradient Satellite, Report RRC-66-R-59, Rocket Research Corporation, Seattle, Washington, May 1966.

Discussion of the design, analysis, test, propellant selection, performance and status of a valveless subliming solid rocket designed for a classified NRL satellite.

Development of the Subliming Solid Control Rocket Phase II, NASA CR-712, Rocket Research Corporation, Seattle, Wash., Mar. 1967.

Final Report for Subliming Solid Control Rocket, November 22, 1963 through September 30, 1964, Rocket Research Corp., prepared for Goddard Space Flight Center under Contract NAS 5-3599.

Microrockets for Control of Satellites and Space Vehicles, Report 62-R-9, Rocket Research Corp., November 1962.

Early Papers And General History Of Electric Propulsion

Bostick, W., *Plasma Motors*, Advan. Astronauts Sci. Vol. 2, American Rocket Society, Plenum Press, Inc., N. Y., 1957.

Forrester, A. T., and Kuskevics, G., "Ion Propulsion", in *AIAA Selected Reprints Series*, Vol. III, by Gross, R. A., Published by AIAA, New York, N. Y.

This is an excellent starting point for studies in ion propulsion. This reference contains an extensive bibliography.

Giannini, G. M., *The Plasma Jet and Its Application*, Technical Note 57-520, Office Scientific Research, 1957.

Goddard, R. H., *R. H. Goddard, an Autobiography*, Robert H. Goddard Notebook dated September 6, 1906, *Astronautics*, Vol. V, p. 24, 1959.

Bibliography (contd)

Langmuir, D. B., "Low Thrust Flight: Constant Exhaust Velocity in Field-Free Space," Chap. 9, in H. S. Seifert (ed.), *Space Technology*, John Wiley and Sons, Inc., N. Y., 1959. (Also see chapter 18.)

Oberth, H., *Wege zu Raumschiffahrt*, R. Oldenbourgh KG, Munich, Chap. 22, pp. 409–423, 1929.

Shepherd, L. R., and Cleaver, A. N., "The Atomic Rocket," *Journal of British Interplanetary Society*, Vol. 7, p. 185, 1948; Vol. 8, pp. 23, 50, 1949.

Stuhlinger, E., *Ion Propulsion for Space Flight*, Chap. 1, McGraw-Hill Book Co., N. Y., 1964.

Good book for early history of electric propulsion.

Stuhlinger, E., "Possibilities of Electric Space Ship Propulsion," in Bericht 5th International Astronautical Congress, Innsbruck, p. 100, 1954.

Stuhlinger, E., "Electrical Propulsion Systems for Space Ships with Nuclear Power Source," *Journal of Astronautics*, Vol. 2, p. 149, 1955; Vol. 3, pp. 11, 33, 1956.

Stuhlinger, E., "Flight Path of an Electrically Propelled Space Ship," *Jet Propulsion*, Vol. 27, No. 4, p. 410, Apr. 1957.

Electric Thrusters, Ion Thruster

Anderson, J. R., and Thompson, S. A., *Development and Long Life Performance of Ion Engines for Satellite Control* (Contract No. 3-7927), Paper 66-234, AIAA 5th Electric Propulsion Conference, San Diego, Calif., Mar. 1966.

Discussion of single-strip cesium-contact ion engines under development at Hughes Research Labs. Thrust levels of 10,300, and 500 μlbf were obtained by the devices presented. A 2000-h test was performed on one thruster at an average thrust of 560 mlbf.

Collett, C. R., Dulgeroff, C. R., and Simpkins, J. M., "Cesium Microthruster System," Paper 69-292, AIAA 7th Electric Propulsion Conference, Williamsburg, Va., Mar. 1969.

Data on a 20-μlbf cesium contact microthrust system is presented. A porous tungsten button is utilized as an ionizer in this Hughes Research Lab. thruster.

Forsnight, V. V., Sohl, G., Caplinger, E., Schrout, E. H., and Dillion, T. R., *A Cesium Electron-Bombardment Microthruster System* (Air Force Contract F 33615-67-C-1268), AIAA Paper 69-293, AIAA 7th Electric Propulsion Conference, Williamsburg, Va., Mar. 1969.

A 100–200 μlbf cesium bombardment thruster system under study at Electro-Optical Systems is presented. Data for the thruster and feed system are presented.

Hunter, R. E., Bartlett, R. O., Worlock, R. M., and James, E. L., *Cesium Contact Ion Microthruster Experiment Aboard Applications Technology Satellite (ATS) IV*, Paper 69-297, AIAA 7th Electric Propulsion Conference, Williamsburg, Va., Mar. 1969.

Results of the ATS experimental thruster performance in space are provided. The thruster demonstrated an absence of detectable EMI and the zero-g feed system operation was satisfactory.

Bibliography (contd)

James, E. L., et al., "A One Millipound Cesium Ion Thruster System," Paper 70-1149, to be presented at the AIAA 8th Electric Propulsion Conference, September 1970.

A description of the north-south station keeping system on ATS-F. Two systems each carrying 3.4-kg of propellant and operating at a nominal specific impulse of 2500 lbf-s/lbm, provide capability for 28 mo of station keeping.

James, E. L., and Goldner, S. J., *Ion Engine Systems Testing*, Air Force Report AFAPL-TR-69-112, Feb. 1970.

This report documents engine lift testing of micropound thrust cesium contact thrusters. Thrusters were tested for in excess of 3000 h.

Kerslake, W. R., Wasserbauer, J. R., and Morgosian, P. M., "Experimental Mercury Bombardment Thruster at Submillipound Thrust," *AIAA Journal*, No. 4, pp. 683–691, April 1967.

Results from low-thrust tests of a 5-cm mercury bombardment thruster operating at 520 and 650 μlbf thrust. The cathode was endurance tested for 1553 h.

Moore, R. D., "Magneto-Electrostatically Contained Plasma Ion Thruster" Paper 69-760, AIAA 7th Electric Propulsion Conference, Williamsburg, Va., Mar. 1969.

Discussion of a new type electrostatic electron bombardment ion thruster. Discharge performance exceeds all previous EOS cesium bombardment thruster designs.

Reader, P. E., et al., "A Sub-Millipound Mercury Electron-Bombardment Thruster," Paper 70-616, AIAA 6th Propulsion Joint Specialist Conference, San Diego, Calif., June 1970.

Studies of 5-cm mercury bombardment thruster research at NASA Lewis are reported. Specific impulse of the thruster has been lowered to 1800 lbf-s/lbm to improve the power-to-thrust ratio at 360 μlbf thrust.

Richley, E. A., and Kerslake, W. R., "Bombardment Thruster Investigation at the Lewis Research Center," Paper 68-542, AIAA 4th Propulsion Joint Specialist Conference, Cleveland, Ohio, June 1968.

The current status of various programs on mercury-bombardment thrusters is reviewed. Included is a 5-cm bombardment thruster. The work on the high-thrust bombardment systems (greater than 1 mlbf) such as the SERT II is applicable to low-thrust engines; however, these references have been omitted from this list. The January 1970 issue of the *Journal of Spacecraft and Rockets* provides a more in-depth discussion of high-thrust mercury-bombardment thrusters.

Sohl, G., et al., "Cesium Electron-Bombardment Ion Microthrusters," Paper 67-81, AIAA 5th Aerospace Sciences Meeting, New York, N. Y., Jan. 1967.

Early paper on Electro-Optical Systems cesium bombardment research. Data for thrusters of 10–1000 μlbf is presented.

Staggs, J. F., and Lathern, W. C., "Experimental Performance of a Low-Thrust, Divergent Flow, Contact-Ionization Electrostatic Thruster," Paper 66-569, AIAA 2nd Propulsion Joint Specialist Conference, Colorado Springs, Colo., June 1966.

Performance of a 350-μlbf cesium contact ionization thruster operating at 2000 lbf-s/lbm is presented. Analysis of electrode erosion is presented.

Worlock, R. M., et al., "A Contact Ion Microthruster System," Paper 67-80, AIAA 5th Aerospace Sciences Meeting, New York, N. Y., Jan. 1967.

One of the first cesium contact microthruster systems developed is presented in this paper. The thruster operates at a nominal 10-μlbf with 5 deg of beam deflection possible.

Worlock, R. M., et al., "An Advanced Contact Ion Microthruster System," Paper 68-552, AIAA 4th Propulsion Joint Specialist Conference, Cleveland, Ohio, June 1968.

Description of the ATS-D and E cesium contact ion microthruster system. This thruster is capable of 5-, 10-, 15-, and 20-μlbf thrust with 10-deg thrust vectoring.

Worlock, R. M., et al., "Characteristics of Micropound Range Ion Thrusters," Paper 66-212, AIAA 5th Electric Propulsion Conference, San Diego, Calif., Mar. 1966.

Performance dates of a 10-μlbf and a 24-μlbf thrust cesium contact ionization thruster is presented.

Worlock, R. M., et al., *Cesium Bombardment Ion Engine System Development*, Air Force Technical Report AFAPL-TR-69-87, Oct. 1969.

This report covers the development of a 100-μlbf cesium bombardment ion engine system. The results of a millipound-range thruster using the magneto-electrostatic plasma containment concept are presented.

Electric Thrusters, Colloid

Cohen, E., Burson, W. C., and Herren, P. C., Jr., "Colloid Thruster Technology '69," 8th International Symposium on Space Technology and Science, Tokyo, 1969.

A good survey of the present status of colloid thruster technology, including thruster performance, pulsed operation for spin-stabilized satellites, and beam vectoring.

Cohen, E., *Research on the Electrostatic Generation and Acceleration of Submicron Size Particles*, ARL 32-88-WPAFB, May 1963.

Early work at TRW on colloids.

Courtney, W. G., and Budnik, C., "Colloid Propulsion Using Chemically-Formed Particles," Paper 66-254, AIAA 5th Electric Propulsion Conference, San Diego, Calif., Mar. 1966.

Goldin, D. S., and Norgren, C. T., "Thrust Measurements of Colloidal Particles as an Indication of Particle Size and Thrustor Operation," Paper 63-050, AIAA Electric Propulsion Conference, Colorado Springs, Colo., Mar. 1963.

Discussion of NASA-Lewis colloid thruster operating with mercurous chloride as propellant.

Hendricks, C. D., and Pfeifer, R. J., "Parametric Studies of Electrohydrodynamic Spraying," Paper 66-252, AIAA 5th Electric Propulsion Conference, San Diego, Calif., Mar. 1966.

Presentation of mathematical models of colloid thruster operation.

Kidd, P. W., "Parametric Studies With a Single Needle Colloid Thrustor," AIAA paper 67-530, AIAA Electric Propulsion and Plasmadynamics Conference, Colorado Springs, Colo., Sept. 1967.

An extensive single needle parametric study is presented. Glycerol solutions of ($SnCl_4$ and $FeCl_3$) at negative potentials and (NaI) at positive potential are included.

Norgren, C. T., and Goldin, D. S., "Experimental Analysis of the Exhaust From A Colloid Thrustor," Paper 64-674, AIAA 4th Electric Propulsion Conference, Philadelphia, Pa., Aug.–Sept. 1964.

Studies of the NASA-Lewis mercurous chloride colloid thruster.

Perel, J., et al., "Research on a Charged Particle Bipolar Thruster," Paper 57-728, AIAA Electric Propulsion and Plasmadynamics Conference, Sept. 1967.

Discussion of a 73 needle bipolar thruster tested at Electro-Optical Systems.

Wineland, S. H., and Hunter, R. E., "Negatively Charged Colloid Generation Research," Paper 66-251, AIAA Fifth Electric Propulsion Conference, San Diego, Calif., Mar. 1966.

Colloid research at Wright-Patterson Aero Propulsion Laboratory.

Zafran, S., et al., "Colloid Microthruster System Development," Paper 68-84, AIAA 6th Aerospace Sciences Meeting, New York, N. Y., Jan. 1963.

Experimental data are presented for a colloid microthruster system which was developed for satellite yaw control.

Zafran, S., and Beynon, J. C., "Colloid Microthruster Life Test", Paper 70-1110 to be presented at AIAA 8th Electric Propulsion Conference, Stanford, Calif., Sept. 1970.

Results from a 1750-h life test of a colloid microthruster system.

Electric Thrusters, Pulsed Plasma

Dailey, C. R., *Development of a Pulsed Inductive Plasma Thruster*, TRW Systems, Redondo Beach, Calif., Oct. 1968.

Discussion of a gaseous pulsed plasma thruster operating at 1-mlbf thrust.

Gilmour, A. S., "Concerning the Feasibility of a Vacuum Arc Thruster," Paper 66-202, AIAA 5th Electric Propulsion Conference, San Diego, Calif., Mar. 1966.

Early studies at Cornell Aeronautical Laboratory in pulsed plasma thrusters.

Gilmour, A. S., Clark, R. J., and Vernon, H., "Pulsed Vacuum-Arc Microthrusters," Paper 67-737, AIAA Electric Propulsion and Plasmadynamics Conference, Colorado Springs, Colo., Sept. 1967.

Early research program at Cornell Aeronautical Laboratory on a pulsed plasma thruster designed for Lincoln Laboratory. This thruster operates at 1000 lbf-s/lbm specific impulse with a 10% efficiency.

Bibliography (contd)

Gilmour, A. S., et al., "Recent Progress in Pulsed Vacuum-Arc Microthruster Research," Paper 68-555, AIAA 4th Propulsion Specialist Conference, Cleveland, Ohio, June 1968.

Description of the Cornell Aeronautical Laboratory pulsed vacuum-arc Microthruster. This thruster uses zinc wire for fuel. Life test data is included in this study.

Gloersen, P., "Current Status of Pulsed Plasma Engine Development," Paper 66-566, AIAA 2nd Propulsion Joint Specialist Conference, Colorado Springs, Colo., June 1966.

General discussion of pulsed plasma thruster research in the U.S. Included in the survey of thrusters were the Convair/Astronautics (coaxial gun), General Electric (coaxial gun), Lewis Research Center (coaxial gun), Republic Aviation (pinch-coaxial), and General Motors/Allison Division (double wire rail gun). All the thrusters discussed in this survey operated with power requirements in excess of a kilowatt.

Gorowitz, B., Karras, T. W., and Gloersen, P., "Performance of an Electrically Triggered Repetitively Pulsed Coaxial Plasma Engine," *AIAA Journal*, Vol. 4, No. 6, pp. 1027–1031, June 1966.

Description of General Electric pulsed plasma coaxial gun thruster.

Guman,, W. J., and Nathanson, D. M., "Pulsed Plasma Microthruster Propulsion System for Synchronous Orbit Satellite," AIAA 7th Electric Propulsion Conference, Williamsburg, Va., Mar. 1969.

Description of the LES-6 pulsed plasma thrusters. This paper describes a program that led to the development of a complete microthruster system. Performance of the pulsed plasma thrusters is provided along with life testing data.

Guman, W. J., et al., "Pulsed Plasma Propulsion System Studies," Paper 70-1141, to be presented at the AIAA 8th Electric Propulsion Conference, Stanford, Calif., Sept. 1970.

Discussion of a 70-μlbf-sec impulse bit pulsed teflon thruster. This is similar to the LES-6 thruster which Fairchild Hiller designed.

Jarrett, O. et al., "Thrust Measurements on a Pulsed Vacuum-Arc Thruster," Paper 70-1146, to be presented at the AIAA 8th Electric Propulsion Conference, Stanford, Calif., Sept. 1970.

Thrust measurements of the Sanders Associates (Cornell thruster) pulsed plasma thruster at the NASA-Langley 21-ft vacuum chamber.

John, R. R., Bennett, S., and Jahn, R., "Current Status of Plasma Propulsion," Paper 66-565, AIAA 2nd Propulsion Joint Specialist Conference, Colorado Springs, Colo., June 1966.

This paper presents a good survey of the plasma propulsion industry. Included in this paper are steady state and quasi-steady state pulse plasma thrusters. Most of the data in this paper pertains to thrusters with large power requirements; however, the pulsed thruster discussion is excellent.

LaRocca, A. V., and Perkins, G. S., "Development of Solid Propellant Electric Thruster Systems for Attitude Control and Station Keeping of Spacecraft," Paper 67-661, AIAA Electric Propulsion and Plasmadynamics Conference, Colorado Springs, Colo., Sept. 1967.

Discussion of the early concept investigations for the General Electric Solid Propellant Electric Thruster (SPET).

LaRocca, A. V., and Perkins, G. S., "Pulsed Plasma Microthruster Applications and Techniques."

Discussion of the SPET inside-out thruster design. System applications are presented, and performance data on the inside-out concept are listed.

LaRocca, A. V., "Pulsed Plasma and Low-Pressure Detonator Thrusters," Paper 70-1147, to be presented at the AIAA 8th Electric Propulsion Conference, Stanford, Calif., Sept. 1970.

Discussion of current studies at General Electric in plasma thruster research. Included in this paper is data on an electrically triggered exothermic fast reaction thruster. (Detonation SPET.)

Pulsed Plasma Microthruster Propulsion System Application Notes, Report PCD-TR-694, Fairchild Hiller, Farmingdale, N. Y., Jan. 1967.

This report presents parametric performance data along with parametric mass and volume data. It is a good reference for system designing.

Thruster Heaters, Resistojets

Bennett, S., *Electrothermal Engine Research and Development*, NASA Report CR-54104.

Cygnarowicz, T. A., and Gibson, R. N., "Design and Performance of a Thermal Storage Resistojet," AIAA paper 67-662, Sept. 1967.

Performance data on the General Electric Thermal Storage Resistojet. At 2300°R the 20-mlbf thrust resistojet developed a specific impulse of 230 lbf-s/lbm for short pulses. Power requirements were 30 W.

Greco, R. V., and Charhut, D. E., "Resistojet Systems Manned Spacecraft Applications," AIAA Paper 69-255, Mar. 1969.

Discussion on the use of resistojets on the MORL and the Orbital Workshop. The use of biowaste, NH_3, and other propellants are discussed. The use of resistojets for spiral orbit injection is also discussed.

Halbach, C. R., and Yoshida, R. Y., "Development of a Biowaste Resistojet," Paper 70-1133, to be presented at the AIAA 8th Electric Propulsion Conference, Stanford, Calif., Sept. 1970.

Most recent data on 10-mlbf Marquardt resistojets, utilizing methane, carbon dioxide, water, hydrogen, and biowaste mixtures.

Howard, J. M., *Investigation of Electric Resistance-Heated Rocket for Feasibility In Space Propulsion Applications*, ASDT PR-62-487, June 1962.

Howard, J. M., The Resistojet, *ARS Space Flight Report to the Nation*, ARS preprint 61-2126 (Oct. 1961); also *ARS J*, 33, No. 6, pp. 961–962, June 1962.

Bibliography (contd)

Jack, J. R., "Theoretical Performance of Propellants Suitable for Electrothermal Jet Engines," 15th annual meeting, ARS, Washington, D. C., ARS Preprint No. 1506-60; Dec. 1960; also *ARS J*, 31, pp. 1685–1689, 1961.

One of the earliest papers on resistojets in the U.S. Presents some of the theoretical performance data of propellants suitable for resistojets.

Jack, J. R., "NASA Research on Resistance-Heated Hydrogen Jets," AIAA Electric Propulsion Conference, Colo., Mar. 1963.

Third paper by J. R. Jack on early NASA-Lewis work on resistance-heated hydrogen jets.

Jackson, F. A., Stansel, J. C., Fortner, D., and Hagelberg, C. F., "An Operational Electrothermal Propulsion System for Spacecraft Reaction Control," AIAA Paper 66-213, March 1966.

A discussion of the first operational use of an electrothermal thruster aboard an orbiting spacecraft (*Vela*) is presented. The engine operates on 90 W of power and produces 0.002 lbf thrust at a specific impulse of 123 lbf-s/lbm (N_2). The advanced *Vela* resistojet is also discussed.

John, R. R., *Resistojet Research and Development, Phase II, Final Report*, NASA CR-54688, Avco Report AVSSD-0356-66-CR, Dec. 1966.

This report pursues research and development of an ammonia-fueled electrothermal thruster system. Thrust range of 100–1000 μlb and power levels (to 50 W) to be compatible with satellite limitations. Fast heat up and thermal storage resistojets are considered. The report contains a wealth of information on thruster propellants, materials and performance.

Jeffries, N. P., *Analytical Methods for Resistance Jet Design*, General Electric Technical Info Series Report No. R 64SD3008.

Murch, C. K., "Electrothermal Thruster Performance with Biowaste Propellants," Paper 70-1161, to be presented AIAA 8th Electric Propulsion Conference, Stanford, Calif., Sept. 1970.

The performance of biowaste propellants in the TRW resistojets thruster.

Page, R. J., and Halbach, C. R., "Resistojet Engine Performance, A Comparison of Experiment with Theory," presented at the AIAA 4th Electric Propulsion Conference, Philadelphia, Pa., Aug. 1964.

Page, R. J., Halbach, C. R., and Short, R. A., "3 KW Concentric Tubular Resistojet Performance compared with Theory," AIAA Paper 66-224, March 1966.

This paper presents a little history of resistojet work in the U.S. along with the performance during a 25-h test of a hydrogen, 140-mlb thrust resistojet. The resistojet was of the concentric tube configuration and delivered a specific impulse of 838 lbf-s/lbm at 3.04 kW.

Page, R. J., and Short, R. A., "Ten-Milli pound Resistojet Performance," AIAA Paper 67-664, October 1967.

This report parameterizes the required power, delivered specific impulse, and thruster resistance as a function of gas temperature. Both hydrogen and ammonia are utilized as propellants.

Bibliography (contd)

Page, R. J., Halbach, C. R., Short, R. A., and Ownby, M. L., "Life Test of Six High Temperature Resistojets," AIAA Paper 69-299, March 1969.

High performance 10-mlbf resistojet life tests are discussed. Test results through 3565 h of testing are discussed. Both ammonia and hydrogen propellants are utilized. Little or no degradation of resistojet performance has been noted. These tests have since been completed at 8000 h.

Page, R. J., and Short, R. A., "Advanced Resistojet Propulsion and Control Systems for Spacecraft", ASME paper 70-Av/SpT-10, Space Technology and Heat Transfer Conference, Los Angeles, Calif., June 1970.

Discussion of an advanced resistojet system under study at Advanced Rocket Technology Corporation.

Pisciotta, A., and Eusanio, E., "Subsystems Analyses for a MORL Resistojet Control System," AIAA Paper 67-721, Sept. 1967.

This report presents the results of the first phase of a program to define a resistojet control system for the manned orbiting research laboratory (MORL).

Pugmire, T. K., and Shaw, R., "Applied Resistojet Technology," Paper 70-211, AIAA 8th Aerospace Sciences Meeting, New York, N. Y., Jan. 1970.

Presentation of performance of Avco resistojets operating at zero to 200 W. Engines were optimized for thrust levels of 10 and 20 mlbf.

Pugmire, T. K., *Flight Prototype Ammonia Storage and Feed System*, Avco Space Systems Division Report AVSSD-0100-67-RR (Contract NAS5-10128), January 1967.

Work on an early NASA Goddard prototype flight unit.

Pugmire, T. K., *Design, Development, Fabrication, Test, and Delivery of Electrothermal Engine Systems, Final Report*, Report AVSSD-0062-68-RR (NASA CR-72362), Avco Space Systems Division, Nov. 1967.

Continuation of early resistojet research for NASA Lewis, culminating in a flight type resistojet system.

Pugmire, T. K., and Lund, W., "ATS-III Resistojet Thruster System Performance," AIAA Paper 68-553, June 1968.

Discussion of an ammonia-fueled resistojet engine developed, qualified, and subsequently tested on the ATS-III spacecraft. This system was flown as an experiment. Measurements of micropound thrust performance were obtained for both cold flow and electrically heated flow. Measurements compared well with ground measurements.

Pugmire, T. K., Shaw, R., and Collens, R. A., "Ammonia Resistojet Station Keeping Subsystem Aboard Applications Technology Satellite (ATS)-IV," AIAA Paper 69-296, March 1969.

A 50-μlb thrust, ammonia-fueled resistojet system on board the ATS-IV is discussed. The system was provided for station keeping, and operated 825 h consuming 35% of its fuel (equivalent to 1 yr). Flight test compares with laboratory calibration. Extensive valve selection and qualification contributed to flight success.

Bibliography (contd)

Pugmire, T. K., and John, R. R., "Thermal and Material Considerations Pertinent to the Biowaste Resistojet," Paper 70-1135, to be presented at the AIAA 8th Electric Propulsion Conference, Stanford, Calif., Sept. 1970.

Potential material problems with biowaste propellants have been studied.

Tinling, B. E., *Measured Steady-State Performance of Water-Vapor Jets for Use In Space Attitude-Control Systems*, NASA TN D-1302, May 1962.

Tobias, Ivan, and Kasson, R. L., "A resistojet system for attitude control of unmanned Earth Satellites," AIAA Paper 66-225, Mar. 1966.

The use of small resistojet thrusters as part of a reaction control system that might provide attitude control and orbit maintenance of manned and unmanned earth satellites is discussed.

Todd, J. P., "Resistance-Heated Thrustor Research," Report ITR 093-18628, Plasmadyne, Sept. 1963.

Early work on a 30-kW resistance-heated thruster utilizing hydrogen as propellant.

White, A. F., "Electrothermal Microthrust Systems," AIAA Paper 67-423, July 1967.

A limited treatment of design and performance characteristics of several electrothermal microthrust systems is presented. Included in the study are the TRW *Vela* resistojet, Avco resistojet, GE resistojet, GE radioisojet, and Marquardt resistojet.

Thruster Heaters, Radioisojet

Grossman, I., Jones, T. R., and Lee, D. N., *Auxiliary Propulsion Survey, Part III*, Technical Report AFAPL-TR-68-67, Part III, Air Force Aero Propulsion Laboratory, Sept. 1968.

Data on the GE radioisojet, project POODLE, and DART are presented in the heated fluids section of this report. This report gives good general information (unclassified) on the DART system.

Radioisotope Propulsion Technology Program (POODLE) Final Report Volume I, II, & III, Report STL-517-0049 (Contract No. AT (04-3)-517), TRW Systems, Redondo Beach, Calif., Apr. 1967.

Description of the POODLE thruster and its performance.

Viventi, R. E., et al., *Simulated Radioisotope Thrust System and Component Development, Final Report*, Report GESP-87, General Electric Nuclear Systems Programs, Cincinnati, Ohio.

Includes a discussion of the General Electric Radioisojet system. Included in this report is a discussion of simulated (electric) thruster development and catalyst studies.

Viventi, R., and Isley, W. C., "Design and Demonstration of a Radioisojet," AIAA Paper 67-425, July 1967.

General discussion of a radioisojet system developed at General Electric.

NASA — JPL — Coml., L.A., Calif.